BorneO JOURNAL

OF RESOURCE SCIENCE AND TECHNOLOGY

Advisory Board

BJRST International Advisory Board Members:
Prof. Dr. Arvind Bhatt, Kuwait Institute for Scientific Research, Kuwait
Prof. Dr. Colin Llewellyn Raston, Flinders University, Australia
Prof. Dr. Flavio M Vichi, Universidade de São Paulo, Instituto de Química, Brazil
Prof. Dr. Kuangyu Yen, Southern Medical University, Guangzhou, China
Prof. Dr. Liu Chao, Lanzhou Institute of Chemical Physics, China
Prof. Dr. Marc Arlen Anderson, IMDEA Energy Institute, Spain
Prof. Dr. Muchlisin Zainal Abidin, Universitas Syiah Kuala, Indonesia
Prof. Dr. Motokawa Masaharu, Kyoto University, Japan
Prof. Dr. Koji Fukui, Shibaura Institute of Technology, Japan
Assoc. Prof. Dr. Tingga Kingston, Texas Tech University, USA
Assoc. Prof. Dr. Lien Luong, University of Alberta, Canada
Assoc. Prof. Dr. Tommy Tsan Yuk Lam, The University of Hong Kong, Hong Kong
Dr. Justin Jong-Leong Wong, University of Sydney, Australia
Dr. Nicolas Hubert, Institut de Recherche pour le Développement, UMR 226 ISEM (UM2-CNRS-IRD), France

BJRST National Advisory Board Members:
Prof. Emeritus Dato Dr. Latiff Mohamad, Universiti Kebangsaan Malaysia, Malaysia
Prof. Dato' Dr. Mohd Tajuddin bin Abdullah, Universiti Malaysia Terengganu, Malaysia
Prof. Dr. Latiffah Zakaria, Universiti Sains Malaysia, Malaysia
Prof. Dr. Kasing Apun, Universiti Malaysia Sarawak, Malaysia
Prof. Dr. Mustafa Ab Rahman, Universiti Malaysia Sarawak, Malaysia
Prof. Dr. Son Radu, University Putra Malaysia, Malaysia
Prof. Dr. Zainab Ngaini, Universiti Malaysia Sarawak, Malaysia
Prof. Dr. Indraneil Das, Universiti Malaysia Sarawak, Malaysia
Prof. Dr. Mhd Ikhwanuddin, Universiti Malaysia Terenganu, Malaysia
Prof. Dr. Sin Yeng Wong, Universiti Malaysia Sarawak, Malaysia
Assoc. Prof. Dr. Syafiq Lee Nung Kion, Universiti Malaysia Sarawak, Malaysia
Dr. Hafizi Rosli, Universiti Sains Malaysia, Malaysia
Dr. Dzarifah Zulperi Universiti Putra Malaysia, Malaysia

Reviewers:
AP Dr Noor Haliza Hasan – Universiti Sains Malaysia
AP Dr Mohamad Hasnul Bolhassan – Universiti Malaysia Sarawak
AP Dr Lee Seong Wei – Universiti Malaysia Kelantan
AP Dr Annita Yong Seok Kian – Universiti Malaysia Sabah
AP Dr Vivien Jong – Universiti Teknologi MARA
Dr Mohd Akmal Mohd Raffi – Universiti Malaysia Sarawak
Dr Yusralina Yusof – Universiti Malaysia Sarawak
Dr Intan Azura Shahdan – International Islamic University Malaysia
Dr Nurul 'Ain Elias – Universiti Sains Malaysia
Dr Mohd Ridwan bin Abd Rahman @ Tahir – Universiti Malaysia Sarawak
Dr Ngieng Ngui Sing – Universiti Malaysia Sarawak
Dr Shairul Izan Binti Ramlee – Universiti Putra Malaysia
Dr Azma Hanim binti Ismail – Universiti Sains Malaysia
Dr Noor Afeefah Nordin – Universiti Tenaga Nasional
Dr Farah Akmal Idrus – Universiti Malaysia Sarawak
Dr Faddrine Jang – Monash University Malaysia
Dr Mugunthan Perumal – Universiti Malaysia Sarawak
Dr Mohd Hadi Akbar Basri – Universiti Putra Malaysia
Dr Rafida binti Razali – Universiti Malaysia Sarawak
Dr Ahmad Riduan Bahauddin – Universiti Sains Islam Malaysia
Dr Gaurav Arora – King Mongkut's University of Technology North Bangkok

BORNEO JOURNAL OF RESOURCE SCIENCE AND TECHNOLOGY

Borneo Journal of Resource Science and Technology (BJRST) publishes scientific articles in all fields of resource sciences. The journal welcomes the submission of manuscripts that meet the general criteria of significance and scientific excellence from but not limited to Borneo. Acceptance for publication is based on contributions to scientific knowledge, original data, ideas or interpretations and on their conciseness, scientific accuracy and clarity.

BJRST publishes scientific articles in all fields of resource sciences including land and forest resources, aquatic science, biodiversity and ecology, biotechnology and molecular biology, chemistry, microbiology, bioinformatics, plant science and zoology. It offers a forum for the discussion of local issues that are of global concern. It is a double-blind refereed online journal published bi-annually. Currently it is indexed by Scopus, MyCITE (Malaysian Citation Index),UDL edge Beta, DOAJ Directory of Open Access Journals, Index Copernicus, MyJurnal and Google Scholar.

When submitting the work, contributors are requested to make a declaration that the submitted work has not been published, or is being considered for publication elsewhere. Contributors have to declare that the submitted work is their own and that copyright has not been breached in seeking the publication of the work.

Views expressed by the author(s) in the article do(es) not necessarily reflect the views of the Editorial Committee.

Manuscripts can be submitted via https://publisher.unimas.my/ojs/index.php/BJRST

Correspondence on editorial matters should be addressed to:

Contents

Epiphyte Diversity in Forests and Oil Palm Plantations: Effects of Age and Distance

BRIDGETTE PHILIP, GABRIEL TONGA NOWEG* & JULIA NELSON

Institute of Biodiversity and Environmental Conservation, Universiti Malaysia Sarawak, 94300 Kota Samarahan, Sarawak, Malaysia
*Corresponding author: gabriel.noweg@gmail.com

ABSTRACT

Epiphytes play a vital role in the rainforest ecosystems, contributing to biodiversity and ecological balance. This study investigates the diversity and abundance of epiphytes in the Jagoi area, Bau, Sarawak, focusing on the impact of forest and oil palm plantation ages, as well as the proximity to the forest-oil palm plantation boundary. We conducted a comprehensive comparative study across 34 sampling plots located within secondary forests and oil palm plantations, with the plots carefully categorised based on their age and distance from the boundary to capture variations in environmental conditions. To ensure consistency and accuracy, the diversity and abundance of epiphytes within these plots were assessed using well-established standard ecological survey methods, which allowed for reliable data collection and analysis. This approach provided valuable insights into how land-use types and spatial factors influence epiphyte communities. Our findings reveal that the age of both forests and oil palm plantations significantly affects the diversity and abundance of epiphytes. In contrast, the distance to the forest-oil palm plantation boundary showed no significant relationship with these parameters. The study highlights the importance of forest and plantation age as key factors influencing epiphyte populations. These insights contribute to understanding the ecological dynamics of forest ecosystems adjacent to agricultural landscapes and highlight the need for sustainable management practices to preserve epiphytic biodiversity.

Keywords: Abundance, age, distance, diversity, forest-oil palm boundary

INTRODUCTION

Epiphytes, a fascinating and diverse group of plant species, are integral components of rainforest ecosystems, contributing significantly to the biodiversity and functioning of these intricate habitats. Found abundantly in tropical rainforest climates, they are adapted to thrive in conditions characterised by consistent temperature, high humidity, dappled light, and frequent rainfall (Zotz, 2013; Zhao *et al*., 2015). These unique plants, which include species such as orchids, ferns, and bromeliads, have evolved remarkable strategies to survive without rooting in soil, instead relying on other plants for structural support. Often mistaken for parasitic plants, epiphytes form a symbiotic relationship with their host trees, utilising them as anchors rather than as sources of nutrients. Unlike parasitic plants, which extract water and nutrients directly from their host, epiphytes derive their sustenance from rainwater, organic debris, and atmospheric nutrients. This distinction highlights their unique ecological niche, as they coexist harmoniously with their hosts without causing harm (Zotz, 2016; Twyford, 2018).

The diversity and distribution of epiphytes in rainforest ecosystems are influenced by a variety of factors, particularly the characteristics of their host trees. Key determinants include the diameter, species, and canopy structure of the host, which directly affect the availability of space, light, and moisture. Larger trees with extensive canopies often support a greater abundance and diversity of epiphytes, providing multiple niches within their branches and bark for colonisation. These factors highlight the complex interdependence between epiphytes and their host trees, as well as their role in rainforest dynamics. Given their significant contribution to the microclimates of rainforest ecosystems, epiphytes also support a variety of other organisms, including insects, birds, and small mammals, by providing shelter, food, and

breeding grounds. Their role extends beyond mere cohabitation as they are essential to maintaining ecological balance and biodiversity in tropical rainforests.

While tropical forests provide ideal conditions, land-use changes, particularly oil palm expansion, disrupt epiphyte communities (Bohnert *et al.*, 2016). Logging, agriculture, and natural disturbances reduce canopy cover and alter microclimates, limiting epiphyte colonisation. Secondary forests, with younger trees and simpler structures, support lower epiphyte diversity than primary forests, reflecting the impact of past disturbances on forest recovery. Epiphytes are less abundant near oil palm plantations due to habitat conversion (Altenhovel, 2013). These plantations lack the shaded, humid environments epiphytes require, as land clearing, chemical inputs, and soil disturbances degrade their habitat. Edge effects, including increased sunlight, wind, and temperature fluctuations, further hinder their survival. In contrast, undisturbed forests provide microclimates, higher humidity, and diverse host trees, fostering richer epiphyte communities. The transition from forests to oil palm plantations disrupts these conditions, emphasising the need for sustainable land-use practices (Luke *et al.*, 2020). Despite the known biodiversity loss, studies on epiphyte density and diversity in oil palm landscapes remain limited (Dunnett, 2004; Luke *et al.*, 2019).

This study investigates the diversity, abundance, and distribution of epiphytes across contrasting land-use types, namely the forests and oil palm plantations in the Jagoi area of Bau, Sarawak. By comparing epiphyte communities in these landscapes, the study aims to examine how factors such as plantation and forest age, as well as proximity to forest edges, influence epiphytic plant populations. The study also examines how environmental shifts associated with oil palm cultivation such as reduced canopy cover, altered microclimates, and chemical use, affect these sensitive plants.

A specific focus is placed on the ecological effects of forest-plantation boundaries, where edge effects, including increased sunlight and wind exposure, may intensify habitat stress for epiphytes. By adopting a comparative approach, this study provides a complete view of how land-use changes shape biodiversity. Ultimately, this study fills a critical knowledge gap by highlighting the ecological consequences of oil palm expansion on epiphyte communities. The findings offer insights for conservation strategies and sustainable land management, supporting efforts to reconcile agricultural development with biodiversity conservation in tropical ecosystems.

MATERIALS AND METHODS

Study Sites

The study was conducted in Sarawak, Malaysia, which has the largest oil palm planted area in the country, accounting for 28.6% of the total planted area of 5.67 million ha in 2022 (Malaysia Palm Oil Board, 2022). The focus was on the Bau-Lundu region, where the oil palm plantation spans 12,701 ha. These plantations are managed by the Sarawak Land Consolidation and Rehabilitation Authority (SALCRA), with smaller plots owned by smallholders (SALCRA, 2022). The study was specifically conducted at the Jagoi (1°22'06.6"N 110°04'45.1" E) and Bratak (1°26'41.1"N 110°06'22.9" E) SALCRA oil palm plantations in Bau, Sarawak (Figure 1).

The Bau District, located within the Kuching Division, is known for its gold mining activities and unique limestone hills that provide habitat for a variety of endemic plants. The primary rainforest covers approximately 40% of the land area in this district, primarily on barren limestone hills and high mountains (Pour *et al.*, 2013).
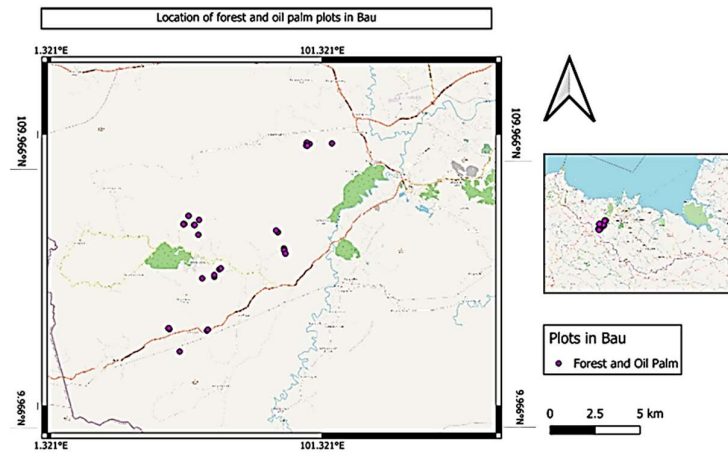
Figure 1. Map of the study area

Sampling Design Overview

This study is designed to assess the diversity and abundance of epiphytes on host trees across two distinct land-use types i.e., neighbouring forests and the Jagoi and Bratak SALCRA oil palm plantations. To ensure comprehensive coverage of the study sites, 34 sampling plots were established in both forested and plantation areas. These plots were categorised based on the age of the ecosystems. For the forest plots, the age categories include young forests (< 25 years old), mid-aged forests (25–40 years old), and mature forests (> 40 years old). Similarly, the oil palm plantations were divided into plots representing young plantations (< 10 years old), mid-aged plantations (10–15 years old), and mature plantations (> 15 years old) (Descals *et al.*, 2019). This classification allowed for a comparative analysis of how vegetation age influences epiphytic diversity and abundance, providing critical insights into the ecological dynamics of these landscapes.

Tree Sampling Strategy

The methodology for tree sampling was carefully structured to capture the diversity of tree hosts and their associated epiphytes. Within each 10 m x 10 m plot, all trees meeting the inclusion criteria of a diameter at breast height (DBH) of at least five cm and a height of at least three m were sampled. These parameters were chosen to ensure that only substantial trees with the potential to host epiphytes were included in the study. Voucher specimens were collected from sampled trees to facilitate accurate

identification and serve as a permanent record for future reference. This detailed sampling strategy aimed to establish a robust dataset on host tree characteristics and their relationship with epiphyte communities, particularly in disturbed and anthropogenic landscapes.

Epiphyte Sampling Methodology

The survey extended beyond trees to include epiphytes growing on oil palms. For epiphyte sampling, all plants occurring on trees or oil palms with a DBH exceeding five cm and a height of less than three m were systematically counted. This study ensured that juvenile host structures and their associated epiphytes were not overlooked by including smaller oil palms and trees within this height range. This inclusion provided a more holistic understanding of epiphyte distribution patterns across different host types and age groups. The consistent sampling approach across forest and plantation plots enabled the researchers to make valid comparisons and derive meaningful conclusions regarding epiphyte community structures in these two contrasting habitats.

Inclusion of Oil Palm Host Trees

To specifically address the role of oil palms as hosts for epiphytes, five oil palms were selected and surveyed within each plantation plot. The focus on a fixed number of oil palms ensured uniformity in data collection and minimised variability introduced by sampling bias. These oil palms were assessed for their ability to support epiphyte communities, and the findings

were compared with those from forest trees. The inclusion of oil palms highlighted the impact of monoculture plantations on epiphyte abundance and diversity, shedding light on how different host characteristics influence the establishment and survival of epiphytes in anthropogenic landscapes.

Proximity to the Forest-Oil Palm Boundary

Another critical factor examined in the study was the distance of oil palm plots from the forest-oil palm plantation boundary. Plots were strategically placed at distances of 10 m and 100 m from the boundary to assess the effects of proximity on epiphyte communities. The 10 m plots were expected to exhibit higher diversity and abundance due to edge effects, such as increased light availability and a transitional microclimate. In contrast, the 100 m plots were anticipated to reflect the harsher environmental conditions characteristic of interior plantation areas. The study integrated distance as a key variable to explore the spatial patterns of epiphyte distribution and to evaluate the impact of edge effects on their diversity and abundance.

Integration and Visualisation of Sampling Design

The arrangement of sampling plots was carefully planned to maximise the representativeness of the data and facilitate the identification of trends across different land-use types and age groups. The systematic placement of plots (Figure 2), combined with rigorous sampling methods, ensured that the study captured a broad spectrum of ecological conditions influencing epiphyte communities. Figure 3 illustrates the spatial distribution of sampling plots, highlighting their alignment with the study objectives. This integrative approach not only enabled a detailed examination of epiphyte diversity and abundance but also provided a framework for future study on biodiversity conservation and sustainable management in tropical landscapes. The study's findings highlight the importance of maintaining ecological connectivity and habitat complexity to support the persistence of epiphyte populations amidst ongoing land-use changes.
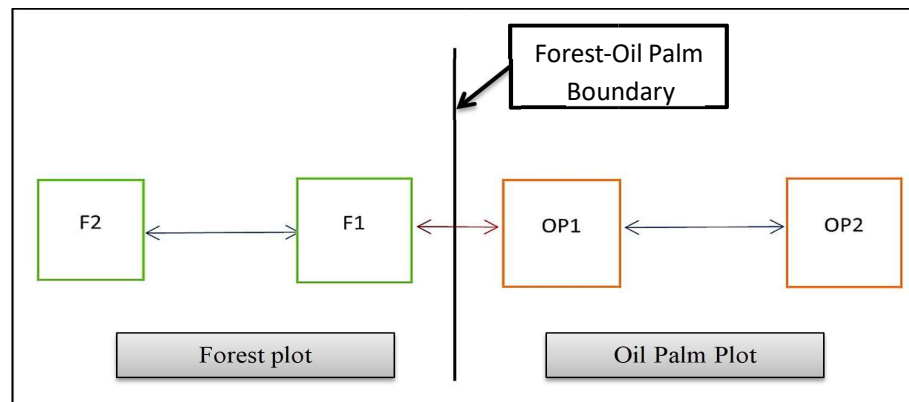
Figure 2. Sampling plots. (F2 (Forest 2), 100 m from F1 (Forest 1); OP2 (Oil Palm 2), 100 m from OP1 (Oil Palm 1); Distance from F1 and OP1 is 20 m, and black line indicates the forest-oil palm boundary)
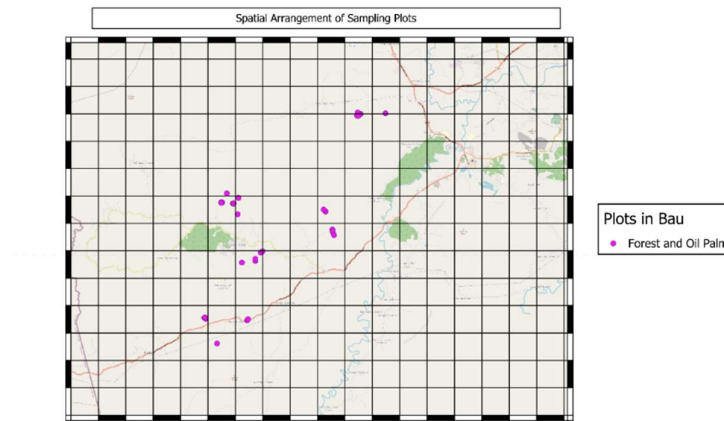
Figure 3. Spatial arrangement of sampling plots

Methods

The methodology used in this study is based on standard protocols for assessing the abundance of epiphytes on host trees (Oswaldo *et al.*, 2022). The choice of these methods was justified by their widespread use in similar studies and their proven effectiveness in providing accurate and reliable data. The categorisation of the plots into different age groups allowed for a more nuanced understanding of the impact of age on the abundance of epiphytes. The use of voucher specimens ensured the accurate identification of the species observed.

The study's design, including the size and placement of the plots, was carefully chosen to ensure a representative sample of the study area. The decision to include trees and oil palms with a diameter of more than five cm and a height of less than three m in the count was based on the assumption that these would be the most likely hosts for epiphytes (Hatta *et al.*, 2023). The enumeration of five oil palms in each oil palm plot plantation plots provided additional data on the abundance of epiphytes in these specific environments.

The placement of the oil palm plantation plots at distances of 10 m and 100 m to the forest-oil palm plantation boundary allowed for an assessment of the impact of proximity to the forest on the abundance of epiphytes. This design choice was based on previous study indicating that the abundance of epiphytes can vary significantly depending on the distance from the forest edge (Bartemucci *et al.*, 2022).

Data Analysis

The objective of this study was to compare the diversity and abundance of epiphytes across forest and oil palm plantations of varying ages and distances to the forest-oil palm boundary. The data collection involved counting the total number of epiphytes in each location, which represented the abundance of epiphytes. The diversity of the epiphyte community was quantified using the Shannon-Weiner's Diversity Index, a widely accepted measure of ecological diversity (Spellerberg and Fedor, 2003). This index provides a numerical value that reflects both the number of species present and their relative abundances. It is calculated using the following equation Eq. (1):

$$H = \sum_{i=1}^{s}[(p_i) \times \ln(p_i)] \qquad \text{Eq. (1)}$$

where:
H is the Shannon-Index Value,
S is the number of species present in the population, and,
p_i is the proportion of individuals belonging to the ith species.

The index value obtained reflects the diversity of the community, where higher values indicate greater species richness and evenness, suggesting a more diverse and balanced

community. Conversely, lower values indicate lower diversity. To determine the significant difference between the means of two or more groups, the non-parametric Kruskal-Wallis H-test was conducted. The mean rank was then used to rank the groups according to the mean differences.

To examine the relationship between epiphyte diversity and frequency concerning age and distance within both forested areas and oil palm plantations, Spearman's Rho rank coefficient of correlation was applied. This non-parametric statistical technique is known for its robustness, as it remains unaffected by the distribution of the population. Additionally, it does not require data to be collected at regular intervals and is suitable for small sample sizes (Gauthier, 2001).

RESULTS AND DISCUSSIONS

A total of 1,416 individual epiphytes from 39 families were recorded in the forest plots (Table 1). Blechnaceae, primarily *Stenochlaena palustris* (Burm.f.) Bedd., was the most dominant at 13.4% of the total population, followed by Fabaceae (10.7%) and Similacaceae (10.5%). These dominant families contribute to nutrient cycling and habitat structuring, suggesting specific ecological adaptations within the forest ecosystem.

Plantation age significantly influenced epiphyte diversity and abundance. Older plantations supported greater species richness due to their developed canopy structures, stable microclimates, and diverse microhabitats. Younger plantations, with sparser canopies, lacked the structural complexity required for epiphyte colonisation. Proximity to forest boundaries also played a role, as epiphytes near the forest edge exhibited higher diversity and abundance, likely due to favourable microclimatic conditions such as increased humidity and moderated temperature fluctuations (Altenhovel, 2013).

Within the oil palm plantations, 1,365 epiphyte individuals from 50 families were identified. Polypodiaceae was the most abundant (24.6%), followed by Davalliaceae (9.2%) and Arecaceae (8.8%). The most dominant species included *Davallia denticulata* (Burm.f.) Mett. (121 individuals) and *Elaeis guineensis* Jacq.

saplings (119 individuals). Other significant contributors were *Pyrrosia longifolia* (Burm.f.) C.V.Morton (Figure 4 (a)) and *Goniophlebium percussum* (Cav.) W.H. Wagner & Grether, each with over 100 individuals. These findings indicate that some epiphyte species exhibit resilience in agricultural landscapes despite altered environmental conditions.

Comparative analysis showed that *Centrosema pubescens* Benth., *Asplenium nidus* L. (Figure 4 (b)), and *D. denticulata* (Figure 4 (c)) were prevalent in both forest and plantation environments. *Hoya coronaria* Blume was also found in both settings, contributing to biomass accumulation and nutrient cycling (Rahayu *et al.*, 2018). *Ophioglossum pendulum* L., favouring humid microclimates, was primarily associated with mature forests, aligning with findings by Zamora and Co (1986) on its moisture-dependent morphology.

Forest age significantly affected epiphyte populations. Mature forests (n = 734) supported the highest number of epiphytes, likely due to their complex microhabitats. Young (n = 364) and old (n = 318) forests exhibited lower counts, possibly due to insufficient structural complexity in young forests and environmental stress in older ones. Epiphyte abundance was also higher near forest boundaries (10m, n = 762) than in interior plots (100m, n = 654), indicating edge effects that modify environmental conditions (Nomura *et al.*, 2019; Li *et al.*, 2023).

The Kruskal-Wallis H-test (Table 2) confirmed significant differences in epiphyte diversity across plantation ages (p = 0.05) and forest ages (p = 0.00), with older plantations supporting greater diversity due to prolonged colonisation opportunities (Bohnert *et al.*, 2016). However, no significant correlation was found between epiphyte diversity and distance from the forest-oil palm boundary, suggesting that proximity alone may not strongly influence epiphyte distribution (Dittrich *et al.*, 2013).

The study corroborates previous study on forest maturity and plantation age shaping epiphyte communities. Large, old-growth trees provide stable microhabitats (Johansson *et al.*, 2007; Wirth *et al.*, 2009), but epiphyte abundance may decline in over-mature forests due to reduced light penetration (Laman, 1995). Findings align with de Frenne *et al.* (2021),

highlighting the role of canopy structure in regulating temperature and humidity for epiphyte growth.

Despite the resilience of some epiphytes in plantations, their diversity remains lower than in natural forests due to habitat simplification. Integrating native trees into plantations, as suggested by Li *et al.* (2023), could enhance biodiversity conservation. The minimal variation in epiphyte numbers across distances from the forest edge suggests that plantation management, rather than proximity to forests, plays a more critical role in maintaining epiphyte communities (Aragon *et al.*, 2015).

Table 1. The epiphytic flora in forest and oil palm plots

Category	Details
Total Epiphytes in Forest Plots	1,416 individuals across 39 families
Total Epiphytes in oil palm plots	1,365 epiphytes across 50 families
Notable Epiphytic Species	*S. palustris* (220), *A. nidus* (127), *S. hypoleuca* (88), *Spatholobus ferrugineus* (62), *Spatholobus sp.* (55), *S. odoratissima* (57), *M. umbellata* (52)
Most Abundant Family (Forest)	Blechnaceae with 220 individuals of *Stenochlaena palustris* (13.4%)
Most Abundant Family (Oil Palm)	Polypodiaceae (24.6%)
Common Species in Both Environments	*Asplenium nidus, Centrosema pubescens, Davallia denticulata, Hoya coronaria, Ophioglossum pendulum*
Epiphyte Count Variation by Forest Age	Mature forest (n = 734) > Young Forest (n = 364) > Old Forest (n = 318)
Epiphyte Count by Proximity to Boundary	Closer to boundary (n = 762) > Farther from boundary (n = 654)
Epiphyte Count in Oil Palm by Age	Old (>15 years) (n = 682), Mature (10-15 years) (n = 451), Young (<10 years) (n = 232)
Epiphyte Count in Oil Palm by Proximity	Farther from boundary (n = 684) > Near boundary (n = 681)
Impact of Forest Age on Epiphytes	Mature forest supports higher diversity and abundance compared to young and old forests
Influence of Boundary Proximity	Higher epiphyte counts near the forest-oil palm boundary due to increased light and seed scattering
Species Density and Light Availability	Greater species density at boundary due to light favouring certain epiphytes' establishment and reproduction
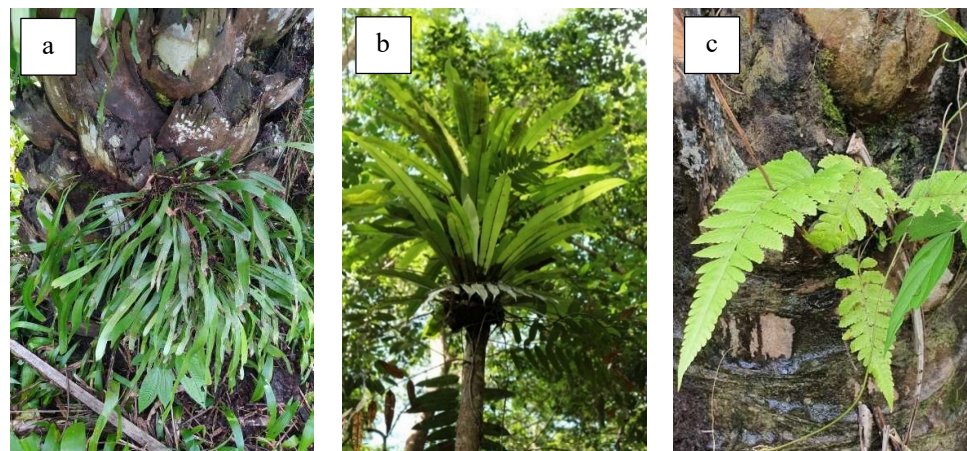
Figure 4. Examples of fern species. (a) *Pyrrosia longifolia,* (b) *Asplenium nidus,* (c) *Davallia denticulata*

Table 2. The Kruskal-Wallis H-test result

Variables			Age	Distance
Diversity	Forest	Chi-square	1.23	0.58
		df	2	1
		Sig (p-value)	0.54	0.45
	Oil palm plantation	Chi-square	6.17	0.05
		df	2	1
		Sig (p-value)	0.05*	0.82
Number of species	Forest	Chi-square	15.82	0.50
		df	2	1
		Sig (p-value)	0.00*	0.48
	Oil palm plantation	Chi-square	11.60	0.07
		df	2	1
		Sig (p-value)	0.00*	0.79
Total count of epiphytes	Forest	Chi-square	26.82	0.06
		df	2	1
		Sig (p-value)	0.00*	0.81
	Oil palm plantation	Chi-square	12.05	0.17
		df	2	1
		Sig (p-value)	0.00*	0.68

*Correlation is significant at $p < 0.05$

Comparative Species Diversity in Oil Palm Plantations and Forests in Bau

The study documented a total of 1,416 individual epiphytes across 39 families in the forest plots, with a significant representation from the Blechnaceae family, predominantly *S. palustris* (220 individuals, 13.4%). Similarly, the oil palm plantation plots contained 1,365 individual epiphytes from 50 families, with the Polypodiaceae family dominating at 24.6%. Notable species, such as *Spatholobus ferrugineus* (Zoll. & Moritzi) Benth. and *H. coronaria* were found in both environments, highlighting shared ecological traits despite the contrasting habitats. Species such as *D. denticulata* and *O. pendulum* were also common, suggesting their adaptability to varying light and humidity conditions across the forest and plantation settings. The comparative dominance of different families in the two habitats highlights variations in ecological preferences and the effects of anthropogenic influences like plantation practices.

Relationships Between Tree Components and Epiphyte Abundance

Tree sampling within the forest plots included host trees with a DBH of at least five cm and a height of at least three m, while oil palm enumeration was conducted for palms exceeding five cm in diameter and less than three m in height. Forests, particularly mature ones (25-40 years old), showed higher epiphyte abundance (n = 734) compared to young (n = 364) and old forests (n = 318). These findings suggest that mature forests provide optimal structural and microclimatic conditions for epiphyte establishment. Conversely, oil palm plantations demonstrated a reverse trend, where older plantations (>15 years) supported the highest epiphyte count (n = 682), likely due to increased structural complexity and light penetration over time. The arrangement of sampling plots at distances of 10 m and 100 m from the forest-oil palm boundary further revealed an edge effect, with more epiphytes recorded closer to the boundary (n = 762).

Effects of Age on Diversity and Abundance

Forest and plantation age significantly influenced the diversity and abundance of epiphytes. As indicated by the Kruskal-Wallis H-test, age was a strong predictor of diversity and species count in both forests and plantations, with statistically significant values for the diversity of oil palm plantations (p = 0.05) and the total count of epiphytes in forests (p = 0.00).

Younger forests (<25 years old) and plantations (<10 years old) displayed reduced epiphyte diversity, likely due to limited canopy structure and lower host tree availability. However, as the forest aged into the mature phase, the species richness and total counts peaked, underscoring the critical role of time in supporting epiphyte colonisation and succession. For plantations, older plots (>15 years) exhibited a higher mean rank for both diversity and abundance, highlighting the progressive adaptation of epiphytes to monoculture systems over time.

Influence of Proximity to the Forest-Oil Palm Boundary

Proximity to the forest-oil palm boundary emerged as a key factor affecting epiphyte distribution (Table 3). Sampling plots situated 10 m from the boundary showed a higher count of epiphytes (n = 762) compared to those 100 m away (n = 654). This pattern was mirrored in oil palm plantations, albeit with a marginal difference, as farther plots contained slightly more individuals (n = 684) than those closer to the boundary (n = 681). The edge effect was particularly evident in forests, where light availability and seed dispersal mechanisms likely contributed to the elevated counts near the boundary. In oil palm plantations, the relatively uniform distribution of epiphytes across distances could reflect the limited ecological differentiation within monoculture systems.

Table 3. The mean rank value between diversity and total count of epiphytes based on age and distance

Categories		Diversity				Number of species				Total count of epiphytes			
		Forest		Oil palm plantation		Forest		Oil palm plantation		Forest		Oil palm plantation	
		N	Mean rank	N	Mean rank	N	Mean rank	N	Mean rank	N	Mean rank	N	Mean rank
Age	Young	10	14.60	6	23.50	197	479.18	30	58.80	197	485.15	30	72.83
	Mature	16	18.94	10	20.95	417	443.98	50	86.08	417	451.67	50	105.34
	Old	8	18.25	18	13.58	257	389.95	90	94.08	257	372.90	90	78.70
Distance	10 m	17	18.88	17	17.88	465	430.57	85	84.48	465	437.88	85	83.95
	100 m	17	16.12	17	17.12	406	442.22	85	86.52	406	433.85	85	87.05

Statistical Analysis of Diversity and Abundance

The Spearman's Rho correlation analysis revealed significant associations between age and diversity for oil palm plantations (p = 0.01) but not for forests, as observed from Table 4. The negative correlation coefficient (-0.43) in plantations indicates that younger plantations support fewer species, consistent with observations of progressive ecological adaptation. For forests, a significant correlation was observed between age and total epiphyte counts (p = 0.00), highlighting the dependency of epiphyte abundance on forest maturity. Interestingly, distance to the forest-oil palm boundary had a minimal influence on diversity and total counts, as reflected in non-significant p-values for both habitats. These findings suggest that while age is a critical determinant of epiphyte diversity, distance effects are more nuanced and habitat-dependent.

Supporting Evidence and Comparative Insights

The observed trends align with recent studies emphasising the role of forest age and structural complexity in supporting epiphyte communities. The study of Cruickshanks *et al.* (2024) emphasises that older forests, with their well-developed canopy layers and higher availability of host trees, offer more niches for epiphyte colonisation and growth compared to younger forests. The increased structural complexity and microhabitat variety in older forests create favourable conditions for epiphyte establishment and survival. Study conducted in tropical rainforests and plantation landscapes highlights the ecological significance of mature forests in harbouring epiphytic diversity due to their stable microclimate and canopy stratification. Study in tropical montane forests showed that mature forests harbour greater epiphyte diversity due to the stability and availability of diverse substrates like tree trunks and branches (Glime, 2024). Younger forests, with less canopy cover and

structural development, tend to support fewer epiphytes. Studies on monoculture plantations have demonstrated the potential for older plantations to develop surrogate habitats for epiphytes, albeit with reduced species richness compared to natural forests (Hekkala *et al*. 2023). The inclusion of current references ensures that these findings are grounded in contemporary ecological study, providing a robust framework for interpreting the spatial and temporal dynamics of epiphyte communities in fragmented landscapes.

Table 4. The Spearman's Rho Correlation Coefficients analysis between diversity and total count of epiphytes based on age and distance to the forest-oil palm plantation boundary

Variables			Age	Distance
Diversity	Forest	Correlation coefficient	0.15	-0.14
		Sig (p-value)	0.40	0.43
		N	34	34
	Oil palm plantation	Correlation coefficient	-0.43	-0.04
		Sig (p-value)	0.01*	0.83
		N	34	34
Number of species	Forest	Correlation coefficient	-0.08	0.02
		Sig (p-value)	0.01*	0.48
		N	871	871
	Oil palm plantation	Correlation coefficient	0.22	0.02
		Sig (p-value)	0.00*	0.79
		N	170	170
Total count of epiphytes	Forest	Correlation coefficient	-0.14	-0.00
		Sig (p-value)	0.00*	0.81
		N	871	871
	Oil palm plantation	Correlation coefficient	-0.04	0.03
		Sig (p-value)	0.57	0.68
		N	170	170

*Correlation is significant at $p < 0.05$

CONCLUSIONS

This comprehensive study evaluated the diversity and abundance of epiphytes in the Jagoi area, Bau, Sarawak, comparing forested regions and oil palm plantations while analysing the influence of habitat age and proximity to the forest-plantation boundary. Addressing the impact of agricultural practices, specifically oil palm cultivation, on epiphyte biodiversity, a critical component of tropical rainforest ecosystems, the study aimed to assess diversity and abundance, understand the role of habitat age, and examine the effects of boundary proximity on these ecological parameters. Through meticulous sampling of 34 plots across secondary forests and oil palm plantations categorised by age and distance from the boundary, the study documented 1,416 individual epiphytes from 39 families in forest plots and 1,365 individuals from 51 families in plantation plots. Significant variation in epiphyte diversity and total count was observed across different ages of oil palm plantations, emphasising the pivotal role of habitat maturity in supporting epiphyte populations. However, contrary to expectations, no significant differences in diversity or total count of epiphytes were observed concerning proximity to the forest-plantation boundary, suggesting that habitat age is a more crucial factor than boundary effects in shaping the epiphyte community. These findings highlight the importance of conservation strategies that incorporate the age dynamics of forests and plantations to sustain epiphyte diversity. The study highlights the need for further study into the long-term effects of oil palm cultivation on epiphyte populations and the development of sustainable agricultural practices that conserve epiphytic biodiversity. Additionally, exploring the microclimatic changes induced by plantation proximity and their impact on epiphyte communities could provide valuable insights. This study enhances our understanding of epiphyte ecology in disturbed habitats, laying a foundation for future studies and conservation efforts in Malaysian forest and plantation ecosystems. It emphasises the crucial role of epiphytes in maintaining ecological balance and

species richness, which are essential for tropical rainforest health.

ACKNOWLEDGEMENTS

REFERENCES

Altenhovel, C. (2013). *Diversity of vascular epiphytes in lowland rainforest and oil palm plantations in Sumatra (Indonesia)* (Master's thesis), University of Göttingen.

Aragon, G., Abuja, L., Belinchón, R., & Martínez, I. (2015). Edge type determines the intensity of forest edge effect on epiphytic communities. *European Journal of Forest Research*, 134(3): 443-451. DOI: 10.1007/s10342-015-0863-5

Bartemucci, P., Lilles, E., & Gauslaa, Y. (2022). Silvicultural strategies for lichen conservation: Smaller gaps and shorter distances to edges promote recolonization. *Ecosphere*, 13(1): DOI: 10.1002/ecs2.3898

Bohnert, T., Wenzel, A., Altenhövel, C., Beeretz, L., Tjitrosoedirdjo, S. S., Meijide, A., Katja, R., & Kreft, H. (2016). Effects of land-use change on vascular epiphyte diversity in Sumatra (Indonesia). *Biological Conservation*, 202: 20-29. DOI: 10.1016/j.biocon.2016.08.008

Cruickshanks, K., Haughian, S. R., Clayden, S. R., Frison, M., Anderson, F., & McMullin, R. T. (2024). Vertical differentiation of epiphyte communities in old growth hemlock forests in Nova Scotia, Canada. *The Bryologist*, 127(4): 413-426. DOI:10.1639/0007-2745-127.4.413

de Frenne, P., Lenoir, J., Luoto, M., Scheffers, B. R., Zellweger, F., Aalto, J., Asgcroft., M. B., Christiansen, D.M., Decocq, G., De Pauw, K., Govaert, S., Greiser, C. Gril, E., Hampe, A., Jucker, T., Klinges, D. H., Koelemeijer, I. A., Lembrechts, J.J., Marrec, R., Meeuseen, C., Ogee J., Tyystjarvi., V., Vangansbeke, P., &

Hylander, K. (2021). Forest microclimates and climate change: Importance, drivers and future research agenda. *Global Change Biology*, 27(11): 2279-2297. DOI:10.1111/gcb.15569

Descals, A., Szantoi, Z., Meijaard, E., Sutikno, H., Rindanata, G., & Wich, S. (2019). Oil palm (*Elaeis guineensis*) Mapping with details: Smallholder versus industrial plantations and their extent in Riau, Sumatra. *Remote Sensing*, 11(21): 2590. DOI: 10.3390/rs11212590.

Dittrich, S., Hauck, M., Jacob, M., Rommerskirchen, A., & Leuschner, C. (2013). Response of ground vegetation and epiphyte diversity to natural age dynamics in a Central European Mountain spruce forest. *Journal of Vegetation Science*, 24(4): 675687. DOI:10.2307/23467152

Dunnett, N. (2004). The dynamic nature of plant communities—pattern and process in *The Dynamic Landscape* (pp.127-149). Taylor & Francis.

Gauthier, T. D. (2001). Detecting trends using Spearman's rank correlation coefficient. *Environmental forensics*, 2(4): 359-362. DOI:10.1006/enfo.2001.0061

Glime, J. M. (2024). Roles of bryophytes in forest sustainability—positive or negative? sustainability, 16(6): 2359. DOI:10.3390/su16062359

Hatta, S. K. M., Quinnell, R. J., & Compton, S. G. (2023). Pollinator attraction in the *Ficus deltoidea* complex: Varietal specificity in a fig wasp that likes to stay close to home. *Acta Oecologica,* 121: 103939. DOI: 10.1016/j.actao.2023.103939

Hekkala, A. M., Jönsson, M., Kärvemo, S., Strengbom, J., & Sjögren, J. (2023). Habitat heterogeneity is a good predictor of boreal forest biodiversity. *Ecological indicators*, 148: 110069. DOI:10.1016/j.ecolind.2023.110069

Johansson, P., Rydin, H., & Thor, G. (2007). Tree age relationships with epiphytic lichen diversity and lichen life history traits on ash in southern Sweden. *Ecoscience*, 14(1): 81-91. DOI:10.2980/1195-6860(2007)14[81:TARWEL]2.0.CO;2

Laman, T. G. (1995). *Ficus stupenda* germination and seedling establishment in a Bornean rainforest canopy. *Ecology*, 76(8): 2617-2626. DOI: 10.2307/2265832

Li, K., Grass, I., Zemp, D.C., Lorenz, H., Sachsenmaier, L., Nurdiansyah, F., Hölscher, D., Kreft, H., & Tscharntke, T. (2023). Tree identity and canopy openness mediate oil palm biodiversity enrichment effects on insect herbivory and pollination. *Ecological Applications*, 33(5): e2862. DOI: 10.1002/eap.2862

Luke, S. H., Advento, A. D., Aryawan, A. A. K., Adhy, D. N., Ashton-Butt, A., Barclay, H., Dewi, J. P., Drewer, J., Dumbrell, A. J., Edi, Eycott, A. E., Harianja, M. F., Hinsch, J. K., Hood, A. S. C., Kurniawan, C., Kurz, D. J., Mann, D. J., Matthews Nicholass, K. J., Naim, M., Pashkevich, M.D., Prescott, G.W., S., Pujianto, Purnomo, D., Purwoko, R.R., Putra, S., Rambe, Soeprapto, Spear, D.M., Suhardi, Tan, D.J.X., Tao, H., Tarigan, R.S., Wahyuningsih, R., Waters, H.S., Widodo, R.H., Whendy, Woodham, C.R., Caliman, J., Slade, E.M., Snaddon, J.L., Foster, W. A., & Turner, E. C. (2020). Managing oil palm plantations more sustainably: Large-scale experiments within the biodiversity and ecosystem function in tropical agriculture (BEFTA) programme. *Frontiers in Forests and Global Change*, 2(75). DOI:10.3389/ffgc.2019.00075

Luke, S. H., Purnomo, D., Advento, A. D., Aryawan, A. A. K., Naim, M., Pikstein, R. N., Sudharto, Rambe, T.D.S., Soeprapto, Caliman, J., Snaddon J. L., Foster, W.A., & Turner, E. C. (2019). Effects of understory vegetation management on plant communities in oil palm plantations in Sumatra, Indonesia. *Frontiers in Forests and Global Change*, 2(33). DOI: 10.3389/ffgc.2019.00033

Malaysia Palm Oil Board (MPOB). (2022). *Overview of the Malaysian Oil Palm Industry 2022.* Retrieved August 10, 2024, from https://bepi.mpob.gov.my/images/overview/Overview2022.pdf

Nomura, K., Mitchard, E. T. A., Patentee, G., Bastide, J., Oswald, P., & Nwe, T. (2019). Oil palm concessions in southern Myanmar consist mostly of unconverted forest. *Scientific Reports,* 9(1): 11931. DOI:10.1038/s41598-019-48443-3

Oswaldo, J., Hugo, C., Wilmer, T., Ismael, P., Wilson, Q., & Omar, C. (2022). Successional forests stages influence the composition and diversity of vascular epiphytes communities from Andean Montane Forests. *Ecological Indicators*, 143(4): 109366. DOI:10.1016/j.ecolind.2022.109366

Pour, A. B., Hashim, M., & Van, G. J. (2013). Detection of hydrothermal alteration zones in a tropical region using satellite remote sensing data: Bau goldfield, Sarawak, Malaysia. *Ore geology reviews,* 54: 181-196. DOI:10.1016/j.oregeorev.2013.03.010

Rahayu, S., Fakhrurrozi, Y., & Putra, H. F. (2018). Hoya species of Belitung Island, Indonesia, utilization, and conservation. *Biodiversitas Journal of Biological Diversity*, 19(2): 369-376. DOI:10.13057/biodiv/d190203

Sarawak Land Consolidation and Rehabilitation Authority (SALCRA). (2022). *Oil Palm*. Retrieved August 5, 2024, from https://www.salcra.gov.my/en/development-project/oil-palm

Spellerberg, I. F., & Fedor, P. J. (2003). A tribute to Claude Shannon (1916–2001) and a plea for more rigorous use of species richness, species diversity and the 'Shannon–Wiener' Index. *Global Ecology and Biogeography*, 12(3): 177-79. DOI:10.1046/j.1466-822X.2003.00015.x

Twyford, A. D. (2018). Parasitic plants. *Current Biology*, 28(16): 857-859. DOI: 10.1016/j.cub.2018.06.030

Wirth, C., Gleixner, G., & Heimann, M. (2009). *Old-growth forests: Function, fate, and value–an overview* (pp. 3-10). Springer.

Zamora, P. M., & Co, L. (1986). *Guide to Philippine flora and fauna: Economic ferns, endemic ferns, gymnosperms* (Vol. II). Natural Resources Management Center, Ministry of Natural Resources, Philippines and University of the Philippines.

Zhao, M., Geekiyanage, N., Xu, J., Khin, M. M., Nurdiana, D. R., Paudel, E., & Harrison, R. D. (2015). Structure of the epiphyte community in a tropical montane forest in SW China. *PLOS One*, 10(4): e0122. DOI:10.1371/journal.pone.0122210

Zotz, G. (2013). The systematic distribution of vascular epiphytes—a critical update. *Botanical Journal of the Linnean Society*, 171: 453–481. DOI:10.1111/boj.12010

Zotz, G. (2016). Plants on plants—the biology of vascular epiphytes. Switzerland: Springer International Publishing.

SHORT COMMUNICATION

Antagonistic Potential of Phosphate Solubilizing Bacteria (*Bacillus* spp.) from Peat Soil against *Erwinia* sp. (BP1) from the Leaves Zig-Zag Spots Symptoms Disease of the Pontianak Siamese Citrus Plants (*Citrus nobilis* var. *microcarpa*)

MUKARLINA[*], SITI KHOTIMAH, RAHMAWATI & SHELLA MIDA JUNIARTI

Faculty of Mathematics and Natural Sciences, Tanjungpura University, Pontianak, West Kalimantan, Indonesia
[*]Corresponding author: mukarlina@fmipa.untan.ac.id

ABSTRACT

The Pontianak Siamese orange (*Citrus nobilis* var. *microcarpa*) is one of the horticultural crops that is a leading commodity in the West Kalimantan area. However, in recent years, the production of Siamese oranges has decreased. One of the causes of the decline in the production of Siamese orange plants is the presence of diseases caused by bacteria. The *Erwinia* sp. bacteria, as the test pathogenic bacteria, were isolated from orange leaves with symptoms of zig-zag spots. Diseases in plants can be controlled using rhizosphere bacteria as biological agents. The phosphate-solubilising bacteria used as biological control agents in this research are rhizosphere bacteria originating from forest peat soil in Kubu Raya Regency, West Kalimantan. This research used a Completely Randomized Design (CRD) with five treatments. The *in vitro* antagonist test uses the dual culture method. The results showed that all phosphate-solubilising bacteria originating from peat soil *Bacillus* sp. (SGB1), *Bacillus* sp. (SGB2), and *Bacillus* sp. (SGB3) had antagonistic potential against the bacteria *Erwinia* sp. BP1.

Keywords: Antagonist test, *Erwinia sp.*, Phosphate-solubilizing bacteria, Siamese lime leaf

Pontianak Siamese oranges (*Citrus nobilis* var. *microcarpa*) are one of the local citrus varieties which are very popular because they have a sweet taste and contain high levels of vitamin C. Sambas Regency is the production center for Pontianak Siamese oranges in West Kalimantan. Sambas Regency produces 107,096 tons out of 142,917 tons, or around 75% of Pontianak Siamese orange production in West Kalimantan. The productivity of Pontianak Siamese orange plants from 2018 to 2020 decreased from 12.69 to 9.75, a decline of 30% (Kristiandi *et al*., 2021). One of the reasons for the decline in the productivity of Siamese orange plants is disease. Some symptoms of leaf disease on Siamese orange plants include Citrus Vein Phloem Degeneration (CVPD), scab, spots, powdery mildew, melanose, and leaf cancer, caused by fungi and bacteria (Setyaningsih *et al.,* 2021; Puspito *et al.*, 2018). The pathogenic bacterium used in this study was *Erwinia* sp., which was isolated from Siamese orange leaves with zigzag spot symptoms. This bacterium does not cause symptoms on citrus leaves but causes symptoms on citrus fruit. Several species of *Erwinia* include *E. carotovora*, *E. amylovora*, *E. tracheiphila*, and *E. rhapontici*, which cause disease in fruits, tubers, corn, carrots, and beans (Huang *et al*., 2003; Sasu, *et al*., 2010; Fatmi, *et al*., 2011).

Disease control in citrus plants generally still relies on the application of synthetic compounds such as imazalil, azoxystrobin, mefenoxam, thiabendazole, pyrimethanil, and fludioxonil (Panebianco *et al.*, 2015; Torres, 2021). The continued use of these chemicals can have negative impacts on

plants and the environment. As an alternative to controlling diseases in plants, rhizosphere bacteria can be used. Phosphate-solubilizing bacteria (PSB) are one type of rhizosphere bacteria that can act as biological control agents in plants. This group of bacteria is termed plant growth-promoting rhizobacteria, which includes many genera such as *Serratia*, *Rhizobium*, *Pseudomonas*, *Paenibacillus*, *Flavobacterium*, *Enterobacter*, *Burkholderia*, *Bacillus*, *Azospirillum*, *Arthrobacter*, *Acinetobacter*, and *Alcaligenes* (Marra *et al.*, 2012; Zeng *et al.*, 2011). These bacteria can indirectly inhibit pathogens through antibiotic compounds and serve as a form of biological control (Asril *et al.*, 2022; Qingwei *et al.,* 2023).

In this study, three test strains of phosphate-solubilizing bacteria (PSB) from different *Bacillus* genera were used, namely, *Bacillus* sp. SGB 1, *Bacillus* sp. SGB 2, and *Bacillus* sp. SGB 3, which were isolated from the rhizosphere of forest peat soil in West Kalimantan. The aim of the research was to determine the ability of the three bacterial strains to inhibit the growth of Erwinia sp. BP 1 bacteria.

In this study, bacterial strains *(Erwinia* sp. BP1), (*Bacillus* sp. SGB1), (*Bacillus* sp. SGB2), and (*Bacillus* sp. SGB3) were selected. The bacterial strains were obtained from the Laboratory of the Biology Department, Faculty of Mathematics and Natural Sciences, Tanjungpura University, West Kalimantan. The treatments used in this research are: a negative control that uses distilled water, a positive control that uses amoxicillin, and the antagonist bacteria used are *Bacillus* sp. (SGB1), *Bacillus* sp. (SGB2), and *Bacillus* sp. (SGB3). Three isolates of phosphate-solubilizing bacteria (PSB) were re-cultured by taking 0.1 ml of each PSB isolate from the stock culture and adding it to 10 ml of liquid NB medium (composition: beef extract and peptone) in each test tube, followed by shaking for 24 hours at a speed of 120 rpm. The bacterial suspension was then spread onto solid Pikovskaya agar medium and incubated at room temperature at pH 7 for 24 hours. An isolate of *Erwinia* sp. was recultured by taking two doses from the stock culture, placing them in a test tube containing 10 ml of sterile distilled water, and shaking it for 24 hours at a speed of 120 rpm. The bacterial suspension was taken from the test tube and spread evenly onto a petri dish containing solid NA medium, then incubated at 37°C and pH 7 for 24 hours.

The antagonism test uses a double-test method or dual-culture method, which is carried out by making a suspension of *Erwinia* sp. isolates and a suspension of antagonistic bacterial isolates, namely taking 1–2 loop of each bacterial isolate, placing them in separate test tubes that contain 10 ml of NB media, then shaking for 24 hours. A 1 ml suspension of pathogenic bacteria and antagonistic bacteria were pipetted into each test tube containing 9 ml of sterile distilled water, and the turbidity was equalised with a 1 McFarland's solution. The NA medium was poured into a petri dish (approximately 20 ml) and cooled. Then, the suspension of pathogenic bacteria, which had been equalized with a 1 McFarland's solution, was taken using a cotton swab and spread evenly over the surface of the NA medium (once solidified) until evenly distributed. Next, pieces of sterile filter paper (diameter ~0.5 cm) were immersed in each of the antagonistic bacterial suspensions, antibiotic suspensions, and sterile distilled water for approximately 30 minutes. The filter paper pieces were placed on the edge of the petri dish containing pathogenic bacteria and incubated for 24 hours at room temperature (Bonev *et al*., 2008)

The observation method is carried out by measuring the horizontal and vertical diameters, as well as the diameter of the filter paper. The average diameter of the inhibition zone for antagonistic bacteria, based on the theory put forward by Jawetz *et al.* (2008), can be calculated using the following formula, Eq. (1):

Zone of Resistance, $R = \dfrac{(Dv-Dc)+(Dh-Dc)}{2}$ Eq.(1)

Where:
R = Average zone of resistance that appears (mm)
Dv = Vertical diameter
Dh = Horizontal diameter

Dc = Diameter of filter paper

From the data, the mean values for the zones of growth inhibition of the plant extracts were calculated using statistical analysis of variance (ANOVA), and the result was expressed with a 95% level of confidence (p<0.05) (Kumar *et al*., 2006).

The results of the ANOVA test showed that the positive control treatment, negative control treatment, and the three tested strains of *Bacillus* sp. (SGB1), *Bacillus* sp. (SGB2), and *Bacillus* sp. (SGB3) applied against *Erwinia* sp. (BP1) at a 24-hour incubation period had a significant effect ($F4.10 = 42.697$, $P = 0.000$), as did the 48-hour incubation period ($F4.10 = 120.237$, $P = 0.000$), both affecting the diameter of the inhibition zone formed. Duncan's further test results at incubation times of 24 hours and 48 hours showed that the positive control treatment was significantly different from the negative control treatment and the phosphate-solubilizing bacteria *Bacillus* sp. (SGB1), *Bacillus* sp. (SGB2), and *Bacillus* sp. (SGB3). The testing of the inhibitory power of phosphate-solubilizing bacteria against *Erwinia* sp. (BP1) from the leaves of Siamese orange plants at incubation times of 24 hours and 48 hours showed the highest inhibition zone diameter in the *Bacillus* sp. (SGB2) treatment namely, 0.80 mm and 0.85 mm (Table 1). This condition indicates that bacteria belonging to the species *Bacillus* spp., with isolate codes SGB1, SGB2, and SGB3, have the ability to act as antagonistic agents against pathogenic bacteria from the leaves of Siamese orange plants through different inhibitory mechanisms and are thought to produce compounds that inhibit growth, varying in type and amount.

Several studies have reported the effects of the genus *Bacillus* isolated from the rhizosphere as having antimicrobial properties. The mechanism of action of antagonistic substances produced by *B. subtilis* against *Erwinia* spp. involved damaging the K^+ ion transport of sensitive phytopathogenic bacteria through their cell walls (Amin *et al*., 2015; Asril *et al*., 2022; Qingwei *et al.,* 2023).

The inhibitory activity of *Bacillus* is also due to the presence of synthesised siderophore compounds (Eman *et al*., 2018). The research results of Khotimah (2021) showed that isolates of phosphate-solubilizing bacteria of the genus *Bacillus* spp. that were isolated from the rhizosphere of forest peat soil in Kubu Raya, West Kalimantan, were able to produce exopolysaccharides, which are siderophores.

The resulting inhibition zone is classified as weak (Table 1). It is suspected that the antagonist bacteria used in this study have weak antagonistic activity against Gram-negative bacteria. *Erwinia* spp. are Gram-negative bacteria (Huang *et al*., 2003; Fatmi *et al.*, 2011). Oscariz *et al.* (1999) reported that *B. cereus* strains isolated from soil were active against most Gram-positive, but not Gram-negative bacteria. Aslim *et al.* (2002) demonstrated that *Bacillus* strains had greater effects on Gram-positive bacteria than on Gram-negative bacteria. As conclusion, phosphate-solubilizing bacteria *Bacillus* spp. with isolate codes SGB-1, SGB-2, and SGB-3, originating from peat soil in this study showed antagonistic potential against the pathogenic bacteria *Erwinia* sp. (BP1).

Table 1. Mean Diameter of the Inhibition Zone for the Antagonist Test of All Treatments Against *Erwinia* sp. BP1 from Siamese Orange Plant Leaves with Zig-Zag Spot Symptoms of the Disease.

Treatment	Diameter of Inhibition zone (mm)		Diameter Inhibition Zone Category (Surjowardojo *et al*., 2015)
	24 hours	48 hours	
BP1 vs K^{+}	$5,73 \pm 1,35^b$	$7,2 \pm 0,95^b$	Medium
BP1 vs K[-]	0.00 ± 0.00^a	0.0 ± 0.00^a	Weak
BP1 vs SGB1	$0,63 \pm 0,03^a$	$0,73 \pm 0,15^a$	Weak
BP1 vs SGB2	$0,80 \pm 0,25^a$	$0,85 \pm 0,30^a$	Weak
BP1 vs SGB3	$0,63 \pm 0,24^a$	$0,68 \pm 0,31^a$	Weak

Numbers followed by the same letter indicate results that are not significantly different with a confidence level of 95%.

REFERENCES

Amin, M., Rakhizi, Z.& Ahmadi, A.Z. (2015). Isolation and identification of *Bacillus* species from soil and evaluation of their antibacterial properties. *Avicenna Journal of Clinical Microbiology and Infection,* 22(1): e23233. DOI: 10.17795/ajcmi-23233.

Aslim, B., Saglam, N. & Beyatli , Y. (2002). Determination of some properties of *Bacillus* isolated from soil. *Turkish Journal of Biology,* 26 (1) 41–48.

Asril, M., Lisafitri, Y. & Siregar, B.A. (2022). Antagonism activity of phosphate solubilizing bacteria against *Ganoderma philippii* and *Fusarium oxysporum* of Acacia plants. *Journal of Multidisciplinary Applied Natural Science*, 2(2): 82-89. DOI: 10.47352/jmns. 2774- 3047.118

Bonev, B., Hooper, J.& Parisot, J. (2008). Principles of accessing bacterial susceptibility to antibiotics using agar diffusion method. *Journal of Antimicrobial Chemotherapy,* 61(6): 1295- 1301. DOI:10.109/jac/dkn090.

Eman, A., Mohamed, H., Farag, A.G. & Youssef, S.A. (2018). Phosphate solubilization by *Bacillus subtlis* and *Serratia marcescens* isolated from tomato plant rhizosphere. *Journal of Environmental Protection,* 9(3): 266-277. DOI**:** 10.4236/jep.2018.93018

Fatmi, M., Yaich, M., Bougsiba , M., Valentini, F., Scuderi, D., D'Onghia, A.M. & Cirvileri, G. (2011). Fire blight (*Erwinia amylovora* [Burrill] Winslow) in Morocco: importance, geographical distribution and characterization, *Phytopathologia. Mediteranea,* 50 (2): 212−227. DOI: https://doi.org/10.14601/Phytopathol_Medit err-9132

Huang, H.C., Hsieh, T.F. & Erickson, R.S. (2003). Biology and epidemiology of *Erwinia rhapontici,* causal agent of pink seed and crown rot of plant. *Plant Pathology Bulletin*, 12:69-76.

Jawetz, E., Melnick, J. L.& Adelberg, E. A. (2008). Medical Microbiology. Jakarta: Medica Salemba Press.

Khotimah, S. (2021). *Potential of Cellulose Degrading Fungi and Bacteria as well as Phosphate Solubilizing Bacteria, Non Symbiotic Nitrogen Fixing, and IAA Producing at Various Peat Maturity Levels as Biofertilizer Candidates* (Dissertation). Brawijaya University, Malang.

Kristiandi, K., Fertiasar, R., Yunita, N.F., Astuti, T. & Sari, D. (2021). Analisis produktivitas dan luas tanaman jeruk siam Sambas tahun 2015-2020. *Jurnal Pemikiran Masyarakat ilmiah Berwawasan Agribisnis*, 7(2): 1747-1755.DOI: http://dx.doi.org/10.25157/ma.v7i2.5607

Kumar, V.P., Chauhan, N.S., Padh, H. & Rajani, M. (2006). Search for antibacterial and antifungal agents from selected indian medicinal plants. *Journal of Ethnopharmacology*, 107(2): 182-188.DOI: 10.1016/j.jep.2006.03.013

Kumar, A.,Verma, S.K., Ashis. & Choudary, D.K. (2014). Biochemical and molecular characterization of antagonistic bacteria against yellow blotch of oyster mushroom. *International Journal of Research in Engineering and Technology*, 3(4): 294-297.

Marra, L.M., Soares, C.R.F.S., Oliveira, S.M., Ferreira, P.A.A., Soares, B.L., Carvalho, R.F., Lima, J.M. & Moreira, F.M.S. (2012). Biological nitrogen fixation and phosphate solubilization by bacteria isolated from tropical soils. *Plant and Soil*, 357:289-307. DOI: 10.1007/s11104- 012-1157-z.

Oscariz, J.C., Lasa, I., Pisabarro, A.G. (1999). Detection and characterization of cerein 7, a new bacteriocin produced by *Bacillus cereus* with a broad spectrum of activity. *FEMS Microbiology Letters,* 178(2):337–341.

Panebianco, S., Vitale, A., Polizzi, G., Scala, F. &Cirvillieri, G. (2015). Enhanced control of postharvest citrus fruit decay by means of the combined use of compatible biocontrol agents. *Biological Control,* 84 :19-27. https://doi.org/10.1016/j.biocontrol.2015.02. 001

Puspito, M.A., Hidayat, N. & Suprapto. (2018). Decision support system for citrus plant disease diagnosis using naive bayes classifier method. *Journal of Information Technology and Computer Science Development,* 2(7): 2578-2683.

Qingwei, Z., Lushi, T., Yu, Z., Yu, S., Wanting, W., Jiangchuan, W., Xiaolei, D., Xuejiao, H. & Bilal, M. (2023). Isolation and characterization of phosphate solubilizing bacteria from rhizosphere of poplar on road verge and their antagonistic potential against

various phytopathogens. *BMC Microbiology,* 23: 1-12. https://doi.org/10.1186/s12866-023-02953-3.

Sasu, M.A., Adams, S.I., Wall, K., Winsor, J.A. & Stephenson, A.G. (2010). Floral transmission of *Erwinia tracheiphila* by cucumber beetle in a wild *Cucurbita pepo*, *Environmet. Entomology,* 39(1): 140-148. DOI: 10.1603/EN09190

Setyaningsih, F.A., Rahmawati. & Mukarlina. (2020), Expert system analysis to identify diseases in siamese orange plants (*Citurus nobilis* var microcarpa) from Setapok village plantations, Singkawang city. *Computer Science Group Journal*, 8(2):162-171.

Suryowardojo, P., Susilawati, T.& Sirait, G.R. (2015). Daya hambat dekok kulit apel Manalagi (Malus sylvesters Mill.) terhadap pertumbuhan Staphylococcus aureus dan Pseudomonas sp penyebab mastitis pada sapi perah. *Jurnal Ternak Tropika*, 16(2): 40-48. DOI: 10.21776/ub.jtapro.2015.016.02.6

Torres, P.S. (2021). Molecular mechanisms underlying fungicide resistance in citrus. *Journal of Fungi,* 7(9):1-18, https://doi.org/10.3390/jof7090783:

Zeng, Q.G., Luo, F., Zhang, Z.B., Yan, R. & Zhu, D. (2011) Phosphate solubilizing rhizosphere bacterial T21 isolated from Dongxian wild rice species promotes cultivated rice growth. *Applied Mechanics and Materials*, 108: 167-175. DOI: https://doi.org/10.4028/www.scientific.net/AMM.108.167

Growth Performance of *Pentaspadon motleyi* Seedlings Inoculated with Arbuscular Mycorrhiza Fungi for Waterway Rehabilitation

CLARY SINAWAT[1], JOHN KEEN CHUBO*[2] & GARY LEEHAN LUHAT[3]

[1]Forest Research Centre, Sepilok, Sabah Forestry Department, P.O. Box 1407, 90715 Sandakan Sabah;
[2]Department of Forestry Sciences, Universiti Putra Malaysia Bintulu Sarawak Campus, 97008 Bintulu, Sarawak;
[3]Samling Timber Malaysia, Wisma Samling, Lot 296, Jalan Temenggong Datuk Oyong Lawai Jau, 98000 Miri, Sarawak
* Corresponding author: johnkeen@upm.edu.my

ABSTRACT

Stream development causes changes to the ecosystems of an area. Planting of trees in cleared area along waterways can help in reviving and create new habitats. Planting of riverine species such as *Pentaspadon motleyi* is one way to rehabilitate disturbed riverine area. The ability of seedlings to survive in new and harsh open environment depends on the seedlings' early growth as well as species adaptability. Arbuscular mycorrhiza fungi (AMF) have the capability to promote superior and stronger seedlings with better growth performance when planted in the fields. Thus, the objectives of this study were: (i) to measure the growth performance of *P. motleyi* seedlings planted along a waterway in Universiti Putra Malayisa Bintulu Sarawak Campus and (ii) to determine the effect of AMF on the growth of *P. motleyi* seedlings. A total of 30 seedlings were planted along a waterway stretch in UPMKB and 15 seedlings were treated with AMF while another 15 seedlings were left untreated. Parameters measured include plant height, collar diameter and leaf number were recorded for a period of 10 weeks. Leaf area and root morphology of *P. motleyi* seedlings were compared after the tenth week. AMF treated seedlings showed five times higher height and collar diameter growth than non-AMF treated seedlings while leaf number and leaf area were superior for all AMF treated seedlings. Roots of AMF treated seedlings were healthier with more fibrous and fine roots. AMF inoculation contributed to *P. motleyi* seedlings by forming mycorrhiza hyphae that helped the root system with the exploration and access to more soil nutrients from the surrounding area. Better nutrient uptake improved plant health including plant biomass. AMF treatment showed good potential in enhancing early growth performance of *P. motleyi* seedlings thus promoting better survival when being transplanted in the open field. Such conditions will benefit the rehabilitation activities of disturbed waterways.

Keywords: Arbuscular Mycorrhiza Fungi (AMF), growth, *Pentaspadon motleyi,* seedlings, waterway

INTRODUCTION

Riparian forests are ecotones delineating the transition from terrestrial ecosystems into aquatic ones. The high-water content in the soil resulted in unique vegetation and soil characteristics, differentiating it from the surrounding landscapes (Ring *et al*., 2018; Dufour *et al*., 2019). Vegetations in the riparian zones are more severely influenced by edaphic factors rather than the climate (van der Maarel *et al*., 2013). Riverine floodplains represent a challenging environment for plant to grow due to their heterogenous physico-chemical soil characteristics (Dai and Nimasow, 2024).

Pentaspadon motleyi of the Anacardiaceae family and a common species found in marshes at elevations of up to 200 m, extending from Sumatra to New Guinea and the Solomon Islands (Adnan *et al*., 2018). Also known as *Pelong* (Peninsular Malaysia); *Empelanjau, Pelajau* (Dayak, Sabah)*, Lakacho*, *Plajau* and *Plasin Uping* (Sarawak); *Djuping, Empit*, *Empelanjau, Letjut, Panjau, Pelajau, Peladjau, Pelasit, Pilajau, Plajau, Planjau, Polajo, Praju, Tampison, Umpit* (Indonesia); *Ttoei-na*, *Oei-nam* (Thailand), *Vi hùng trung* (Vietnam) and *Ailala*, *Laleua*, *Laleva* (New Guinea). The main reason for the selection *P. motleyi* for waterway rehabilitation is related to its natural habitat which is commonly found in swamps, along streams and rivers (Adnan *et al*., 2018). The tree can grow to be quite large, reaching up to 36 m in height and 80 cm in diameter at breast height, with spreading buttresses and beautiful, fluffy

crowns. Browne *et al.* (1955) noted that the trees can reach a height of 21 m after 11 years.

The tree has spirally organised compound leaves with 4 to 5 pairs of leaflets that are grouped at the ends of the twig tips and pinkish in colour when young. The leaves are 10 to 30 cm long and have 7 to 9 leaflets; the leaflets are normally opposite, pointed at the apex with a rounded base, and pinkish in colour when young (Kochummen, 1989). The blooms are yellowish white in colour and 4 mm in diameter. The sweeping canopies are loaded with flowers while in bloom. It blooms twice a year, from March to May and again from October to November and when in bloom, the trees stand out with full bloom and no leaves (Lim, 2012). Burgess (1966) and Wong (1975) recorded the bark of *P. motleyi* as grey, white with pink inner bark and pale sap. The wood is classified as a light hardwood with a pale yellow-green heart wood. When young, the sapwood is white with a green tint or light yellow with a pink tinge, 2 to 3 cm broad, and not usually clearly separated.

The wood is of good quality with straight stem which is quite strong and not cracked when used as building materials. The wood is simple to work with and is appropriate for general utility interior furnishing, panelling, partitioning, moulding, and other planking projects. Extractive compounds from the *P. motleyi* tree have been applied as medicinal components, including in the treatment of scabies (tinea) and malignant rashes (Heyne, 1987; Wiart, 2006). According to Yusro *et al.*, (2009), past research indicated that wood extract of *P. motleyi* showed the ability to inhibit the development of fungus *Candida albicans* and *Trichophyton mentagrophytes. Pentaspadon motleyi* seeds (endocarp) can be consumed either eaten raw, fried, cooked, or roasted (Lim, 2012).

Soil consolidation influences structural stability, soil nutrient content, and microbial biomass (Lin *et al.*, 2020). The potential of seedlings to grow well in the field can be influenced by many factors including soil compactness and erosion that can occur on the riverbank. Land along a waterway is commonly exposed to occasional short-term flood. Such situation can be detrimental to plants as flooding causes hypoxia or anoxia in soils creating low solubility and diffusion of oxygen in water while increased in the use of dissolved oxygen by

microorganisms and roots (Fougnies *et al.*, 2007). The survival of seedlings when planted in flooded and open field depends much on the ability and period required by the seedlings to adopt different physiological, morphological and biochemical strategies (Jia *et al*, 2021) to cope with the stress in the new environment.

The introduction of arbuscular mycorrhiza fungi (AMF) has been found crucial for plant growth and survival, enhancing nutrient acquisitions and tolerance to biotic and abiotic stresses (Dai and Nimasow, 2024). Inoculation of AMF on seedlings planted on flooded soil have shown variable effects with some plants recording improvement in growth (Miller and Sharitz, 2000), some showing decreased growth (Neto *et al.*, 2006) while others failed to indicate any clear relationship (Hartmond *et al.*, 1987). AMF have been reported to promote the development of a strong root system to help seedlings strive when a site is flooded (Fougnies *et al.*, 2007) during heavy rainfall.

Research on the response of *P. motleyi* seedlings to AMF is lacking and this study can help in providing some insight into such relationship. The introduction of AMF to *P. motleyi* seedlings is expected to assist the initial growth when transplanted in the open field. Therefore, the objectives of this study are to compare the effect of AMF on the growth of *P. motleyi* seedlings when planted along the waterway in Universiti Putra Malaysia Bintulu Sarawak Campus (UPMKB). Changes in the plant height, stem diameter, leaf number, leaf area and root growth were evaluated and related to the potential of AMF in promoting *P. motleyi* seedlings growth.

MATERIALS AND METHODS

Study Site

The area along a waterway in Universiti Putra Malaysia Bintulu Sarawak Campus was selected for the project. The site is occasionally inundated with rainwater during heavy rain which will usually subside once the rain stopped. The area along the waterway was cleared during the construction of the waterway to reduce the incidence of flooding in the area. The soil was of the Bekenu series (Typic Paleudult) with a pH of 4.84 and undulating slopes. The soil nutrient contents were recorded as 0.48% N, 0.90 mg/kg

P, 102 mg/kg K, 17.2 cmol/kg exchangeable Ca and 27.0 cmol/kg exchangeable Mg.

Seedlings Source and Planting

Pentaspadon motleyi seedlings were obtained from UPMKB Forest Nursery and placed in an open area for a week for the hardening process in order to reduce stress on the seedlings when planted in the open field. Few days before planting, the seedlings were moved on site and kept under tree shade for further hardening while waiting for the planting holes to be ready. Fertilizers were added into the planting holes before planting. This was done to ensure that most of the fertilizer can reach the root system and did not escape due to water runoff. A single seedling was then planted in each hole which was then covered using soil. Each seedling was gently removed from the polybag to ensure that the roots were kept intact as much as possible to avoid root disturbance. A polyvinyl chloride (PVC) pipe was used to cover the seedling's stem in order to protect the stem from injury, particularly due to grass cutting activities. The PVC pipe was cut to approximately 45 cm in length and one vertical cut was made to ease the insertion of the seedling's stem into the pipe.

AMF Treatments

Fifteen seedlings were treated with AMF while another fifteen were left untreated. Thus 50% of the seedlings will be selected for AMF treatment while another 50% will be left untreated. Both treated and untreated seedlings were planted alternately in a row at a 8 m distance between seedlings on both sites of the waterway. AMF treatment was applied on *P. motleyi* seedlings by digging two holes on an opposite direction around the root of the treated seedlings. Each hole was added with 20 gm of the AMF inoculum (RHIZAgold®). The product is documented to contain a mixture of 12 AMF species (including the genera *Glomus*, *Acaulospora*, *Gigaspora*, *Scutellospora* and *Sclerocystis*) and every 10 g of product has 250-300 mixed viable AMF spores. After addition of the AMF inoculum, the seedlings were left out in the field until the first measurement was conducted.

Data Collection

The first growth measurement was conducted one month after the application of the AMF inoculum. Measurements were conducted for a period of ten weeks from 14 September 2022 until 25 November 2022. Parameters included in determining the growth performance of *P. motleyi* seedlings were height, stem diameter and leaf number. Height growth was measured using a meter tape and measured from the root collar until the shoot tip of each seedling. Meanwhile, stem diameter was measured slightly above the root collar using a digital calliper. Data of height and diameter growth rate per week was conducted by deducting the measurement of height and diameter of the present week with the measurement of the past week. Leaf number was recorded based on manual counting. Recording of these parameters were conducted fortnightly.

Leaf area as well as root development of the seedlings were conducted during the last week of measurement using destructive methods. All leaves and roots from three random seedlings representing non-AMF and AMF treated seedlings were harvested. Photograph and leaf area were taken and determined using a web application software called Petiole®. The software is a mobile application designed for leaf area measurement that leverages on a smartphone's camera and a calibration plate to accurately determine leaf area. As to reduce destructive sampling, only two seedlings per treatment were dug out to sample to roots. Roots of the seedling were dug out carefully, and all soil and debris were washed with care under running water to avoid destruction to the root system. Photographs of the root system was taken to record the differences in root development due of the treatments.

Data Analysis

Data analysis was conducted using an independent T-test at 5% probability ($P < 0.05$) to determine the significant difference between the two-treatment means and performed using the Statistical Package for the Social Sciences (SPSS).

RESULTS

Growth Rate of *Pentaspadon motleyi* Seedlings

Table 1 shows the height growth rate of *P. motleyi* seedlings as recorded per week in terms of height growth. Height growth rates ranged from 0.13 to 0.93 cm in non-AMF treated seedlings and 1.13 to 3.27 cm for AMF treated seedlings. Comparison of height growth rate between the non-AMF treated and AMF treated seedlings found significant differences in eight of nine weeks of measurements. Two weeks indicated highly significant differences (P ≤ 0.001) between the two treatments, while the other two weeks and four weeks were

significantly different at p≤0.01 and p≤0.05, respectively. Insignificant difference was detected only in week 7.

The cumulative height growth of *P. motleyi* seedlings shows the height growth of AMF treated seedlings were far superior to the non-AMF treated seedlings (Figure 1). The mean height of AMF treated seedlings increased by 17.12 cm from 133.00 cm during the first measurement to 150.12 cm during the last measurement. Meanwhile, the non-AMF treated seedlings observed only 3.69 cm increment from 130.00 cm to 133.69 cm. After nine weeks of measurements, the AMF treated seedlings were five times taller than the non-AMF treated seedlings.

Table 1. Height growth rate per week recorded for *P. motleyi* seedlings

Week	Height Growth Rate (cm) Per Week		P-value
	Non-AMF Treated	AMF Treated	
1	0.47 ± 0.17	1.20 ± 0.28	0.032
2	0.16 ± 0.12	2.33 ± 0.33	<0.001
3	0.33 ± 0.21	1.53 ± 0.34	0.005
4	0.80 ± 0.28	2.60 ± 0. 81	0.045
5	0.40 ± 0.21	3.27 ± 0.42	<0.001
6	0.20 ± 0.14	1.93 ± 0.53	0.004
7	0.93 ± 0.32	1.60 ± 0.47	0.246
8	0.13 ± 0.09	1.13 ± 0.48	0.049
9	0.27 ± 0.12	1.53 ± 0.52	0.023

Note: Significant difference in height increment between treatment means were conducted at P ≤ 0.05.
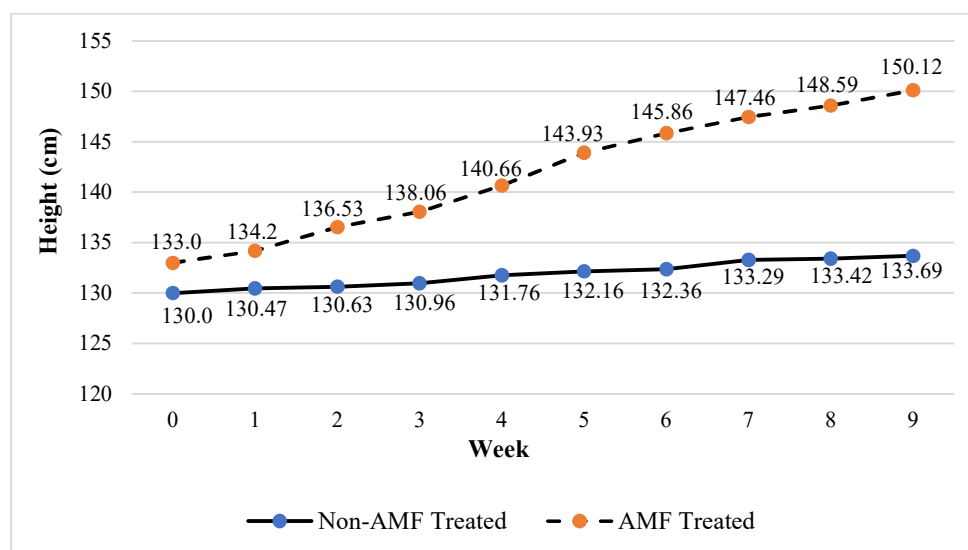
Figure 1. Cumulative height growth of *P. motleyi* seedlings

Diameter Growth Rate

Significant differences in the diameter growth rate per week for non-AMF and AMF treated *P. motleyi* seedlings were detected as shown in Table 2. Comparisons of treatments during weeks 1, 3, 4 and 6 were found to be highly significant (P ≤ 0.001) while other weeks indicated significant differences at P ≤ 0.01. Diameter growth rate per week ranged from 0.07 to 0.17 mm and 0.24 to 1.07 mm for non-AMF and AMF treated seedlings, respectively.

As indicated in Figure 2, the AMF treated seedlings showed superior cumulative diameter growth than the non-AMF treated seedlings. The non-AMF treated seedlings recorded an increase of 0.96 mm in total diameter growth while the AMF treated seedlings observed an increase of 4.36 mm to the initial diameter size. After nine weeks of measurement, AMF treated seedlings exhibited four to five times greater cumulative diameter growth than non-AMF treated seedlings.

Table 2. Diameter growth per week of *Pentaspadon motleyi* seedlings

Week	Diameter Growth Rate (mm) Per Week		P-value
	Non-AMF Treated	AMF Treated	
1	0.16 ± 0.05	1.07 ± 0.09	<0.001
2	0.17 ± 0.09	0.74 ± 0.19	0.012
3	0.07 ± 0.01	0.42 ± 0.07	<0.001
4	0.06 ± 0.01	0.52 ± 0.09	<0.001
5	0.14 ± 0.02	0.40 ± 0.10	0.013
6	0.08 ± 0.02	0.24 ± 0.03	<0.001
7	0.09 ± 0.01	0.36 ± 0.72	0.001
8	0.07 ± 0.01	0.24 ± 0.06	0.012
9	0.12 ± 0.02	0.37 ± 0.07	0.002

Note: Significant difference in diameter increment between treatment means were conducted at P ≤ 0.05.
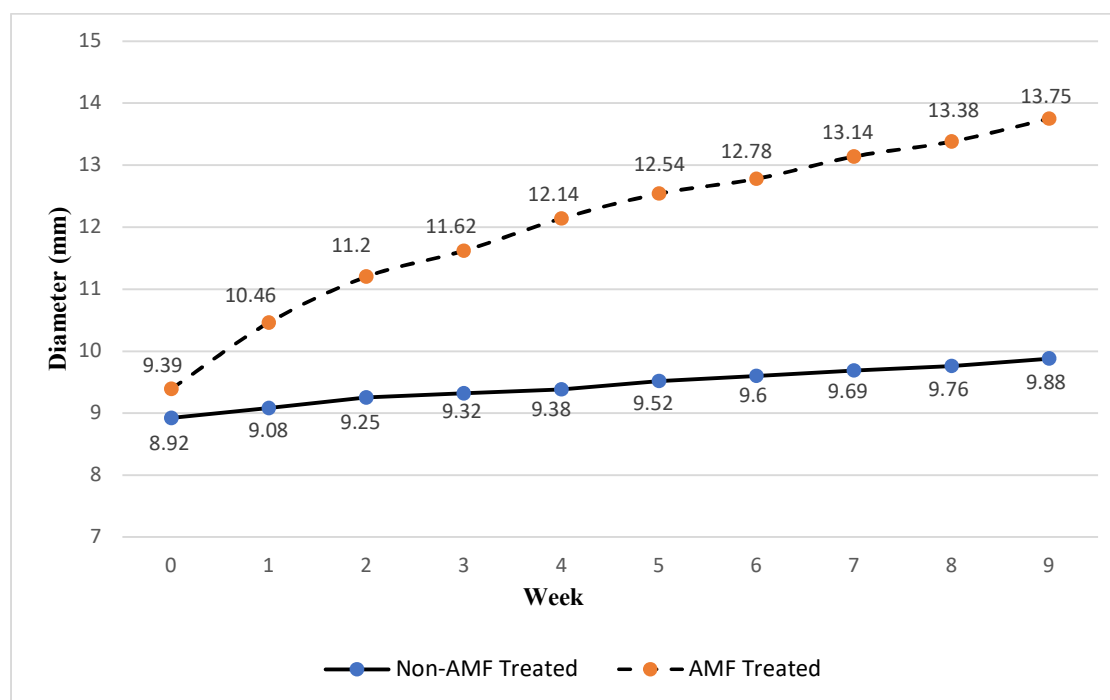
Figure 2. Cumulative diameter growth of *P. motleyi* seedlings

Leaf Number of *P. motleyi* Seedlings

Leaf number of *P. motleyi* seedlings also indicated significant difference between the non-AMF treated and AMF treated seedlings as shown in Figure 3. A decreased in leaf number was observed in non-AMF treated seedlings from 24 leaves during the beginning of the study to only 19 leaves at week 10. This is in contradiction with the number of leaves on AMF treated seedlings which showed an increase in numbers from 33 leaves at week 1 to 56 at week 10. Therefore, AMF treated seedlings has approximately 2 to 3 times more leaves than the non-AMF treated seedlings which were more obvious from week 2 onwards.
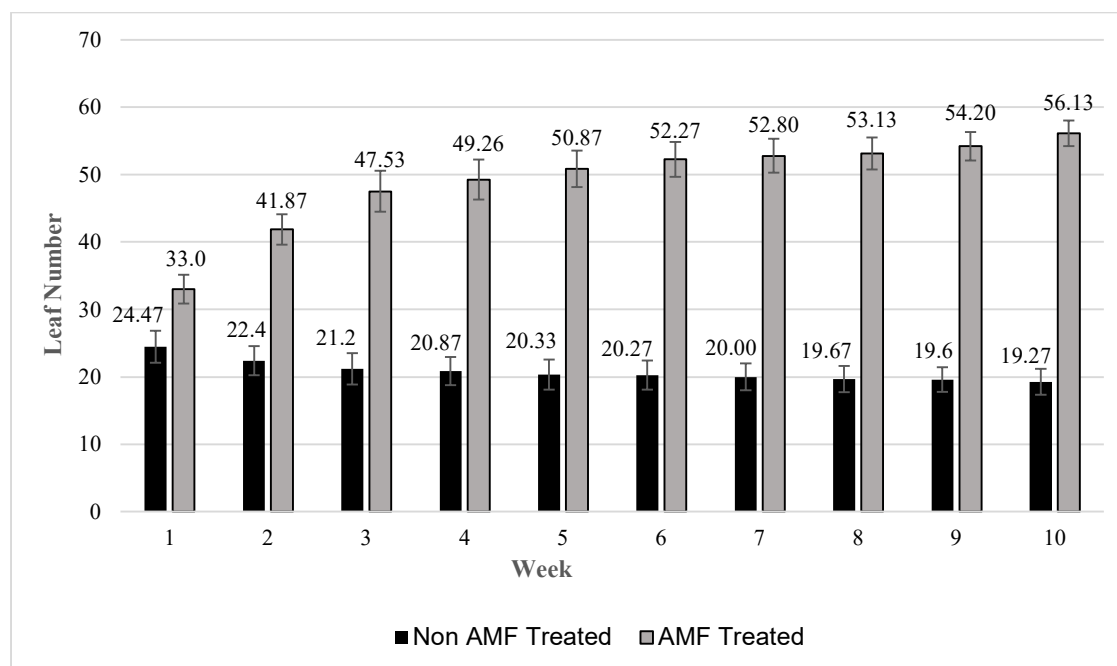
Figure 3. Cumulative leaf number of *P. motley*i seedlings

Root growth and leaf area of AMF and non-AMF treated *P. motleyi* seedlings

Root growth of AMF treated *P. motleyi* seedlings were found better with more fibrous and fine roots as compared to the non-AMF treated seedlings after 10 weeks of transplanting (Figure 4). Besides that, the roots of AMF treated seedlings also looked darker and healthier. Higher leaf number and better leaf area expansion was observed in AMF treated seedlings. The leaf areas for non-AMF treated seedlings ranged from 21.10 cm^2 to 28.1 cm^2 with a mean value of 21.10 cm^2. Meanwhile, the mean leaf area recorded for AMF treated seedlings was 32.43 cm^2 with values ranging from 30.1 cm^2 to 35.1 cm^2.

Figure 4. Comparison of root growth on AMF treated and non-AMF treated seedlings

DISCUSSION

As plants depend much on the root system for its physiological processes such as obtaining water and nutrients, plants need a well-developed root system to survive the harsh environment in the field (Rani *et al.* 2019). A good root system is vital for the survival of the seedlings after transplanting. As the research location involves a waterway which is occasionally affected by temporary flooding, the capability of young *P. motleyi* seedlings to overcome stress during the transplanting activities is an indication on the ability of the seedlings adapting to the new environment. In *Pterocarpus officinalis*, flooding has induced physiological and morphological changes in AMF inoculated seedlings making them more tolerant to flooding (Foughies *et al.*, 2007). Thus, AMF can help in improving soil characteristics and encourage continuous plant development even under stressful environment (Navarro *et al.*, 2014; Alqarawi *et al.*, 2014).

The enhancement of plant growth and budding potential are very important biological processes for rapid growth of plants, as well as improving the survival rate of seedlings (Morgan and Connolly 2013). AMF provides a lot of advantages to plants as young seedlings inoculated with efficient AMF will not only have stronger root system but have superior growth and can better establish themselves in the field (Navarro-Garcia *et al.*, 2011).

AMF treated *P. motleyi* seedlings showed better vegetative growth in terms of plant height and collar diameter increment besides higher shoot, root, and total dry weights similar to the report by Kumar *et al.* (2017) as well as greater leaf length and leaf number by Mathur *et al.* (2016). Chinnathambi *et al.* (2024) reported that mycorrhizal plants showed greater shoot and root dry weight, leaf area and root length than non-mycorrhizal plants. Better growth performances demonstrated by the AMF treated *P. motleyi* seedlings indicated that the application of AMF has helped with the improvement and enhancement of the seedlings' growth rate. However, these findings must be interpreted with caution as this study has its limitations such as the short study duration (only 10-weeks), besides effect of other environmental factors that were not controlled during the data collection.

Plants with thriving mycorrhizal root systems can perform better in comparison to their non-inoculated counterparts (Smith and Smith, 2012). AMF enhances root growth of treated plants and assists plants in water and nutrient uptake (Kim *et al.*, 2017). Better root growth can be observed in AMF inoculated *P. motleyi* seedlings where finer roots, better root spread, and more root hairs can be observed (Morgan and Connolly 2013). Similarly, high flooding tolerance by AMF inoculated *P. officinalis* seedlings was found to be attributed to the production of adventitious roots (Foughies *et al.*, 2007). AMF inoculation dramatically increase root biomass by increasing the number of 1st and 2nd order lateral root, root total length, root surface area and root volume in *Prunes persica* seedling under flooding (Zheng *et al.* 2020). Improvement of plant growth and nutrient accumulation is the effect of AMF inoculation that extends the absorption area to the root system of the host plant (Bourles *et al.*, 2020).

AMF inoculated plants can explore more soil volume for available nutrients and water (Kumar *et al.* 2017). AMF plant roots can significantly improve the access of roots to a large soil surface area through the formation of hyphal network (Bowles *et al.*, 2016). AMF improves plant nutrition acquisition by increasing the availability as well as translocation of various nutrients (Rouphael *et al.*, 2015). The fungal hyphae can help in accelerating the decomposition process of soil organic matter (Paterson *et al.*, 2016) and improves the quality of soil by influencing its structure and texture (Zou *et al.*, 2016; Thirkell *et al.*, 2017). In this study, quantitative root parameters such as root length, surface area, and biomass were not assessed. To strengthen the understanding of the root system's role in influencing nutrient uptake, these factors should be incorporated in future research.

The leaf blade is an important organ particularly for plant photosynthesis, respiration, and transpiration. The leaf size and shape can influence photosynthetic efficiency and are closely related to plant growth potential, nutrient supply, yield, quality, and resistance (Nicotra *et al.*, 2011). In cotton seedlings, AMF supports better nutrient uptake thus promotes good vegetative growth by improving photosynthesis rate, CO_2 concentration, transpiration and

energy use efficiency (Peng *et al*., 2024). AMF also contributes to an increase in chlorophyll a, photosynthetic rate, stomatal conductance, and transpiration rate (Mathur *et al*., 2016) that leads to higher plant photosynthates production and biomass development.

In the present study, AMF treated *P. motleyi* seedlings showed larger leaf area, that may contribute to better light reception by the seedlings' blade, allowing the seedlings to photosynthesize better and produce more food stock through rapid photosynthesis. Plants inoculated with AMF has been known to enhance plant growth as indicated by the increase in leaf area as well as N, P, Ca, and K contents (Balliu *et al*., 2015). According to Begum *et al*. (2019), increased in photosynthetic activities and other leaf functions are directly linked to the uptake of N, P, and carbon that improved growth of AMF inoculated plants.

AMF inoculation provides plenty of advantages to plants particularly to young seedlings (Navarro-Garcia *et al*., 2011). AMF assist plants during the initial growth by enhancing plant growth performances. AMF treatment assists growth promotion not only by improving water and mineral nutrient uptake from the soil but has also been found to safeguard the plants from fungal pathogens (Smith and Read, 2008; Jung *et al*., 2012). Similarly, long term association with AMF is speculated to enhance the survival and establishment of *P. motleyi* seedlings by improving nutrient acquisition, water relations and soil structure thus facilitating successful establishment in waterway rehabilitation.

CONCLUSION

Significant differences were observed between the AMF treated and non-AMF treated seedlings with better growth performance observed from *P. motleyi* seedlings inoculated with AMF. Plant height and collar diameter of AMF treated seedlings observed five times higher values than non-AMF treated seedlings. Leaf number and leaf area also observed similar superior trends while root morphology of AMF treated seedlings were found to be better developed and look heathier.

AMF treatment supports good root growth among *P. motleyi* seedlings. AMF that colonizes

the plant root system, provide better plant growth by increasing nutrient accumulation as the inoculated roots can extend the root absorption area. In addition, AMF inoculation promotes the development of mycorrhizal hyphae that contribute to better soil exploration and nutrient uptake by the root system. Better nutrient uptake by the root system eventually enhances photosynthate production by the leaves contributing to other vegetative growth and biomass accumulation such as diameter, height, and leaf number.

Better growth performance by AMF treated *P. motleyi* seedlings is an indication that inoculated seedlings were stronger and performed better when planted in the open field. The well-developed root system of AMF treated seedlings promotes the establishment of the seedlings in the fields. This study indicates that the inoculation of *P. motleyi* seedlings with AMF can enhance early growth of the seedlings which can be a determining factor in the ability of seedlings to survive the harsh environment such as along waterways which was exposed to direct sunlight and flood.

However, it must be highlighted that this study was conducted within a short period of 10-weeks using a very small sample size thus require caution when interpreting the results. Longer monitoring period with larger sample size may be required to confirm the broader applicability of these findings. Nonetheless, this study still provides some insights into the potentials of using AMF inoculated *P. motleyi* seedlings to rehabilitate disturbed waterways by promoting better early growth when being transplanted in the open field.

REFERENCES

Adnan, M., Zainuddin, A.F., Hamzah, M.A., Moorthy, M. & Mohamad Zaki, M.I. (2018). *Koleksi Pokok Taman Botani Kepong*. Institut Penyelidikan Perhutanan Malaysia (FRIM), Malaysia. 234 p.

Alqarawi, A.A., Abd Allah, E.F. & Hashem, A. (2014). Alleviation of salt-induced adverse impact via mycorrhizal fungi in *Ephedra aphylla* Forssk. *Journal of Plant Interactions*, 9(1): 802-810.

Balliu, A., Sallaku, G. & Rewald, B. (2015). AMF Inoculation enhances growth and improves the

nutrient uptake rates of transplanted, salt-stressed tomato seedlings. *Sustainability*, 7: 15967–15981. DOI: 10.3390/su71215799

Begum, N., Qin, C., Ahanger, M.A., Raza, S., Khan, M.I., Ashraf, M., Ahmed, N. & Zhang, L. (2019). Role of arbuscular Mycorrhizal fungi in plant growth regulation: Implications in abiotic stress tolerance. *Frontiers in Plant Science,* 10:1068. DOI: 10.3389/fpls.2019.01068

Bourles, A., Guentas, L., Charvis, C., Gensous, S., Majorel, C., Crossay, T., Cavaloc, Y., Buret-Sarramegna, V., Jourand, P & Amir, H. (2020). Co-Inoculation with a bacterium and arbuscular mycorrhizal fungi improves root colonization, plant mineral nutrition, and plant growth of a Cyperaceae plant in an ultramafic soil. *Mycorrhiza,* 30: 121–131. DOI: 10.1007/ s00572-019-00929-8

Bowles, T.M., Barrios-Masias, F.H., Carlisle, E.A., Cavagnaro, T.R., and Jackson, L.E. (2016). Effects of arbuscular mycorrhizae on tomato yield, nutrient uptake, water relations, and soil carbon dynamics under deficit irrigation in field conditions. *Science of the Total Environment,* 566: 1223–1234. DOI: 10.1016/j.scitotenv. 2016.05.178.

Browne, F.G. (1955). Forest Trees of Sarawak and Brunei. Government Printer, Kuching, Sarawak. 112 p.

Burgess, P.F. (1966). Timbers of Sabah. Sabah Forest Records No. 6., Forest Department Sabah. pp. 30-32.

Chinnathambi, S., Peeran, M.F., Srinivasan, V., Sankar, S.M. & George, P. (2024). Optimizing mycorrhizal fungi application for improved nutrient uptake, growth, and disease resistance in cardamom seedlings (*Elettaria cardamomum* (L.) Maton). *Heliyon*, 10: e39227.

Dai, M. and Nimasow, O.D. (2024). An investigation on soil-plant-AMF relationships in lateral transitional zones of a Riverine Island. *Journal of Bioresources*, 11: 77-83.

Dufour, S. & Piégay, H. (2019). From the myth of a lost paradise to targeted river restoration: Forget natural references and focus on human benefits. *River Research and Applications*, 25: 568-581.

Fougnies, L, Renciot, S., Muller, F., Plenchette, C., Prin, Y., de Faria, S.M., Bouvet, J.M., Sylla, S. Nd., Dreyfun, B. & Bâ, A.M. (2007). Arbuscular mycorrhizal colonization and nodulation improve

flooding tolerance in *Pterocarpus officinalis* Jacq. seedlings. *Mycorrhiza,* 17: 159-166.

Hartmond, U., Schaesberg, N.V., Graham, J.H. & Syvertsen, J.P. (1987). Salinity and flooding stress effects on mycorrhizal and nonmycorrhizal citrus rootstock seedlings. *Plant and Soil*, 104: 37-43.

Heyne, K. (1987). *Tumbuhan Berguna Indonesia. Jilid II*. Jakarta: Badan Litbang Kehutanan. pp. 1233-1244.

Jia, W., Ma, M., Chen, J. & Wu, S. (2021). Plant morphological, physiological and anatomical adaptation to flooding stress and the underlying molecular mechanisms. *International Journal of Molecular Sciences*, 22: 1088.

Jung, S.C., Martinez Medina, A., Lopez-Raez, J.A. & Pozo, M.J. (2012). Mycorrhiza-induced resistance and priming of plant defences. *Journal of Chemical Ecology*, 38: 651-664. DOI: 10.1007/s10886-012-0134-6

Kim, S.J., Eo, J.K., Lee, E.H., Park, H. & Eom, A.H. (2017). Effects of arbuscular mycorrhizal fungi and soil conditions on crop plant growth. *Mycobiology*, 45(1): 20-24.

Kochummen, K.M. (1989). Anacardiaceae. In: Ng, F.S.P. (ed.). *Tree Flora of Malaya*, Vol. 4. Longman Malaysia, Petaling Jaya, Malaysia. pp. 9-57.

Kumar, A., Gupta, A., Aggarwal, A., Singh, J.P. & Parkash, V. (2021). Ethno-medicinal and AMF diversity conservation aspects of some weeds of Himachal Pradesh, India. *Journal of Research in Weed Science*, 4(1): 43-56.

Lim, T.K. (2012). *Edible Medicinal and Non-Medicinal Plants*, Vol. 1. Dordrecht, The Netherlands: Springer. pp. 656-687.

Lin, Y., Ye, Y., Wu, C. & Shi, H. (2020). Changes in microbial structure under land consolidation in paddy soils: A case study in eastern China. *Ecological Engineering,* 145: 105696.

Mathur, S., Sharma, M.P. and Jajoo, A. (2016). Improved photosynthetic efficacy of maize *Zea mays* plants with arbuscular mycorrhizal fungi (AMF) under high temperature stress. *Journal of Photochemistry and Photobiology B: Biology*, 180: 149-154. DOI: 10.1016/j. jphotobiol.2018.02.002.

Miller, S.P. & Sharitz R.R. (2000). Manipulation of flooding and arbuscular mycorrhiza formation

influences growth and nutrition of two semi-aquatic grass species. *Functional Ecology*, 14: 738-748

Morgan, J.B. & Connolly, E.L. (2013). Plant-soil interactions: Nutrient uptake. *Nature Education Knowledge*, 4(8): 2.

Navarro-Garcia, A., Del Pilar Banon Arias, S., Morte, A. & Snachez-Blanco, M.J. (2011). Effects of nursery preconditioning through mycorrhizal inoculation and drought in *Arbutus unedo* L. plants. *Mycorrhiza*, 21: 53-64.

Neto, D., Carvalho, L.M., Cruz, C. & Martin-Louçao, M.A. (2006). How do mycorrhizas affect C and N relationships in flooded *Aster tripolium* plants? *Plant and Soil*, 279: 51–63.

Nicotra, A.B., Leigh, A., Boyce, C.K., Jones, C.S., Niklas, K.J., Royer, D.L. & Tsukaya, H. (2011). The evolution and functional significance of leaf shape in the angiosperms. *Functional Plant Biology*, 38(7): 535-552. DOI: 10.1071/FP11057

Paterson, E., Sim, A., Davidson, J. & Daniell, T.J. (2016). Arbuscular mycorrhizal hyphae promote priming of native soil organic matter mineralization. *Plant and Soil*. 408: 243-254. DOI: 10.1007/s11104-016-2928-8

Peng, Z., Zulfiqar, T., Yang, H., Wang, M. & Zhang, F. (2024). Effect of Arbuscular mycorrhizal fungi (AMF) on photosynthetic characteristics of cotton seedlings under saline-alkali stress. *Scientific Reports*. 14: 8633.

Rani, A., Kumar, N., Ram, A., Dev, I., Uthappa, A.R., Shukla, A. & Parveen, S. (2019). Effect of growing media and arbuscular mycorrhiza fungi on seedling growth of Leucaena leucocephala (Lam.) de Wit. *Indian Journal of Agroforestry*, 21(2): 22-28.

Ring, E., Andersson, E., Armolaitis, K., Eklöf, K., Finér, L., Gil, W., Glazko, Z., Janek, M., Lībieté, Z., Lode, E., Małek, S. & Piirainen, S. (2018). *WAMBAF - Good Practices for Forest Buffers to Improve Surface Water Quality in the Baltic Sea Region*. http://urn.fi/URN:ISBN:978-952-326-576-9. Downloaded on 10 June 2022.

Rouphael, Y., Franken, P., Schneider, C., Schwarz, D., Giovannetti, M. & Agnolucci, M. (2015). Arbuscular mycorrhizal fungi act as bio-stimulants in horticultural crops. *Scientia Horticulturae*, 196: 91–108. DOI: 10.1016/j.scienta.2015.09.002.

Smith, S. & Read, D. (2008). *Mycorrhiza Symbiosis*. Third Edition. San Diego, California: Academic Press.

Smith, S.E. & Smith, F.A. (2012). Fresh perspectives on the roles of arbuscular mycorrhizal fungi in plant nutrition and growth. *Mycologia*, 104: 1–13.

Thirkell, T. J., Charters, M. D., Elliott, A. J., Sait, S. M. & Field, K. J. (2017). Are mycorrhizal fungi our sustainable saviours? Considerations for achieving food security. *Journal of Ecology*, 105: 921–929. DOI: 10.1111/1365-2745.12788.

van der Maarel, E. & Franklin, J. (Eds) (2013). *Vegetation Ecology: Historical notes and outline*. pp. 1-27. DOI:10.1002/9781118452592

Wiart, C. (2006). *Medicinal Plants of Asia and the Pacific*. CRC Press, Boca Raton. pp.177-182.

Wong, T.M. (1975). *Wood Structure of the Lesser-Known Timbers of Peninsular Malaysia*. Malayan Forest Records No. 28. Forest Research Institute Malaysia, Kepong, Kuala Lumpur. 115 p.

Yusro, F. (2011). Aktivitas anti rayap tanah (*Coptotermes curvignathus* Holmgren) tiga fraksi ekstrak kayu pelanjau (*Pentaspadon motleyi* Hook. f). *Jurnal Wana Tropika*, 1(2): 42-50.

Zheng, F-L., Liang, S-M., Chu, X-N., Yang, Y.L. & Wu, Q.S. (2020). Mycorrhizal fungi enhance flooding tolerance of peach through inducing proline accumulation and improving root architecture. *Plant, Soil and Environment*, 66: 624-631.

Zou, Y.N., Srivastava, A.K. & Wu, Q.S. (2016). Glomalin: a potential soil conditioner for perennial fruits. *International Journal of Agriculture and Biology*, 18, 293–297. DOI: 10.17957/ IJAB/15.0085.

Modelling of Schiff Base Vanillin Derivatives Targeting *Streptococcus Pneumoniae* Bacterial Neuraminidase

WOON YI LAW* & MOHD RAZIP ASARUDDIN

Department of Chemistry, Faculty of Resource Science and Technology, Universiti Malaysia Sarawak, 94300 Kota Samarahan, Sarawak, Malaysia
*Corresponding author: mendah_wylaw@hotmail.com

ABSTRACT

Streptococcus pneumoniae is a pathogenic bacterium which has led to serious pneumococcal infections. Despite the fact that efficient therapeutic agents and vaccinations are available for the treatment of *Streptococcus pneumoniae* infections, more strains of *Streptococcus pneumoniae* have acquired significant resistance towards the available antibiotics. The neuraminidase of *Streptococcus pneumoniae* possess significant contribution in pathogenesis, aiding the release and spread of virus. Simultaneously, Schiff base vanillin derivatives were reported in past literature for their great deal of potential as inhibitors of influenza virus neuraminidase. Hence, the research aims to evaluate the inhibitory activity of Schiff base vanillin derivatives against *Streptococcus pneumoniae* neuraminidase via ligand-based pharmacophore modelling and structure-based molecular docking using LigandScout 4.4.9 and AutoDock 4.2. Ligand-based pharmacophore modelling was performed to analyse the anti-neuraminidase activity of Schiff base vanillin derivatives based on their pharmacophore fit values and matching pharmacophore features with a pharmacophore model, generated from a list of training sets, which are reported drugs against *Streptococcus pneumoniae* neuraminidase. In structure-based molecular docking, the Schiff base vanillin derivatives were evaluated based on their docking performances with the active sites of the crystal structure of PDB:2YA8. Evaluations were based on their pharmacophore scores, binding affinity and matching interactions with the inhibitory ligand of 2YA8. 20 out of 21 Schiff base vanillin derivatives successfully show good results in ligand-based pharmacophore modelling, as well as satisfying docking performances in structure-based molecular docking. Furthermore, they also fulfill the Lipinski's Rule of 5, thus displaying appreciable potential as inhibitors of *Streptococcus pneumoniae* neuraminidase.

Keywords: Molecular docking, neuraminidase, pharmacophore modelling, Schiff base vanillin derivatives, *Streptococcus pneumoniae*

INTRODUCTION

Pneumococcal infections are any infections caused by the bacteria *Streptococcus pneumoniae*, also known as pneumococcus, as shown in Figure 1. The bacteria commonly reside in the human upper respiratory tract, nasal cavity and sinuses (World Health Organization, 2022). As a pathogenic bacterium, it has cause significant morbidity and mortality all over the world, especially among the children and elder people in developing areas (Lv *et al*., 2020). *Streptococcus pneumoniae* is alpha-hemolytic, which means that it is able to produce hydrogen peroxide (H_2O_2) which oxidizes hemoglobin within the erythrocytes. The presence of H_2O_2 may lead to destruction of DNA and apoptosis of lung cells (Oliver, 2019). On top of that, for inhabiting human nasopharynx asymptomatically, it has led to numerous invasive pneumococcal infections, such as pneumonia, meningitis, otitis media and bacteremia (Nguyen & Bhattacharya, 2022). The infections were responsible for at least 1-2 million infant deaths all over the world (Bogaert *et al*., 2004), and before the development and availability of antibiotics, about 95% of the cases of pneumonia were caused by *Streptococcus pneumoniae* (Dion & Ashurst, 2022).

Figure 1. *Streptococcus pneumoniae* (Oliver, 2019)

Pneumococcal infections can affect all age groups, but children younger than 2 years old and senior citizens who are 65 years old and above possess a higher risk of infection (European Centre for Disease Prevention and Control, 2023). Apart from that, patients with health conditions that may lead to immune deficits such as diabetes mellitus and HIV infections, as well as health conditions associated with decreased pulmonary clearance functions such as asthma, chronic bronchitis, or chronic obstructive pulmonary disease are also at higher risk (Iyer & Perloff, 2023). There are many *Streptococcus pneumoniae* serotypes being discovered, however only a few of them are responsible for most of the serious and invasive infections (European Centre for Disease Prevention and Control, 2023). Based on the epidemiological surveillance of *Streptococcus pneumoniae* infections within the Malaysian population carried out by the Bacteriology Division of the Institute for Medical Research (IMR) from 1994 to 1995, out of 273 *Streptococcus pneumoniae* isolations from different clinical samples, most of them belong to only 5 serotypes, which were serotypes 1, 6B, 19B, 19F and 23F (Rohani *et al*., 1999). Back then in the 1990s, *Haemophilus influenzae* type b vaccine successfully decreases the invasive Hib infections in most of the European countries, but on the other hand causing *Streptococcus pneumoniae* to become the leading outbreak of meningitis and sepsis among children (European Centre for Disease Prevention and Control, 2023). Thereupon, vaccines for pneumococcal infections have been developed to overcome the situation. The introduction of 7-valent Pneumococcal Conjugate Vaccine (PCV 7) has successfully altered the epidemiology of pneumococcal infections in many countries, in which pneumococcal infections had decrease by 94% in the United States (European Centre for Disease Prevention and Control, 2023). Other pneumococcal conjugate vaccines include PCV13, PCV15, and PCV20, as well as pneumococcal polysaccharide vaccine (PPSV23) (Centers for Disease Control and Prevention, 2023). Antibiotics have been prescribed as the main treatment for *Streptococcus pneumoniae* infections. The commonly used antibiotics include penicillin, macrolides, clindamycin, cephalosporin, rifampin, vancomycin, and trimethoprim-sulfamethoxazole, which were utilized until the 70s (Iyer & Perloff, 2023). Other than that, amoxicillin is given to patients with pneumonia, otitis media and sinusitis (Musher, 2019). Despite significant studies, developments and availability of effective therapeutic agents and vaccines, the mortality rate has remained high due to the increasing number of strains that are resistant to the available antibiotics which complicates the medications (Lv *et al*., 2020). Due to antibiotic abusage in hospitals, multidrug-resistant and vancomycin-resistant strains have drastically increased, with 15 - 30% of the pneumococcal strains being multi-drug resistant (Li *et al*., 2009). It was reported by Centers of Disease Control and Prevention (CDC) that up to 40% of the pneumococcal infections until 2000 were due to resistance of pneumococcal bacteria to at least one type of antibiotic (Centers for Disease Control and Prevention, 2024). For the increasing emergence of antibiotic-resistance *Streptococcus pneumoniae* isolates, the greater increase of more serious and risky complications may be a possible concern in the future.

Streptococcus pneumoniae possesses a number of virulence factors which plays an important role in infection, which are capsules, pneumolysin, sortase A, pneumococcal surface protein A, hyaluronidase and neuraminidase (Maragakis *et al*., 2008). A great deal of research was performed to discover and develop drugs, natural compounds or novel compounds based on their inhibitory activity against these proteases. For instance, quercetin, polyhydroxy flavonoid compound which is found in the leaves, fruits and flowers of plants, was found out to be able to inhibit pneumolysin via hemolysis assay and oligomerization assay (Nguyen & Bhattacharya, 2022). Interestingly, honeys from Malaysia origin were found out to be able to inhibit hyaluronidase of *Streptococcus pneumoniae*, with honeys from Kelulut to be reported for its highest inhibitory activity against hyaluronidase (Nayian & Yusof, 2020). Other than inhibiting the proteases, another research reported the *in silico* discovery of 6 novel compounds, 1 from imidazole analogue, 4 from furan derivatives and 1 from thiophene derivative, being able to inhibit the histidine kinase (HK) VicK protein, which is important for the growth of bacterium (Li *et al*., 2009).

Neuraminidase A of *Streptococcus pneumoniae*, NanA, played an imperative role by catalyzing the release and removal of terminal sialic acid residues from cell membrane glycostructures, hence decreasing the binding of complement regulator factor H to cell surfaces (Parker *et al*., 2009; Syed *et al*., 2019). There were three homologous neuraminidase encoded: NanA, NanB and NanC, based on different sequence of amino acids, choice of substrates and types of reactions. The specific roles of the three neuraminidases were still not completely discovered, however, NanA was confirmed for its significant importance in pathogenesis (Sharapova *et al*., 2018). Nonetheless, research related to the findings of drugs or inhibitors against *Streptococcus pneumoniae* neuraminidase were very limited and inadequate. This is because most of the research related to the search of *Streptococcus pneumoniae* neuraminidase were at the early stages of study, such as the search of prenylated flavonoids against neuraminidase of both influenza virus and *Streptococcus pneumoniae* (Grienke *et al*., 2016). Additionally, most of the research focuses on the study of influenza virus neuraminidase inhibitors. Chlorogenic acid was reported to show strong inhibitory activity against neuraminidase of influenza virus, but inhibitory activity against neuraminidase of *Streptococcus pneumoniae* was still considered limited (Guan *et al*., 2020). Hence, it has been a great interest and potential in research of development and findings of compounds that possess inhibitory activity against neuraminidase of *Streptococcus pneumoniae*.

Schiff base vanillin derivatives are compounds derived from the Schiff base synthesis reaction between vanillin and primary amines. Previously, a research has reported that neuraminidase of influenza virus was able to be inhibited by Schiff base vanillin derivatives, compounds derived from the Schiff base synthesis mechanism between vanillin and primary amines, by *in silico* pharmacophore modelling, virtual screening and molecular docking, as well as via 2′-(4-Methylumbelliferyl)-α-D-N-acetylneuraminic acid (MUNANA) assay (Asaruddin, 2016). This raises a great interest and potential as the viral neuraminidase and bacterial neuraminidase play the same role by cleaving sialic acid residues from cell surfaces and facilitates the release and spread of virus from infected cells (Benton *et al*., 2017). Thereupon, the research focuses on the inhibitory activity of Schiff base vanillin derivatives against neuraminidase of *Streptococcus pneumoniae*. This study is done by performing *in silico* screenings, which include ligand-based pharmacophore modellings and structure-based molecular dockings.

MATERIALS & METHODS
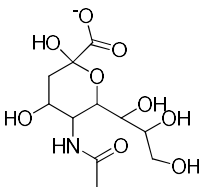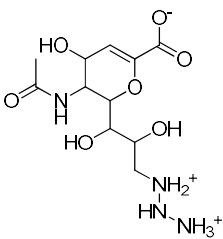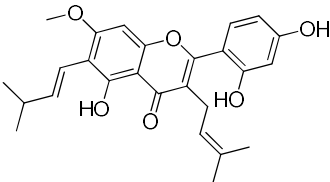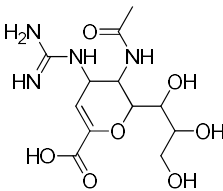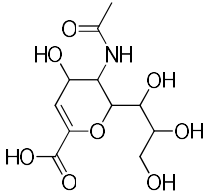
Pharmacophore Model Preparation

Preparation of pharmacophore model was done by using LigandScout 4.4.9 software. A list of chemical compounds with diverse chemical structures that were reported for their inhibitory activity against neuraminidase of *Streptococcus pneumoniae* were selected as training sets to generate a pharmacophore model for the evaluation of Schiff base vanillin derivatives as inhibitors of *Streptococcus pneumoniae* neuraminidase. The chemical structures of the training sets were initially drawn by using ChemDraw Ultra 12.0 and downloaded in the MDL-mol file formats. The training sets include zanamivir (Gut *et al*., 2011), atorcarpin (Walther *et al*., 2015), DANA (2-deoxy-2,3-dehydro-N-

acetyl-neuraminic acid) (Owen *et al.*, 2015), NANA (N-acetyl-alpha-neuraminic acid) (Hsiao *et al.*, 2009) and 9N3Neu5Ac2e (5-acetamido-2,6-anhydro-3,5,9-trideoxy-9-triazan-1-yl-D-glycero-D-galacto-non-2-enonic acid). They were later imported into the ligand-based perspective of LigandScout 4.4.9. Table 1. shows the chemical structures of training sets used to generate pharmacophore model.

Table 1. Chemical structures of training sets used to generate pharmacophore model

Name of training sets	Chemical structures
NANA (N-acetyl-alpha-neuraminic acid)	
9N3Neu5Ac2e (5-acetamido-2,6-anhydro-3,5,9-trideoxy-9-triazan-1-yl-D-glycero-D-galacto-non-2-enonic acid)	
Artocarpin	
Zanamivir	
DANA (2-deoxy-2,3-dehydro-N-acetyl-neuraminic acid)	

Based on Table 1, NANA, DANA and 9N3Neu5Ac2e are sialic acid residues, zanamivir is a synthetic neuraminidase inhibitor, whereas artocarpin is a natural isoprenylated flavone. Due to their diverse chemical structures and different nature, they were able to generate a good pharmacophore model which account for different binding interactions with the neuraminidase of *Streptococcus pneumoniae*.
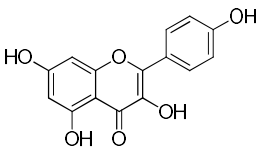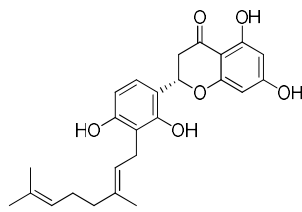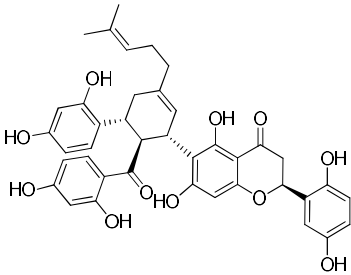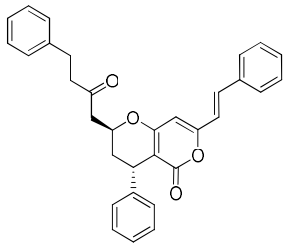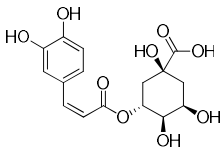
The generated pharmacophore model is validated for its reliability by analysis with a list of test sets. Therefore, a list of chemical compounds from natural products which were previously reported to exhibit inhibitory activity

against *Streptococcus pneumoniae* neuraminidase were selected as test sets to perform such validation. The 2D structure of the chemical structures of the test sets were also drawn by using ChemDraw Ultra 12.0, downloaded in the MDL-mol file format and imported into the ligand-based perspective of LigandScout 4.4.9 together with the list of training sets. Due to limited studies, the natural products available to be selected as test sets in literature review were also limited. Based on literature study, the test sets that were reported for their strong and affirm inhibitory activity against *Streptococcus pneumoniae* neuraminidase include kaempferol (Xu *et al*., 2023), Sanggenol A, Sanggenon G (Grienke *et al*., 2016), Katsumadain A (Walther *et al*., 2015) and chlorogenic acid (Guan *et al*., 2020), with chemical structures as depicted in Table 2. Not only due to the reported literature review, the test sets were all greatly diverse chemical structures among themselves and in comparison with training sets. This provides further fundamental support to confirm the reliability of the generated pharmacophore model due to their different chemical properties.

Table 2. Chemical structures of test sets to validate the reliability of generated pharmacophore model

Name of test sets	Chemical structures
Kaempferol	
Sanggenol A	
Sanggenon G	
Katsumadain A	
Chlorogenic acid	

When all MDL-mol files of training and test sets were imported, the MMFF94 energy of the chemical structures were minimised to reach the closest local minimum. Conformations of the ligand sets were generated by using the FAST settings, and the ligand sets were clustered based on pharmacophore RDF-code similarity and average cluster distance calculation. Subsequently, ligand-based pharmacophore modelling was run based on pharmacophore fit scoring function, and the pharmacophore model was generated based on merged pharmacophore feature. The evaluation of the generated model was based on matching pharmacophore features, model scores and pharmacophore fit values depicted by training sets and test sets. If the test sets were able to depict more than half of the matching features and fit values of the training sets, then the generated pharmacophore model is said to be reliable for evaluation of potential inhibitory activity against *Streptococcus pneumoniae* neuraminidase. Additionally, the root mean square deviation (RMSD) values of

the test sets in alignment with the pharmacophore model, as well as their cosine similarities were also evaluated to further validate the reliability of the generated pharmacophore model.

Ligand-based Pharmacophore Modelling of Schiff Base Vanillin Derivatives

A total of 21 Schiff base vanillin derivatives were selected to be evaluated for their inhibitory activity against *Streptococcus pneumoniae* neuraminidase. The chemical structures of these compounds were drawn using ChemDraw Ultra 12.0, downloaded in the MDL-mol file format and imported as test sets in the generated pharmacophore model. The general synthetic route of Schiff base vanillin derivatives was as illustrated in Figure 2.

The chemical structures of the primary amines and the Schiff base vanillin derivatives are as shown in Table 3.
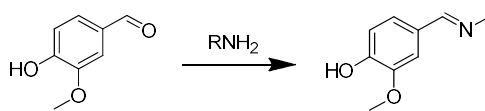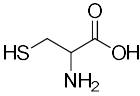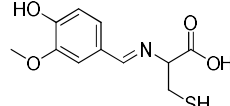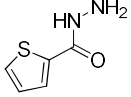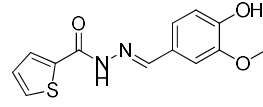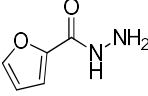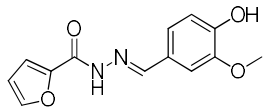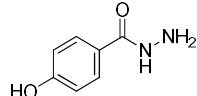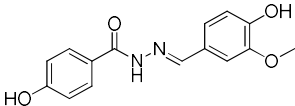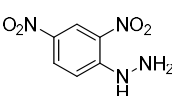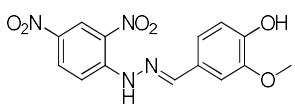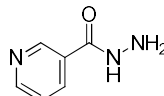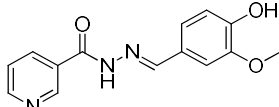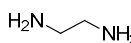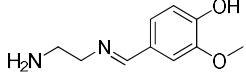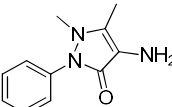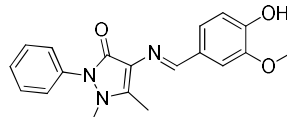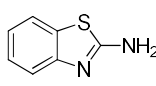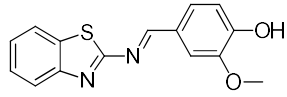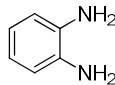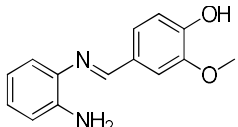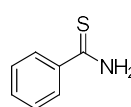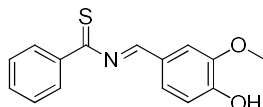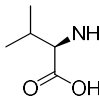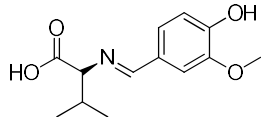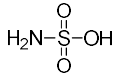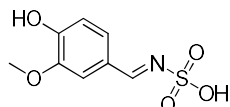
Figure 2. General synthetic route of Schiff base vanillin derivatives

Table 3. Chemical structures of primary amines and resulting Schiff base vanillin derivatives

Name of primary amines	Chemical structures of primary amine	Schiff base vanillin derivatives
(1) Salicyl hydrazide		
(2) Serine		
(3) Hydrazide hydrate		
(4) Phenylhydrazine		

(5) Cysteine		
(6) 2-thiophene carboxylic acid hydrazide		
(7) 2-furoic acid hydrazide		
(8) 4-hydroxybenzhydrazide		
(9) 2,4-dinitrophenylhydrazine		
(10) Nicotinic hydrazide		
(11) Ethylenediamine		
(12) 4-aminoantipyrine		
(13) 2-aminobenzothiazole		
(14) O-phenyldiamine		
(15) Thiobenzamide		
(16) L-valine		
(17) Sulfamic acid		

(18) Benzamide

(19) Benzophenone hydrazone

(20) Aniline

(21) Isonicotinic acid hydrazide
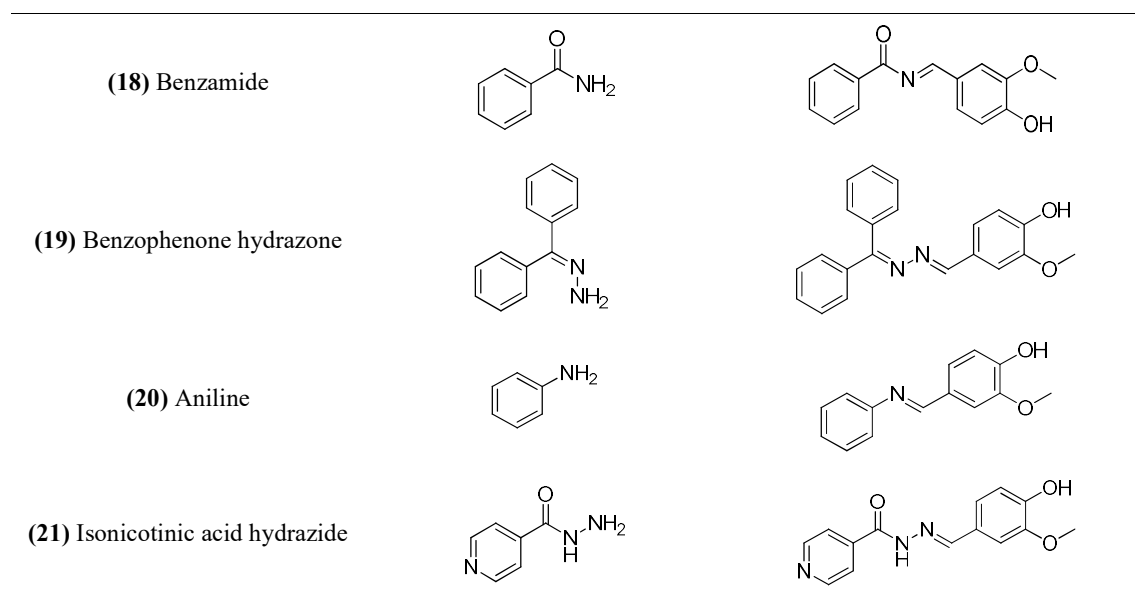
After the import of Schiff base vanillin derivatives as test sets, similarly, MMFF94 energies of all datasets were minimised. Conformations of the ligand sets were generated, and the ligand sets were clustered based on pharmacophore RDF-code similarity and average cluster distance calculation. Ligand-based pharmacophore modelling was run and the Schiff base vanillin derivatives were analysed for their potential inhibitory activity against *Streptococcus pneumoniae* neuraminidase based on their matching pharmacophore features and fit values with the generated pharmacophore model. Schiff base vanillin derivatives that were able to depict satisfied results in ligand-based pharmacophore modelling were later subjected to structure-based molecular docking for further assessment.

Molecular Docking

The crystal structure of *Streptococcus pneumoniae* neuraminidase A, NanA (TIGR4) in complex with oseltamivir carboxylate (PDB code: 2YA8), as shown in Figure 3., was first retrieved from Protein Data Bank (PDB), and imported into the structure-based perspective of LigandScout 4.4.9. The oseltamivir carboxylate is the inhibitory ligand in the active site of the crystal structure as shown in Figure 4. and Figure 5., which possess inhibitory activity against *Streptococcus pneumoniae* neuraminidase. Hence, the Schiff base vanillin derivatives were evaluated based on their alignment with the pharmacophore model of the oseltamivir carboxylate ligand, as well as the protein-ligand interaction in the active site *via* molecular docking of the vanillin derivatives in the active site of 2YA8.
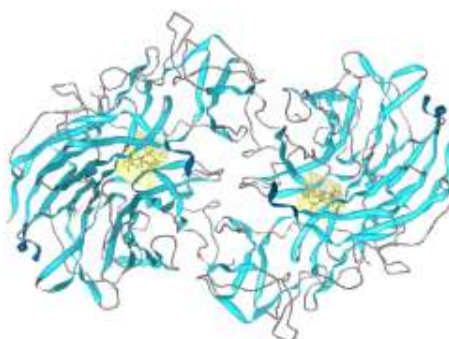
Figure 3. Crystal structure of *Streptococcus pneumoniae* neuraminidase A in complex with oseltamivir carboxylate (2YA8)

Figure 4. Pharmacophore model of the ligand, oseltamivir carboxylate in the active site of 2YA8
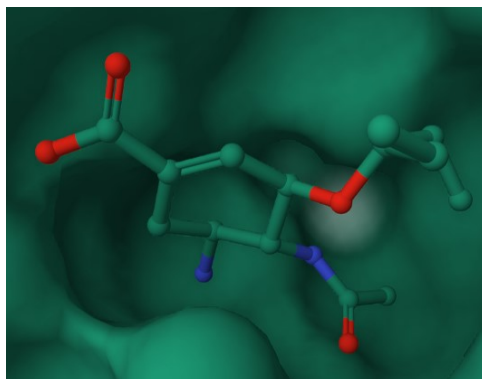
Figure 5. Illustration of oseltamivir carboxylate ligand in the active site of 2YA8

All Schiff base vanillin derivatives were first converted to the MDL-sdf file formats by using Open Babel GUI 2.3.1. They were imported one at a time into the alignment perspective of LigandScout 4.4.9 together with the pharmacophore model and ligand structure of oseltamivir carboxylate. In the alignment perspective, beginning from the first Schiff base vanillin derivative, alignment was performed to oseltamivir carboxylate. Upon successful alignments, common pharmacophore features between both chemical structures were analysed as shown in Figure 6, depicted by the orange spots.
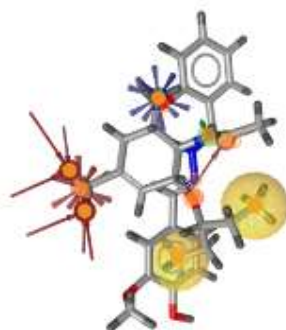
Figure 6. Successful alignment between Schiff base vanillin derivative and oseltamivir carboxylate

Based on the common features shared between the two structures, a shared pharmacophore model was generated, and the pharmacophores were merged, followed by interpolation of overlapping features. All ligands and pharmacophore models were injected into the active site of 2YA8. Interactions shown by the Schiff base vanillin derivatives towards the active site of 2YA8 were analysed and compared with the oseltamivir carboxylate ligand, with an example as depicted in Figure 7.
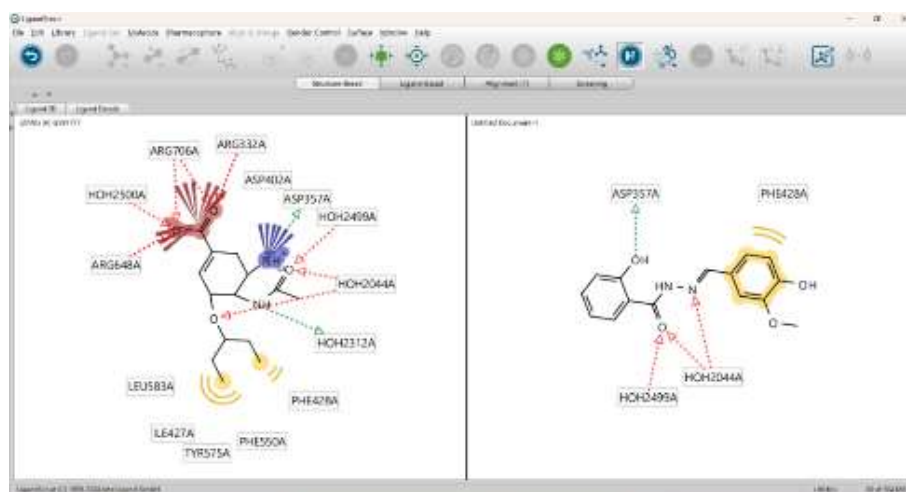
Figure 7. Interactions depicted by the vanillin derivative in the active site of 2YA8 in comparison with oseltamivir carboxylate ligand

The binding affinities of all Schiff base vanillin derivatives were determined by docking using AutoDock 4.2. Schiff base vanillin derivatives that successfully show good alignment with the oseltamivir carboxylate ligand, interactions with the active site of 2YA8, as well as good binding affinity and pharmacophore scores were recorded.

Druglikeness Evaluation

Schiff base vanillin derivatives that successfully showed good results in ligand-based pharmacophore modelling and structure-based molecular docking were evaluated for their druglikeness properties based on Lipinski's Rule of 5 (RO5). The vanillin derivatives were considered potential orally active drugs if they possess not more than 5 hydrogen bond donors (HBD) (nitrogen-hydrogen and oxygen-hydrogen bonds), not more than 10 hydrogen bond acceptors (HBA) (nitrogen and oxygen atoms), molecular weight less than 500 g/mol and partition coefficient log P not greater than 5 (Benet *et al*., 2016).

RESULTS & DISCUSSION

Generation and Validation of Pharmacophore Model in Ligand-based Pharmacophore Modelling

A pharmacophore model was successfully generated by the 5 training sets. The training sets depicted pharmacophore fit values ranging from 74.09 to 98.79 in the generated model, which is considerably high. The model is made up of 10 common pharmacophore features, which is composed of 5 hydrogen bond acceptors (HBA) and 5 hydrogen bond donors (HBD). The generated model is as illustrated in Figure 8.
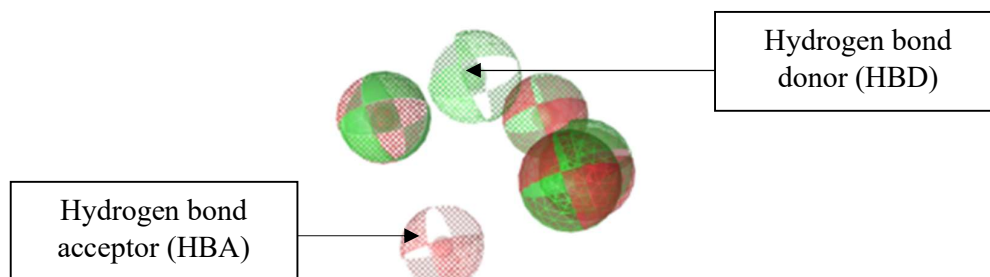
Figure 8. Generated pharmacophore model by training sets

Upon validation of the model by test sets, all test sets successfully depict good pharmacophore fit values in the generated model, ranging from 46.79 to 90.43, which is more than half of the fit values shown by training sets. On top of that, out of the 10 common pharmacophore features, the test sets were able to show good alignment with 4 to 9 features, thus

depicting satisfying matching alignment. On top of that, chlorogenic acid, sanggenol A and sanggenon G even showed pharmacophore fit values higher than a few training sets, depicting good matching result. Katsumadain A showed lower pharmacophore fit values than the rest of the test sets, which may be due the lack of hydroxyl groups compared to other test sets, as well as larger chemical structure which may not fit in the pharmacophore model well.

On top of that, the RMSD value further affirm the reliability of the pharmacophore model. Theoretically, an RMSD value less than 2 Å is considerably good, but the lower the RMSD value, the better the agreement of the pharmacophore model with the actual binding pose (Al-Shar'i & Musleh, 2020). It was concluded that all 5 test sets were able to show RMSD value less than 1.5 Å. This provides further fundamental support to the validation of the reliability of the pharmacophore model.

Cosine similarity is a mathematical method utilized to measure the similarity values between two vectors. By measuring the similarity values between a pharmacophore model and the pharmacophore features of the test sets, the reliability of the pharmacophore model can be further affirmed. Based on the values ranging from -1 to 1, cosine similarities from 0 to 1 indicate strong similarity between the pharmacophore model and the test sets (Neela & Peram, 2025). Cosine similarities were calculated by using the formula, Eq. (1) as shown:

$$\text{Cosine similarity} = \cos\theta = \frac{A \cdot B}{\|A\| \cdot \|B\|} \quad \text{Eq. (1)}$$

where $A \cdot B$ = Dot product of vectors A and B
  A = magnitude of vector A (pharmacophore model)
  B = magnitude of vector B (test set)

By calculating cosine similarities with pharmacophore vector of [5, 5, 0, 0, 0] due to 5 HBA and 5 HBD in the model, all 5 test sets were able to show cosine similarity values in between 0 and 1, showing strong similarity with the pharmacophore model. This further validate the reliability of the generated pharmacophore model.

As a whole, the generated pharmacophore model was said to be validated for its reliability as model for evaluation of Schiff base vanillin derivatives as potential inhibitors against neuraminidase of *Streptococcus pneumoniae*. The overall matching features and pharmacophore fit values of training and test sets in the model were shown in Table 4. The matching features shown by respective functional groups of the chemical structures of Schiff base vanillin derivatives were shown in Table 5, the RMSD-based evaluation of test sets alignment to the pharmacophore model was shown in Table 6, whereas the cosine similarities of test sets and the pharmacophore model was as illustrated in Table 7.

Table 4. Matching features and pharmacophore fit values of training sets and test sets in the pharmacophore model, and RMSD values of test sets

Training sets / Test sets	Matching features	Pharmacophore fit values
NANA	🟥🟥🟥🟥🟥🟩🟩🟩🟩	98.59
9N3Neu5Ac2e	🟥🟥🟥🟥🟥🟩🟩🟩🟩	90.28
Artocarpin	🟥🟥🟥🟥🟥 🟩🟩	74.09
Zanamivir	🟥🟥🟥🟥🟥🟩🟩🟩🟩	98.27
DANA	🟥🟥🟥🟥🟥🟩🟩🟩🟩	98.79
Kaempferol	🟥🟥 🟥🟥🟩🟩🟩	72.02
Sanggenol A	🟥🟥🟥🟥🟥🟩🟩🟩	82.28
Sanggenon G	🟥🟥🟥🟥🟥🟩🟩🟩	82.65
Katsumadain A	🟥🟥🟥🟥	46.79
Chlorogenic acid	🟥🟥🟥🟥🟥🟩🟩🟩 🟩	90.43

Table 5. Matching features shown by respective functional groups of Schiff base vanillin derivatives
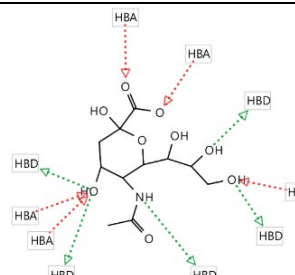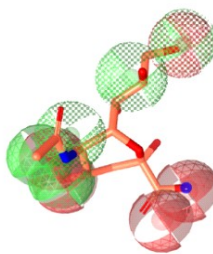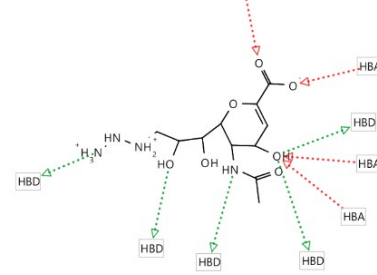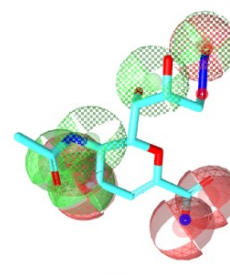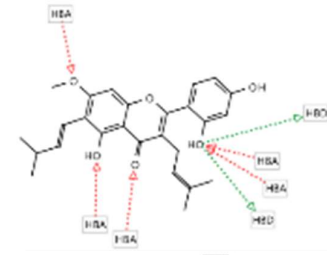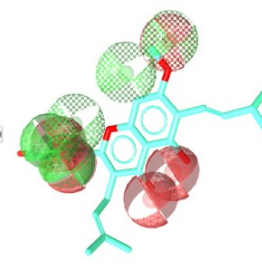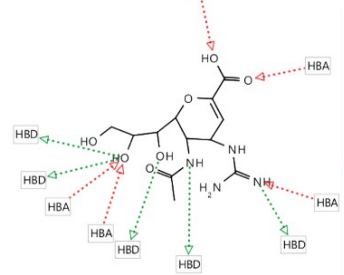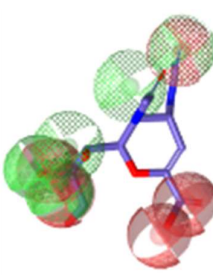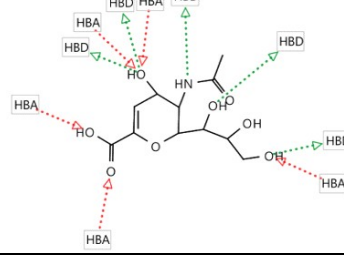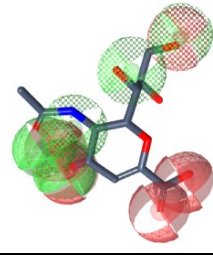
Training sets	Matching features
Test sets	
NANA	
9N3Neu5Ac2e	
Artocarpin	
Zanamivir	
DANA	

Kaempferol		
Sanggenol A		
Sanggenon G		
Katsumadain A		
Chlorogenic acid		
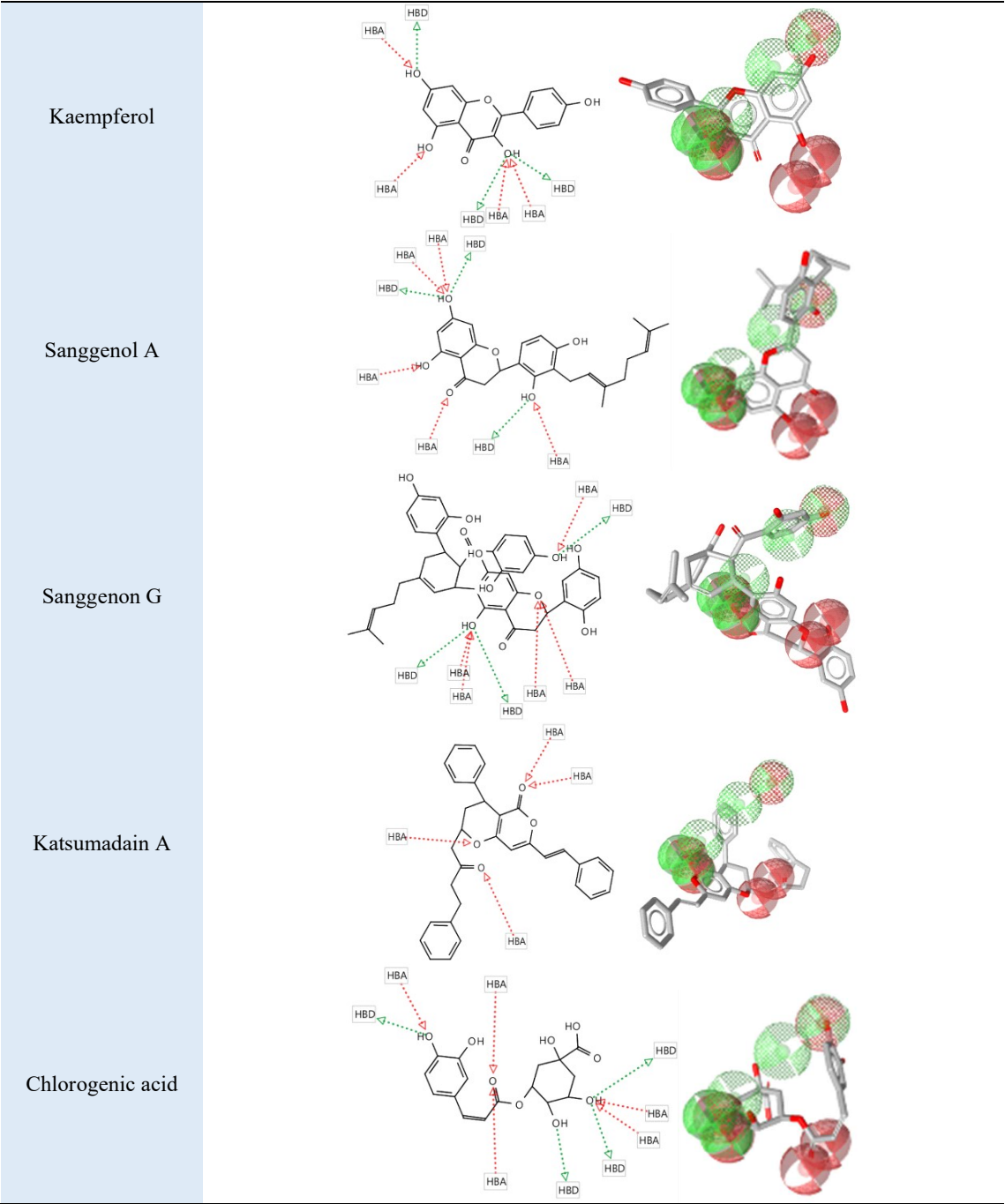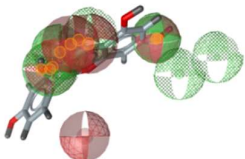
Table 6. RMSD-based evaluation of test sets alignment to the pharmacophore model

Test sets	Alignment of test sets with pharmacophore model	RMSD values
Kaempferol		0.835
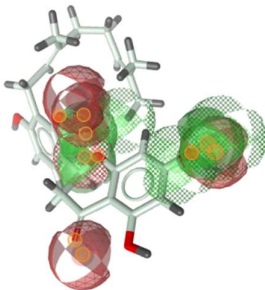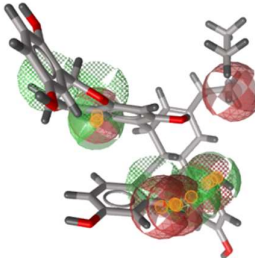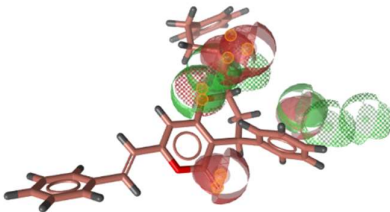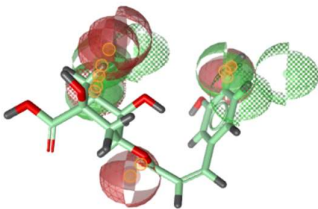
Sanggenol A — 1.219

Sanggenon G — 0.546

Katsumadain A — 1.052

Chlorogenic acid — 0.932

Table 7. Cosine similarities of test sets and pharmacophore model

Test sets	Vector of test sets	Cosine similarity
Kaempferol	[1, 6, 2, 0, 0]	0.77
Sanggenol A	[2, 3, 2, 1, 0]	0.83
Sanggenon G	[1, 2, 3, 1, 0]	0.55
Katsumadain A	[1, 4, 2, 1, 0]	0.75
Chlorogenic acid	[2, 5, 1, 0, 0]	0.90

Analysis of Schiff Base Vanillin Derivatives as Potential Neuraminidase Inhibitors of *Streptococcus Pneumoniae* in Ligand-based Pharmacophore Modelling

It was found out that out of all 21 Schiff base vanillin derivatives, compounds (1) to (10) were able to show good matching features and pharmacophore fit values greater than 70 in the generated pharmacophore model. Compounds (11) to (21) showed slightly lowered pharmacophore fit values and less optimal fit.

This is greatly due to the lack of proper functional groups to fit in the pharmacophore model, thus lack of suitable molecular structure. This can be explained by the depiction of pharmacophore features. Out of 10 pharmacophore features depicted by the pharmacophore model, compounds (1) to (10) successfully depicted 7 to 8 pharmacophore features, whereas compounds (11) to (21) depicted 6 pharmacophore features. Additionally, it was also noted that 2 derivatives show fit values higher than one of the training

sets, therefore having great potential as neuraminidase inhibitors of *Streptococcus pneumoniae*. Table 8 shows the matching features and pharmacophore fit values of the list of Schiff base vanillin derivatives in the pharmacophore model, arranged in descending order of pharmacophore fit values and number of matching features. Table 9 shows the matching features depicted by respective functional groups of the chemical structures of Schiff base vanillin derivatives in the pharmacophore model.

Table 8. Matching features and pharmacophore fit values of the list of Schiff base vanillin derivatives in the pharmacophore model

Schiff base vanillin derivatives	Matching features	Pharmacophore fit values
(1) Salicyl hydrazide		81.50
(2) Serine		81.31
(3) Hydrazide hydrate		74.49
(4) Phenylhydrazine		74.42
(5) Cysteine		74.35
(6) 2-thiophene carboxylic acid hydrazide		74.20
(7) 2-furoic acid hydrazide		74.16
(8) 4-hydroxybenzhydrazide		74.12
(9) 2,4-dinitrophenylhydrazine		73.99
(10) Nicotinic hydrazide		73.29
(11) Ethylenediamine		65.81
(12) 4-aminoantipyrine		64.68
(13) 2-aminobenzothiazole		64.61
(14) O-phenylenediamine		64.61
(15) Thiobenzamide		64.58
(16) L-Valine		64.56
(17) Sulfamic acid		64.56
(18) Benzamide		64.56
(19) Benzophenone hydrazine		64.55
(20) Anilline		64.54
(21) Isonicotinic acid hydrazide		64.25

Table 9. Matching features depicted by respective functional groups of Schiff base vanillin derivatives

Schiff base vanillin derivatives (Vanillin + …)	Matching features
(1) Salicyl hydrazide	
(2) Serine	
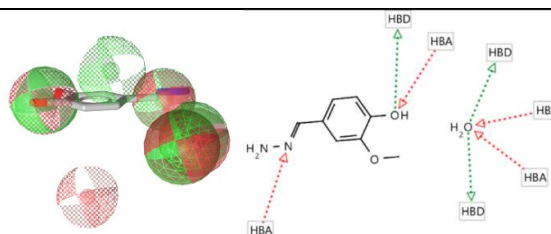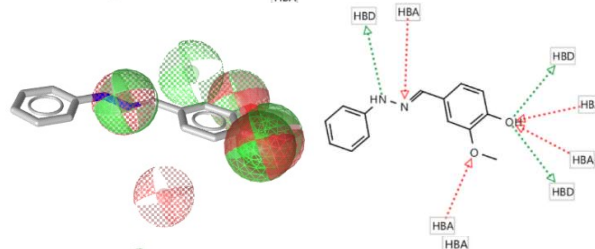
(3) Hydrazide hydrate

(4) Phenylhydrazine

(5) Cysteine

(6) 2-thiophene carboxylic acid hydrazide

(7) 2-furoic acid hydrazide

(8) 4-hydroxybenzhydrazide

(9) 2,4-dinitrophenylhydrazine

(10) Nicotinic hydrazide

(11) Ethylenediamine

(12) 4-aminoantipyrine

(13) 2-aminobenzothiazole

(14) O-phenylenediamine

(15) Thiobenzamide

(16) L-Valine

(17) Sulfamic acid

(18) Benzamide

(19) Benzophenone hydrazine
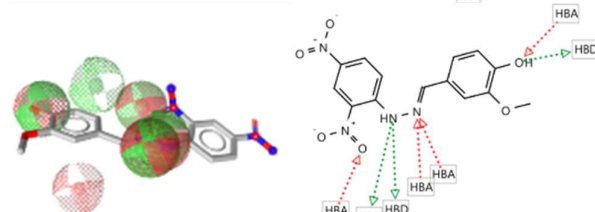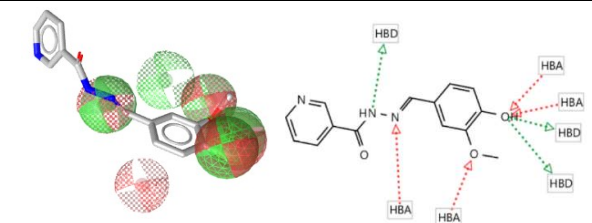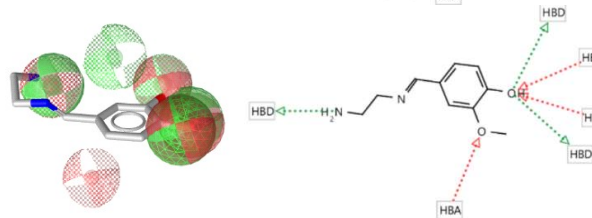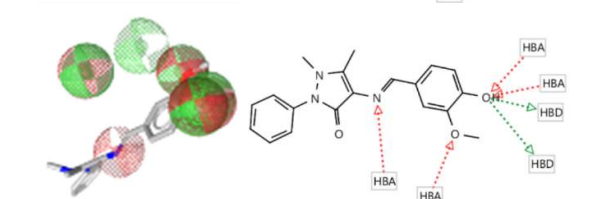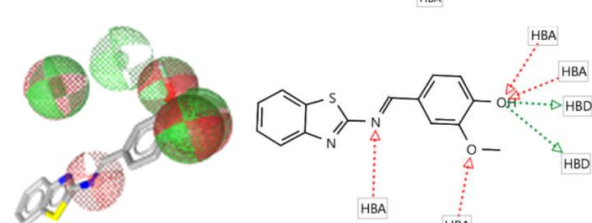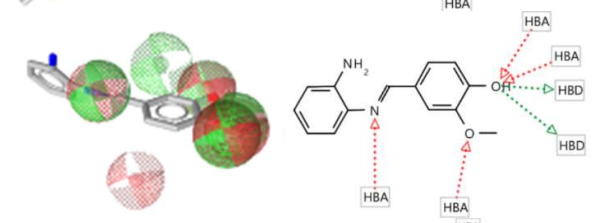
(20) Anilline
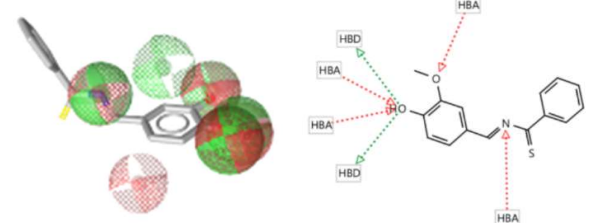
(21) Isonicotinic acid hydrazide
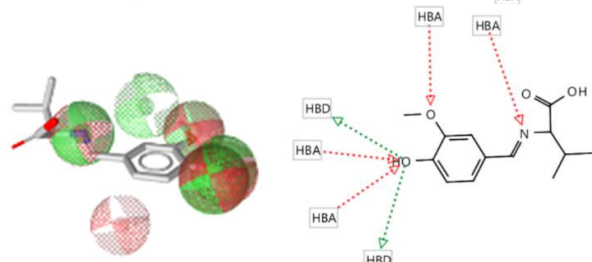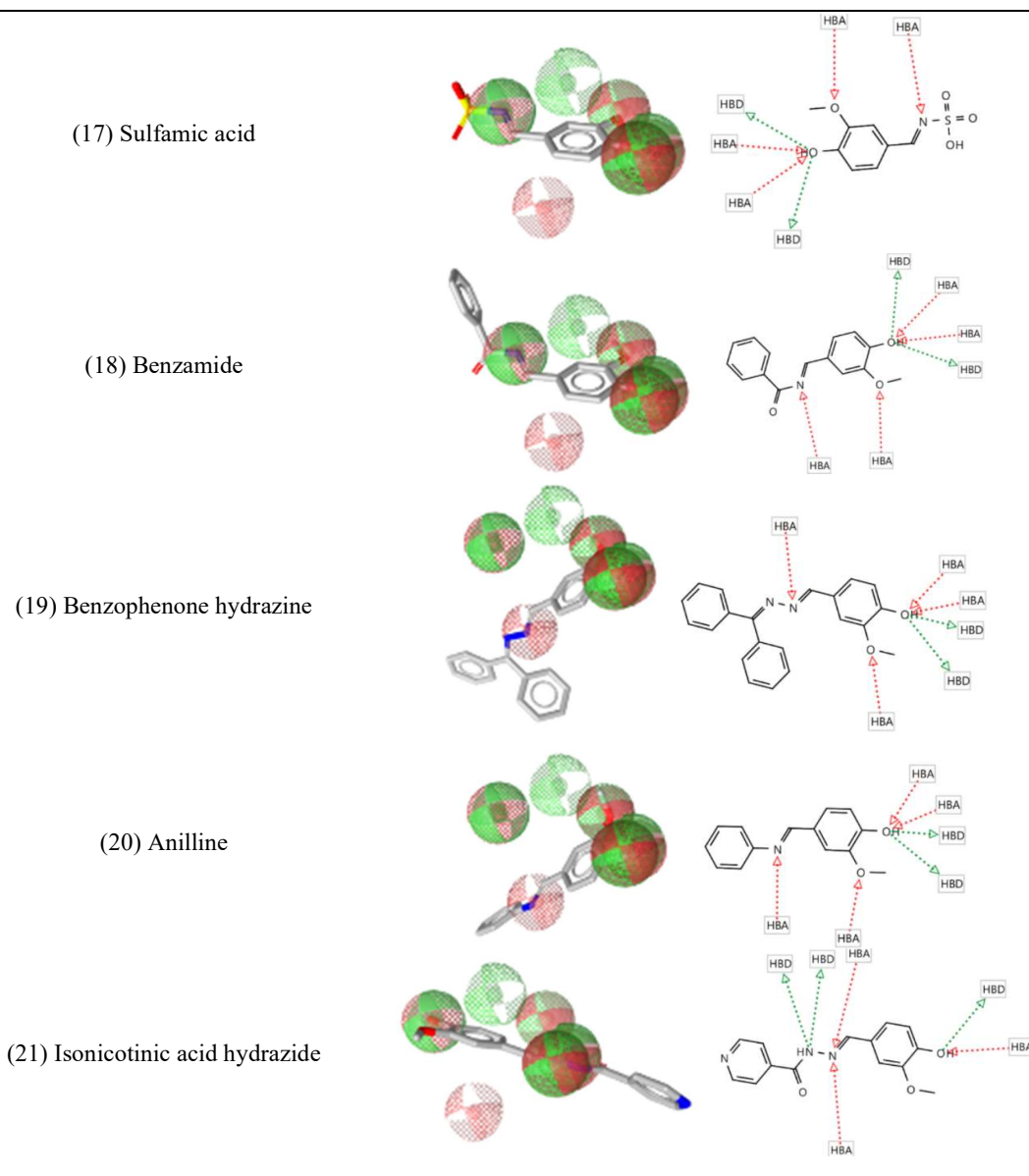
The matching features and pharmacophore fit values shown by the Schiff base vanillin derivatives are based on their functional groups and their molecular orientations. The MMFF94 energies of all Schiff base vanillin derivatives were minimised, thus they depict the most stable orientation. Schiff base vanillin derivatives were derived from a reaction between vanillin and primary amine. HBA and HBD interactions were discovered at the hydroxyl (OH) groups and ether group (C-O-C) of the vanillin part of all derivatives. Therefore, this indicates the importance of vanillin structure in matching with the pharmacophore feature. Vanillin has not only been reported previously for its antibacterial activity against various strains of bacteria, but

also as alternative against multidrug-resistant bacteria (Maisch *et al.*, 2022). This supports the potential inhibitory activity of vanillin against neuraminidase of *Streptococcus pneumoniae*. Secondly, most interactions are shown at the imine linkage (C=N) which is formed between vanillin and primary amine, indicating the significance and potential of Schiff base derivatives as neuraminidase inhibitors of *Streptococcus pneumoniae*. The antibacterial activities of Schiff bases against a variety of bacteria species such as *Staphylococcus aureus*, *Escherichia coli*, *Klebsiella pneumoniae* and *Proteus vulgaris* have been reported, which includes a comparative study as well such that Schiff base ligands showed greater antimicrobial

activity than their respective free ligands (Joseyphus & Nair, 2008). This further supports Schiff base derivatives' potential anti-neuraminidase activity. As for the primary amines which were bonded to the vanillin, most of the interactions are shown at OH group, amino group (NH$_2$), nitrogen atom (N), thiol group (SH), and nitro group (NO$_2$). Most of the Schiff base vanillin derivatives with high pharmacophore fit values and more matching features have OH groups in the chemical structures, as oxygen atom has lone pairs of electrons to be a potentially good HBA, and hydrogen atom as a good HBD. Vanillin derivatives such as (18), (19), (20) and (21) lack of OH group in their primary amine chemical structure, hence this may result in lower pharmacophore fit values and less matching features. Vanillin derivatives such as (4), (6) and (7), (9) and (10) are still able to show good pharmacophore fit values even without OH group in their primary amine, this may be due to suitable molecular orientation which fits in the pharmacophore model well. Despite the fact that 10 out of 21 Schiff base vanillin derivatives showed good results in ligand-based pharmacophore modelling, the remaining 11 Schiff base vanillin derivatives showed only slightly less optimal fit value. Thus, all Schiff base vanillin derivatives were subjected to structure-based molecular docking for further analysis and evaluations.

Pharmacophore Model of Ligand in the Active Site of 2YA8 in Structure-based Molecular Docking

Pharmacophore model of the oseltamivir carboxylate ligand in the active site of 2YA8 is generated to evaluate the interactions of Schiff base vanillin derivatives depicted in the active site of 2YA8. The pharmacophore model generated is composed of 20 pharmacophore features; 2 HBD to active sites HOH2312A and ASP357A, 8 HBA to active sites HOH2499A, HOH2044A, HOH2500A, ARG648A, ARG706A and ARG332A, 5 hydrophobic interactions (HI) to active sites PHE428A, LEU583A, PHE550A, TYR575A and ILE427A, 2 positive ionisable areas (PI) to ASP357A and ASP402A, and 3 negative ionisable areas (NI) to ARG648A, ARG706A and ARG332A. The pharmacophore model is as illustrated in Figure 9, whereas the pharmacophore features to respective active sites in 2YA8 is shown in Figure 10.
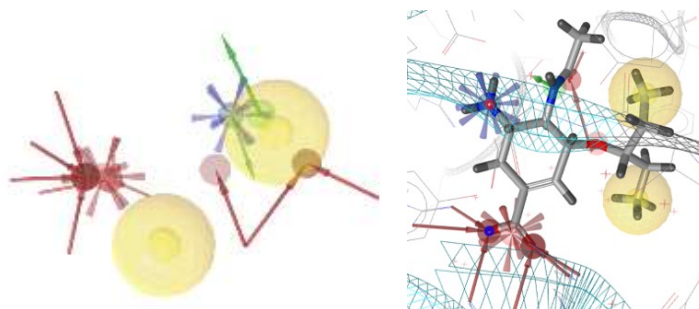
Figure 9. Generated pharmacophore model from oseltamivir carboxylate ligand in active site of 2YA8
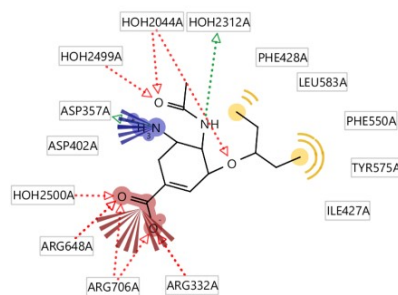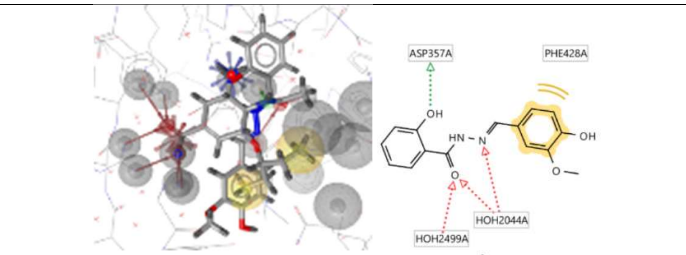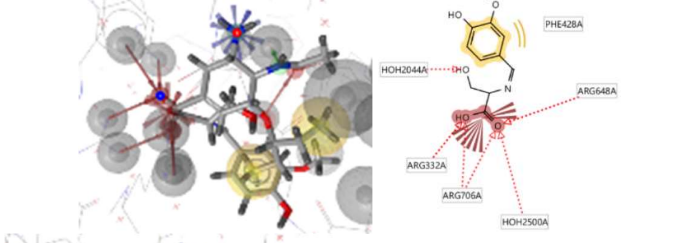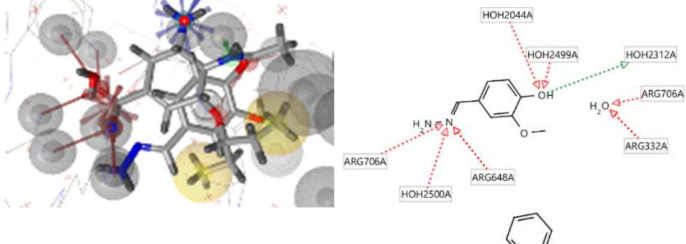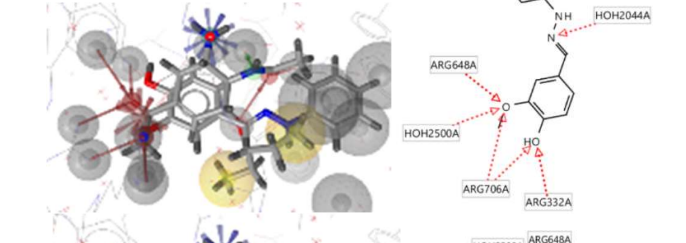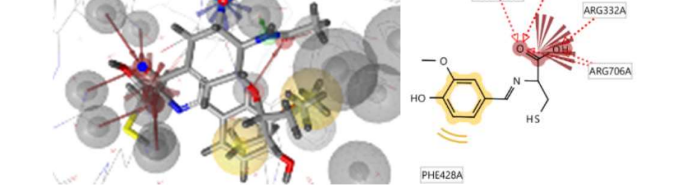
Figure 10. Pharmacophore features depicted by oseltamivir carboxylate ligand to respective active sites in 2YA8

Analysis of Schiff Base Vanillin Derivatives as Potential Neuraminidase Inhibitors of *Streptococcus Pneumoniae* in Structure-based Molecular Docking

Out of 21 Schiff base vanillin derivatives, only 19 of them successfully aligned with the pharmacophore model of the oseltamivir carboxylate ligand, showing matching pharmacophore features towards the active sites of 2YA8. Vanillin derivatives (6) and (20) failed to align with the ligand, thus fail to show matching features to interact with the actives sites of 2YA8. Table 10 shows the alignment and matching features portrayed by the Schiff base vanillin derivatives to the ligand in 2YA8 active site.

Table 10. Alignment and matching features of Schiff base vanillin derivatives to 2YA8 active site

Schiff base vanillin derivatives (Vanillin + …)	Alignment and matching features
(1) Salicyl hydrazide	
(2) Serine	
(3) Hydrazide hydrate	
(4) Phenylhydrazine	
(5) Cysteine	

(7) 2-furoic acid hydrazide
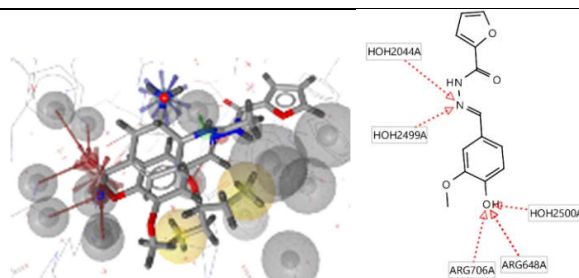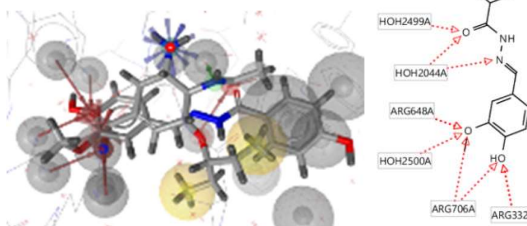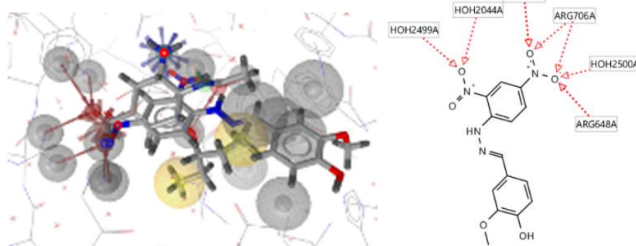
(8) 4-hydroxybenzhydrazide

(9) 2,4-dinitrophenylhydrazine

(10) Nicotinic hydrazide

(11) Ethylenediamine

(12) 4-aminoantipyrine

(13) 2-aminobenzothiazole

(14) O-phenylenediamine

(15) Thiobenzamide

(16) L-Valine

(17) Sulfamic acid

(18) Benzamide		
(19) Benzophenone hydrazine		
(21) Isonicotinic acid hydrazide		
(6) 2-thiophene carboxylic acid hydrazide	No successful alignment	
(20) Anilline	No successful alignment	
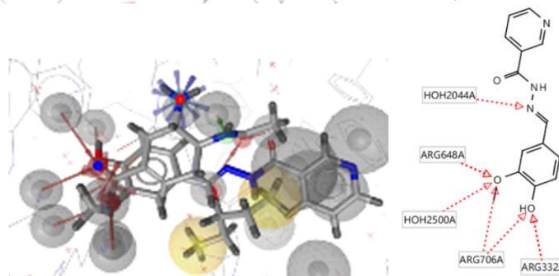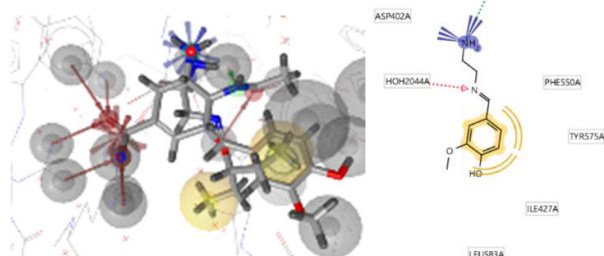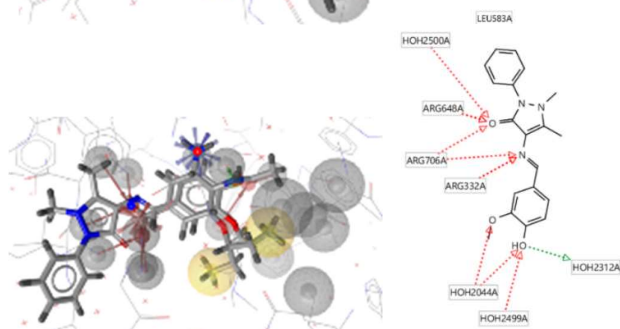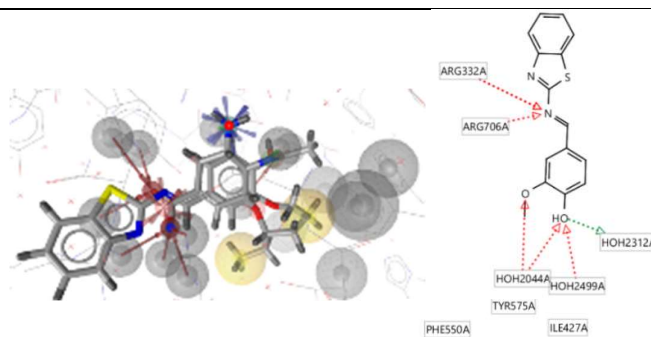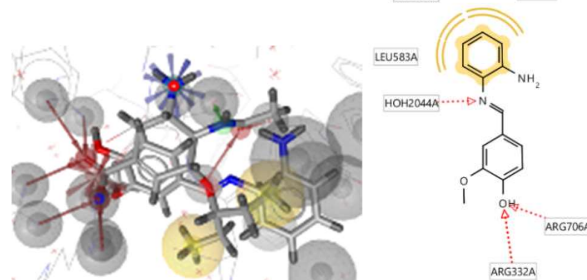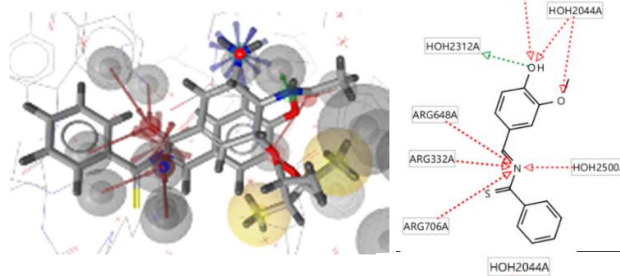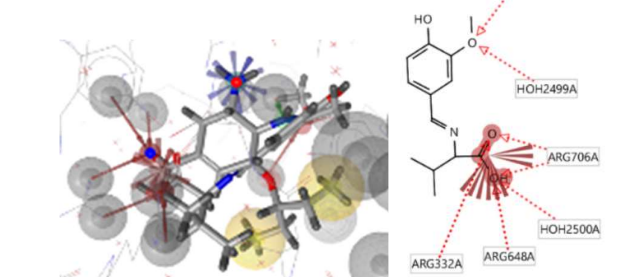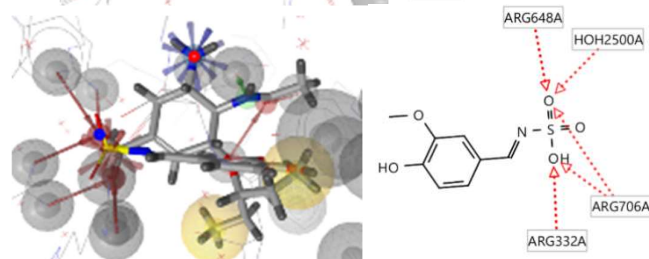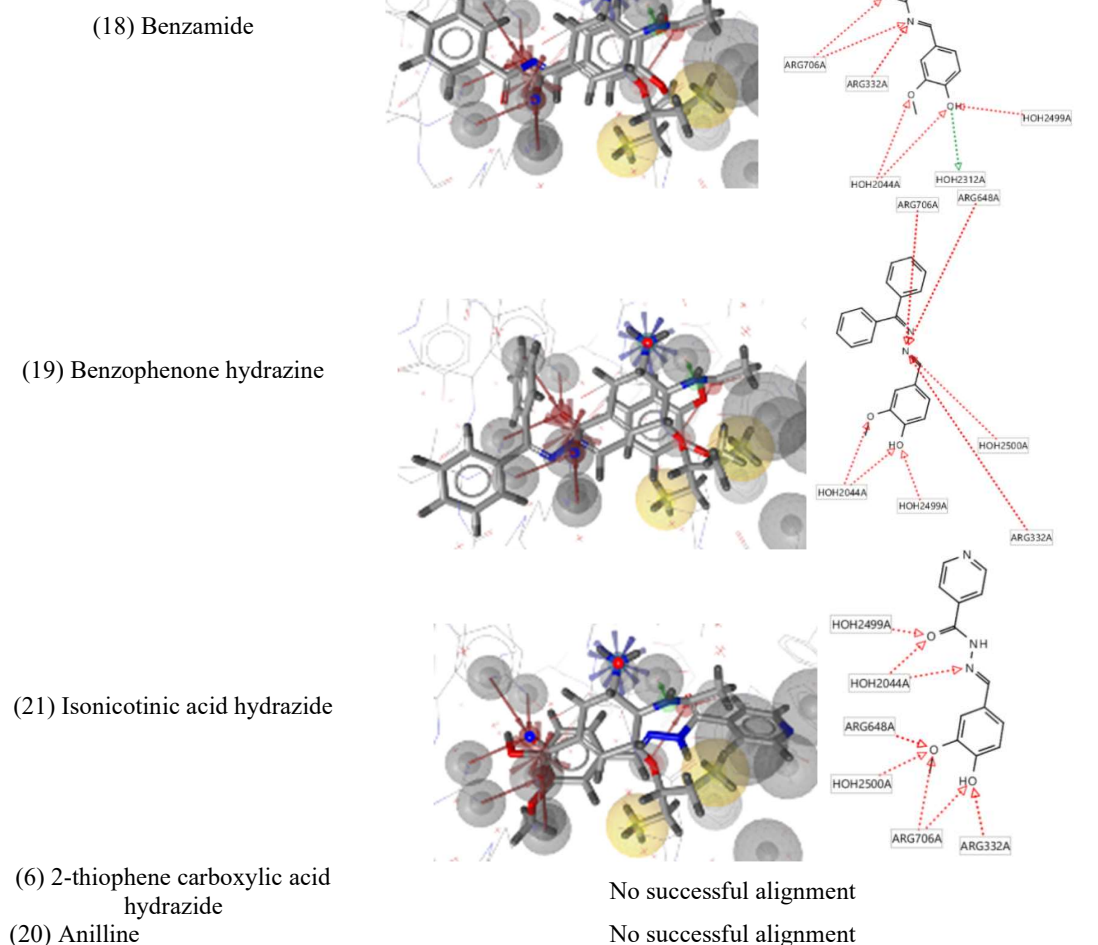
The key active site residues of the catalytic domain in 2YA8 include ARG332, ASP357, GLU632, ARG648, ARG706, and TYR737 (Sharapova *et al*., 2021). Out of 6 active sites, the Schiff base vanillin derivatives showed interactions towards 4 of them, which include HBA and NI interactions to ARG332, ARG648 and ARG706, as well as HBD and PI interactions to ASP357. In the same protein structure of 2YA8, zanamivir ligand was also reported to show strong binding interaction towards most of the active sites of *Streptococcus pneumoniae* neuraminidase, which include ARG332, ARG648, ARG706 and ASP357 (Sharapova *et al*., 2021). On top of that, the same bindings are also discovered in the interaction between DANA ligand and the active site of *Streptococcus pneumoniae* neuraminidase (Sharapova *et al*., 2021). These reported research proved the importance of the active sites in the evaluation of inhibitory activity against *Streptococcus pneumoniae* neuraminidase, thus further supported the inhibitory potential of the 19 Schiff base vanillin derivatives. Most interactions were depicted at the OH group and C-O-C group of the vanillin part, as well as the C=N linkage between the vanillin and primary amine, giving more fundamental support to the significance of not only Schiff bases, but vanillin as well in inhibitory interaction against *Streptococcus pneumoniae* neuraminidase. As for the primary amines, interactions were mostly shown by NO_2 group, C=O group, benzene ring, carboxylate group (COOH) and sulfonyl group (SO_2). Despite the fact that most Schiff base vanillin derivatives successfully showed good interaction results towards the active site of 2YA8, other than the molecular formulae of the vanillin derivatives, the structural formulae and molecular orientations are also responsible for

their alignment and matching features to the oseltamivir carboxylate ligand. This may explain the unsuccessful alignment of (6) and (20) to the ligand, as well as failed docking into the active site of 2YA8 even though their chemical structures are similar to the other Schiff base vanillin derivatives. Furthermore, (6) and (20) may also be lack of important functional groups to align with the significant active sites.

Binding Affinity Values of Schiff Base Vanillin Derivatives

Binding affinity values determine the strength of binding interaction between the Schiff base vanillin derivatives and the active site of 2YA8. The smaller the binding affinity values, the stronger the binding interaction. Being a function of Gibbs free energy, binding affinity values less than -6.00 kcal/mol are considered as active molecules with strong binding interaction (Shityakov & Förster, 2014). Binding affinity values shown by the Schiff base vanillin

derivatives based on the docking outcome are ranged between -6.00 kcal/mol to -7.60 kcal/mol, thus showing strong binding affinity towards the active site of 2YA8. However, (3) was unable to show good binding affinity value, with great probability due to the lack of suitable molecular structure. (3), which is vanillin synthesised with hydrazide hydrate has a water molecule. The water molecule may cause steric hindrance which interfere binding interactions. When water molecule is removed from (3), the Schiff base vanillin derivative of hydrazide was only able to dock with binding affinity value of -5.90. Thus, (3) was unable to show good binding interaction with the pocket of 2YA8, with or without the water molecule. Despite the fact that it is able to align with the oseltamivir carboxylate ligand, the separated chemical structure affects its docking efficiency into the active site of 2YA8. Table 11 summarises the binding affinity values of 18 Schiff base vanillin derivatives towards 2YA8 active site.

Table 11. Binding affinity values of Schiff base vanillin derivatives to 2YA8 active site

Schiff base vanillin derivatives (Vanillin + …)	Binding affinity values (kcal / mol)
(1) Salicyl hydrazide	-7.10
(2) Serine	-6.50
(4) Phenylhydrazine	-7.00
(5) Cysteine	-6.40
(7) 2-furoic acid hydrazide	-7.60
(8) 4-hydroxybenzhydrazide	-6.00
(9) 2,4-dinitrophenylhydrazine	-7.40
(10) Nicotinic hydrazide	-6.60
(11) Ethylenediamine	-6.60
(12) 4-aminoantipyrine	-6.20
(13) 2-aminobenzothiazole	-6.30
(14) O-phenylenediamine	-6.20
(15) Thiobenzamide	-6.10
(16) L-Valine	-6.50
(17) Sulfamic acid	-7.50
(18) Benzamide	-6.50
(19) Benzophenone hydrazine	-6.70
(21) Isonicotinic acid hydrazide	-7.20

Lipinski's Rule of 5

Lipinski's Rule of 5, or known as RO5, is a rule that is used to evaluate the drugability or druglikeness of chemical compounds, which is their potential as orally active drugs. The evaluation is based on the drug's pharmacokinetics in human body, including their absorption, distribution, metabolism, and excretion (ADME). For a chemical compound to

possess druglikeness, the chemical compound should have no more than 5 HBD, no more than 10 HBA, molecular mass less than 500 g/mol and partition coefficient value less than 5 (Benet *et al*., 2016). It was concluded that all 18 Schiff base vanillin derivatives fulfilled all the rules in RO5, indicating their potential as promising drug candidates for having druglikeness as orally active drugs. Table 12 summarises the number of HBD, HBA, molecular masses and partition

coefficient values depicted by the 18 Schiff base vanillin derivatives.

Table 12. The number of HBD, HBA, molecular masses and partition coefficient values of Schiff base vanillin derivatives

Schiff base vanillin derivatives (Vanillin + …)	c log P	Hydrogen bond donors (HBD)	Hydrogen bond acceptors (HBA)	Molecular weight (g/mol)
(1) Salicyl hydrazide	1.639	3	5	286.287
(2) Serine	0.265	2	6	239.227
(4) Phenylhydrazine	2.847	2	3	242.278
(5) Cysteine	1.583	2	6	255.292
(7) 2-furoic acid hydrazide	1.526	2	4	260.249
(8) 4-hydroxybenzhydrazide	1.639	3	5	286.287
(9) 2,4-dinitrophenylhydrazine	2.663	2	7	332.272
(10) Nicotinic hydrazide	1.328	2	5	271.276
(11) Ethylenediamine	0.778	2	3	194.234
(12) 4-aminoantipyrine	2.949	1	4	337.379
(13) 2-aminobenzothiazole	3.761	1	4	284.337
(14) O-phenylenediamine	2.734	2	3	242.278
(15) Thiobenzamide	3.195	1	4	271.338
(16) L-Valine	1.929	1	5	251.282
(17) Sulfamic acid	1.703	1	6	231.226
(18) Benzamide	2.428	1	4	255.273
(19) Benzophenone hydrazine	4.272	1	4	330.387
(21) Isonicotinic acid hydrazide	1.328	2	5	271.276

CONCLUSION

As a whole, out of 21 Schiff base vanillin derivatives, 8 compounds showed potential inhibitory activity against neuraminidase of *Streptococcus pneumoniae* in combination of both results from ligand-based pharmacophore modelling and structure-based molecular docking. These compounds are (1), (2), (4), (5), (7), (8), (9) and (10). 10 out of 21 Schiff base vanillin derivatives, which were compounds (1) to (10) were able to show good pharmacophore fit values of 70 and above and satisfied matching pharmacophore feature with the validated pharmacophore model. On top of that, except for compounds (3), (6) and (20), the remaining 18 Schiff base vanillin derivatives were able to show good docking results in the active site of *Streptococcus pneumoniae* neuraminidase, as well as depicting good alignment with the inhibitory oseltamivir carboxylate ligand in the active site. For showing good binding affinity values and fulfilling Lipinski's Rule of 5 simultaneously, the 8 Schiff base vanillin derivatives were concluded as promising drug candidates opened to be further evaluated for their inhibition activity against *Streptococcus pneumoniae* neuraminidase by other biological assays, including MUNANA assay, which is an assay based on cleavage of neuraminidase on the 2′-(4-methylumbelliferyl)-α-D-N-acetylneuraminic acid.

REFERENCES

Al-Shar'i, N., & Musleh, S. (2020). Identification of CHK1 Kinase Inhibitors Using Structure-Based Pharmacophore Modelling and Molecular Docking. *Indian Journal of Pharmaceutical Sciences*, 82: 472–482. DOI: 10.36468/pharmaceutical-sciences.670

Asaruddin, M. R. (2016). *Modelling and Syntheses of Vanillin Derivatives Targeting Influenza Virus Neuraminidase*. (PhD thesis), Universiti Sains Malaysia, Malaysia.

Benet, L. Z., Hosey, C. M., Ursu, O. & Oprea, T. I. (2016). BDDCS, the Rule of 5 and Drugability. *Advanced Drug Delivery Reviews*, 101: 89–98.

Benton, D. J., Wharton, S. A., Martin, S. R. & McCauley, J. W. (2017). Role of Neuraminidase in Influenza A(H7N9) Virus Receptor Binding. *Journal of Virology*, 91(11): e02293–16. DOI: 10.1128/jvi.02293-16

Bogaert, D., de Groot, R. & Hermans, P. W. M. (2004). *Streptococcus Pneumoniae* Colonisation: The Key to Pneumococcal Disease. *The Lancet Infectious Diseases*, 4(3): 144–154. DOI: 10.1016/S1473-3099(04)00938-7

Centers for Disease Control and Prevention. (2023). *Pneumococcal Vaccination*. Retrieved June 15, 2024, from https://www.cdc.gov/pneumococcal/vaccines/index.html

Centers for Disease Control and Prevention. (2024). *Antibiotic-Resistant Streptococcus Pneumoniae*. Retrieved June 16, 2024, from https://www.cdc.gov/pneumococcal/php/drug-resistance/index.html

Dion, C.F. & Ashurst, J.V. (2022). *Streptococcus Pneumoniae*. Retrieved June 16, 2024 from https://www.ncbi.nlm.nih.gov/books/NBK470537/

European Centre for Disease Prevention and Control. (2023). *Factsheet About Pneumococcal Disease*. Retrieved June 13, 2024, from https://www.ecdc.europa.eu/en/pneumococcal-disease/facts

Grienke, U., Richter, M., Walther, E., Hoffmann, A., Kirchmair, J., Makarov, V., Nietzsche, S., Schmidtke, M. & Rollinger, J. M. (2016). Discovery of Prenylated Flavonoids with Dual Activity Against Influenza Virus and *Streptococcus Pneumoniae*. *Scientific Reports*, 6: 27156. DOI: 10.1038/srep27156

Guan, S., Zhu, K., Dong, Y., Li, H., Yang, S., Wang, S. & Shan, Y. (2020). Exploration of Binding Mechanism of a Potential *Streptococcus Pneumoniae* Neuraminidase Inhibitor from Herbaceous Plants by Molecular Simulation. *International Journal of Molecular Sciences*, 21(3): 1003. DOI: 10.3390/ijms21031003

Gut, H., Xu, G., Taylor, G. L. & Walsh, M. A. (2011). Structural Basis for *Streptococcus Pneumoniae* NanA Inhibition by Influenza Antivirals Zanamivir and Oseltamivir Carboxylate. *Journal of Molecular Biology*. 409(4): 496–503. DOI: 10.1016/j.jmb.2011.04.016

Hsiao, Y. S., Parker, D., Ratner, A. J., Prince, A. & Tong, L. (2009). Crystal Structures of Respiratory Pathogen Neuraminidases. *Biochemical and Biophysical Research Communications*. 380(3): 467–471. DOI: 10.1016/j.bbrc.2009.01.108

Iyer, U. & Perloff S. (2023). *Pneumococcal Infections (Streptococcus Pneumoniae)*. Medscape. Retrieved June 13, 2024, from https://emedicine.medscape.com/article/225811-overview

Joseyphus, R. S. & Nair, M. S. (2008). Antibacterial and Antifungal Studies on Some Schiff Base Complexes of Zinc(II). *Mycobiology*, 36(2): 93–98. DOI: 10.4489/MYCO.2008.36.2.093

Li, N., Wang, F., Niu, S., Cao, J., Wu, K., Li, Y., Yin, N., Zhang, X., Zhu, W. & Yin, Y. (2009). Discovery of Novel Inhibitors of *Streptococcus Pneumoniae* Based on the Virtual Screening with the Homology-Modeled Structure of Histidine Kinase (VicK). *BMC Microbiology*, 9(1): 129. DOI: 10.1186/1471-2180-9-129

Lv, Q., Zhang, P., Quan, P., Cui, M., Liu, T., Yin, Y. & Chi, G. (2020). Quercetin, a Pneumolysin Inhibitor, Protects Mice Against *Streptococcus Pneumoniae* Infection. *Microbial Pathogenesis*, 140: 103934. DOI: 10.1016/j.micpath.2019.103934

Maisch, N. A., Bereswill, S. & Heimesaat, M. M. (2022). Antibacterial Effects of Vanilla Ingredients Provide Novel Treatment Options for Infections with Multidrug-Resistant Bacteria - A Recent Literature Review. *European Journal of Microbiology & Immunology*, 12(3): 53–62. DOI: 10.1556/1886.2022.00015

Maragakis, L. L., Perencevich, E. N. & Cosgrove, S. E. (2008). Clinical and Economic Burden of Antimicrobial Resistance. *Expert Review of Anti-Infective Therapy*, 6(5): 751–763. DOI: 10.1586/14787210.6.5.751

Musher, D. M. (2019). *Streptococcus Pneumoniae*. Haymarket Medical Network. Retrieved June 15, 2024, from https://www.infectiousdiseaseadvisor.com/ddi/streptococcus-pneumoniae/

Nayian, N. A. & Yusof, H. A. (2020). Inhibition of *Streptococcus pneumoniae* Hyaluronidase by Honeys of Malaysian origins. *Bioremediation Science and Technology Research,* 8(1): 1–6.

Neela, M. M. V. & Peram, S. (2025). Computational Approaches for Drug-Protein Interaction Analysis in Cancer: Machine Learning and Structural

Bioinformatics Perspectives. Journal of Information Systems Engineering and Management, 10, 231–247. https://doi.org/10.52783/jisem.v10i10s.1368

Nguyen, T. L. A. & Bhattacharya, D. (2022). Antimicrobial Activity of Quercetin: An Approach to Its Mechanistic Principle. *Molecules*, 27(8): 2494. DOI: 10.3390/molecules27082494

Oliver, F. (2019). *Streptococcus Pneumoniae (pneumococcus)*: *Overview*. News-Medical. Retrieved June 12, 2024, from https://www.news-medical.net/health/Streptococcus-pneumoniae-(pneumococcus)-Overview.aspx

Owen, C. D., Lukacik, P., Potter, J. A., Sleator, O., Taylor, G. L. & Walsh, M. A. (2015). *Streptococcus Pneumoniae* NanC: Structural Insights into The Specificity and Mechanism of a Sialidase That Produces a Sialidase Inhibitor. *The Journal of Biological Chemistry*, 290(46): 27736–27748. DOI: 10.1074/jbc.M115.673632

Parker, D., Soong, G., Planet, P., Brower, J., Ratner, A. J. & Prince, A. (2009). The NanA Neuraminidase of *Streptococcus Pneumoniae* is Involved in Biofilm Formation. *Infection and Immunity*, 77(9): 3722–3730. DOI: 10.1128/IAI.00228-09

Rohani, M. Y., Raudzah, A., Ng, A. J., Ng, P. P., Zaidatul, A. A., Asmah, I., Murtaza, M., Parasakthy, N., Mohd Yasmin, M. Y. & Cheong, Y. M. (1999). Epidemiology of *Streptococcus Pneumoniae* Infection in Malaysia. *Epidemiology and Infection*, 122(1): 77–82. DOI: 10.1017/s0950268898001605

Sharapova, Y., Suplatov, D. & Švedas, V. (2018). Neuraminidase A from *Streptococcus Pneumoniae* Has a Modular Organization of Catalytic and Lectin Domains Separated by a Flexible Linker. *The FEBS Journal*, 285(13): 2428–2445. DOI: 10.1111/febs.14486

Sharapova, Y., Švedas, V. & Suplatov, D. (2021). Catalytic and Lectin Domains in Neuraminidase A from *Streptococcus Pneumoniae* are Capable of an Intermolecular Assembly: Implications for Biofilm Formation. *The FEBS Journal*, 288: 3217–3230. DOI: 10.1111/febs.15610

Shityakov, S. & Förster, C. (2014). *In Silico* Predictive Model to Determine Vector-Mediated Transport Properties for the Blood-Brain Barrier Choline Transporter. *Advances and Applications in Bioinformatics and Chemistry*, 7: 23–36. DOI: 10.2147/AABC.S63749

Syed, S., Hakala, P., Singh, A. K., Lapatto, H. A. K., King, S. J., Meri, S., Jokiranta, T. S. & Haapasalo, K. (2019). Role of Pneumococcal NanA Neuraminidase Activity in Peripheral Blood. *Frontiers in Cellular and Infection Microbiology*, 9: 218. DOI: 10.3389/fcimb.2019.00218

Walther, E., Richter, M., Xu, Z., Kramer, C., von Grafenstein, S., Kirchmair, J., Grienke, U., Rollinger, J. M., Liedl, K. R., Slevogt, H., Sauerbrei, A., Saluz, H. P., Pfister, W. & Schmidtke, M. (2015). Antipneumococcal Activity of Neuraminidase Inhibiting Artocarpin. *International Journal of Medical Microbiology*. 305(3): 289–297. DOI: 10.1016/j.ijmm.2014.12.004

World Health Organization. (2022). *Pneumonia in Children*. Retrieved June 12, 2024, from https://www.who.int/news-room/fact-sheets/detail/pneumonia

Xu, L., Fang, J., Ou, D., Xu, J., Deng, X., Chi, G., Feng, H. & Wang, J. (2023). Therapeutic Potential of Kaempferol on *Streptococcus Pneumoniae* Infection. *Microbes and Infection*, 25(3): 105058. DOI: 10.1016/j.micinf.2022.105058

Knowledge and Perceptions of Bat Guano Among Diverse Demographics in Malaysia

SITI-SYAMIM NURFATIHAH ABD RAHMAN[*1], MOHAMAD FHAIZAL MOHAMAD
BUKHORI[2], ROBERTA CHAYA TAWIE ANAK TINGGA[2] & FAISAL ALI ANWARALI KHAN[1]

[1]Faculty of Resource Science and Technology, Universiti Malaysia Sarawak, 94300, Kota Samarahan, Sarawak,
Malaysia; [2]Centre for Pre-University Studies, Universiti Malaysia Sarawak, 94300, Kota Samarahan, Sarawak,
Malaysia.
[*]Corresponding author: sitisyamim98@gmail.com

ABSTRACT

Bat guano, or bat faeces, plays a crucial role in cave ecosystems, serving as a source of energy and impacting habitat dynamics. Its utilisation had been beneficial worldwide since centuries ago. However, a lack of awareness on bat guano's role in the ecosystem particularly in Malaysia can be identified. Hence, the study delves into the perceptions and knowledge of the local Malaysian community regarding bat guano. A virtual survey was conducted through platforms like WhatsApp, Facebook, and LinkedIn. Analysis of the chi-square test using SPSS Version 37 Software was done to show the correlation between respondents' demographics, guano knowledge, its importance, and their willingness to use it. Among 103 respondents, mostly aged 18 to 25, 64.08% were aware of bat guano, but few had used guano-derived products. Positive perceptions were linked to the age group (p = 0.002), indicating younger individuals were more receptive. Challenges to broader acceptance included cleanliness and safety concerns heightened by the ongoing COVID-19 pandemic. Despite efforts to provide information and change perceptions, 78.64% remained undecided about using bat guano in their daily lives due to persistent misconceptions. Public awareness and education are crucial for promoting its benefits, necessitating collaboration among researchers, educators, and government entities.

Keywords: bat awareness, bat droppings, benefits, community, ecosystem

INTRODUCTION

Bat guano, the excrement deposited by bats, is predominantly found on cave floors and plays a crucial role in the cave ecosystem (Ferreira & Martins, 1999; Sakoui *et al*., 2020). It serves as a primary energy source in caves, significantly influencing their dynamics and structural habitat (Fenolio *et al*., 2006). Guano supports a complex food web involving bacteria, fungi, protozoa, nematodes, arthropods, and other invertebrates (Harris, 1970). The composition of bat guano varies based on environmental factors, age, and the diet of bats (Ferreira & Martins, 1999; Karagoz, 2014).

Historically, the utilisation of bats guano in previous centuries had been recorded in various studies. A few examples of records were written by Buchannan (1800) where harvesting of guano from *Chaerephon plicatus*, the cave-dwelling Asian wrinkle-lipped bat, had been occurring for decades in Cambodia (Sothearen *et al*., 2014).

Bat guano was also used to produce gunpowder due to its high phosphorus content (Ghanem & Voigt, 2012; Linn & Myint, 2018). It has also been utilised in radiocarbon dating to record environmental changes, revealing a savanna ecosystem in Borneo during the Pleistocene epoch (Wurster *et al*., 2019). In Western countries, guano has been used non-invasively to identify bats, particularly after the rise of white-nose syndrome (Kanuch *et al*., 2007; Puechmaille *et al*., 2007). In Malaysia, bat guano has been found in various locations in Borneo, with significant deposits in Racer Cave -part of Mulu National Park, and in Niah Cave located in Niah National Park, highlighting its mineral diversity through degradation processes (McFarlane & Lundberg, 2018).

In the field of mycology, guano obtained from Madai Cave, Sabah were found to contain 32 species of fungi such as *Penicillium* spp., *Aspergillus* spp., and *Purpureocillium lilnacium* as well as several pathogenic yeasts and

microbes used in developing biological control agents for harmful plants nematodes and other harmful plant microbes (Wasti *et al*., 2021).

Studying guano morphology is crucial for understanding the dietary habits of bats and developing effective conservation strategies. By analysing guano, researchers can gain insights into bat habitats and diet partitioning. Additionally, assessing prey availability helps determine the potential for bats to coexist with other species, thereby reducing competition with other predators in the area such as other bat species, nocturnal birds and some herpetofaunas (Ware *et al*., 2020). Dietary specialisation is one of the key factors contributing to extinction risk in bats. Through guano analysis, researchers can identify the dietary preferences of bat species and implement targeted conservation strategies to maintain a balanced prey-predator relationship (Ware *et al*., 2020).

However, community discussions about the utilisation of bats guano revealed mixed perceptions. Addressing public perceptions of bat guano is vital for successful conservation efforts. Studies from various regions showed that local communities often viewed bat guano negatively. For instance, in Fort Collins, Colorado, 76% of surveyed participants had negative views on bat guano, with only 7% expressing positive thoughts (Sexton & Stewart, 2007). Similarly, in Mexico, coffee farmers considered bat guano usage detrimental to disease-resistant agroecosystems, and 59% had limited knowledge about it (Torres-Jiménez *et al*., 2020).

Conversely, in Balla and Guidimouni, Niger, 96.7% of horticulturists used bat guano to enhance plant growth. Guano extraction was also prevalent in nearby Magarawa Village, where workers, aware of the risks, often wore protective clothing (Harouna *et al*., 2021). In Southeast Asia, 26% of caves in the Philippines were used for guano collection (Tanalgo *et al*., 2016). In Thailand, significant guano mining activities occurred in Lopburi and Chiang Rai, managed by local Buddhist temples, providing income for villagers (Suwannarong *et al*., 2020).

Despite numerous studies on bat guano worldwide, a survey at Kuala Gandah Interpretive Centre (Krau Wildlife Reserve) is one of two surveys that touched on bats guano

knowledge in Malaysia (Kingston *et al*., 2006). The survey, which was an effort from the Malaysian Bat Conservation Research Unit (MBRCU) was determined to establish an environmental education programme for bats. The survey found that only 3.4% of visitors were aware of its agricultural benefits. The second survey on the public perception of bats guano in Peninsular Malaysia had found that a major participants of the survey acknowledge the utility of bats guano as organic fertiliser. However, the participants agree that bat droppings have a pungent odour and is not comfortable living with bats in proximity (Lim & Wilson, 2019).

This perceptions and low awareness level underscores a significant educational gap on bats guano utilisation, this may be due to the unfavourable public opinion on the matter. Appreciation of guano as a sustainable source of fertiliser and research values would indicate a better management in guano mining. Tanalgo *et al*. (2016) mentioned that the threats of bats declination in Thailand were contributed by the destruction of cave habitats from the lack of protocol and regulation for guano mining in the area becomes a big threat to the population. Management in guano extraction activities is of the utmost importance to hinder the destruction of geological cave features and bat roosts' damages (Tanalgo *et al*., 2016). Hence, the objective of this virtual study is to assess the level of awareness and knowledge about bat guano among various demographic groups in Malaysia, including differences based on age, gender, education level, and geographic location, to inform targeted educational and conservation efforts.

MATERIALS AND METHODS

A social survey was conducted where 17 questions was published through social media platforms such as Facebook, LinkedIn, WhatsApp, and Instagram. The questionnaire was distributed randomly, and it was available for a two-month period, from February to April 2023. Utilising a virtual form provided numerous advantages, including convenience, scalability, and efficient data management and analysis. Respondents could participate at their own pace and convenience, removing geographical constraints and enabling broader participation. A pre-survey trial was not in place

as the study's goal is to gather as much data as possible within the available timeframe, prioritising broad participation over preliminary testing. To accommodate a wider audience, the questionnaire was offered in both Malay and English.

The information sheet included the purpose of the study, participants' right to withdraw, ensuring confidentiality and anonymity, and information on data storage. An informed consent that confirmed their voluntary participation in the study was included at the beginning of the questionnaire. The participants were informed that no identifiable data would be published.

The survey was adapted from questionnaire done by Lim and Wilson (2019), where it covers demographics, familiarity, perception, and knowledge, as well as responses to bats. Certain questions were modified to align with the objectives of this study. The survey aimed to assess general perceptions and knowledge of bat guano based on respondents' educational levels and demographic characteristics. Demographic variables included gender, age group, place of residence, level of education, and occupation. The questionnaire was divided into four sections: respondents' demographics (Questions 1 to 5), general knowledge of bat guano (Questions 6 to 13), understanding of its importance (Questions 14 and 15), and willingness to use bat guano after learning about its benefits (Questions 16 and 17).

Some questions required elaboration on choice through open-ended questions (Table 1). The questions provide flexibility to discuss aspects of the answers that might not have been considered. Other than that, it gives an understanding of the respondents' experiences in their own words. Most of the questions provided are closed-ended questions to ensure efficiency in respondents answer time, and the compilation of data. It also provides consistency in uniform data, to be easily compared across respondents. Scores from true or false questions gauged knowledge levels. A Likert scale was not utilised in the survey questions to ensure a simplified question structure and to ease the response for participants with varying education levels. Survey results were compiled in Excel and imported into SPSS Version 37 for analysis. Statistical analysis using a chi-square test through SPSS was done to test the significance of each demographic character against the knowledge and utilisation of bat guano by the respondents, followed by linear regression to assess knowledge scores. Analysis of the chi-square test was used to determine the correlation between the demographic characters and the yes or no variables.

Table 1. List of questions of the social survey conducted through Microsoft Forms.

Section Number	Question Number	Question
1 Demographic	1	Gender
	2	Age
	3	Place of residence
	4	Level of education
	5	Occupation
2 Knowledge and Experience	6	Are you familiar with the term bat guano before?
	7	If your previous answer was yes, where did you first hear about bat guano before?*
	8	What was your perception of bat guano before?
	9	Why do you have that perception?*
	10	Have you encountered bat guano anywhere before?
	11	If your previous answer was yes, where did you encounter the bat guano before?
	12	Have you utilised bat guano derived product before in any matters?
	13	If your previous answer was yes, how long have you been using bat guano derived product before?
3 Knowledge of Bats Guano Importance	14	Do you understand the importance of bat guano before?
	15	According to your knowledge, which do you think is the importance of bat guano?
4 Final Personal Thoughts	16	After reading the information, do you wish to use bat guano in your life?
	17	If your previous answer was no, what is the reason?*

*Open-ended questions

RESULTS

Demographic

A total of 103 respondents was obtained from 29 males, 72 females, 1 undisclosed (prefer not to say). The age group of respondents (Question 2) were described in Figure 1. The answers comprised of 65 respondents in the age group of 18 to 25 years old (63.11%), 22 respondents from 26 to 35 years old (21.36%), 6 respondents from 36 to 45 years old (5.83%), 5 respondents from 46 to 55 years old (4.85%), and the others were from above 55 years old (4.85%). The localities of respondents (Question 3) were dispersed around the states of Malaysia with the highest number of respondents from Sarawak at 40.78% (42 respondents) while the lowest number was 1 respondent (0.97%) from Kelantan, Melaka, Pahang and Perak (Figure 2). The results show 99% of the respondents had obtained or currently pursuing their tertiary education ranging from diploma or matriculation (11 respondents – 10.67%), Bachelor's degree (73 respondents – 70.87%), Master's degree (16 respondents – 15.53%) and Doctorate degree (2 respondents – 1.94%), while only 1 respondent obtained primary and secondary education (0.97%).
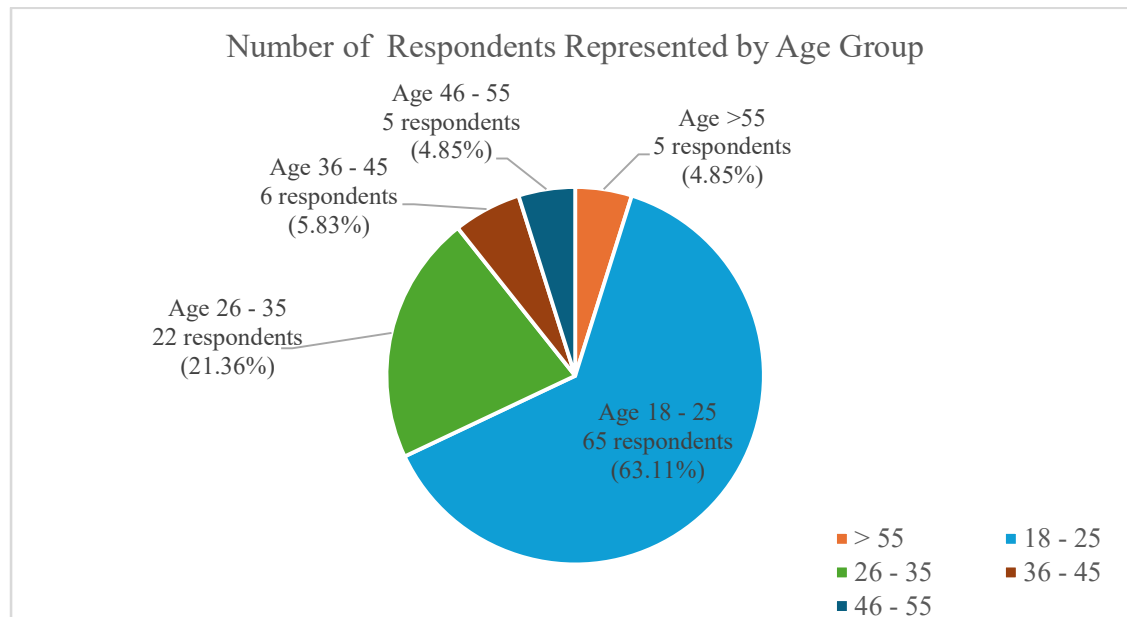
Figure 1. The pie chart on the age groups of 103 respondents in the survey**.** The biggest age group of the respondents is from the age of 18 to 25 at 63.11%, while the lowest is the age group 46 to 55 years old and above 55 years old at 5 respondents, respectively.
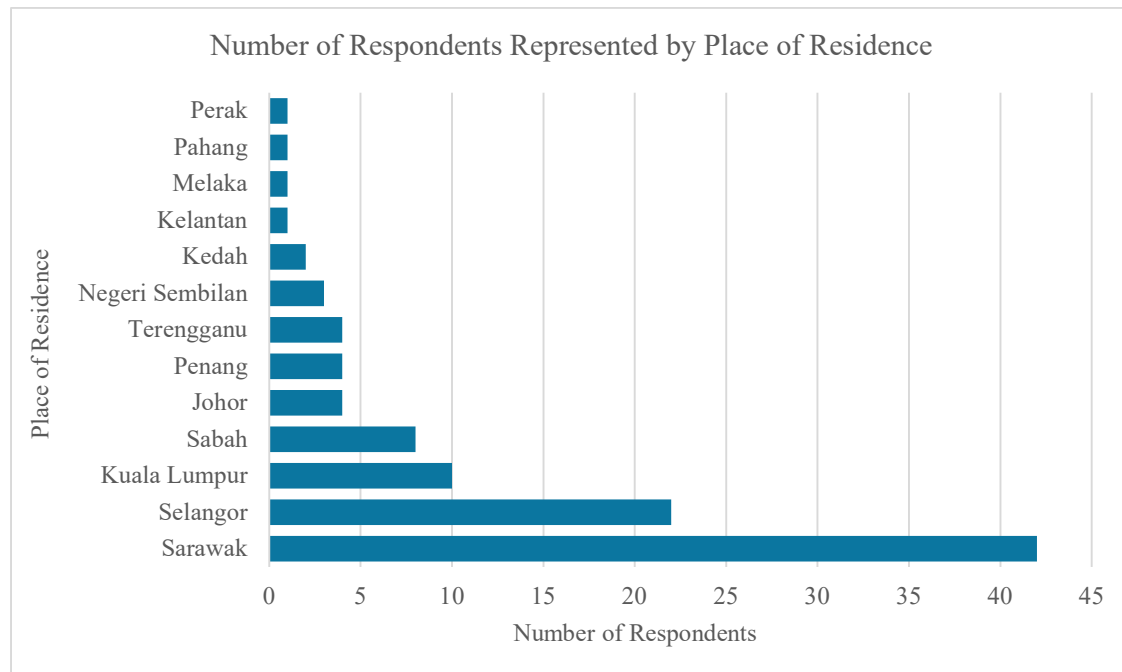
Figure 2. The bar chart on the place of residence of 103 respondents in the survey**.** The highest place of residence of the respondents in the survey is from Sarawak at 42 respondents, while the lowest number was 1 respondent each, from Kelantan, Melaka, Pahang and Perak

Knowledge and Experience

Through the questionnaire, it was found that 64.08% of the respondents were familiar with bats guano (66 respondents), while 37 respondents (35.92%) answered 'no' to the question (Question 6). The chart was presented in Figure 3. Among all of the respondents, the term bats' guano was mostly discovered through word of mouth (42 respondents), scientific readings (34 respondents) and social media (33 respondents) (Question 7). Additionally, 52 of the 66 respondents (78.79%) perceived bat guano in a positive way (Question 8). Few of the respondents' negative view of bats' guano was said due to the unhealthy nature of the bats' guano and the high number of microbes in it (Question 9).

Respondents' experiences in encountering bat guano (Question 10) are varied, with 60.19% (62 respondents) having come across bat guano and 41 respondents (39.81%) having never encountered bat guano before. Most of the respondents said to had encountered bats guano in the cave (51 respondents) while a few had seen it in urban buildings (26 respondents), and only 5 respondents had encountered bat guano or bat guano-derived products in stores (Question 11). Utilisation of bat guano among the respondents is weighted on one response, where 96.12% (99 respondents) have never used bat guano at all (Question 12), three of the respondents used bat guano in less than a year and only one respondent had used bats guano derived product for one to five years (Question 13). The results of the chi square test are shown in Table 2. Through the data, a significant correlation ($p < 0.05$) was only found in the relation between the age group and the positive perception of bat guano, while others were not significant.
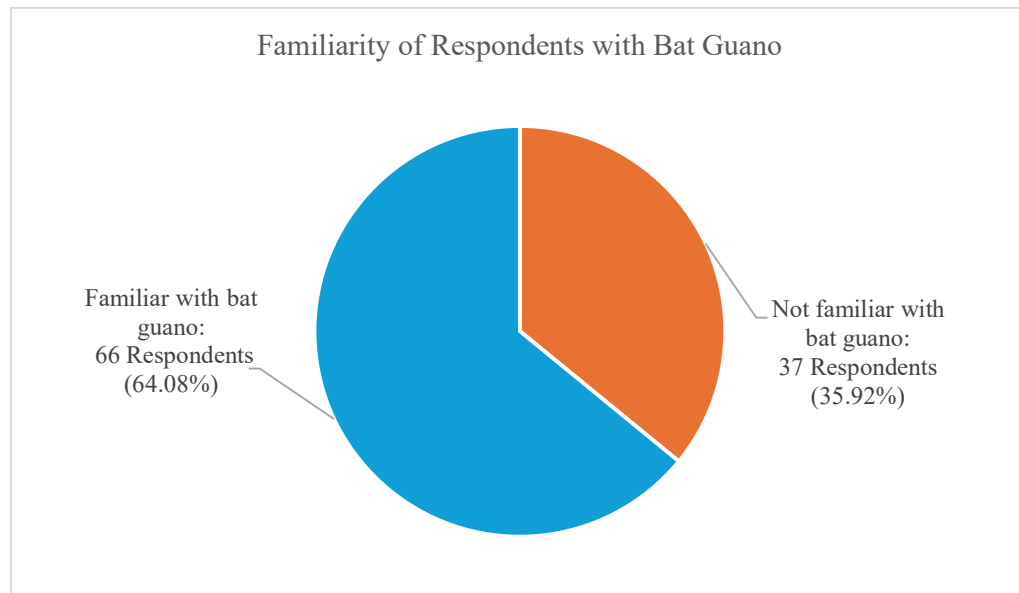
Figure 3. The pie chart on the familiarity with bat guano for 103 respondents in the survey. 66 respondents or 64.08% were found to be familiar with bat guano while the others (37 respondents – 35.92%) are not familiar with bat guano.

Table 2. p values of demographic characters against key knowledge of bats guano by the respondents. Analysis of the chi-square test shows the correlation between the demographics characters and the yes or no variables.

	Gender	Age Group	Level of Education	Place of Residence
Familiarity with the term bats guano	0.346 ± 0.03	0.532 ± 0.17	0.493 ± 0.19	0.398 ± 0.14
Positive perception of bat guano	0.707 ± 0.23	$0.002 \pm 0.28*$	0.254 ± 0.33	0.341 ± 0.03
Had encountered bats guano previously	0.357 ± 0.22	0.838 ± 0.10	0.599 ± 0.04	0.406 ± 0.13
Experience in using bat guano-derived products	0.075 ± 0.21	0.902 ± 0.32	0.874 ± 0.32	0.804 ± 0.04
Understand the importance of bat guano	0.643 ± 0.14	0.976 ± 0.03	0.229 ± 0.29	0.455 ± 0.09

*Note*s: All values are p value ± standard error of P.
*$p<0.05$ The Association between the two variables is statistically significant.

Knowledge of Bats Guano Importance

In the true or false section of the knowledge on the importance of bat guano (Question 15), eight questions were asked about the importance of bats guano which are (a) as plants fertilisers; (b) in carbon dating; (c) as ecosystem stabiliser; (d) as animal's habitat; (e) in the field of research; (f) in traditional medicine; (g) as aesthetical value; and (h) as a product of biomass. The result established that a major number of respondents knew the importance of bats guano as plant fertiliser (99 participants – 96.1%) and in the field of research (98 participants – 95.1%). As expected, a few of the respondents are unaware of the aesthetic value of bats guano (32 participants – 31.1%) and the utilisation of bats guano in carbon dating (36 participants – 35%).

A multiple linear regression analysis in the study examined the relationship between demographic factors (gender, age, place of residence, and level of education) and knowledge of bat guano. The model explained 8.5% of the variance in bat guano knowledge ($R^2 = 0.085$), with an adjusted R^2 of 4.7%, indicating a relatively low explanatory power. Despite this, the overall model was tested for statistical significance. Table 3 presents the regression coefficients for each independent variable. The results indicate that age was the only significant predictor of bat guano knowledge ($p = 0.008$),

suggesting that the age group influenced, the knowledge on bat guano. Gender (p = 0.483), place of residence (p = 0.163), and level of education (p = 0.950) were not statistically significant predictors, indicating that these demographic factors do not have a strong influence on bat guano knowledge in this sample.

Table 3. Analysis of multiple linear regression between the demographics characters and knowledge score of bats guano utilisation

	Coefficient (B)	Std. Error	t-value	Sig. (p value)
(Constant)	5.783	1.191	4.856	<0.001
Gender	0.227	0.322	0.705	0.483
Age	-0.403	0.150	-2.690	0.008
Place of residence	-0.052	0.037	-1.406	0.163
Level of Education	0.015	0.245	0.063	0.950

Final Personal Thoughts

In the final section of the questionnaire, a short passage about bats guano was described as follows.

"Guano" (from the Spanish Quecha: *wanu*) is the accumulation of bats, seabirds and seals' excrement (Ferreira, 2019). Bat guano specifically refers to the excrement of bats. Cave roosts are the main provider of guano (Ghanem and Voigt, 2012). Guano fertiliser is a suitable fertiliser as it has high phosphorus and nitrogen levels (Tuttle and Moreno, 2005). A diverse number of invertebrates inhabit the guano in caves (Ferreira and Martin, 1998). Research on guano can also determine records of environmental changes in the cave in the past (Wurster *et al.*, 2019). Hence, there are multiple values of bats guano that should be inserted into the education syllabus of Malaysia to change the community's perception."

Upon the information, respondents were asked whether they choose to use bats guano in their daily life (Question 16), the results were described in Figure 4. Only 33.01% (34) of the respondent would choose to use bats guano, while eight chose the contrary (7.7%), 61 respondents (59.22%) were undecided. A mixture of age groups was identified in refusing utilisation of bat guano, where two respondents from four age groups (18 – 25, 26 – 35, 36 – 45, and >55) each, answered 'no' to the question.

Question 17 noted that few of the respondents that are unsure in using bats guano is due to the doubtfulness in bats' guano cleanliness and safety while another respondent from the same group answered that bats guano is hard to come by. Respondents that refuse to use bat guano also mentioned on the cleanliness and safety of bat guano, while some respondents from the group admitted on not using any fertilisers in their day-to-day life. One respondent that refused to use bats guano voiced out on the lack of understanding on bats guano importance which shows the vitality on exposure and education regarding the matter.
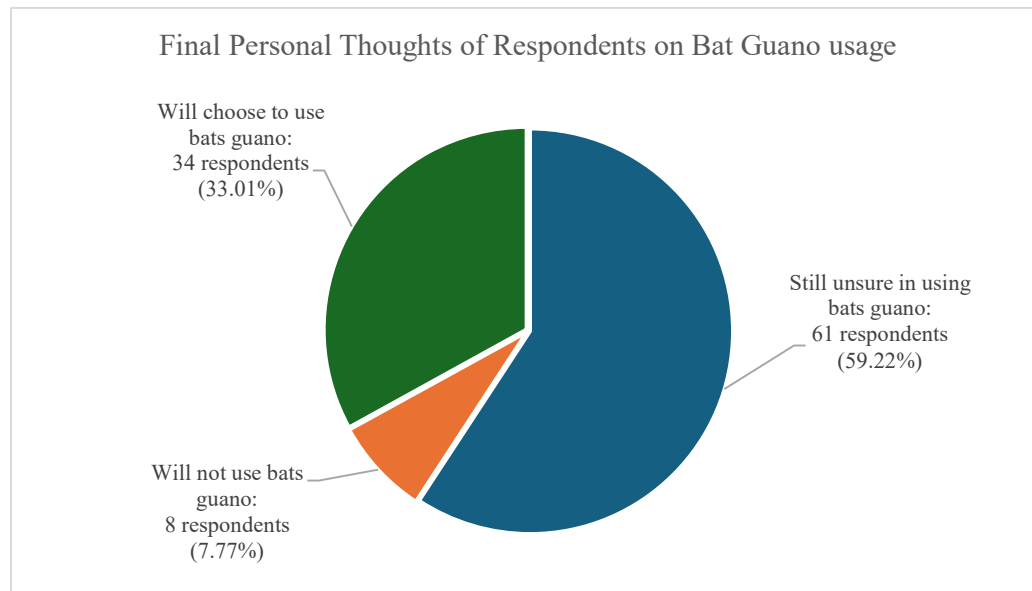
Figure 4. The pie chart on the final personal thoughts of bat guano for 103 respondents in the survey**.** Among the respondents, 61 respondents are still unsure about using bat guano, while 8 respondents refuse to use bat guano in their day-to-day life. 34 respondents expressed willingness to use bat guano.

DISCUSSION

The demographic data revealed a significant concentration of respondents from Sarawak. Despite the survey being distributed across multiple social media platforms and through secondary networks, most responses were collected through the primary researcher's network, which predominantly includes university students aged 18-25 years. This demographic skew reflects the researcher's connections and may impact the generalisability of the results to a broader Malaysian population.

Mixed perceptions of bat guano were discovered through the questionnaire, where 64.1% of the respondents are aware of the presence of bats guano. This is similar to the finding reported by Torres-Jimenez *et al.* (2020) on the perception of bat guano among coffee farmers in Mexico with 59% of the interviewees having little to no knowledge of bat guano benefits to the local community. This is due to the negative perception of the community towards bats as well as feeling fearful of bats (chiroptophobia). The negative perception of the community towards bats is rooted from fearing their appearance, the stigma of bats as a vector of human diseases and viewing bats as 'bloodsuckers' (Torres-Jimenez *et al.*, 2020).

Establishing the channels of information platforms can be the first step in bats' guano introduction and awareness for bat conservation goals. Since word of mouth achieved the highest scoring in introducing bat guano to the survey's participants, an outreach programme through talks and showcase is one of the possible methods in widening the positive viewpoints of bat guano in the community. Responses to the questionnaires vary in terms of the countenance of bat guano and experience in handling bat guano. A major portion of the respondents had never used bat guano-derived products which might be due to the lack of market awareness of bat guano as fertiliser where the study by Kingston *et al.* (2006) recorded that only 3.4% of the survey participants knew about the utilisation of bats guano as fertiliser.

In the current survey, one of the respondents claims the denial of using bat guano products is due to the scarcity of bat guano supplies in stores. Although there are no scientific publications or records to support the claim, through online surfing, the market for bats guano in Malaysia were investigated. The market for bat's guano as organic fertilisers in Malaysia comprises of local producers and international brands, where Pok Asia Marketing which is a local company based in Kelantan, supplies 100% natural and pure bat guano organic fertiliser. Other than that, the company Serbajadi also

offers the Natural Pure Guano fertiliser in their range of products. 'Bat guano fertiliser mix' by international companies 'Down to Earth' and Plagron has also penetrated the Malaysian market. Since the availability of bats guano in local agriculture market is not widespread, the current existing companies that promotes the usage of bats guano as fertiliser in Malaysia is a good model to be expanded nationwide.

The number of respondents who acknowledge the usage of bat guano as plant growth fertiliser and its value in research is high at 96.1% and 95.1%, respectively. This shows a hopeful path for the conservation work of bats guano and bats generally. The data is also reflected in the survey done by Lim and Wilson (2019) where 72.9% of 340 respondents agreed with the utility of bats droppings as organic fertilisers. The increment of percentage between the current survey and the survey done by Lim and Wilson (2019) might be due to the influence of educational level of the participants. Where only 86% of the respondents in the previous study in comparison to 99% of the current study had received or is receiving tertiary education.

However, relations between demographic factors and knowledge of bat guano were found to be independent of one another except for age group and positive perceptions of bat guano. This contradicts the conclusion of surveys done by Lim and Wilson (2019) on the public perception and knowledge of the chiropterans' group, as the research done reported that most demographic factors can affect the communities' knowledge, perception and response to bats. The contradiction could be due to the lack of variability in other demographic factors such as gender, localities and education level that could affect coefficient value of the relations. A higher number of respondents should be sourced through other platforms such as face-to-face interviews, physical questionnaires and phone calls to ensure a wide range of demographic variability can be obtained for a more significant data.

Positive perceptions of bats guano were significantly contributed by the age group. Thornton and Quinn (2009), and Shafie *et al*. (2017) also reached a similar consensus in their study, where it is noted that there is a high association between the knowledge of current wildlife issues and age group. On the topic of bat guano, a major part of the younger age groups had a more positive take towards the usage of bat guano among the community. This might be due to the reliability of social media which is being used largely by the younger groups in information exchange and publications (Auxier & Anderson, 2021). This was supported by the significant correlation between the age group and the knowledge of bat guano's importance coefficients. When looking at the apprehension on the importance of bat guano, the lowest number of results were obtained for recognition of bat guano for aesthetic purposes. Although it is not commonly known and sought for, bat guano was once used as an art medium in the Caribbean and Bulgaria cave art due to its high availability in caves (Samson *et al*., 2017; Sassoni *et al*., 2020).

Finally, the doubt about the cleanliness and safety of bat guano will always be the driving force in the denial of bat guano. Bat guano emits a strong, unpleasant odour due to the high levels of ammonia from decomposed urine and faeces. This strong smell can be off-putting and creates a perception of uncleanliness. The accumulation of guano can also lead to an unsanitary environment, promoting the growth of bacteria, fungi, and other microorganisms, some of which can be harmful to humans (Wasti *et al*., 2021). The perceived filthiness and the health risks associated with these microorganisms contribute to the scepticism around bat guano.

Other than that, with the lingering pandemic of Covid-19 and its devastating casualties, usage of bats-derived products (such as bushmeat, in research and fertilisation) has proceeded with caution. A recent study by Tan *et al*. (2021) in Wind Cave Nature Reserve, Bau, Sarawak found a high diversity of alpha and beta coronaviruses which are unique to Borneo Island in almost half of the samples collected. This study which was done in the heights of Covid-19 pandemic was expected to add on the negative perception of the utilisation of bats guano in day-to-day activities. Considering the current issues influencing the bats and bats guano perception, the survey found that more than a quarter of the respondents would choose to use bat guano in their daily life at the end of the questionnaire which shows the willingness of Malaysian community in switching to an organic material in fertilisation as well as utilising bats guano efficiently.

The study on the health hazards of bat guano increased an urge for better management of health safety in bat guano collection (Jayasvasti & Jayasvasti, 2018). This can be done through training and management systems that can be empowered by the government (Jayasvasti & Jayasvasti, 2018). Further research and education on the utilisation of bat guano in Malaysia and the steps to handle them are of the utmost importance to ensure an improvisation of bat guano benefit in the eyes of Malaysian perspective. Strategic approaches to increasing acceptance and awareness of bats guano can be planned thoroughly using education and advocacy through platforms social media and scientific publications. Other than that, policies on the training and management system of bat guano utilisation should also be outlined in by Malaysian governments to safely manage the collection of guano and to control the disruption of the ecosystem in guano harvesting.

CONCLUSION

Bat guano utilisation has been proven throughout the centuries. From the usage of bat guano as gunpowder to its vast usage in the agriculture industry, tapping into the reservoir of bat guano can be beneficial to the economy. Despite that, the acceptance of bat guano in the Malaysian community is still lacking. The study highlights the mixed perceptions of bat guano among the Malaysian public, with significant awareness but persistent concerns regarding cleanliness, safety, and potential health risks. The significant demographic factor of age group affecting the perception of bats guano in the community suggests a growing acceptance of bat guano, influenced by higher education levels and social media exposure. However, factors such as fear of bats, stigma, and limited market awareness will continue to restrict acceptance and usage. Future research should explore changes in public perception over time, particularly in response to educational initiatives. Health risk assessments related to guano use, economic market studies, and ecological research on harvesting impacts are also essential. Furthermore, establishing standardised methods for guano collection and processing can improve quality control and consumer confidence. With comprehensive education, scientific advocacy, and government-backed safety measures, bat guano has the potential to become a widely accepted and valuable resource in both economic and environmental contexts.

ACKNOWLEDGEMENTS

REFERENCES

Auxier, B. & Anderson, M. (2021). *Social media use in 2021.* Pew Research Center. https://www.pewresearch.org/internet/2021/04/07/social-media-use-in-2021/. Downloaded on 20 January 2025.

Fenolio, D.B., Graening, G. O., Collier, B. A. & Stout, J. F. (2006). Coprophagy in a cave-adapted salamander; The importance of bat guano examined through nutritional and stable isotope analyses. *The Royal Society B: Biological Sciences,* 273(1585): 439-443. DOI: 10.1098/rspb.2005.3341

Ferreira, R. L. & Martins, R. P. (1998). Diversity and distribution of spiders associated with bat guano piles in Morrinho cave (Bahia State, Brazil). *Diversity and Distribution,* 4(5), 235-241.

Ferreira, R. L. & Martins, R. P. (1999). Trophic structure and natural history of bat guano invertebrate communities, with special reference to Brazilian caves. *Tropical Zoology,* 12(2): 231-252. DOI: 10.1080/03946975.1999.10539391

Ferreira, R.L. (2019). Guano communities. In White, W. B., Culver, D. C., and Tanja, P. (eds.) *Encyclopedia of caves*. Massachusetts, United States, Academic Press. pp. 474-484.

Ghanem, S. J. & Voigt, C.C. (2012). Increasing awareness of ecosystem services provided by bats. In Brockmann H. J., Roper T. J., Naguib M., Mitani, J. C., Simmons L. W. (eds.) *Advances in the Study of Behavior Vol. 44.* Massachusetts, United States, Academic Press. pp. 279-302.

Harris, J. A. (1970). Bat-guano cave environment. *Science,* 169(3952): 1342-1343. DOI: 10.1126/science.169.3952.1342.c

Harouna, K. A., Tidjani, A. D., Fanna, A. G. & Yadji, G. (2021). Bats guano from Magarawa in Niger: Exploitation, marketing and peasant perception. *International Journal of Innovation and Applied Studies, 32*(3), 426-436.

Jayasvasti, I. & Jayasvasti, M. (2018). Bat guano as the component of fertiliser or the health hazard? *Southeast Asian Journal of Tropical Medicine and Public Health,* 49(2), 331-339.

Kanuch, P., Hajkova, Z. Rehak, R. & Bryja, J. (2007). A rapid PCR-based test for species identification of two cryptic bats *Pipistrellus pipistrellus* and *P. pygmaeus* and its application on museum and dropping samples. *Acta Chiropterologica,* 9: 277–282. DOI: 10.3161/150811007781694516

Karagoz, K. (2014). Bat guano in agricultural production. *Alınteri Zirai Bilimler Dergisi, 27*, 35-42.

Kingston, T., Zubaid, A., Lim, G. & Hatta, F. (2006). From research to outreach: Environmental education materials for the bats of Malaysia. In Yahya, N.A., Philip, E. and Ong, T. (eds.) *Proceedings of the Best of Both Worlds International Conference on Environmental Education for Sustainable Development,* 6–8 September 2005, Kuala Lumpur, Forest Research Institute Malaysia (FRIM). pp. 21-29

Lim, V. C. & Wilson, J. J. (2019). Public perceptions and knowledge of, and responses to, bats in urban areas in peninsular Malaysia. *Anthrozoos,* 32(6): 825-834. DOI: 10.1080/08927936.2019.1673063

Linn, K. Z. & Myint, P. P. (2018). Study on the effectiveness of natural organic fertilisers on cassava (*Manihot esculenta* Crantz.) cultivation. *Asian Journal of Soil Science and Plant Nutrition,* 3(3): 1-10. DOI: 10.9734/AJSSPN/2018/42912

McFarlane, D. A. & Lundberg, J. (2018). New records of guano-associated minerals from caves in northwestern Borneo. *International Journal of Speleology,* 47(2): 119-126. DOI:10.5038/1827-806X.47.2.2169

Puechmaille, S. J., Mathy, G. & Petit. E. J. (2007). Good DNA from bat droppings. *Acta Chiropterologica*, 9: 269–276. DOI: 10.3161/150811007781694435

Sakoui, S., Derdak, R., Addoum, B., Serrano-Delgado, A., Soukri, A. & El Khalfi, B. (2020). The life hidden inside caves: Ecological and economic importance of bat guano. *International Journal of Ecology,* 2020: 1-7. DOI: 10.1155/2020/9872532

Samson, A. V., Wrapson, L. J., Cartwright, C. R., Sahy, D., Stacey, R. J. & Cooper, J. (2017). Artists before Columbus: A multi-method characterization of the materials and practices of Caribbean cave art. *Journal of Archaeological Science,* 88: 24-36. DOI: 10.1016/j.jas.2017.09.012

Sexton, N. R. & Stewart, S. C. (2007). *Understanding knowledge and perceptions of bats among residents of Fort Collins, Colorado.* Colorado: US Geological Survey.

Sassoni, E., Franzoni, E., Stefanova, M., Kamenarov, Z., Scopece, P. & Verga, F. E. (2020). Comparative study between ammonium phosphate and ethyl silicate towards conservation of prehistoric paintings in the Magura cave (Bulgaria). *Coatings,* 10(3): 250. DOI: 10.3390/coatings10030250

Shafie, N. J., Sah, S. A. M., Mutalib, A. H. A. & Fadzly, N. (2017). General perceptions and awareness level among local residents in Penang Island toward bats conservation efforts. *Tropical Life Sciences Research,* 28(2): 31-44. DOI: 10.21315/tlsr2017.28.2.3

Sothearen, T., Furey, N. M. & Jurgens, J. A. (2014). Effect of bat guano on the growth of five economically important plant species. *Journal of Tropical Agriculture,* 52(2), 169-173.

Suwannarong, K., Balthip, K., Kanthawee, P., Suwannarong, K., Khiewkhern, S., Lantican, C., Ponlap, T., Bunhap, N. & Amonsin, A. (2020). Bats and belief: A sequential qualitative study in Thailand. *Heliyon,* 6(6): e04208. DOI: 10.1016/j.heliyon.2020.e04208

Tan, C.S., Noni, V., Seelan, S., J. S., Denel, A. & Khan, F. A. A., (2021). Ecological surveillance of bat coronaviruses in Sarawak, Malaysian Borneo. *BMC Research Notes,* 14(1): 1-6. DOI: 10.1186/s13104-021-05880-6

Tanalgo, K.C., Teves, R. D., Salvana, F. R. P., Baleva, R. E. & Tabora, J. A. G. (2016). Human-bat interactions in caves of South-Central Mindanao, Philippines. *Wildlife Biology in Practice,* 12(1): 1-14. DOI: 10.2461/wbp.2016.12.2

Thornton, C. & Quinn, M. S. (2009). Coexisting with cougars: public perceptions, attitudes, and awareness of cougars on the urban-rural fringe of

Calgary, Alberta, Canada. *Human-Wildlife Conflicts,* 3(2): 282–295. DOI: 10.26077/xvx2-ba39

Torres-Jiménez, M. G., Murrieta-Galindo, R., Bolívar-Cimé, B., Wojtarowski-Leal, A., & Piñar-Álvarez, M.Á. (2020). Coffee farmers' perception of bat guano as fertiliser in agroecosystems of Mexico. *Regions and Cohesion,* 10(1): 22-35. DOI: 10.3167/ reco.2020.100103

Tuttle, M. D. & Moreno, A. (2005). Cave-dwelling bats of Northern Mexico: Their value and conservation needs. In Kunz, T. H., and Fenton, M. B. (eds.) *Bat Ecology.* Illinois, United States, University of Chicago Press. pp. 49-62.

Ware, R. L., Garrod, B., Macdonald, H. & Allaby, R. G. (2020). Guano morphology has the potential to inform conservation strategies in British bats. *Public Library of Science ONE,* 15(4): e0230865. DOI: 10.1371/journal.pone.0230865

Wasti, I. G., Khan, F. A. A., Bernard, H., Hassan, N. H., Fayle, T. & Sathiya, J. S. S. (2021). Fungal communities in bat guano, speleothem surfaces, and cavern water in Madai cave, Northern Borneo (Malaysia). *Mycology,* 12(3): 188-202. DOI: 10.1080/21501203.2021.1877204

Wurster, C. M., Rifai, H., Zhou, B., Haig, J. & Bird, M. I. (2019). Savanna in equatorial Borneo during the late Pleistocene. *Scientific reports,* 9(1): 1-7. DOI: 10.1038/s41598-019-42670-4

Microplastics Quantification in *Meretrix lyrata* through Rapid Screening Method using Nile Red

NGIE-HAO ERIC LAU[1*], AAZANI MUJAHID[1*], CINDY PETER[2] & MORITZ MÜLLER[3]

[1]Faculty of Resource Science and Technology, Universiti Malaysia Sarawak, 94300 Kota Samarahan, Sarawak, Malaysia; [2]Institute of Biodiversity and Environmental Conservation, Universiti Malaysia Sarawak, 94300 Kota Samarahan, Sarawak, Malaysia; [3]Faculty of Engineering, Computing and Science, Swinburne University of Technology Sarawak Campus, Kuching, Sarawak, Malaysia
*Corresponding author: 18020217@siswa.unimas.my; maazani@unimas.my

ABSTRACT

Microplastics have emerged as a significant form of plastic pollution. Many ingestions in biota were reported worldwide. Filter feeder such as bivalves are prone to microplastics ingestion due to the non-selective feeding behavior. Bivalves are usually consumed as whole, without gut removal, which can pose a threat towards human consumption. This study focused on *Meretrix lyrata* to examine the level of microplastics ingestion under two factors: size class and weather seasons. The rapid screening approach with the fluorescent tagging using Nile red on microplastics for biota samples was used to quantify *M. lyrata* samples ($n = 81$) in this study. The high lipid content of the clams presented a significant challenge to the effectiveness of the method. As an alternative, high temperatures from acidification were used to disrupt lipid membranes and improve extraction efficiency. A total of 15,867 microplastics were quantified, with the average microplastics ingestion of 195.90±43.6 items/individuals. The statistical analysis indicated that clam size had a significant effect on the rate of microplastics ingestion ($p<0.05$), whereas weather season did not show a significant effect ($p>0.05$). Polyvinylchloride (66.5%), polypropylene with silicate mix (8.5%), resin dispersion (8.5%) and polydimethylsiloxane (16.5%) were from the 12 isolated items. The higher rate of microplastics ingestion observed in smaller clam size *M. lyrata* and similar rate between weather season (dry season and wet season) indicate that these contaminated seafood increases the human exposure through consumption. The type of polymer identified in this study indicate that most of the microplastic may sources from human daily products.

Keywords: Fluorescent tagging, High lipid content samples, Microplastics, Nile red, Rapid screening method

INTRODUCTION

Plastics pollution have become a prominent environmental issue in aquatic environments. The increasing demand for plastic in various industries is due to its low cost, strength, durability, corrosion resistance, and good thermal and electrical insulation properties (Geyer *et al*., 2017). However, plastics have, finite lifespans and are quickly discarded, often ending up in landfills, being burned, or littering the environment. Research indicates that plastic materials constitute 95% of floating marine debris (Lebreton *et al*., 2018). The persistence of plastics in the environment is the primary factor contributing to their dominance as the leading component of marine debris (Auta *et al*., 2017).

Among the various forms of plastic pollution, small plastic particles typically less than 5 mm in size which also commonly known as microplastics have emerged as a critical environmental contaminant. These particles originate from direct source as such personal care products, industrial processes and synthetic textiles (primary microplastics) and from the degradation of larger plastic items (secondary microplastics) (Hartmann *et al*., 2019). Their minute sizes and extensive distribution make them particularly challenging, as they penetrate even the most secluded aquatic ecosystems, from freshwater rivers to deep-sea sediments.

The small size of microplastics leads to increase accumulation of contaminants due to their hydrophobic nature and high surface area (Shahul Hamid *et al*., 2018; Deng *et al*., 2021). Microplastics pollution has been reported in many marine ecosystems worldwide due to massive input from land source, the persistence

of microplastics in environment and the fact that they are readily transported by ocean current (Lavers & Bond, 2017; Brach *et al.*, 2018; Reed *et al.*, 2018). Lebreton *et al.* (2019) suggested that buoyant macroplastic accumulate in offshore surface water should be lesser than predicted as a series of repeated activity like stranding, settling and resurfacing in coastal environment tend to trap most of the marine litters. The intertidal zone, situated between land and ocean, experiences more human activity compared to other marine environments and can be exposed to microplastics from both land-based and marine sources (Cole *et al.*, 2011; Zhang *et al.*, 2020; Zhang *et al.*, 2022).

Rapid screening method using fluorescent tagging is a new alternative to aid in increasing the precision of the microplastics quantification and identification through visual identification. Nile red is recommended by Maes *et al.* (2017) as the dye for fluorescent tagging due to the lipophilic characteristics, which allow selective staining of plastic polymers when appropriate protocols are employed.

Microplastics pose significant risks to aquatic organisms and can enter the food webs, as they can be ingested by organisms (Hasbudin *et al.,* 2022). *M. lyrata* is particularly susceptible to microplastic ingestion due to its filter-feeding behavior (Woods *et al.,* 2018). Chinfak *et al.* (2021) had shown the possibility of higher microplastics ingestion rate of in small-sized shellfish for *Perna viridis* and *M. lyrata*. Similar trends were also reported in *Mythilus edulis* and *Donax cuneatus* (Scott *et al.,* 2019; Sathish *et al.*, 2020). Studies reported negative effects of microplastics on bivalves such as reduced filtration activity and altered feeding behavior (Rist *et al.,*2016; Green *et al.,* 2017), potentially causing physical and chemical stress (Woods *et al.,* 2018), impairing feeding efficiency, and acting as vectors for harmful substances such as persistent organic pollutants (POPs) (Zhang *et al.,* 2020) and heavy metals (Fu *et al.,* 2020; Idrus *et al.,* 2022a). This not only impacts the health of *M. lyrata* populations but also raises significant concerns about the transfer of microplastics and associated contaminant to humans through the consumption of contaminated seafood.

Despite increasing research research on microplastics in aquatic ecosystems, there remains a critical need to understand the specific pathways, interactions, and impacts of microplastics on key species such as M. lyrata. Previous studies (Kolandhasamy *et al.*,2018; Li *et al.*, 2019; Hasbudin *et al.*, 2022) highlight three pathways of microplastic accumulation in mussels including ingestion, adherence and fusion. Tang *et al.* (2022) suggested quantifying amount of microplastics in clams could provide insight of microplastics contamination in intertidal zones and thus suggested their use as a bio-indicator for environmental monitoring of microplastics.

As bivalves have high potential to serve as bioindicators (Ding *et al.*, 2021) for microplastics pollution in sediment and water, investigating the prevalence of microplastics in *M. lyrata* and their surrounding habitats is essential for assessing ecosystem health and potential risks to food safety, where these organisms can serve as vectors, transferring microplastics to humans.

Thus, the aims of this study were to quantify microplastics in *M. lyrata* and to address the impact of size classes and weather seasons towards microplastics ingestion in *M. lyrata*.

MATERIALS AND METHODS

The laboratory benchtop was cleaned, and surfaces were wiped with 70 % ethanol using a cotton cloth. A full cotton lab coat and nitrile gloves were worn during the experiment. All solutions (distilled water, 10 % potassium hydroxide (KOH), zinc chloride (ZnCl$_2$), 10 % hydrochloric acid (HCl) were pre-filtered with 0.5 μm Whatman GC50 filter paper to prevent contamination from other sources. Filter papers used were GF/C (ADVANTEC GC-50, 0.5 μm). Apparatus materials were either glass or stainless steel. Glassware and stainless-steel tweezers were pre-cleaned with filtered deionized water and rinsed with filtered 70 % ethanol.

Sample Processing and Microplastics Extraction

The clams (n = 81) with random sizes were purchased from the local fish market in Kampung Buntal (1° 41' 43.58" N, 110° 22' 19.87" E), from October 2020 to March 2021. The determination of monsoon seasons was

based on the dates provided by the Malaysian Meteorological Department (May 2020 – September 2020: Southwest monsoon; November 2020 – Mac 2021: Northeast monsoon). Additionally, Kampung Buntal is one the most active artisanal fishing communities in Kuching Bay where there is an overlap between fisheries activities with cetacean occurrence (Ambie *et al*., 2023).

Upon acquisition, the clams were stored in a freezer at –20 °C after their shells were rinsed with filtered distilled water to remove any surface contaminants. For subsequent processing, the clams were thawed to room temperature, then each clam was dissected, and transferred into a glass bottle for digestion process.

The KOH digestion method was based on the study by Lusher and Hernandez-Milian (2018), where the details of this protocol can be found in their study.

After the digestion process, the microplastics in the clam samples were separated by applying density separation technique based on the study by Maes *et al*. (2017) using $ZnCl_2$ to reduce the possible interference from other non-plastic substances such as shell, wood, sand and clay.

An additional step adapted from Prata *et al*. (2021) is added prior to the density separation steps as clogging and precipitation were observed. High temperature can aid in disrupt lipid membranes and improve extraction efficiency. Acidification is an exothermic process which can achieve the mentioned condition to reduce clogging and prevent precipitation.

Nile Red Staining for Quantification of Microplastics

Nile red stock solutions were prepared in propanol with the ratio of 1:100. Approximately 0.06 g of Nile red powder were measured and mixed with 60 ml of propanol. The stock solution was then stored in a 60 ml Scott bottle pre-wrapped with aluminum foil and kept at 4 ˚C. The stock solution was diluted 100 times in filtered distilled water to make a working solution (1 mg/ml). The filtrate (microplastics) collected from density separation were pre-washed with a small volume of 10 % HCl to remove residual $ZnCl_2$. Subsequently, 10 ml of the Nile red working solution were added to the microplastics and left for 10 – 15 minute to obtain optimum staining results. After staining, the excess Nile red solution was removed by filtering, and the stained microplastics on the filter paper were washed with a small amount of filtered distilled water to eliminate any remaining excess dye.

Lowering the pH of the digested residue extract (10 % HCl) improved the dissolution, thus increased the filtration rate and inhibited precipitation when mixed with $ZnCl_2$. To avoid quenching and false positives (Erni-Cassola *et al*., 2017), additional steps were incorporated.

The filter paper with stained microplastics, was then placed in an automated filter-scanning rig (Maes *et al*., 2017) combines with a commercial micro-milling machine and a DSLR (EOS 90D) camera that was adjusted to create a dim background to enhance the visibility of the fluorescent microplastics. G-code routines controlled the scanning process, dividing the 47 mm filter paper into 24 segments, with each segment being captured individually. This segmentation aimed to produce detailed images with minimal noise, thereby reducing counting errors during the quantification process.

After that, the optimized samples images were illuminated with blue light (Crime Lite: 450 – 510 nm) and viewed through an orange filter (529 nm). The resulting photographs were then processed using ImageJ software, and saved in TIFF format. The camera settings were calibrated individually for each sample. Prata *et al*. (2020) noted that higher ISO settings tend to introduce more noise and defects in images, thus a lower ISO setting was employed in this study in combination with a longer exposure time (2s).

The TIFF images were reviewed and analyzed to quantify the amount of microplastics, which were identified as fluorescent particles.

Verification of Microplastics using ATR-FTIR

The polymers of the microplastic samples were identified by using The Nicolet IN10 ATR-FTIR (Thermo Scientific). Spectra ranges were set at $4000 – 675$ cm^{-1}, with resolution of 4 cm^{-1} and 32

scans s^{-1}. The resulting spectra were directly compared with the available open-source database OpenSpecy (www.openspecy.org; Cowger *et al*., 2021).

Statistical Analysis

Morphometric data and quantitative data were compiled and tabulated using Microsoft Excel to compare different size classes and different weather seasons. Statistical test was conducted to analyze the significant differences of microplastics ingestion by difference sizes of bivalve and weather seasons. Normality tests were done to determine data sets were close to normal or skewed data. Student's T test was used as the parametric test if the data sets were normally distributed, while the Mann-Whitney U test was used as the non-parametric test if the data sets were not normally distributed.

RESULTS AND DISCUSSION

Microplastics Quantification in *M. lyrata*

A total of 81 clams with variant of clam size were tested for microplastic counts resulting with 12 to 1047 items/individual. A total of 15,867 items were detected, with an average of 195.90±43.6 items/individual.

The average microplastic counts obtained from current study is higher than other findings nearby countries in the same species (*M. lyrata*) 12.73±4.49 items/individual, 13.20±7.66 items/individual (Tran-Nguyen *et al*., 2023), 3.6±2.1 items/individual (Kieu-Le *et al*., 2022) and 0.67±0.15 items/individual (Chinfak *et al*., 2021).

These differences might be due to the method chosen for digestion and separation (Kieu-Le *et al*., 2022; Tran-Nguyen *et al*., 2023). Quinn *et al*. (2017) suggested to use denser solution (such as $ZnCl_2$) for density separation to get higher recovery rates. Study by Zarlf (2019) found out that extracting lower density microplastics using NaCl solution might fail if the plastic particles were agglomerated with mineral particles. Chinfak *et al*. (2021) and Idrus *et al*. (2022b) used oxidative digestion using 30 % hydrogen peroxide (H_2O_2) to degrade labile organic matters. However, Nuelle *et al*. (2014) advised the usage of oxidative digestion method should be only applied to organic rich samples because of the bleaching effect that might aggravate the visual detection process and cause potential exothermic reaction with other chemicals (NaCl) for density separation.

In this study, the *M. lyrata* samples were divided into 6 size classes in which (0 – 29.99 mm, 30.0 – 39.99 mm, 40.0 – 49 mm) representing small size classes and (50.0 – 59.99 mm, 60.0 – 69.99 mm, 70.0 – 79.99 mm) representing big size classes. The microplastics ingestion in smaller sized class clam (0 – 49.9 mm) with the average of 218.63±54.78 items/individual compared to size class (50.0 – 99.9 mm) with the average of 166±68.86 items/individual. Figure 1 shows the number of microplastics ingestion according to size classes.

Prior to analysis, the data set were identified as not normally distributed, non-parametric analysis, Mann-Whitney U test was used. The Mann-Whitney U test revealed a statistically significant difference in the number of microplastics ($p<0.05$), (U= 553, |z| = 2.40, p= 0.018) between the clam size less than 50 mm and the clam size more than 50 mm.

Chinfak *et al*. (2021), obtained about a similar trend where smaller size of Mytilus edulis and M. lyrata recorded higher microplastic particles compared to the larger sizes. Scott *et al*. (2019) and Sathish *et al*. (2020) also reported similar patterns in M. edulis and Donax cuneatus. Woods *et al*. (2018) reported certain bivalves are selective filter feeders with the ability to reject some of the ingested particles such as microplastics through excretion. The capacity of ingestion, accumulation and digestion may differ according to habitat, size, surface characteristics, and concentration microplastics.
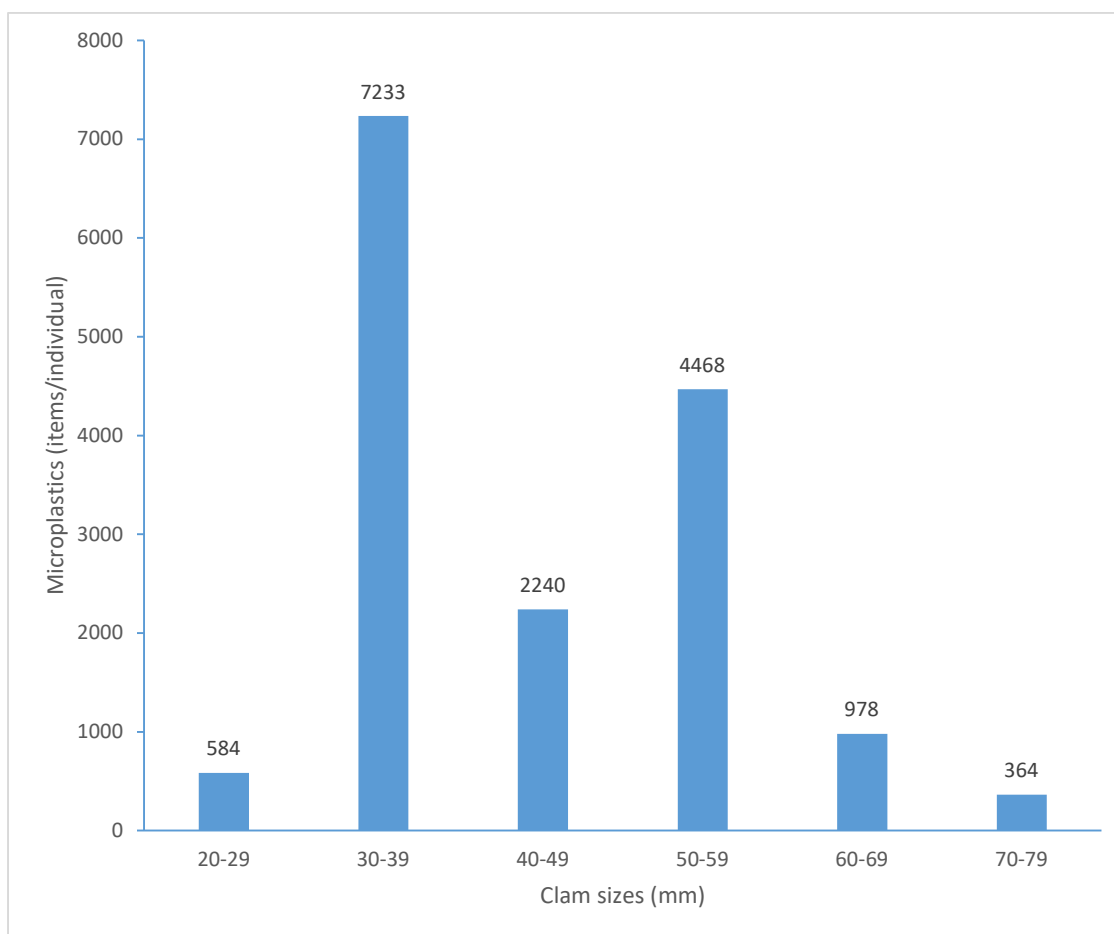
Figure 1. The amount of microplastic ingested by *M. lyrata* according to different size classes which further categorised into small size (<50mm) and large size (>50mm)

The samples were also tested microplastics ingestion according to weather season. The average microplastics ingestion of *M. lyrata* during the dry season is 174.86±21.2 items/individual and is 212.71±71.14 items/individual during the wet season. Figure 2 shows the number of microplastics ingested according to weather seasons. Mann-Whitney U test revealed no significant difference in the number of microplastics (p<0.05), (U= 752, |z| = 0.55, p= 0.581) between the dry season and the wet season.
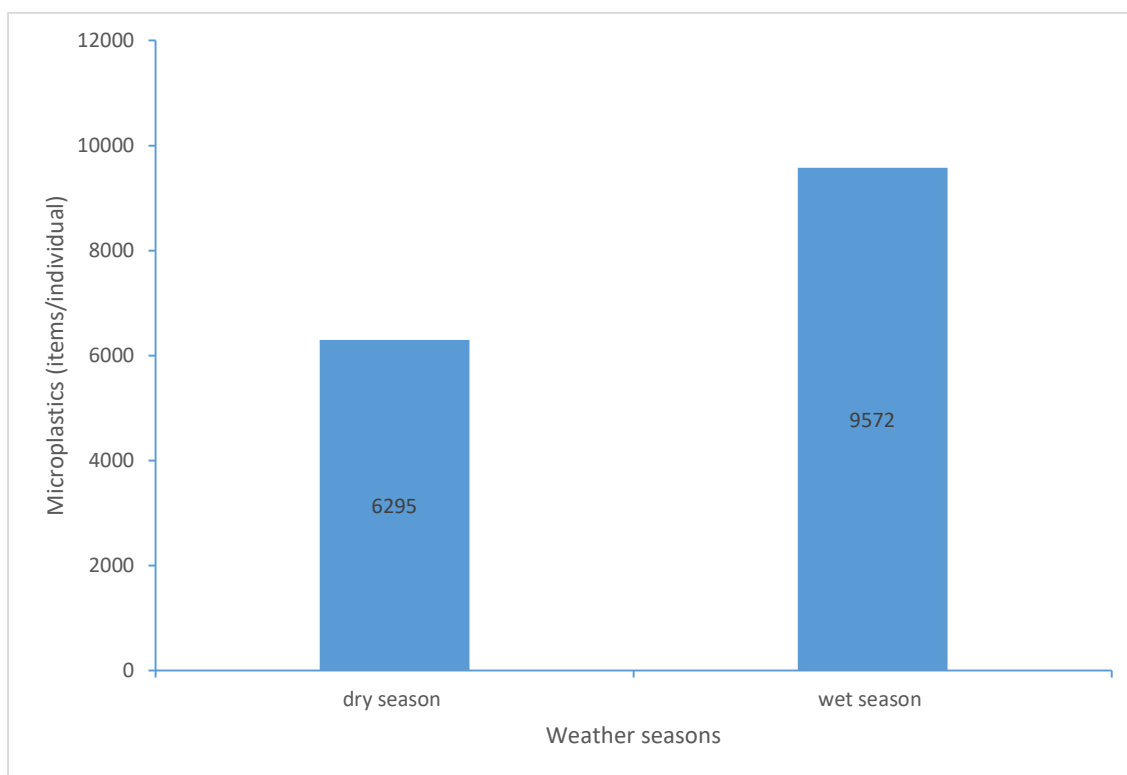
Figure 2. Amount of microplastics ingested by *M. lyrata* according to different weather seasons

The possible microplastics input for the study site is through both land input (human settlement area), input through river systems (oil palm plantation, aquaculture farm) and input through tidal change as well as wave activities. Figure 3 shows the map of the study sites with different land use zonation identified.
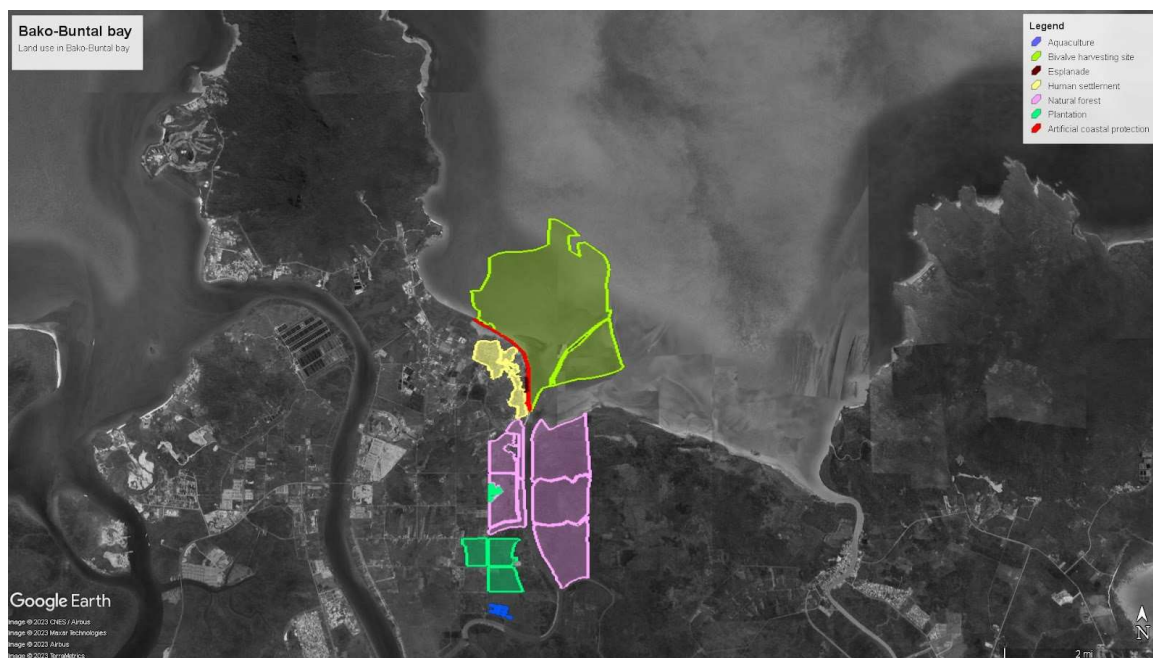
Figure 3. Map of the study site (Kampung Buntal) with the land use surrounding the study site identified based on outcome from informal interviews with the local clam collectors and spatial data from Google Earth.

The zonation indicated in the map were derived from informal interviews with the local bivalve collectors and interpretations based on satellite imagery through Google Earth.

Lebreton *et al*. (2019) hypothesized that most of the plastic marine debris should be settling in the coastal environment through a series of processes such as stranding, settling and resurfacing process. The mentioned process can also break down the bigger plastic marine debris into smaller microplastics (through physical abrasion), therefore the plastic marine debris and the byproduct (microplastics) will be highly polluting the habitat of the *M. lyrata*. Wu *et al*. (2020) reported higher microplastics abundance in surface sediment of intertidal zone during neap tide cycles compared to spring tide cycles. The microplastics settled at surface sediment during the neap tide cycle can either be brought away by strong tidal actions during spring tide cycles or buried in the sediment column. *M.*

lyrata as one of the common bivalves inhabits at intertidal zone were highly at risk of microplastics contamination due to the high bioavailability of microplastics within the region.

Polymer Identification Result

About 12 items were isolated for polymer identification due to limitation. 4 plastic polymers were identified in which polyvinyl chloride (PVC) (8 samples), polydimethylsiloxane (PDMS) (2 samples), resin dispersion (1 sample), and polypropylene with silicate mix (PP with silicate mix) (1 sample). Figure 4a shows the type of polymer identified from the isolated items and Figure 4b shows the result of spectral comparison with OpenSpecy database of the polymers. Figure 4c shows some photos of the isolated items to be process with polymer identification using Nicolet IN10 ATR-FTIR (Thermo Scientific).
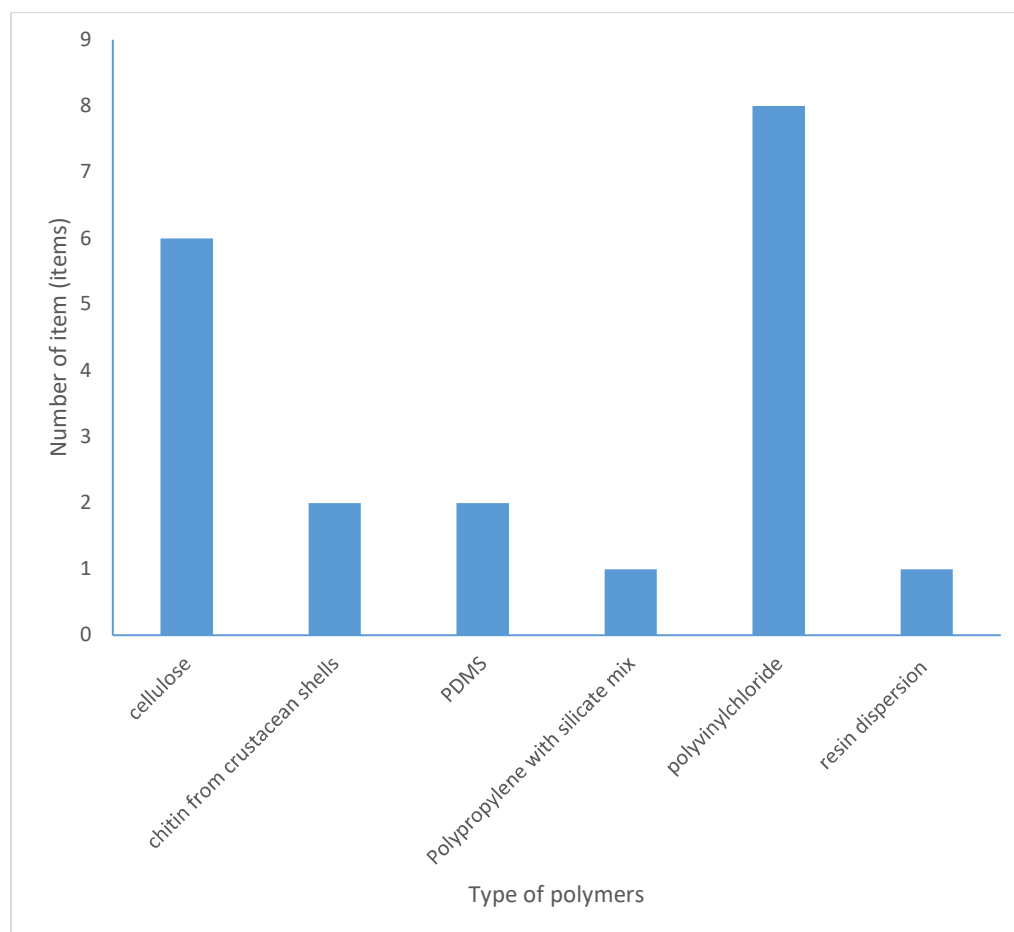
Figure 4(a). Four (4) types of identified polymers (polydimethylsiloxane, polypropylene with silicate mix, polyvinylchloride and resin dispersion) sorted according to the size class and harvesting season of the clam in which the microplastics were isolated for polymer identification.
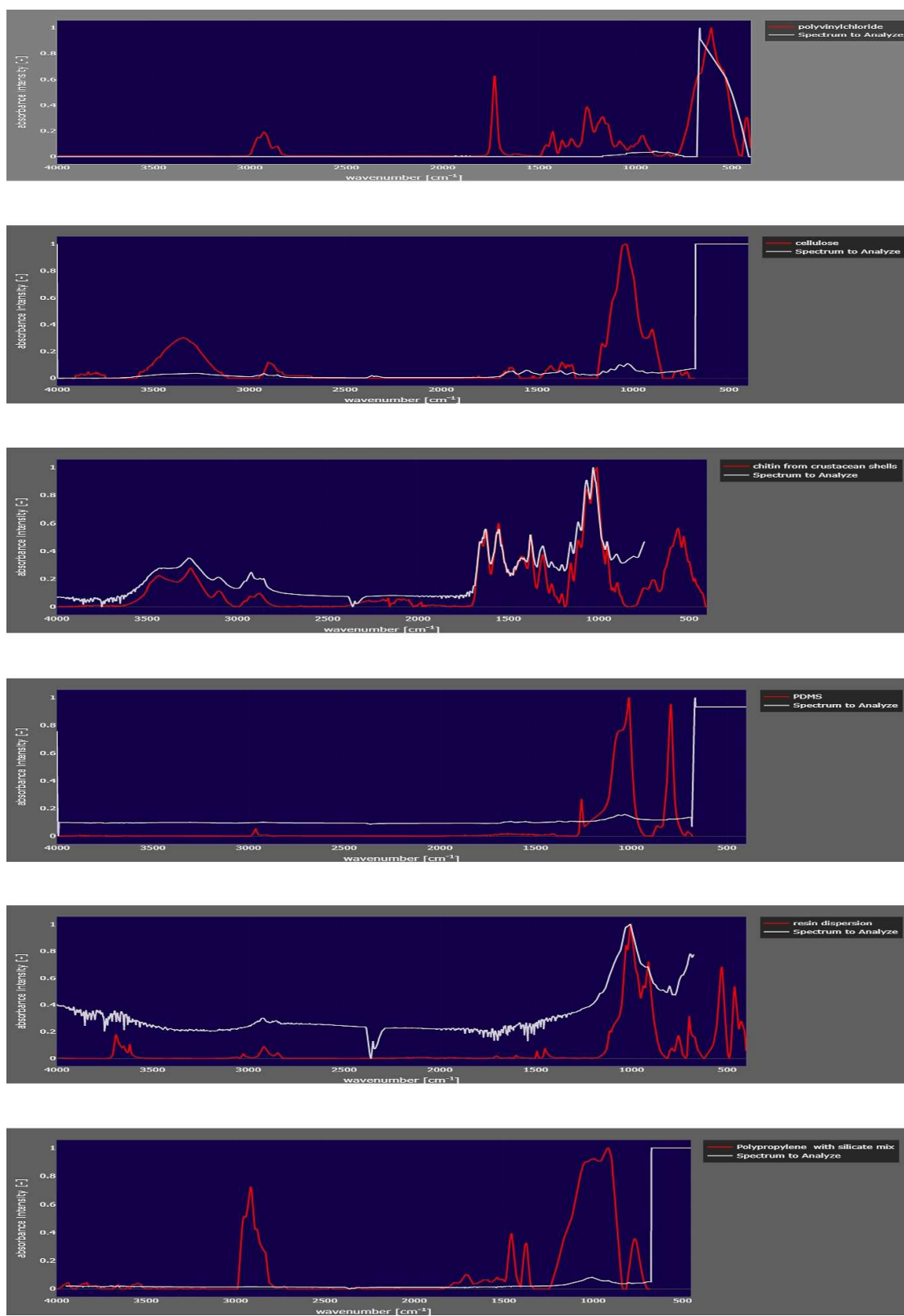
Figure 4(b). Comparison of the spectral data from the isolated items spectral comparison of the isolated particles with OpenSpecy database.
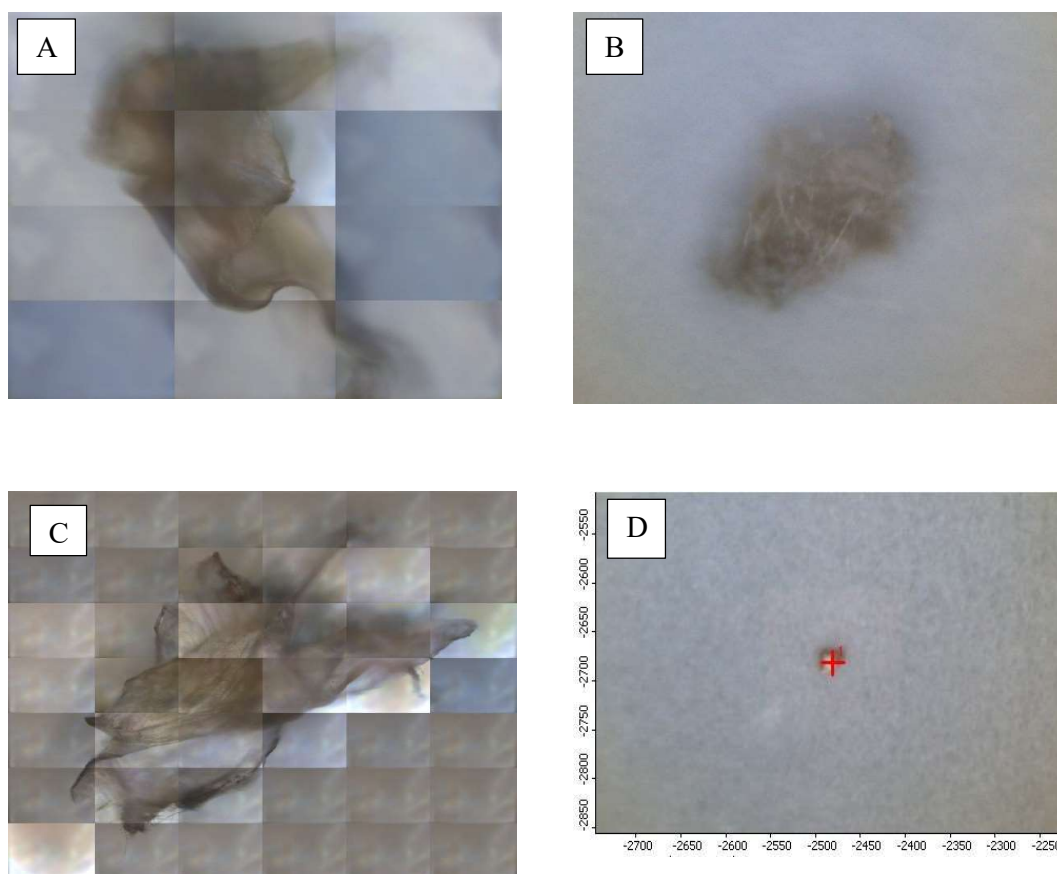
Figure 4(c). Photos of the isolated items to be process with polymer identification using Nicolet IN10 ATR-FTIR (Thermo Scientific). A, B and C are fragment and D particles.

Local publications also reported similar detection of plastic polymer, polyvinyl chloride and polypropylene in both *Corbicula fluminea* and *Polymesoda expansa* (Karim *et al*., 2023) and polypropylene in *Perna veridis* (Mazni *et al*., 2022).

All four types of detected plastic polymers (PVC, PDMS, PP and resin) were either common additives or building materials and easily entered the environment if there were human settlements around the area.

PVC is commonly used in the building and construction sector. It is a thermoplastic having a good resistance to alkalis, salt and highly polar solvents. Despite the relatively high density of PVC in nature, formation of biofilm may also alter the density through increasing the density and decreasing the buoyancy of the particles. (Rummel *et al*., 2017). PDMS is an elastomeric polymer used as fuel additives in car waxes,

cleaners and polishers, and biomedical application such as implants for cosmetic surgery. One of the routes that PDMS can enter the aquatic environment is through wastewater treatment plants or directly introduced into the aquatic environment as wastewater (Álvarez-Muñoz *et al*., 2016). PDMS adsorb strongly to sludge which reduces the volatility of PDMS (Whelan *et al*., 2009). The combination of PDMS with sludge will settle down in the environment, therefore PDMS is usually found in high concentration near the wastewater discharge areas (Sparham *et al*., 2011). PP with silicate mix is one of the common plastics used in human daily life. Single use plastic bags are a good example of polypropylene products. Fishing lines and nets were mostly composite of PP and polyethylene (PE) Improper discard of broken nets may break down into smaller pieces and form microplastics. Resin dispersion according to Yoshida (2014) is formed from epoxy resin after mixing with different

component such as basic epoxy resin, curing agents, accelerators and additives to produce epoxy with specific performance, therefore it's hard to determine the density of the dispersed resin. Current fishing boats materials are shifting from wood to glass fiber boats due to its durability and lightweight. Resins were commonly used as the main adhesion agent in repairing fiber boats. This might explain the availability of this polymer within the study site.

Ke *et al*. (2019) and Luan *et al*. (2019) reported that the exposure of microplastics (PP and PS) to clams (*Meretrix meretrix*) can lead to reduction in total oocyte number, oocyte diameter peroxidation damage of embryo membrane and death of *M. meretrix* larvae.

The possibility of microplastics entering humans usually through consumption of seafood for example, bivalves are usually consumed as whole organisms and rarely with gut removal (Cho *et al*., 2019). The toxicity of the plastic additives and chemicals adhered to the surface of microplastics during exposure in the environment may affect humans upon consumption of bivalves or other seafood that are contaminated with microplastics (Karbalaei *et al*., 2018).

CONCLUSION

This study provides compelling evidence of widespread microplastic contamination in *Meretrix lyrata* from an intertidal coastal habitat, with 100% of individuals found to contain microplastics. The average ingestion was 195.90±43.6 items per individual and a total count of 15,867 items across all samples. These concentrations are significantly higher than those reported in similar species from neighboring countries, suggesting local environmental and methodological factors may influence microplastic accumulation. Notably, smaller clams (<50 mm) exhibited significantly higher microplastic ingestion than larger individuals, a pattern consistent with previous studies and potentially linked to size-related differences in filtration capacity or feeding behavior. Although no significant seasonal variation was observed, the overall high prevalence of microplastics across seasons underscores the persistent nature of contamination in the study area. The identification of four distinct polymer types—

polyvinyl chloride (PVC), polydimethylsiloxane (PDMS), polypropylene with silicate mix (PP), and resin dispersion—points to multiple anthropogenic sources, including urban runoff, aquaculture, and maritime activities. Given that bivalves are commonly consumed whole, the detection of high microplastic loads in *M. lyrata* raises potential concerns regarding food safety and human health risks.

REFERENCES

Álvarez-Muñoz, D., Llorca, M., Blasco, J. & Barceló, D. (2016). Contaminants in the Marine Environment. In Blasco. J., Chapman, P, M., Campana, O. & Hampel, M. (eds.) *Marine Ecotoxicology: Current knowledge and future issue,* Cambridge: Academic Press. pp. 1-34.

Ambie, S., Peter, C., Minton, G., Ngeian, J., Zulkifli Poh, A. N., Mujahid, A. & Tuen, A. A. (2023). Utilizing interview-based data to measure interactions of artisanal fishing communities and cetacean populations in Kuching Bay, Sarawak, East Malaysia. *Ocean & Coastal Management*, 239: 106592. https://doi.org/10.1016/j.ocecoaman.2023.106592

Auta, H. S., Emenike, C. U. & Fauziah, S. H. (2017). Distribution and importance of microplastics in the marine environment: A review of the sources, fate, effects, and potential solutions. *Environment International*, 102: 165-176. 10.1016/j.envint.2017.02.013

Brach, L., Deixonne, P., Bernard, M. F., Durand, E., Desjean, M. C., Perez, E., Sebilie, E. V. & Ter Halle, A. (2018). Anticyclonic eddies increase accumulation of microplastics in the North Atlantic subtropical gyre. *Marine Pollution Bulletin,* 126: 191-196. 10.1016/j.marpolbul.2017.10.077

Chinfak, N., Sompongchaiyakul, P., Charoenpong, C., Shi, H., Yeemin, T. & Zhang, J. (2021). Abundance, composition, and fate of microplastics in water, sediment, and shellfish in the Tapi Phumduang river system and Bandon Bay, Thailand. *Science of The Total Environment,* 781: 146700. 10.1016/j.scitotenv.2021.146700

Cho, Y., Shim, W. J., Jang, M., Han, G. M. & Hong, S. H. (2019). Abundance and characteristics of microplastics in market bivalves from South Korea. *Environmental Pollution*, 245: 1107-1116. 10.1016/j.envpol.2018.11.091

Cole, M., Lindeque, P., Halsband, C. & Galloway, T. S. (2011). Microplastics as contaminants in the marine environment: A review. *Marine Pollution Bulletin.* 62: 2588–2597. 10.1016/j.marpolbul.2011.09.025

Cowger, W., Steinmetz, Z., Gray, A., Munno, K., Lynch, J., Hapich, H. & Herodotou, O. (2021). Microplastics spectral classification needs an open source community: Open specy to the rescue! *Analytical Chemistry*, 93(21): 7543–7548. 10.1021/acs.analchem.1c00123

Deng, H., He, J., Feng, D., Zhao, Y., Sun, W., Yu, H. & Ge, C. (2021). Microplastics pollution in mangrove ecosystems: A critical review of current knowledge and future directions. *Science of The Total Environment,* 753: 142041. 10.1016/j.scitotenv.2020.142041

Ding, J. F., Sun, C. J., He, C. F., Li, J. X., Ju, Peng., & Li, F. M. (2021). Microplastics in four bivalve species and basis for using bivalves as bioindicators of microplastic pollution. *Science of The Total Environment*, 782: 146830. https://doi.org/10.1016/j.scitotenv.2021.146830

Erni-Cassola, G., Gibson, M. I., Thompson, R. C. & Christie-Oleza, J. A. (2017). Lost, but found with Nile Red: A novel method for detecting and quantifying small microplastics (1 mm to 20 µm) in environmental samples. *Environmental Science & Technology,* 51(23): 13641–13648. 10.1021/acs.est.7b04512

Fu, Z., Chen, G., Wang, W. & Wang, J. (2020). Microplastics pollution research methodologies, abundance, characteristics and risk assessments for aquatic biota in China. *Environmental Pollution*, 266: 115098. 10.1016/j.envpol.2020.115098

Geyer, R., Jambeck, J. R. & Law, K. L. (2017). Production, use, and fate of all plastics ever made. *Science Advances,* 3(7): e1700782. 10.1126/sciadv.1700782

Green, D. S., Boots, B., O'Connor, N. E. & Thompson, R. (2017). Microplastics affect the ecological functioning of an important biogenic habitat. *Environmental Science & Technology*, 51(1): 68-77. 10.1021/acs.est.6b04496

Hartmann, N. B., Hüffer, T., Thompson, R. C., Hassellöv, M., Verschoor, A., Daugaard, A. E., Rist, S., Karlsson, T., Brennholt, N., Cole, M., Herrling, M. P., Hess, M. C., Ivleva, N. P., Lusher, A. L. & Wagner, M. (2019). Are we speaking the same language? Recommendations for a definition and categorization framework for plastic debris. *Environmental Science & Technology,* 53(3): 1039–1047. 10.1021/acs.est.8b05297

Hasbudin, H., Harith, M. N. & Idrus, F. A. (2022). A review on microplastic ingestion in marine invertebrates from Southeast Asia. *Songklanakarin Journal of Science and Technology* 44(3): 609–618. 10.14456/sjst-psu.2022.84

Idrus, F. A., Fadhli, N. M. & Harith, M. N. (2022a). Occurrence of microplastics in the Asian freshwater environments: A Review. *Applied Environmental Research,* 44(2), 1–17. https://doi.org/10.35762/AER.2022.44.2.1

Idrus, F. A., Roslan, N. S. & Harith, M. N. (2022b). Occurrence of macro- and micro-plastics on Pasir Pandak Beach, Sarawak, Malaysia. *Jurnal Ilmiah Perikanan Dan Kelautan* 14(2). https://doi.org/10.20473/jipk.v14i2.34034

Karbalaei, S., Hanachi, P., Walker, T. R. & Cole, M. (2018). Occurrence, sources, human health impacts and mitigation of microplastics pollution. *Environmental Science and Pollution Research,* 25(36): 36046–36063. 10.1007/s11356-018-3508-7

Karim, N., Musa, S. & Mat Lazim, A. (2023). *Microplastics physicochemical properties in commercial bivalves from Malaysia.* SSRN preprint. 10.2139/ssrn.4366421

Ke, A.Y., Chen, J., Zhu, J., Wang, Y.-H., Hu, Y., Fan, Z. L., Chen, M., Peng, P., Jiang, S. W., Xu, X. R. & Li, H. X. (2019). Impacts of leachates from single-use polyethylene plastic bags on the early development of clam *Meretrix Meretrix* (Bivalvia: Veneridae). *Marine Pollution Bulletin,* 142: 54–57. 10.1016/j.marpolbul.2019.03.029

Kieu-Le, T.-C., Tran, Q.-V., Truong, T.-N.-S. & Strady, E. (2022). Anthropogenic fibres in white clams, *Meretrix lyrata*, cultivated downstream a

developing megacity, Ho Chi Minh City, Viet Nam. *Marine Pollution Bulletin,* 174. 113302. 10.1016/j.marpolbul.2021.113302

Kolandhasamy, P., Su, L., Li, J., Qu, X., Jabeen, K. & Shi, H. (2018). Adherence of microplastics to soft tissue of mussels: a novel way to uptake microplastics beyond ingestion. *Science of the Total Environment*, 610: 635-640. 10.1016/j.scitotenv.2017.08.053

Lavers, J. L. & Bond, A. L. (2017). Exceptional and rapid accumulation of anthropogenic debris on one of the world's most remote and pristine islands. *Proceedings of the National Academy of Sciences,* 114(23): 6052-6055. 10.1073/pnas.1619818114

Lebreton, L., Slat, B., Ferrari, F., Sainte-Rose, B., Aitken, J., Marthouse, R., Hajibane, S., Cunsolo, S., Schwarz, A., Levivier, A., Noble, K., Debelijak, P., Maral, H., Schoeneich-Argent, R., Brambini, R. & Reisser, J. (2018). Evidence that the Great Pacific Garbage Patch is rapidly accumulating plastic. *Scientific Reports,* 8(1): 1-15. 10.1038/s41598-018-22939-w

Lebreton, L., Egger, M. & Slat, B. (2019). A global mass budget for positively buoyant macroplastic debris in the ocean. *Scientific Reports*, 9(1): 1–10. 10.1038/s41598-019-49413-5

Li, Q., Sun, C., Wang, Y., Cai, H., Li, L., Li, J. & Shi, H. (2019). Fusion of microplastics into the mussel byssus. *Environmental Pollution*, 252: 420–426g. 10.1016/j.envpol.2019.05.093

Luan, L., Wang, X., Zheng, H., Liu, L., Luo, X. & Li, F. (2019). Differential toxicity of functionalized polystyrene microplastics to clams (*Meretrix meretrix*) at three key development stages of life history. *Marine Pollution Bulletin,* 139: 346–354. 10.1016/j.marpolbul.2019.01.003

Lusher, A. L. & Hernandez-Milian, G. (2018). Microplastic extraction from marine vertebrate digestive tracts, regurgitates and scats: A protocol for researchers from all experience levels. *Bio Protocol,* 8(22): 10.21769/BioProtoc.3087.

Maes, T., Jessop, R., Wellner, N., Haupt, K. & Mayes, A. G. (2017). A rapid-screening approach to detect and quantify microplastics based on fluorescent tagging with Nile Red. *Scientific Reports,* 7(1): 1–10. 10.1038/srep44501

Mazni, M. Z., Azman, S., Mohd Ismail, M. I. & Muhammad, M. K. (2022). Microplastics contents in natural and maricultured shellfish from Pasir Putih estuary in Johor, Malaysia. *Journal of Sustainability Science and Management,* 17(10): 121–135. 10.46754/jssm.2022.10.009

Nuelle, M.-T., Dekiff, J. H., Remy, D. & Fries, E. (2014). A new analytical approach for monitoring microplastics in marine sediments. *Environmental Pollution,* 184: 161–169. 10.1016/j.envpol.2013.07.027

Prata, J. C., Alves, J. R., da Costa, J. P., Duarte, A. C. & Rocha-Santos, T. (2020). Major factors influencing the quantification of Nile red stained microplastics and improved automatic quantification (MP-VAT 2.0*). Science of The Total Environment,* 719: 137498. 10.1016/j.scitotenv.2020.137498

Prata, J. C., Sequeira, I. F., Monteiro, S. S., Silva, A. L. P., da Costa, J. P., Dais Pereira, P., Fernandes, A. J. S., da Costa, F. M., Duarte, A. C. & Rocha Santos, T. (2021). Preparation of biological samples for microplastic identification by Nile Red. *Science of The Total Environment,* 783: 147065. https://doi.org/10.1016/j.scitotenv.2021.147065

Quinn, B., Murphy, F. & Ewins, C. (2017). Validation of density separation for the rapid recovery of microplastics from sediment. *Analytical Methods*, 9(9): 1491–1498. 10.1039/C6AY02542K

Reed, S., Clark, M., Thompson, R. & Hughes, K. A. (2018). Microplastics in marine sediments near Rothera research station, Antarctica. *Marine Pollution Bulletin,* 133: 460–463. 10.1016/j.marpolbul.2018.05.068

Rist, S. E., Assidqi, K., Zamani, N. P., Appel, D., Perschke, M., Huhn, M. & Lenz, M. (2016). Suspended micro-sized PVC particles impair the performance and decrease survival in the asian green mussel *Perna viridis*. *Marine Pollution Bulletin*, 111(1-2): 213–220. 10.1016/j.marpolbul.2016.07.006

Rummel, C. D., Jahnke, A., Gorokhova, E., Kühnel, D. & Schmitt-Jansen, M. (2017). Impacts of biofilm formation on the fate and potential effects of microplastics in the aquatic environment. *Environmental Science & Technology Letters*, 4(7): 258–267. 10.1021/acs.estlett.7b00164

Sathish, M. N., Jeyasanta, K. I. & Patterson, J. (2020). Monitoring of microplastics in the clam *Donax Cuneatus* and its habitat in Tuticorin coast of Gulf of Mannar (GoM), India. *Environmental*

Pollution, 266: 115219. 10.1016/j.envpol.2020.115219

Scott, N., Porter, A., Santillo, D., Simpson, H., Lloyd-Williams, S. & Lewis, C. (2019). Particle characteristics of microplastics contaminating the mussel *Mytilus edulis* and their surrounding environments. *Marine Pollution Bulletin,* 146: 125–133. 10.1016/j.marpolbul.2019.05.041

Shahul Hamid, F., Bhatti, M. S., Anuar, N., Anuar, N., Mohan, P. & Periathamby, A. (2018). Worldwide distribution and abundance of microplastics: How dire is the situation? *Waste Management and Research,* 36(10): 873–897. 10.1177/0734242X18785730

Sparham, C., Van Egmond, R., Hastie, C., O'Connor, S., Gore, D. & Chowdhury, N. (2011). Determination of decamethylcyclopentasiloxane in river and estuarine sediments in the UK. *Journal of Chromatography A*, 1218(6): 817–823. 10.1016/j.chroma.2010.12.030

Tang, R., Zhang, T., Song, K., Sun, Y., Chen, Y., Huang, W. & Feng, Z. (2022) Microplastics in commercial clams from the intertidal zone of the South Yellow Sea, China. *Frontiers in Marine Science,* 9: 905923. 10.3389/fmars.2022.905923

Tran-Nguyen, Q. A., Nguyen, T. Q., Phan, T. L., Vo, M. V. & Trinh-Dang, M. (2023). Abundance of microplastics in two venus clams (*Meretrix Lyrata* and *Paratapes Undulatus*) from estuaries in central Vietnam. *Water,* 15(7): 1312. 10.3390/w15071312

Whelan, M. J., Sanders, D. & Van Egmond, R. (2009). Effect of aldrich humic acid on water–atmosphere transfer of decamethylcyclopentasiloxane. *Chemosphere*, 74

(8): 1111–1116. 10.1016/j.chemosphere.2008.10.037

Woods, M. N., Stack, M. E., Fields, D. M., Shaw, S. D. & Matrai, P. A. (2018). Microplastics fiber uptake, ingestion, and egestion rates in the blue mussel (*Mytilus edulis*). *Marine Pollution Bulletin,* 137: 638–645. 10.1016/j.marpolbul.2018.10.061

Wu, F., Pennings, S. C., Tong, C. & Xu, Y. (2020). Variation in microplastics composition at small spatial and temporal scales in a tidal flat of the Yangtze Estuary, China. *Science of The Total Environment,* 699. 134252. 10.1016/j.scitotenv.2019.134252

Yoshida, S. (2014). Quantitative evaluation of an epoxy resin dispersion by infrared spectroscopy. *Polymer Journal*, 46(7): 430–434. 10.1038/pj.2014.15

Zarfl, C. (2019). Promising techniques and open challenges for microplastics identification and quantification in environmental matrices. *Analytical and Bioanalytical Chemistry,* 411(17): 3743–3756. 10.1007/s00216-019-01763-9

Zhang, F., Man, Y. B., Mo, W. Y., Man, K. Y. & Wong, M. H. (2020). Direct and indirect effects of microplastics on bivalves, with a focus on edible species: A mini-review. *Critical Reviews in Environmental Science and Technology*, 50(20): 2109–2143. 10.1080/10643389.2019.1700752

Zhang, T., Song, K., Meng, L., Tang, R., Song, T., Huang, W. & Feng, Z. (2022). Distribution and characteristics of microplastics in barnacles and wild bivalves on the coast of the Yellow Sea, China. *Frontiers in Marine Science,* 8: 78961. 10.3389/fmars.2021.78961

Molecular Characterisation of Upland and Lowland Rice from Sarawak, Malaysian Borneo

FREDDY KUOK SAN YEO[1*], RENEE PRISCILLA TRAWAS SYLVESTER EMBUAS[1],
ZAZEVIA FRANK CLIFTON[1], MEEKIONG KALU[1], ZINNIRAH SHABDIN[1] & LEE SAN LAI[2]

[1]Faculty of Resource Science and Technology, Universiti Malaysia Sarawak, Jalan Datuk Mohammad Musa,
94300, Kota Samarahan, Sarawak, Malaysia; [2]Agriculture Research Centre Semongok, KM20, Jalan Puncak
Borneo, 93250, Kuching, Sarawak
*Corresponding author: yksfreddy@unimas.my

ABSTRACT

A total of 39 Simple Sequence Repeat (SSR) markers distributed across 12 chromosomes were screened to assess genetic polymorphism among rice accessions. From the 39 tested SSR primer pairs, eight markers (RM1, RM489, RM552, RM444, RM257, RM481, RM166 and RM164) exhibited clear polymorphic banding patterns and strong amplification, while the remaining were excluded due to monomorphism or unclear bands. Among the selected primers, RM257 recorded the highest polymorphic information content (PIC) value (0.9316), while RM552 had the lowest (0.4029), with an average PIC of 0.6891. The observed number of effective alleles (Ne) was 1.543 in the lowland population and 1.566 in the upland population. Nei's gene diversity (h) was 0.329 for lowland and 0.318 for upland populations, suggesting a low level of genetic divergence. Similarly, Shannon's Information Index (I) values were 0.475 and 0.490 for lowland and upland populations, respectively. Analysis of Molecular Variance (AMOVA) revealed that 20% of genetic variation existed among populations, while 80% occurred within populations. Clustering analysis using a UPGMA dendrogram based on SSR genotypes grouped the 44 rice accessions into two major clusters, each further divided into sub-clusters. However, no clear grouping was observed based on morphological traits or geographical origin, likely due to the higher sensitivity of molecular markers in detecting underlying genetic differences that are not always reflected in visible traits. Unlike conventional morphological classification which relies on observable characteristics such as grain shape, plant height or habitat, genome-based clustering captures deeper genetic relationships that offer a more accurate picture of population structure. Simultaneously, the *Maturase-K* barcoding gene marker grouped the accessions into a single large cluster, which also included 94 accessions from diverse origins and three accessions of *Oryza rufipogon*, indicating genome-level similarities. These findings underscore the utility of molecular markers in revealing genetic diversity and population structure. The insights gained from this study can support the development of targeted rice breeding programs essential for advancing sustainable agriculture.

Keywords: *Maturase-K*, Rice, Sarawak, Simple Sequence Repeat

INTRODUCTION

Rice *(Oryza sativa* L.) is a staple food for more than half of the world's population, serving as a crucial source of nutrition and sustenance (Awika, 2011). Rice is one of the few crop species endowed with the richest genetic diversity and has one of the largest ex situ germplasm collections in the world (Dempewolf *et al.*, 2023). Sarawak is well known as a rich biodiversity centre with diverse types of rice, from commercial high yielding cultivars to indigenous traditional varieties or landraces, which will make great contributions to rice breeding if accessible (Lee *et al.*, 2011; Yeo *et al.*, 2018; Frank Clifton *et al.*, 2024).

The Agriculture Research Centre Semongok currently conserves 2011 rice landrace accessions collected from across Sarawak (Department of Agriculture Sarawak, 2020). Although these accessions display morphological variation, comprehensive molecular characterization is lacking. Such information is crucial for optimizing the use of these genetic resources in breeding, conservation and crop improvement.

To address this gap, molecular tools such as Simple Sequence Repeat (SSR) markers and DNA barcoding genes like *Maturase-K* (*matK*) offer powerful and complementary insights. The SSR markers are widely used due to their high polymorphism, codominant inheritance and genome-wide distribution, making them ideal for assessing nuclear genetic variation, population structure and diversity (Akagi *et al.*, 1997; Miah *et al.*, 2013). In contrast, *matK*, a chloroplast-encoded gene, provides information from the maternal genome and is particularly useful for identifying phylogenetic relationships and evolutionary lineage due to its conserved sequences and relatively high mutation rate (Yao *et al.*, 2019; Adriansyah *et al.*, 2021).

By combining these two markers; SSR for fine-scale nuclear diversity and *matK* for broader plastid-based phylogeny, this study adopts an integrated approach to analyze the genetic variation of Sarawak rice landraces more comprehensively. This dual-marker strategy enhances resolution, facilitates more accurate classification and provides insights that would not be possible through a single marker system alone.

While genetic research on Sarawak rice is still at an early stage, the previous work such as a 2006 study using six SSR markers on Bario varieties (Tan *et al.*, 2006) has highlighted the potential of molecular tools in variety certification. However, broader genetic profiling across diverse landraces remains limited.

Therefore, the objective of this study was to evaluate the genetic diversity of rice landraces collected from the North-West region of Sarawak using both SSR markers and *matK* sequences. This research aims to fill a critical gap in molecular data for local rice germplasm, ultimately contributing to more informed conservation strategies and targeted breeding programs that support sustainable agriculture.

MATERIALS & METHODS

Plant Materials Preparation and DNA Extraction

A total of 44 rice accessions (22 upland and 22 rice accessions) from Frank Clifton *et al.* (2024) were used in this study. The 44 rice accessions may have been obtained from the same seed source or different seed sources from farmers, as reported in Frank Clifton *et al.* (2024). The 44 rice accessions were designated as UNIMAS-01 to UNIMAS-44 (Supplementary Table 1). Upland rice is grown in rainfed and non-irrigated areas, often on elevated or hilly terrains, whereas lowland rice is cultivated in paddy fields with irrigated or rainfed conditions, where the soil remains waterlogged for most of the growth cycle (Sohrabi *et al.*, 2012).

The accessions were planted in soil mixture of topsoil, compost and sand (3:2:1 ratio). For upland accessions, each of the accessions were transplanted into pots with the drainage holes at the bottom to drain the excess water. Lowland accessions were transplanted into pots without holes at the bottom but having holes at the top of the pots to maintain the water level about 2 cm above soil surface. Nitrogen, phosphorus, and potassium (NPK) fertilizer (17.5:15.5:10) was used for fertilization, with each plant pot receiving 10 grams per application. The first application was conducted around the time of transplanting.

At one month old, young leaf samples of about 4-5 cm were collected. DNA was extracted using cetyltrimethylammonium bromide protocol following Doyle and Doyle (1987). The concentration of extracted DNA was measured using Nano-drop machine (Model: ND-2800-ODJ Nano DOT Nucleic Acid Analyzer; Hercuvan), where the quality and quantity of genomic DNA were measured. The integrity of the DNA was visually checked by electrophoresis on 1% agarose gel. The DNA stocks were diluted to 20 ng/ul using distilled water and stored at -20°C.

Microsatellite Marker Amplification

A total of 39 Simple Sequence Repeat (SSR) primer pairs were selected randomly from Gramene Markers Database (https://archive.gramene.org/markers/microsat/ssr.html), representing 12 rice chromosomes (Supplementary Table 2).

Polymerase Chain Reaction (PCR) amplification was performed following Zhu *et al.* (2012) in a 20 µL reaction containing 5 ng of genomic DNA, 0.2 µM of each forward and reverse primer, 0.2 mM dNTPs, 1X PCR buffer (First Base Laboratories), 2.5 mM $MgCl_2$ and 1

unit of Taq DNA polymerase (First Base Laboratories). The PCR started with initial denaturation at 94°C for 4 minutes followed by 40 cycles of denaturation at 94°C for 45 seconds, annealing at optimized temperature (Supplementary Table 2) for 45 seconds, extension at 72°C for 1 minute, and with a final extension at 72°C for 10 minutes. The amplified PCR products were electrophoresed on 2% agarose gel stained with ethidium bromide (0.1mg/ml; EtBr). The gel was visualized under an ultraviolet transilluminator.

The final SSR dataset was reviewed for scoring consistency and unclear bands were re-scored to minimize genotyping errors.

SSR Marker Analysis

The amplified bands were visually scored as present (1) or absence (0) separately for each primer pair. Polymorphic Information Content (PIC) was calculated following Anderson *et al.* (1993), Eq. (1):

$$PICi = 1 - \Sigma Pij^2 \qquad \text{Eq. (1)}$$

Where i is the total number of alleles detected for SSR marker and Pij is the frequency of the jth allele for marker i.

The genetic distances as well as Analysis of Molecular Variation where number of alleles, number of effective alleles (*Ne*), Nei's gene diversity (*h*) and Shannon's Information Index (*I*) were calculated in Genetic Analysis in Excel (GenAlEx) version 6.51 (Smouse *et al.*, 2017). Dendrogram was constructed using Unweighted Pair Group Method with Arithmetic Means (UPGMA) generated from Molecular Evolutionary Genetic Analysis (MEGA X) v.10.1 software based on genetic distance.

Amplification of *Maturase-K* Barcoding Marker

The *matK* region was amplified by using forward primer: 5'- TAA TTA AGA GGA TTC ACC AG -3' and reverse primer: 5'- ATG CAA CAC CCT GTT CTG AC -3'. The PCR protocols were based on Patil *et al.* (2015) with expected product size of 1500 bp.

The PCR reaction contains 3-5 ng of genomic DNA, 0.5 µM each of forward and reverse primers, 1.5 mM MgCl$_2$, 0.2 mM dNTPs, 1X PCR buffer (First Base Laboratories), and 2.5 unit of Taq DNA polymerase (First Base Laboratories). The thermocycler profile for amplification of *matK* had initial denaturation at 94°C for 4 minutes, followed by 35 cycles of denaturation at 94°C for 1 minute, 2 minutes of annealing at 57.8°C, extension at 72°C for 2 minutes and ended with final extension at 72°C for 15 min.

The PCR products were electrophoresed in a 1.5% agarose gel, stained with EtBr and visualised under UV transilluminator. The PCR product was purified using QIAquick Gel Extraction Kit (QIAGEN, Germantown, MD, USA) following the provided protocol by the manufacturer. Purified PCR products were subjected for two-way sequencing by Apical Scientific Sdn. Bhd. Malaysia.

Cluster Analysis Based on *Maturase-K*

The *matK* sequences from the 44 accessions of this study were manually edited in BioEdit software. An additional 94 *matK* sequences of *O. sativa* were downloaded from GenBank database at National Centre for Biotechnology Information (NCBI) (Supplementary Table 3). One to three *matK* sequences of *O. rufipogon*, *O. punctata*, *O. officinalis, O. australiensis,* and *O. granulata* were also downloaded (Supplementary Table 3). The *matK* sequences of the 44 accessions of this study were aligned with the sequences from NCBI using ClustalW (MEGA X v. 10.1). Phylogenetic tree was constructed using Maximum Likelihood with Tamura 3-parameter model evolutionary rates among sites with discrete gamma distribution (T92+G) at 1000 bootstrap value.

RESULTS

From 39 tested SSR primer pairs, eight primer pairs displayed polymorphic banding patterns and exhibited strong polymorphism among the accessions. The primers with clear amplification results were RM1, RM489, RM552, RM444, RM257, RM481, RM166 and RM164 (Figure 1). The other primers showing either monomorphic banding patterns or unclear band were excluded from the study.
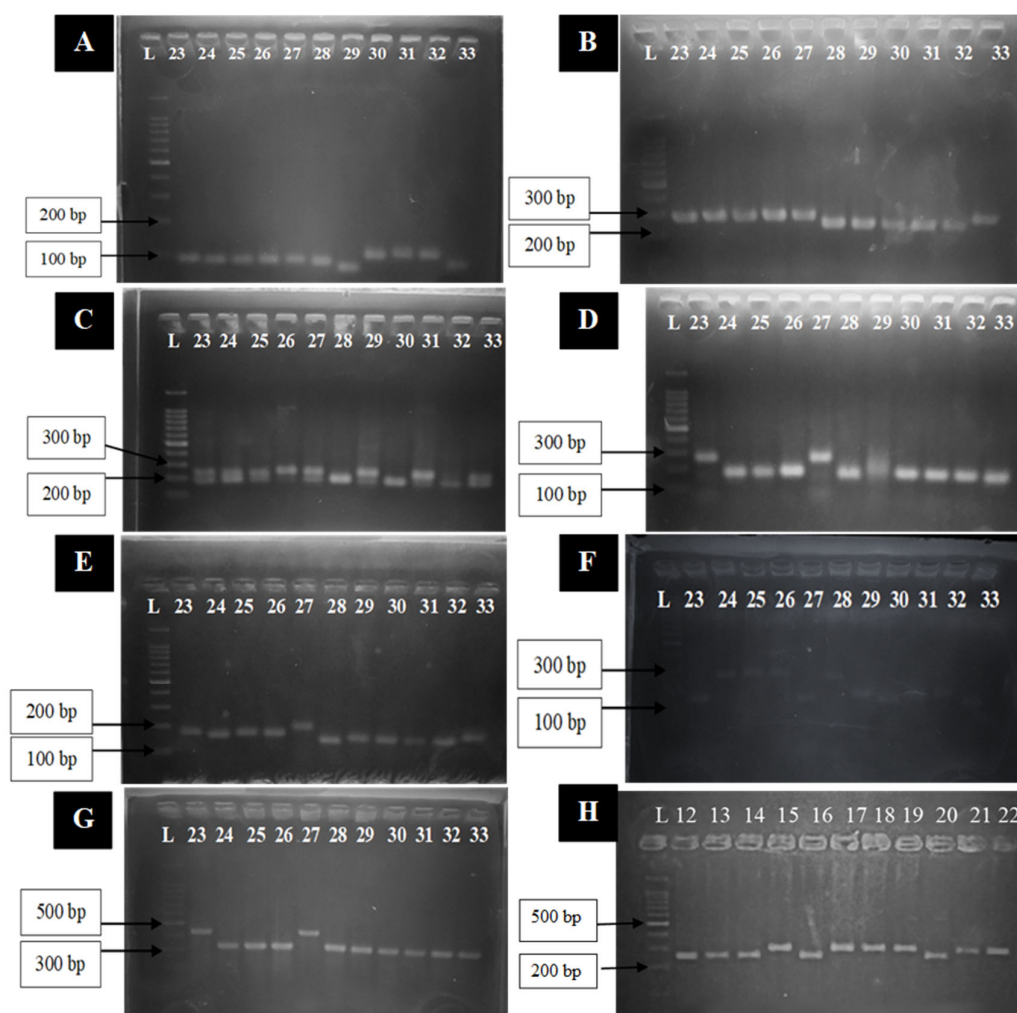
Figure 1. A Representative figure for the banding pattern of the seven polymorphic SSR markers. A: RM1, B: RM489, C: RM552, D: RM444, E: RM257, F: RM481, G: RM166, H: RM164. L= 100 bp ladder. The number represents UNIMAS collection number.

PIC Values and Genetic Diversity

In this study, the highest PIC value (0.9316) was recorded for RM257 (Table 1). The lowest PIC value (0.4029) was recorded for RM552 and the average PIC value for 44 accessions was 0.6891. About 87.5% of the SSR markers (7 out of 8 SSR markers) used in this study showed PIC values higher than 0.5 indicating markers used in the study were highly informative.

Table 2 summarizes the genetic analysis of the two rice populations. The observed number of effective alleles (Ne) in upland rice population recorded 1.566 and 1.543 in lowland rice population.

Nei's gene diversity (h) in upland rice and lowland rice population was 0.329 and 0.318, respectively. Shannon's Information Index (I) recorded 0.490 in upland rice population, and 0.475 in lowland rice population. Analysis of Molecular Variance indicated a 20% of genetic variation among population. Meanwhile, genetic variation within the population was 80%.

Table 1. SSR markers with Polymorphic Information Content.

SSR marker	Number of alleles	PIC
RM1	3	0.5072
RM489	2	0.7371
RM552	2	0.4029
RM444	2	0.7537
RM257	4	0.9316
RM481	3	0.864
RM166	2	0.6984
RM164	2	0.6178
Average	2.5	0.6891

Note. PIC: Polymorphic Information Content

Table 2. Summary of genetic analysis of upland and lowland accessions. The values indicate the means ± standard error of the 22 accessions of the respective upland and lowland rice population.

Population	*Ne*	*h*	*I*
Upland	1.566 ± 0.075	0.329 ± 0.036	0.490
Lowland	1.543 ± 0.077	0.318 ± 0.037	0.475

Note. Ne: Number of effective alleles; *h*: Nei's gene diversity; *I*: Shannon's Information Index

Cluster Analysis Based on SSR Markers

The UPGMA dendrogram was constructed for the 44 accessions using the MEGA X v.10.1 program based on the eight SSR markers genotype. The UPGMA dendrogram classified the 44 rice accessions into two primary clusters, Cluster I and Cluster II. Cluster I was divided into two sub-clusters, sub-cluster IA and sub-cluster IB and Cluster II was splat into sub-cluster IIA and sub-cluster IIB (Figure 2).

As tabulated in Table 3, sub-cluster IA had the highest number of accessions with 19 rice accessions. Sub-cluster IB comprises of seven accessions. Meanwhile, sub-cluster IIA consisted of six accessions and the rest were grouped in sub-cluster IIB. The dendrogram tree did not show clear clustering pattern according to their morphological traits described by Frank Clifton *et al*. (2024), nor according to the division where the seeds were sampled. The clustering was also not clearly according to the rice type (upland vs lowland).

Maturase-K Sequence Characteristics and Genetic Diversity

Bright and clear 1500 bp band of the *matK* gene fragment were successfully amplified from the 44 rice accessions (Figure 3). The aligned sequences resulted in a data matrix of 1470 bp with no alignment gaps. The number of segregating sites showed a value of 140.

Phylogenetic Analysis Based on *Maturase-K*

The phylogenetic tree constructed based on *matK* sequence had one big cluster (Figure 4). All the accessions in this study were grouped in Cluster I with 100% bootstrap value. Also in the same cluster, there were 94 accessions of *O. sativa* which mostly originated from India (88 accessions), followed by Australia (4 accessions), China (1 accession) and one from unknown origin. Other than *O. sativa*, *O. rufipogon* was grouped together in the big cluster (Figure 4; Table 4). The outgroup consists of four species, *viz O. punctata*, *O. granulata*, O. *australiensis*, and *O. officinalis* (Figure 4; Table 4).
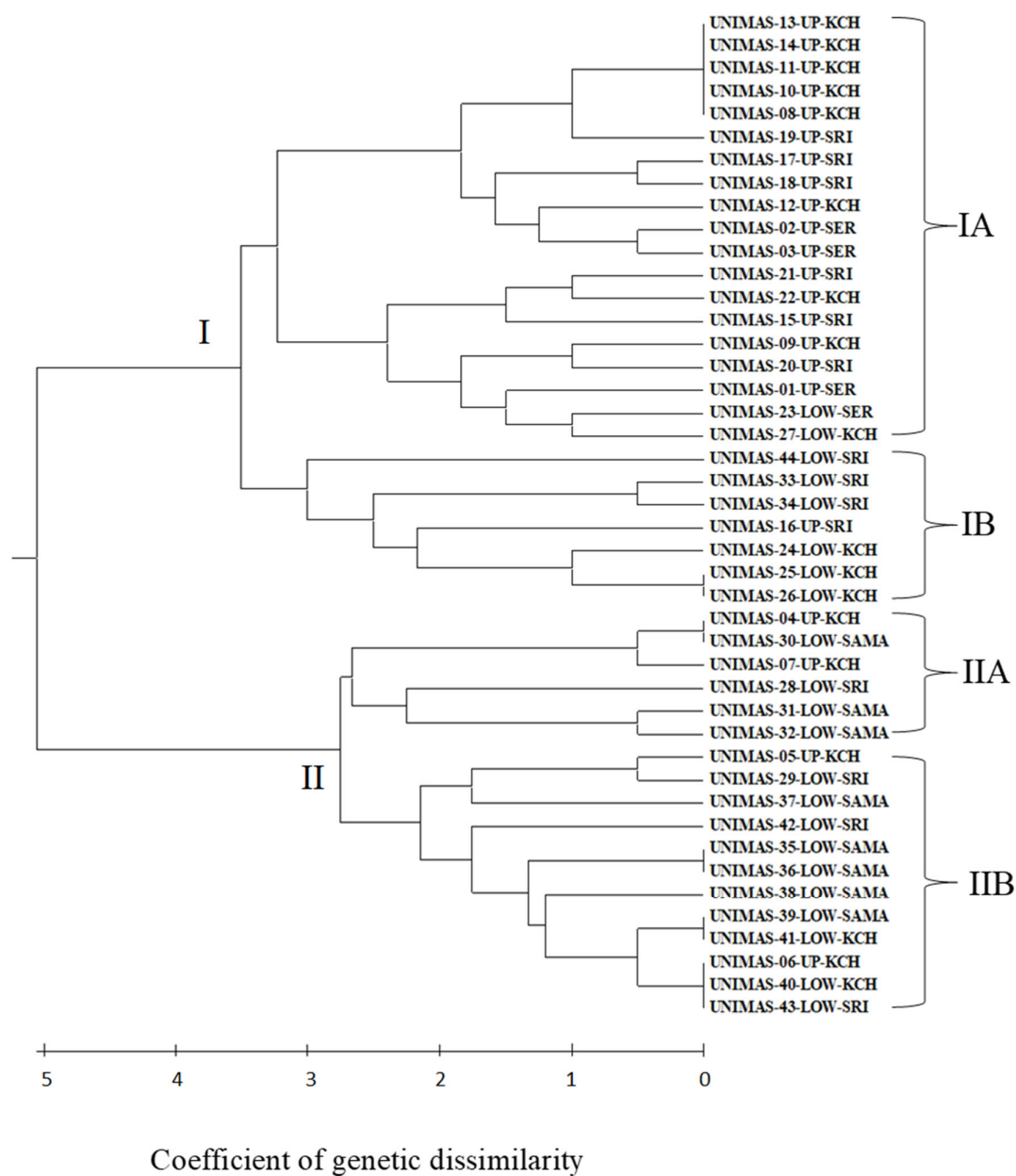
Figure 2. The cluster analysis of 44 rice accessions collected from North-West region of Sarawak based on eight SSR markers. I: Cluster I; IA: Sub-cluster IA; IB: Sub-cluster IB; II: Cluster II; IIA: Sub-cluster IIA; IIB: Sub-cluster IIB. The uppercase abbreviation after the accession number indicates the division where seeds were collected. KCH: Kuching; SER: Serian; SAMA: Kota Samarahan; SRI: Sri Aman.
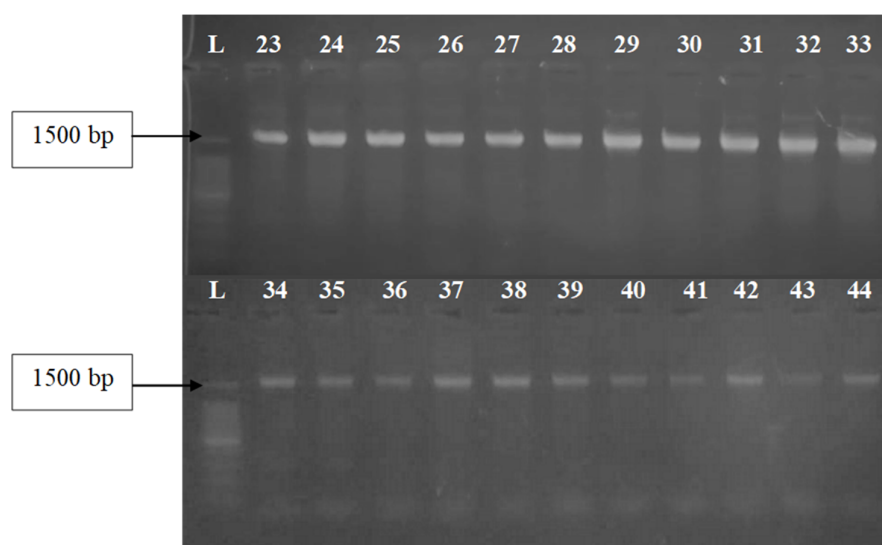
Figure 3. Representative amplification of 22 rice accessions employing *matK* gene specific primer. L= 100 bp ladder. The number represents the 22 UNIMAS collections from UNIMAS-23 to UNIMAS-44.
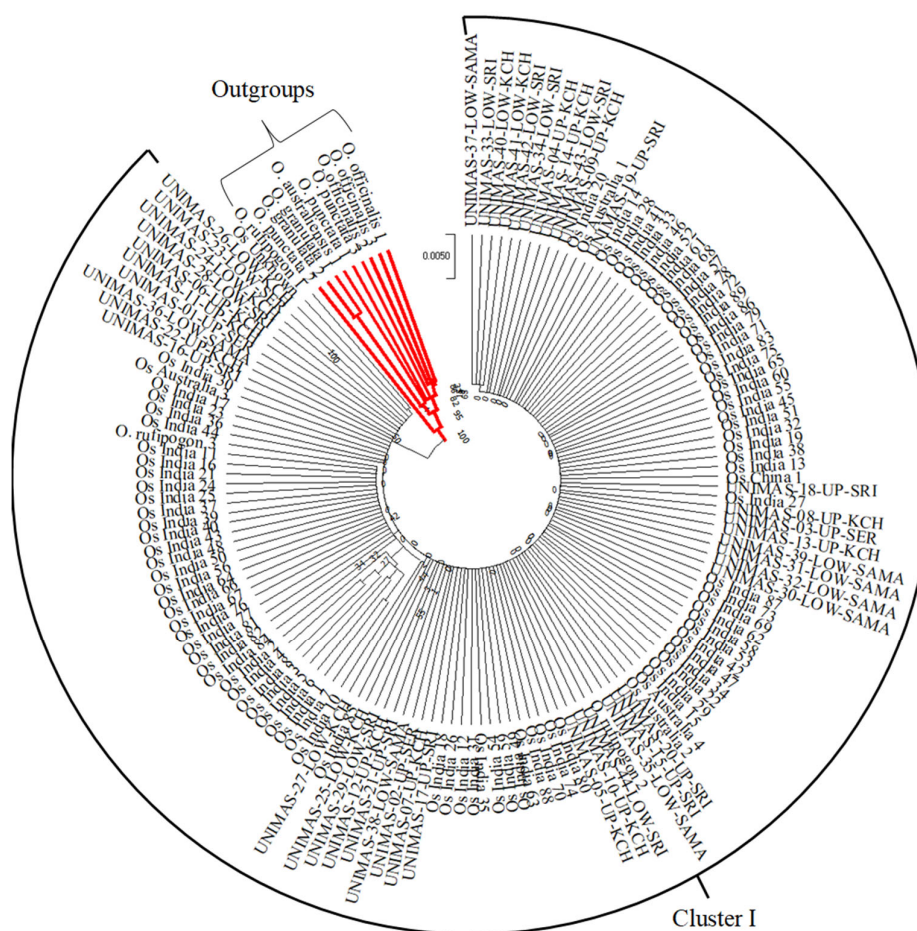
Figure 4. The phylogenetic tree of 44 rice accessions based on *Maturase-K* sequence, constructed using Maximum Likelihood Analysis. Best-fit substitution models: Tamura 3-Parameter Model with discrete gamma distribution evolutionary rates among sites (T92+G) at 1000 replicates bootstrap values. The red line indicates the outgroups.

Table 3. Clustering of the 44 rice accessions based on the eight SSR markers

Cluster	Sub-cluster	Number of accession	Accession
I	IA	19	UNIMAS-13-UP-KCH UNIMAS-14-UP-KCH UNIMAS-11-UP-KCH UNIMAS-10-UP-KCH
			UNIMAS-08-UP-KCH UNIMAS-19-UP-SRI
			UNIMAS-17-UP-SRI UNIMAS-18-UP-SRI
			UNIMAS-12-UP-KCH UNIMAS-02-UP-SER
			UNIMAS-03-UP-SER UNIMAS-21-UP-SRI
			UNIMAS-22-UP-KCH UNIMAS-15-UP-SRI UNIMAS-09-UP-KCH UNIMAS-20-UP-SRI
			UNIMAS-01-UP-SER
			UNIMAS-23-LOW-SER
			UNIMAS-27-LOW-KCH
	IB	7	UNIMAS-44-LOW-SRI
			UNIMAS-33-LOW-SRI
			UNIMAS-34-LOW-SRI
			UNIMAS-16-UP-SRI
			UNIMAS-24-LOW-KCH
			UNIMAS-25-LOW-KCH
			UNIMAS-26-LOW-KCH
II	IIA	6	UNIMAS-04-UP-KCH
			UNIMAS-30-LOW-SAMA
			UNIMAS-07-UP-KCH
			UNIMAS-28-LOW-SRI
			UNIMAS-31-LOW-SAMA
			UNIMAS-32-LOW-SAMA
	IIB	12	UNIMAS-05-UP-KCH
			UNIMAS-29-LOW-SRI
			UNIMAS-37-LOW-SAMA
			UNIMAS-42-LOW-SRI
			UNIMAS-35-LOW-SAMA
			UNIMAS-36-LOW-SAMA
			UNIMAS-38-LOW-SAMA
			UNIMAS-39-LOW-SAMA
			UNIMAS-41-LOW-KCH
			UNIMAS-06-UP-KCH
			UNIMAS-40-LOW-KCH
			UNIMAS-43-LOW-SRI

Note. The uppercase abbreviation after the accession number indicates the location of the collection. KCH: Kuching; SER: Serian; SAMA: Kota Samarahan; SRI: Sri Aman

Table 4. Clusters for 44 upland and lowland rice accessions based on *Maturase-K* marker

Cluster	Species	Country of Origin	No of Accession
I	*Oryza sativa*	India	88
	Oryza sativa	Australia	4
	Orya sativa	China	1
	Oryza sativa	Unknown	1
	*Oryza sativa***	Malaysia	22
	*Oryza sativa**	Malaysia	22
	Oryza rufipogon	Unknown	1
	Oryza rufipogon	China	1
	Oryza rufipogon	India	1
Outgroups	*Oryza punctata*	Unknown	1
	Oryza puntata	Unknown	1
	Oryza granulata	Unknown	1
	Oryza granulata	China	1
	Oryza australiensis	Vietnam	1
	Oryza officinalis	Australia	1
	Oryza officinalis	Phillipines	1
	Oryza officinalis	China	1
	Oryza punctata	Papua New Guinea	1

Note. **Upland rice accessions from UNIMAS collections, *Lowland rice accessions from UNIMAS collections.

DISCUSSION

Characterisation Based on Simple Sequence Repeat

Characterizing rice cultivar using a highly polymorphic microsatellite markers may provide a deeper information on rice germplasm and serves as powerful tools to detect genetic variation and genetic relationship within and among species (Al-Musawi *et al*., 2019). The SSR are markers of choice because SSR demonstrate a higher per-locus information content (García *et al*., 2018). Hodel *et al*. (2016) stated the utilisation of a number of SSR markers are inexpensive and can deliver good results.

A total of 20 alleles were successfully amplified by eight SSR markers in the present study, ranging from two (RM489, RM552, RM444, RM166 and RM164) to four (RM257) alleles per primer with an average of 2.5 alleles per marker. Similarly, Supari *et al*. (2019) and Wong *et al*. (2009) reported an average of 2.26 and 2.60 alleles per SSR locus, respectively, for

their rice genotyping. The number of alleles amplified in the present study is, however, relatively lower compared to Sohrabi *et al*. (2013) and Aljumaili *et al*. (2018) which reported two to eleven alleles from the SSR markers used for genotyping their rice samples.

The PIC value serves as an indicator of allele diversity and frequency (Shete *et al*., 2000). In this study, the SSR markers displayed a range of PIC values from 0.4029 (RM552) to 0.9316 (RM257), averaging 0.6891. Among the eight polymorphic markers examined, only RM552 had a PIC value below 0.5, suggesting lower reliability in assessing genetic diversity according to Dalimunthe *et al*. (2020). The SSR markers with a PIC value above 0.5 are considered highly polymorphic and valuable for genetic research (Melaku *et al*., 2018). The high PIC value of RM257 suggests that this marker is particularly effective in evaluating genetic variability among rice accessions. Overall, the eight SSR markers used in this study had an average PIC value greater than 0.5, indicating

they were highly informative and capable of distinguishing between genotypes.

Following the assessment of PIC values, the study also examined the number of effective alleles (Ne), which reflects the number of alleles that actively contribute to genetic variation within a population. The upland rice population recorded a higher Ne of 1.566 compared to 1.543 in the lowland population. These Ne values are greater than those reported for aromatic rice accessions from Malaysia genotyped using SSR markers by Aljumaili *et al.* (2018), indicating a relatively higher effective allele diversity in the current populations.

The Nei's gene diversity (h) for markers in upland population was 0.329 and 0.318 in lowland population. A study done by Sohrabi *et al.* (2013) showed a much higher value of h in the author's upland rice populations originated from Peninsular Malaysia and Sabah, which was 0.62 and 0.58, respectively. According to Bobokashvili (2016), the h of value 0.95 to 1.00 indicates high divergence in a population. The h value ranging from 0.50 to 0.60 indicates two species were having similar features, however, unable to cross each other. Two subspecies having very similar features in range of one species were likely to have h value ranging from 0.17 to 0.22. This indicates low level of divergence in the 44 accessions of the current study.

The Shannon's Information Index (I) based on SSR markers in upland and lowland rice population were 0.490 and 0.475, respectively. Sohrabi *et al.* (2013) reported much higher value of I with an average of 1.1653 for the author's rice populations from Peninsular Malaysia and 1.0754 for Sabah. The recorded I value in both populations of the current study indicates a low diversity in comparison with the rice accessions from Peninsular Malaysia and Sabah by Sohrabi *et al.* (2013). Higher number of SSR markers were tested in Sohrabi *et al.* (2013) compared to the present study. Several studies highlight the effect of the number of markers on I in rice, emphasizing that a higher number of markers often results in better detection of genetic diversity. Study of rice landraces, such as those from the Honghe Hani Rice Terraces (Ma *et al.*, 2023), used over 200 SSR markers and reported significant genetic diversity, with Shannon's Index values averaging around 1.08. This indicates that a higher number of markers can capture a broader range of allelic variation, contributing to a more robust Shannon Index value.

The Simple Sequence Repeat Cluster Analysis

The clustering analysis did not reveal clear grouping of the lowland and upland rice accessions based on their morphological traits described by Frank Clifton *et al.* (2024), geographical origin or rice type. This lack of clear clustering may be due in part to the small number of SSR markers used in this study, which was only eight markers. Previous studies have used between 32 and 140 markers (Zhang *et al.*, 2010; Ma *et al.*, 2016; Aljumaili *et al.*, 2018; Hassan and Hama-Ali, 2022). Using fewer markers limits the ability to detect small genetic differences among rice accessions, which can reduce clustering accuracy and weaken conclusions about genetic diversity and relationships (Wang *et al.*, 2021). In addition, seed mixing in local farming practices may have contributed to the genetic overlap observed, as seeds from different accessions can be unintentionally combined and this blurs distinct groupings. The observed low genetic diversity is also consistent with morphological findings reported by Frank Clifton *et al.* (2024), where some rice accessions displayed similar traits despite differences in their names or origins. Taken together, these factors of limited marker coverage, possible seed mixing and genuinely low genetic diversity help to explain why genetic clustering in this study did not correspond clearly with morphological traits or geographic origin. Future research should use a larger number of SSR markers or combine different genetic markers to improve resolution and better capture the genetic variation among rice varieties. This could include not only more SSR markers but also different types of genetic markers such as single nucleotide polymorphisms (SNPs), amplified fragment length polymorphisms (AFLPs) or insertions/deletions (InDels), which together can capture a wider range of genetic differences among rice varieties.

Accessions that shared the same name (Padi Merjat) but collected from different villages were found to be genetically different based on SSR genotype as shown in upland rice

accessions namely UNIMAS-04, UNIMAS-05, UNIMAS-06, and UNIMAS-07 (Kampung Mambong) and UNIMAS-22 (Kampung Tabuan Rabak; Table 3; Supplemetary Table 1). Moreover, it can be seen that UNIMAS-17 and UNIMAS-18 from upland rice accessions and UNIMAS-30 from lowland rice accessions were grouped in two different clusters (Cluster IA and Cluster IIA) although both had the same name (Padi Bario).

From the dendrogram obtained using UPGMA cluster analysis of SSR (Figure 2), three lowland rice accessions namely UNIMAS-42, UNIMAS-43 and UNIMAS-44, which derived from a same seed source named Padi Kanowit (Supplemetary Table 1), were separated in different cluster. UNIMAS-42 and UNIMAS-43 were grouped together in Cluster IIB but UNIMAS-44 was separated into Cluster IB. This indicates UNIMAS-44 was genetically different in comparison with UNIMAS-42 and UNIMAS-43 (Table 3). This might be a result from seed impurity or mixture of seed provided by the farmers due to common practice by planting several rice varieties in one field or planting them close to each other without a clear boundary which contribute to diversity in the landrace (Yeo *et al.*, 2018).

According to Yeo *et al.* (2018), the registration of a variety based on the name given by farmers may not serve as a reliable basis for registration. There is a possibility for a variety with a similar name, exhibiting distinct morphological characteristics. To support this, the upland accessions despite being given the same name by local farmers, there were noticeable differences in seed and grain color (Frank Clifton *et al.*, 2024). Meanwhile the lowland rice varieties in Frank Clifton *et al.* (2024) showed various morphological variations. These include differences in panicle type, ligule shape, seed color, secondary branching, and grain shape. Some accessions exhibited variation in both panicle type and ligule, while others showed differences in secondary branching and grain color.

Genetic Relatedness Based on *Maturase-K*

Phylogenetic analysis based on *matK* has clustered the 22 upland accessions and 22 lowland accessions along with 94 *O. sativa* accessions from different origins and three *O.*

rufipogon accessions into one major cluster with 100% bootstrap. Accessions in Cluster I were seen not clustered together with four other *Oryza* species (*O. punctata, O. granulata, O. officinalis* and *O. australiensis*) which marked as outgroups.

The clustering of the upland 22 rice accessions and 22 lowland rice accessions were random. The clustering based on *matK* gene sequence of this study was based on genome rather than geographical or morphological characteristics. *Oryza sativa* and *O. rufipogon* which have AA genome were clustered in one clade but separated from *Oryza* of different genomes [*O. punctata* (BB genome), *O. officinalis* (CC genome), *O. australiensis* (EE genome) and *O. granulata* (GG genome)]. Similar results were obtained by Zodinpuii *et al.* (2013) and Patil *et al.* (2015) in their study by utilizing *matK* gene for the phylogenetic relationships of the *Oryza* genus. *Oryza sativa* and *O. rufipogon* in their study were also grouped in one clade, supporting the previous hypothesis of an Asian origin of *O. sativa*, and *O. rufipogon* as the progenitor (Khush, 1997). This indicates that *matK* marker alone was unable to distinguish closely related species.

The *matK* gene, while commonly used for plant DNA barcoding, often lacks sufficient resolution to distinguish closely related species within the *Oryza* genus. This limitation arises because *matK* is a relatively conserved plastid gene, meaning its DNA sequence evolves slowly and shows little variation among species that have recently diverged (Fazekas *et al.*, 2008; Hollingsworth *et al.*, 2009). As a result, *matK* may not capture enough genetic differences to separate closely related *Oryza* species effectively. Several studies by Zodinpuii *et al.* (2013) and Patil *et al.* (2015) have reported similar findings, where *matK*-based phylogenetic trees clustered *Oryza* species broadly but failed to discriminate subspecies or varieties clearly. To overcome this, combining *matK* with other more variable genetic markers such as intergenic spacers or nuclear genes is recommended, as this approach can increase discriminatory power and provide a more detailed resolution of species relationships.

A combination of barcoding markers from the plastid genome and intergenic spacers should be considered to improve the resolution of the

phylogenetic tree for a higher discrimination power. Such proposition is based on De Mattia *et al.* (2011), where the author manages to discriminate *Ocimum basilicum* from other *Ocimum* species up to cultivar level by using the combination of *matK* and *trnH-psbA* genes. The hypothesis is supported by Ho *et al.* (2021) on phylogenetic analysis of jewel orchid accessions by using *matK* and *ribulose 1,5-biphosphate carboxylase*, where the analysis revealed the combination of the two barcoding markers have higher discrimination power in comparison to analysis based on *matK* gene alone.

CONCLUSION

The 44 upland and lowland rice accessions collected from the North-West region of Sarawak were successfully genotyped using SSR markers and analyzed with the *matK* barcoding marker. The SSR analysis revealed low genetic diversity among the accessions, which may reflect either the limited number of markers used or a narrow genetic base arising from shared ancestry among local landraces. Phylogenetic analysis based on the *matK* gene grouped accessions primarily by genome type rather than by geographic origin or morphological traits.

The low genetic diversity observed among these local landraces carries important implications for both conservation and rice breeding efforts in Sarawak. On one hand, this genetic uniformity may reflect long term adaptation to local environmental conditions, suggesting a certain degree of genetic stability. On the other hand, it also indicates a limited capacity to respond to emerging challenges such as climate change, pest outbreaks and shifting agronomic needs. This potential vulnerability highlights the importance of conserving the remaining genetic variation through both in-situ and *ex situ* approaches to safeguard against further genetic erosion. Furthermore, the narrow genetic base underscores the need to introduce new, diverse germplasm into local breeding programs. Expanding the genetic pool can support the development of rice varieties with greater resilience, adaptability and productivity for sustainable cultivation in Sarawak.

To enhance the resolution and accuracy of genetic diversity assessments, future studies should consider expanding the SSR marker set or incorporating SNP markers. These approaches will provide finer genetic resolution, improve classification accuracy and strengthen molecular-assisted selection strategies in breeding programs. Additionally, combining *matK* with other barcoding markers such as *trnL-trnF* and *rbcL* can improve species discrimination and provide a more comprehensive understanding of the genetic relationships among accessions. Collectively, these strategies can support the development of effective germplasm conservation plans and guide the selection of parental lines for sustainable rice cultivation in Sarawak.

ACKNOWLEDGEMENTS

REFERENCES

Adriansyah, F., Hasmeda, M., Suwignyo, R.A., Halimi, E.S. & Sarimana, U. (2021). Genetic diversity and relationship of South Sumatran local rice and its backcrossed lines based on the *matK* gene. *Journal of Breeding & Genetics*, 53(3): 499-509.

Akagi, H., Yokozeki, Y., Inagaki, A. & Fujimura, T. (1997). Highly polymorphic microsatellites of rice consist of AT repeats, and a classification of closely related cultivars with these microsatellite loci. *Theoretical and Applied Genetics*, 94: 61-67. DOI: 10.1007/s001220050382

Aljumaili, S.J., Rafii, M.Y., Latif, M.A., Sakimin, S.Z., Arolu, I.W. & Miah, G. (2018). Genetic diversity of aromatic rice germplasm revealed by SSR markers. *BioMed Research International*, 2018: 1-11. DOI: 10.1155/2018/7658032

Al-Musawi, B.H., Al-Bdairi, N.A.H. & Al-Anbari, M.A. (2019). Sequence variation and phylogenetic relationship among rice (*Oryza sativa* L.) genotypes in Iraq. *American Institute of Physics Conference Proceedings,* 2144(1): 040001. DOI: 10.1063/1.5123102

Anderson, A., Churchill, G.A., Autrique, J.E., Tanksley, S.D. & Sorrells, M.E. (1993). Optimizing parental selection for genetic linkage

maps. *Genome*, 36(1): 181-186. DOI: 10.1139/g93-024

Awika, J.M. (2011). *Major cereal grains production and use around the world (Advances in cereal science: implications to food processing and health promotion)*. United States, American Chemical Society. DOI: 10.1021/bk-2011-1089.ch001

Bobokashvili, Z. (2016). *Re: How to interpret or infer Nei's phenotypic diversity index?* Retrieved December 10, 2022, from https://www.researchgate.net/post/How_to_ interprete_or_infer_Neis_phenotypic_diversity_i ndex.

Dalimunthe, S.R., Siregar, L.A.M., Putri, L.A.P., Cirunnisa, T. & Hairmansis, A. (2020). Polymorphism levels of some SSR markers (Simple Sequence Repeat) for parental line identification on low temperature tolerance. *Institute of Physics Conference Series: Earth and Environmental Science*, *454*(1): 012165. DOI: 10.1088/1755-1315/454/1/012165

De Mattia, F., Bruni, I., Galimberti, A., Cattaneo, F., Casiraghi, M. & Labra, M. (2011). A comparative study of different DNA barcoding markers for the identification of some members of Lamiacaea. *Food Research International*, 44(3): 693-702. DOI: 10.1016/j.foodres.2010.12.032

Dempewolf, H., Krishnan, S. & Guarino, L. (2023). Our shared global responsibility: Safeguarding crop diversity for future generations. *Proceedings of the National Academy of Sciences,* 120(14): e2205768119. DOI: 10.1073/pnas.2205768119

Department of Agriculture Sarawak. (2020). Agriculture Research Centre: Programmes. Retrieved November 20, 2021, from https://doa.sarawak.gov.my/page-0-0-415-AGRICULTURE-RESEARCH-CENTRE-PROGRAMMES.html

Doyle, J.J. & Doyle, D.J.L. (1987). A rapid DNA isolation procedure for small quantities of fresh leaf tissue. *Phytochemistry*, 19: 1115.

Fazekas, A.J., Burgess, K.S., Kesanakurti, P.R., Graham, S.W., Newmaster, S.G., Husband, B.C., Percy, D.M., Hajibabaei, M. & Barrett, S.C.H. (2008). Multiple multilocus DNA barcodes from the plastid genome discriminate plant species equally well. *PLoS ONE*, 3(7): e2802. DOI: 10.1371/journal.pone.0002802

Frank Clifton, Z., Yeo F.K.S., Sylvester Embuas, R.P.T., Kalu, M., Shabdin, Z. & Lai, L.S. (2024). Preliminary characterisation of lowland and upland rice from Sarawak, Malaysian Borneo. *Borneo Journal of Resource Science and Technology*, 14(1): 123-138. DOI: 10.33736/bjrst.5653.2024

García, C., Guichoux, E. & Hampe, A. (2018). A comparative analysis between SNPs and SSRs to investigate genetic variation in a juniper species (*Juniperus phoenicea* ssp. turbinata). *Tree Genetics & Genomes*, 14: 1-9. DOI: 10.1007/s11295-018-1301-x

Hassan, D.A. & Hama-Ali, E.O. (2022). Evaluation of gene flow and genetic diversty in rice accessions across Kurdistan region-Iraq using SSR Markers. *Molecular Biology Reports*, 49: 1007-1016.

Ho, V.T., Tran, T.K.P., Vu, T.T.T. & Widiarsih, S. (2021). Comparison of *matK* and *rbcL* DNA barcodes for genetic classification of jewel orchid accessions in Vietnam. *Journal of Genetic Engineering and Biotechnology*, 19(1): 93. DOI: 10.1186/s43141-021-00188-1

Hodel, R.G., Segovia-Salcedo, M.C., Landis, J.B., Crowl, A.A., Sun, M., Liu, X. & Soltis, P.S. (2016). The report of my death was an exaggeration: A review for researchers using microsatellites in the 21st century. *Applications in Plant Sciences*, 4(6): 1600025. DOI: 10.3732/apps.1600025

Hollingsworth, P.M., Forrest, L.L., Spouge, J.L., Hajibabaei, M., Ratnasingham, S., van der Bank, M., Chase, M.W., Cowan, R.S., Erickson, D.L., Fazekas, A.J., Graham, S.W., James, K.E., Kim, K.J., Kress, W.J., Schneider, H., van Alphen Stahl, J., Barrett, S.C.H., van den Berg, C., Bogarin, D. & Little, D.P. (2009). A DNA barcode for land plants. *Botanical Journal of the Linnean Society,* 159(1): 1-16. DOI: 10.1073/pnas.0905845106

Khush, G.S. (1997). Origin, dispersal, cultivation and variation of rice. *Plant Molecular Biology*, 35: 25-34. DOI: 10.1023/A:1005810616885

Lee, H.H., Neoh, P.P.N., Bong, W.S.T., Puvaneswaran, J., Wong, S.C., Yiu, P.H. & Rajan, A. (2011). Genotyping of Sarawak rice cultivars using microsatellite markers. *Pertanika Journal of Tropical Agriculture Science*, 34: 123-136.

Ma, M., Liu, Y., Wang, T. & Lu, B. (2016). Cluster analysis of red rice based on SSR markers from Hani's terraced fields in Yunnan Province.

Advances in Computer Science Research, 63. DOI: 10.2991/aiea-16.2016.29

Ma, M., Lei, E., Wang, T., Meng, H., Zhang, W. & Lu, B. (2023). Genetic diversity and association mapping of grain-size traits in rice landraces from the Honghe Hani Rice Terraces system in Yunnan Province. *Plants,* 12(8): 1678.

Melaku, G., Zhang, S. & Haileselassie, T. (2018). Comparative evaluation of rice SSR markers on different *Oryza* species. *Journal of Rice Research and Developments*, 1(1): 38-48. DOI: 10.36959/973/418

Miah, G., Rafii, M.Y, Ismail, M.R., Puteh, A.B., Rahim, H.A., Islam, K.H. & Latif, M.A. (2013). A review of microsatellite markers and their applications in rice breeding programs to improve blast disease resistance. *International Journal of Molecular Sciences*, 14: 22499-22528.

Patil, R.G., Jadhao, K.R., Samal, K.C. & Rout, G.R. (2015). Molecular phylogeny of Indian indigenous aromatic rice based on sequence diversity of the chloroplast-encoded *matK* gene. *Rice Genomics and Genetics*, 6(8): 1-8. DOI: 10.5376/rgg.2015.06.0008

Shete, S., Tiwari, H. & Elston, R.C. (2000). On estimating the heterozygosity and polymorphism information content value. *Theoretical Population Biology*, 57(3): 265-271. DOI: 10.1006/tpbi.2000.1452

Smouse, P.E., Banks, S.C. & Peakall, R. (2017). Converting quadratic entropy to diversity: Both animals and alleles are diverse, but some are more diverse than others. *The Public Library of Science One*, 12(10): e0185499. DOI: 10.1371/journal.pone.0185499

Sohrabi, M., Rafii, M.Y., Hanafi, M.M. & Latif, M.A. (2013). Genetic divergence of Malaysian upland rice revealed by microsatellite markers. *Plant Omics Journal*, 6(3): 175-182.

Sohrabi, M., Rafii, M.Y., Hanafi, M.M., Siti Nor Akmar, A. & Latif, M.A. (2012). Genetic diversity of upland rice germplasm in Malaysia based on quantitative traits. *The Scientific World Journal*, 2012(1), 1-9. DOI: 10.1100/2012/416291

Supari, N., Kaya, Y., Biroudian, M. & Javed, M. (2019). Molecular characterization of Malaysian rice cultivars using SSR markers. *American*

Institute of Physics Conference Proceedings, 2155(1): 020016. DOI: 10.1063/1.5125520

Tan, C.S., Teo, G.K., Jamadon, B. & Tan P.H. (2006). *Microsatellite markers for differentiation of local Bario rice varieties*. Retrieved August 15, 2022, from: https://doa.sarawak. gov.my/web/attachment/show/?docid=https://doa .sarawak.gov.my/web/attachment/show/?docid=b GlYVDZsV3hTU1NkVUQyTHBSOG9EQT09O jr-_vyzGFP5599ncaaN5uaQ

Wang, H., Yang, B., Wang, H. & Xiao, H. (2021). Impact of different numbers of microsatellite markers on population genetic results using SLAF-seq data for *Rhododendron* species. *Scientific Reports*, 11(1): 8597. DOI:10.1038/s41598-021-87945-x

Wong, S.C., Yiu, P.H., Bong, S.T.W., Lee, H.H., Neoh, P.N.P. & Rajan, A. (2009). Analysis of Sarawak Bario rice diversity using microsatellite markers. *American Journal of Agricultural and Biological Sciences*, 4(4): 298-304.

Yao, X., Tan, Y.H., Liu, Y.Y. & Song, Y. (2019). Molecular markers for species identification of medicinal plants: A review. *Evidence-Based Complementary and Alternative Medicine*, 2019: 8746802. DOI: 10.1155/2019/8746802

Yeo, F.K.S., Meekiong, K., Shabdin, Z., Mohamad, N.K., Hussin, N.A. & Chung, H.H. (2018). Diversity of rice in Kampung Lebor, Serian – A first insight. In Yeo, F.K.S., Chong, Y.L. & Khan, F.A.A. (eds.). *Glimpses of Bornean Biodiversity.* Kuching, Malaysia, Universiti Malaysia Sarawak Publisher. pp. 155-167.

Zhang, C.H., Li, J.Z., Zhu, Z., Zhang, Y.D., Zhao, L. & Wang, C.L. (2010). Cluster analysis on japonica rice (*Oryza sativa* L.) with good eating quality based on SSR markers and phenotypic traits. *Rice Science*, 17(2): 111-121. DOI: 10.1016/S1672-6308(08)60113-4

Zhu, Y.F., Qin, G.C., Yang, W., Wang, J.C. & Zhu, S.J. (2012). Fingerprinting and variety identification of rice (*Oryza sativa* L.) based on Simple Sequence Repeat markers. *Plant Omics Journal*, 5(4): 421-426.

Zodinpuii, D., Ghatak, S., Mukherjee, S. & Kumar, N.S. (2013). Genetic relatedness of genus *Oryza* from Eastern Himalayan region as revealed by chloroplast *matK* gene. *Asian Journal of Conservation Biology*, 2(2): 144-151.

SUPPLEMENTARY MATERIALS

Molecular Characterisation of Upland and Lowland Rice from Sarawak, Malaysian Borneo

FREDDY KUOK SAN YEO[1*], RENEE PRISCILLA TRAWAS SYLVESTER EMBUAS[1], ZAZEVIA FRANK CLIFTON[1], MEEKIONG KALU[1], ZINNIRAH SHABDIN[1] & LEE SAN LAI[2]

[1]Faculty of Resource Science and Technology, Universiti Malaysia Sarawak, Jalan Datuk Mohammad Musa, 94300, Kota Samarahan, Sarawak, Malaysia; [2]Agriculture Research Centre Semongok, KM20, Jalan Puncak Borneo, 93250, Kuching, Sarawak
*Corresponding author: yksfreddy@unimas.my

SUPPLEMENTARY DATA

Supplementary Table 1.
List of landraces with its locality and GPS

Upland Landraces					Lowland Landraces				
Name	Accession	Location	GPS	Division	Name	Accession	Location	GPS	Division
Padi Belawi Pandan	UNIMAS-01, UNIMAS-02	Kg Paon Gahat	0° 57' 0" North, 110° 39' 0" East	Serian	Padi Pandan	UNIMAS-23	Kg Paon Gahat	0° 57' 0" North, 110° 39' 0" East	Serian
Padi Belawi	UNIMAS-03	Kg Paon Gahat	0° 57' 0" North, 110° 39' 0" East	Serian	Padi Hitam	UNIMAS-24, UNIMAS-25, UNIMAS-26	Kg Pueh	1° 51' 0" North, 109° 41' 0" East	Kuching
Padi Merjat	UNIMAS-04, UNIMAS-05, UNIMAS-06, UNIMAS-07	Kg Mambong	1° 22' 0" North, 110° 21' 0" East	Kuching	Padi Merah	UNIMAS-27	Kg Pesak	1° 45' 0" North, 110° 46' 0" East	Kuching
Padi Pandan Wangi	UNIMAS-08, UNIMAS-09, UNIMAS-10, UNIMAS-11, UNIMAS-12, UNIMAS-13, UNIMAS-14	Kg Pesak	1° 45' 0" North, 110° 46' 0" East	Kuching	Padi Bajong	UNIMAS-28	Kg Panggil	1°05'48" North, 111°23'23" East	Sri Aman
Padi Limbang	UNIMAS-15	Kg Sg Tenggang	1° 04' 48" North, 111° 03' 28" East	Sri Aman	Padi Arang	UNIMAS-29	Kg Sg Tenggang	1° 04' 48" North, 111° 03' 28" East	Sri Aman
Padi Chelum	UNIMAS-16	Kg Sg Tenggang	1° 04' 48" North, 111° 03' 28" East	Sri Aman	Padi Bario	UNIMAS-30	Kg Baru	1° 33' 28" North, 110° 22' 22" East	Kota Samarahan
Padi Bario	UNIMAS-17, UNIMAS-18	Kg Sg Tenggang	1° 04' 48" North, 111° 03' 28" East	Sri Aman	Padi Sabak Hitam	UNIMAS-31, UNIMAS-32	Kg Baru	1° 33' 28" North, 110° 22' 22" East	Kota Samarahan
Padi Badawi	UNIMAS-19	Kg Sg Tenggang	1° 04' 48" North, 111° 03' 28" East	Sri Aman	Padi Selasih	UNIMAS-33, UNIMAS-34	Kg Melugu Skim	1°07'10" North, 111°25'33" East	Sri Aman

Supplementary Table 1. *(continue)*

Padi Sempang	UNIMAS-20	Kg Melugu Tengah	1° 06'14" North, 111°23'57" East	Sri Aman	Padi Sabak Angin	UNIMAS-35, UNIMAS-36, UNIMAS-37, UNIMAS-38, UNIMAS-39	Kg Baru	1° 33' 28" North, 110° 22' 22" East	Kota Samarahan
Padi Mawang	UNIMAS-21	Kg Melugu Tengah	1° 06' 14" North, 111° 23' 57" East	Sri Aman	Padi Kihuai	UNIMAS-40, UNIMAS-41	Kg Mambong	1° 22' 0" North, 110° 21' 0" East	Kuching
Padi Merjat	UNIMAS-22	Kg Tabuan Rabak	1° 18' 39" North, 110° 20' 59" East	Kuching	Padi Kanowit	UNIMAS-42, UNIMAS-43, UNIMAS-44	Kg Melugu Skim	1° 07' 10" North, 111° 25' 33" East	Sri Aman

Supplementary Table 2.

The 39 sets of SSR markers with sequences and details

SSR	Primer sequence	Ch	EPS (bp)	Ta (°C)	Source
RM1	F: GCGAAAACACAATGCAAAAA	1	90-120	55	
	R: GCGTTGGTTGGACCTGAC				
RM226	F: GAAGCTAAGGTCTGGGAGAAACC	1	280-350	55	
	R: AATGGCCTTAACCAAGTAGGATGG				
RM279	F: GCGGGAGAGGGATCTCCT	2	170-190	55	
	R: GGCTAGGAGTTAACCTCGCG				
RM207	F: CCATTCGTGAGAAGATCTGA	2	N/A	55	
	R: CACCTCATCCTCGTAACGCC				
RM489	F: ACTTGAGACGATCGGACACC	3	250-270	55	
	R: TCACCCATGGATGTTGTCAG				
RM514	F: AGATTGATCTCCCATTCCCC	3	N/A	55	Gramene (https://archive.gramene.org/markers/microsat/all-ssr.html)
	R: CACGAGCATATTACTAGTGG				
RM335	F: GTACACACCCACATCGAGAAG	4	100-200	55	
	R: GCTCTATGCGAGTATCCATGG				
RM567	F: ATCAGGGAAATCCTGAAGGG	4	280-400	55	
	R: GGAAGGAGCAATCACCACTG				
RM317	F: CATACTTACCAGTTCACCGCC	4	160	55	
	R: CTGGAGAGTGTCAGCTAGTTGA				
RM229	F: CACTCACACGAACGACTGAC	4	100-120	55	
	R: CGCAGGTTCTTGTGAAATGT				
RM166	F: GGTCCTGGGTCAATAATTGGGTTACC	4	321-410	61	
	R: TTGCTGCATGATCCTAAACCGG				
RM108	F: TCTCTTGCGCGCACACTGGCAC	4	N/A	67	
	R: CGTGCACCACCACCACCACCAC				
RM413	F: GGCGATTCTTGGATGAAGAG	5	N/A	53	
	R: TCCCCACCAATCTTGTCTTC				
RM480	F: GCTCAAGCATTCTGCAGTTG	5	N/A	58	
	R: GCGCTTCTGCTTATTGGAAG				

Supplementary Table 2. *(continue)*

SSR	Primer sequence	Ch	EPS (bp)	Ta (°C)	Source
RM164	F: TCTTGCCCGTCACTGCAGATATCC R: GCAGCCCTAATGCTACAATTCTTC	5	246-300	58	
RM250	F: GGTTCAAACCAAGCTGATCA R: GATGAAGGCCTTCCACGCAG	5	170-190	57	Gramene (https://archive.gramene.org/markers/microsat/all-ssr.html)
RM469	F: AGCTGAACAAGCCCTGAAAG R: GACTTGGGCAGTGTGACATG	6	100-120	55	
RM454	F: CTCAAGCTTAGCTGCTGCTG R: GTGATCAGTGCACCATAGCG	6	N/A	55	
RM276	F: CTCAACGTTGACACCTCGTG R: TCCTCCATCGAGCAGTATCA	6	100-180	59	
RM125	F: ATCAGCAGCCATGGCAGCGACC R: AGGGGATCATGTGCCGAAGGCC	7	130-600	63	
RM455	F: AACAACCCACCACCTGTCTC R: AGAAGGAAAAGGGCTCGATC	7	140	55	
RM481	F: TAGCTAGCCGATTGAATGGC R: CTCCACCTCCTATGTTGTTG	7	190-300	59	
RM47	F: ACTCCACTCCACTCCCCAC R: GTCAGCAGGTCGGACGTC	7	N/A	59	
RM152	F: GAAACCACCACACCTCACCG R: CCGTAGACCTTCTTGAAGTAG	8	140	53	
RM447	F: CCCTTGTGCTGTCTCCTCTC R: ACGGGCTTCTTCTCCTTCTC	8	100-600	53	
RM210	F: TCACATTCGGTGGCATTG R: CGAGGATGGTTGTTCACTTG	8	120-180	57	
RM444	F: GCTCCACCTGCTTAAGCATC R: TGAAGACCATGTTCTGCAGG	9	190-280	55	
RM215	F: CAAAATGGAGCAGCAAGAGC R: TGAGCACCTCCTTCTCTGTAG	9	150	56.	

Supplementary Table 2. *(continue)*

SSR marker	Primer sequence	Ch	EPS (bp)	Ta (°C)	Source
RM244	F: CCGACTGTTCGTCCTTATCA R: CTGCTCTCGGGTGAACGT	10	N/A	55	
RM228	F: CTGGCCATTAGTCCTTGG R: GCTTGCGGCTCTGCTTAC	10	N/A	55	
RM552	F: CGCAGTTGTGGATTTCAGTG R: TGCTCAACGTTTGACTGTCC	11	200-210	55	
RM206	F: CCCATGCGTTTAACTATTCT R: CGTTCCATCGATCCGTATGG	11	N/A	58.1	
RM257	F: CAGTTCCGAGCAAGAGTACTC R: GGATCGGACGTGGCATATG	11	150-200	55	
RM224	F: ATCGATCGATCTTCACGAGG R: TGCTATAAAAGGCATTCGGG	11	150-200	55	Gramene (https://archive.gramene.org/markers/microsat/all-ssr.html)
RM21	F: ACAGTATTCCGTAGGCACGG R: GCTCCATGAGGGTGGTAGAG	11	140-180	51	
RM247	F: TAGTGCCGATCGATGTAACG R: CATATGGTTTTGACAAAGCG	12	140-190	55	
RM17	F: TGCCCTGTTATTTTCTTCTCTC R: GGTGATCCTTTCCCATTTCA	12	190-220	55	
RM519	F: AGAGAGCCCCTAAATTTCCG R: AGGTACGCTCACCTGTGGAC	12	120-140	55	
RM561	F: GAGCTGTTTTGGACTACGGC R: GAGTAGCTTTCTCCCACCCC	N/A	N/A	55	

Note. SSR: Simple Sequence Repeat; F: Forward primer; R: Reverse primer; Ch: Chromosome; EPS: Expected product size in base pair; Ta: Annealing temperature in degree Celsius; N/A indicates data not available.

Supplementary Table 3.
The accession number for *matK* sequences downloaded from NCBI

Species	Identification Code	Country of Origin	GenBank Accession Number
Oryza sativa	OS India 1	India	KT894765.1
Oryza sativa	OS India 2	India	KT894764.1
Oryza sativa	OS India 3	India	KT894763.1
Oryza sativa	OS India 4	India	KT894762.1
Oryza sativa	OS India 5	India	KT894761.1
Oryza sativa	OS India 6	India	KT894760.1
Oryza sativa	OS India 7	India	KT894759.1
Oryza sativa	OS India 8	India	KT894758.1
Oryza sativa	OS India 10	India	KT894756.1
Oryza sativa	OS India 11	India	KF731111.1
Oryza sativa	OS India 12	India	KF731110.1
Oryza sativa	OS India 13	India	KF731109.1
Oryza sativa	OS India 14	India	KF731108.1
Oryza sativa	OS India 15	India	KF731107.1
Oryza sativa	OS India 16	India	KF731106.1
Oryza sativa	OS India 17	India	KF731105.1
Oryza sativa	OS India 18	India	KF731104.1
Oryza sativa	OS India 19	India	KF731103.1
Oryza sativa	OS India 20	India	KF731102.1
Oryza sativa	OS India 21	India	KF731101.1
Oryza sativa	OS India 22	India	KF731100.1
Oryza sativa	OS India 23	India	KF731099.1
Oryza sativa	OS India 24	India	KF731098.1
Oryza sativa	OS India 25	India	KF731097.1
Oryza sativa	OS India 26	India	KF731096.1
Oryza sativa	OS India 27	India	KF731095.1
Oryza sativa	OS India 28	India	KF731094.1
Oryza sativa	OS India 29	India	KF731093.1
Oryza sativa	OS India 30	India	KF731092.1

Supplementary Table 3. *(continue)*

Species	Identification Code	Country of Origin	GenBank Accession Number
Oryza sativa	OS India 31	India	KF731091.1
Oryza sativa	OS India 32	India	KF731090.1
Oryza sativa	OS India 33	India	KF731089.1
Oryza sativa	OS India 34	India	KF731088.1
Oryza sativa	OS India 35	India	KF731087.1
Oryza sativa	OS India 36	India	KF731086.1
Oryza sativa	OS India 37	India	KF731085.1
Oryza sativa	OS India 38	India	KF731084.1
Oryza sativa	OS India 39	India	KF731083.1
Oryza sativa	OS India 40	India	KF731082.1
Oryza sativa	OS India 41	India	KF731081.1
Oryza sativa	OS India 42	India	KF731080.1
Oryza sativa	OS India 43	India	KF731079.1
Oryza sativa	OS India 44	India	KF731078.1
Oryza sativa	OS India 45	India	KF731077.1
Oryza sativa	OS India 46	India	KF731074.1
Oryza sativa	OS India 47	India	KF731073.1
Oryza sativa	OS India 48	India	KF731072.1
Oryza sativa	OS India 49	India	KF731071.1
Oryza sativa	OS India 50	India	KF731070.1
Oryza sativa	OS India 51	India	KF731069.1
Oryza sativa	OS India 52	India	KF731068.1
Oryza sativa	OS India 53	India	KF731067.1
Oryza sativa	OS India 54	India	KF731066.1
Oryza sativa	OS India 55	India	KF731065.1
Oryza sativa	OS India 56	India	KF731064.1
Oryza sativa	OS India 57	India	KF731063.1
Oryza sativa	OS India 58	India	KF731062.1
Oryza sativa	OS India 59	India	KF731061.1
Oryza sativa	OS India 60	India	KF731060.1
Oryza sativa	OS India 61	India	KF731059.1

Supplementary Table 3. *(continue)*

Species	Identification Code	Country of Origin	GenBank Accession Number
Oryza sativa	OS India 62	India	KF731058.1
Oryza sativa	OS India 63	India	KF731057.1
Oryza sativa	OS India 64	India	KF731056.1
Oryza sativa	OS India 65	India	KF731055.1
Oryza sativa	OS India 66	India	KF731054.1
Oryza sativa	OS India 67	India	KF731053.1
Oryza sativa	OS India 68	India	KF731052.1
Oryza sativa	OS India 69	India	KF731051.1
Oryza sativa	OS India 70	India	KF731050.1
Oryza sativa	OS India 71	India	KF731049.1
Oryza sativa	OS India 72	India	KF731048.1
Oryza sativa	OS India 73	India	KF731047.1
Oryza sativa	OS India 74	India	KF731046.1
Oryza sativa	OS India 75	India	KF731045.1
Oryza sativa	OS India 76	India	KF731044.1
Oryza sativa	OS India 77	India	KF731043.1
Oryza sativa	OS India 78	India	KF731042.1
Oryza sativa	OS India 79	India	KF731041.1
Oryza sativa	OS India 80	India	KF731040.1
Oryza sativa	OS India 81	India	KF731039.1
Oryza sativa	OS India 82	India	KF731038.1
Oryza sativa	OS India 83	India	KF731037.1
Oryza sativa	OS India 84	India	KF731036.1
Oryza sativa	OS India 85	India	KF731035.1
Oryza sativa	OS India 86	India	KF731034.1
Oryza sativa	OS India 87	India	KF731033.1
Oryza sativa	OS India 88	India	KF731032.1
Oryza sativa	OS India 89	India	HG794000.1
Oryza sativa	OS Australia 1	Australia	KU923990.1
Oryza sativa	OS Australia 2	Australia	KU923989.1
Oryza sativa	OS Australia 3	Australia	KU923988.1

Supplementary Table 3. *(continue)*

Species	Identification Code	Country of Origin	GenBank Accession Number
Oryza sativa	OS Australia 4	Australia	KU923987.1
Oryza sativa	OS China 1	China	AF148650.1
O. sativa	OS Unknown	Unknown	EU434287.1
Oryza rufipogon	*O. rufipogon 1*	Unknown	EU434286.1
Oryza rufipogon	*O. rufipogon 2*	India	FJ908261.1
Oryza rufipogon	*O. rufipogon 3*	China	AF148651.1
Oryza punctata	*O. punctata 1*	Unknown	KP864529.1
Oryza punctata	*O. punctata 2*	Unknown	KP864528.1
Oryza punctata	*O. punctata 3*	Unknown	KP864527.1
Oryza officinalis	*O. officinalis 1*	Philippines	AF148658.1
Oryza officinalis	*O. officinalis 2*	China	KP121859.1
Oryza officinalis	*O. officinalis 3*	Papua New Guinea	KP121858.1
Oryza australiensis	*O. australiensis 1*	Australia	AF148667
Oryza granulata	*O. granulata 1*	China	AF148674.1
Oryza granulata	*O. granulata 2*	Vietnam	KP121857.1

The Potential of *Neolamarckia cadamba* Seedling in Improving Growth Performance and Yield of *Zea mays* under Different Precipitation Patterns

ROMIA RONA TAGANG[1], HOLLENA NORI[1], WALFTOR DUMIN[1], WEE SZE YEE[2], HO WEI SENG[1] & MOHAMAD HILMI IBRAHIM*[1]

[1]Faculty of Resource Science and Technology, Universiti Malaysia Sarawak, 94300, Kota Samarahan, Sarawak, Malaysia; [2]Institute of Biodiversity and Environmental Conservation, Universiti Malaysia Sarawak, 94300, Kota Samarahan, Sarawak, Malaysia;
*Corresponding author: imhilmi@unimas.my

ABSTRACT

Climate change is altering rainfall, with more droughts and severe storms that harm agriculture. These shifts in temperature and precipitation disrupt soil moisture, which is essential for the growth of staple crops. Therefore, this study was conducted to investigate the effects of integrating *Neolamarckia cadamba* with *Zea mays* on growth performance under different precipitation patterns: low (T1), normal (T2) and high (T3). The experiment was conducted in a completely randomised block design (CRBD), with the first block representing *N. cadamba* integrated with *Z. mays* as agroforestry, the second block representing only *Z. mays* as a crop and the third block only *N. cadamba* as a tropical tree species. The growth parameters (number of leaves, diameter, plant height and chlorophyll content) were measured 120 days after planting and the yield parameters (fresh weight, dry weight, number of kernels, fresh weight of kernel, dry weight of kernel) were measured after harvesting. The results showed significant effects of rainfall and agroforestry integration on maize yield in term of dry weight, number of kernels, kernels fresh weight and kernel dry weight. Kernel yield parameters, including fresh weight and kernel number, were highest under T2 and T3 in the agroforestry (AGRO), indicating improved availability of resources and soil conditions by *N. cadamba*. In term of practices, AGRO produced higher chlorophyll (SPAD: 29.44 ± 1.44 vs 22.47 ± 2.31; $p< 0.05$) and dry weight (277.24 ± 11.68 g vs 216.84 ± 23.47 g; $p< 0.05$) than NON-AGRO. These results show an ecological trade-off such as in normal and wet conditions *N. cadamba* cools the canopy and conserves soil moisture, raising *Z. mays* performance while under drought, root water pre-emption and reduced light increase competition and depress kernel. At farm level, border or alley planting of *N. cadamba* with *Z. mays* can be promoted under normal and wet conditions, while wider spacing or soil-water conservation is advisable in dry conditions the policymakers can include maize and *N. cadamba* designs in agroforestry extension as part of climate-smart agriculture.

Keywords: Agroforestry, climate change, growth performance, precipitation pattern, *Zea mays*

INTRODUCTION

In response to growing concerns over climate change, the integration of agroforestry practices has gained attention as a sustainable solution to improve the resilience of agriculture. Agroforestry, the combination of trees with agricultural crops, has been shown to be a sustainable practice for agricultural productivity, restoring degraded land, and mitigating the effects of climate change (Jose, 2009; Das *et al*., 2024). By incorporating perennial woody plants into agricultural systems, agroforestry improves biodiversity, carbon sequestration and ecosystem resilience while supporting rural livelihoods (Lorenz & Lal, 2014; Zomer *et al*., 2016). This practice is particularly important in regions that are vulnerable to climate variability as it helps to maintain soil fertility and water availability for plant growth.

Climate change, especially the shift in precipitation patterns, poses a major challenge to agricultural systems worldwide. Anthropogenic activities such as deforestation, the burning of fossil fuels and greenhouse gas emissions have accelerated global warming and contribute to changing precipitation patterns and extreme weather events (Tang, 2019). Changes in precipitation patterns affect soil moisture availability, crop phenology and overall agricultural productivity and pose a threat to

global food security (Hooper *et al.*, 2005; Firdaus *et al.*, 2018). In Malaysia, climate variability has led to prolonged droughts, excessive rainfall and flooding, disrupting agricultural cycles and crop yields (Tang, 2019).

Among agroforestry trees, *Neolamarckia cadamba*, also known as Kelempayan, is a potential tropical tree species due to its fast growth and deep root system that can help improve soil structure and nutrient cycling (Khatta *et al.*, 2023). Its ability to adapt to different environmental conditions and improve soil properties makes it a suitable candidate for agroforestry systems, especially in areas with climatic stress (Khatta *et al.*, 2023). On the other hand, *Zea mays* (maize) is a globally important cereal crop that is essential for food security and economic stability in many regions (Erenstein *et al.*, 2022). However, maize production is very sensitive to climate variability, especially to changes in rainfall patterns. Insufficient rainfall or too much water can have a negative impact on the growth, development and yield of maize and exacerbate food insecurity in regions such as Malaysia (Alam *et al.*, 2017).

Recent studies emphasise the role of rainfall in determining crop productivity, with rainfall variability posing a major challenge to food security (Wang *et al.*, 2024). Changes in rainfall patterns due to climate change in the form of excessive rainfall or prolonged drought can affect the growth, yield and resilience of crops such as maize (Yin *et al.*, 2016). *Zea mays* is highly sensitive to moisture extremes where drought can reduce yield by ~30–90% depending on timing and severity (Széles *et al.*, 2023). *Neolamarckia cadamba* can mitigate some negative effects through water regulation and soil stabilisation, making it an ideal candidate for integration into agroforestry (Wamalwa *et al.*, 2021). Empirical evidence for the integration of *N. cadamba* and *Z. mays* in different rainfall regimes is still limited. Few studies examine both species simultaneously under low, normal and high precipitation to separate microclimatic benefits from subsurface water competition.

The aim of this study is to investigate the effects of *N. cadamba* integration on *Z. mays* growth and yield performance under different precipitation patterns. By assessing low (T1), normal (T2) and high (T3) rainfall, the study aims to provide data on whether the integration of agroforestry can improve crop resilience and productivity in changing climates. We hypothesise that integrating *N. cadamba* with *Z. mays* increases chlorophyll content, biomass, and kernel yield under normal and high precipitation, but shows neutral or negative effects under low precipitation because of water competition. We expect a significant interaction between cropping system and precipitation on growth and yield.

METHODOLOGY

Study Site

The 29ft (L) × 19ft (W) × 8ft (H) shelter was set up at the Faculty of Resource Science and Technology, UNIMAS. *Neolamarckia cadamba* and *Zea mays* were grown in the shelter house to minimise infestation by pests and to ensure uniform sunlight and water supply. The temperature in the shelter was 29 °C with a humidity of 76%, which was determined using a hygrometer.

Experimental Design

A complete randomised block design (CRBD) was conducted to minimise variability and increase the reliability of the results. The study consisted of three blocks with four replications. Each block assigned to one of the three rainfall treatments. The block plot was the integration of *N. cadamba* and *Z. mays* as agroforestry, the second block was only *Z. mays* as a crop and the third block was only *N. cadamba* as a tropical tree. Each agroforestry (AGRO) pot contained two seedlings (1 *N. cadamba* + 1 *Z. mays*; 1:1). Each NON-AGRO pot contained a single seedling (either *Z. mays* or *N. cadamba*). In AGRO pots, the centre-to-centre spacing between the two seedlings was 15 cm within the pot area. Across treatments, n = 4 pots per rainfall regime. These represent the different agricultural practices.

Baseline Soil Composition and Nutrient

Baseline soil (Nyalau series; *Typic paleudults*) was characterised before treatments. Texture was determined by the hydrometer method and classified as sandy clay loam. Soil pH (H_2O) was measured in a 1:2.5 soil-to-water suspension. Bulk density was measured by the core method

(oven-dry mass/volume). Mineral N (NH_4^+–N and NO_3^-–N) was extracted with 2 M KCl (1:5, w/v) and determined using Hach colourimetric methods ammonia salicylate for NH_4^+–N (Hach 8155) and Nitrate by cadmium reduction/Griess for NO_3^-–N (Hach 8039/8171) on a Hach DR spectrophotometer. Available P was extracted with Bray-1 and measured colourimetrically. Total N was determined by the Kjeldahl method. Total organic carbon was analysed by the Walkley–Black method, and organic matter by loss on ignition. Summary values (means of three replicates) are reported in Table 1.

Table 1. Selected soil physico-chemical properties of Nyalau series (*Typic paleudults*) used in the study. Data are expressed as the means of three replications

Parameter	Value
pH in water	4.84
Exchangeable Ammonium NH_4^+	49.04 mgkg^{-1}
Available Nitrate NO_3^-	21.02 mgkg^{-1}
Available Phosphate	0.10 mgkg^{-1}
Total Nitrogen	0.11%
Bulk density	1.20 gcm^{-3}
Total Organic Carbon	6.00%
Organic matter	0.17%
Soil texture: Soil-sandy clays loam	

Precipitation Treatments

The three precipitation treatments were carefully simulated to reflect realistic environmental scenarios. Low precipitation (T1) included water reduction to mimic drought conditions, normal precipitation (T2) corresponded to average precipitation patterns typical of the region, and high precipitation (T3) simulated excessive rainfall from supplemental irrigation. Water was applied by hand to each pot using the average weekly rainfall in Kota Samarahan, Sarawak as the basis. The experiment tested three precipitation levels: the weekly average (W), W decreased by 30% (W−), and W increased by 30% (W+). For example, if the weekly total was 311 mm (approximate ± 30% range: highest 449 mm; lowest 212 mm), treatment volumes were set accordingly. Treatments were administered once every six days in the morning (07:00–09:00). To prevent desiccation, seedlings were also watered once daily.

Measuring the Variables

Growth performance and yield of *Z. mays* and *N. cadamba* were measured over 120 days after planting. The growth parameters included the number of leaves, plant height, stem diameter and chlorophyll, which were measured using a ruler, a tape measure, a digital calliper and a chlorophyll metre (SPAD 502, Plus, Konica Minolta). Yield metrics were assessed at harvest and included *Z. mays* fresh weight, *Z. mays* dry weight, number of kernels, kernel fresh weight and kernel dry. *Zea mays* were harvested fresh in the field and weighed using an electronic scale with an accuracy of 1 g. The grains on the stalk were shelled and weighed. Total dry matter (TDM) was determined by drying in a brown envelope in an oven at 65 °C until a constant weight was reached.

Data Analysis

The data were analysed using SAS Version 9 (SAS Institute Inc., Cary, NC, USA). Growth and yield of *Z. mays* were evaluated under three rainfall treatments where low is T1, normal is T2 and high is T3 for both AGRO and NON-AGRO systems. We used one-way ANOVA to test rainfall effects within each cropping system because rainfall was the single factor with three fixed levels and our primary interest was to compare T1, T2 and T3 within a given system. Duncan's Multiple Range Test (DMRT) identified differences among means at $\alpha = 0.05$. We used unpaired t-tests to compare AGRO versus NON-AGRO within the same rainfall regime, as units experienced the same watering schedule and could be matched; pairing increases power and controls between-unit

variability. We checked normality (Shapiro–Wilk) and homogeneity of variances (Levene's). Results are reported as mean ± SE, and statistical significance was set at p<0.05.

RESULTS

Growth Performance and Yield of *Z. mays* Under Different Precipitation Patterns

Within AGRO, Table 2 shows no significant differences among rainfall treatments for any growth parameter namely leaf number, plant height, stem diameter and chlorophyll (SPAD), were statistically similar across T1–T3. However, there were differences in the number of kernels, and kernel yield (fresh and dry). Fresh weight was significantly higher under T2 (1233.30±72.23 g), closely followed by T3 (1216.70±71.73 g), while T1 had the lower fresh weight (970.00±71.24 g).

Table 2. Effect of precipitation and agroforestry integration on growth and yield of *Zea mays* (mean ± SE; n = 4 per treatment)

Treatment	Number of Leaves	Height (cm)	Diameter (mm)	Chlorophyll content (SPAD)	Fresh weight (Kg)	Dry weight (Kg)	Number of kernels	Kernel fresh weight (g)	Kernel dry weight (g)
Growth Parameter *Zea mays* (AGRO)									
T1	13.00[A]	190.08[A]	13.320[A]	27.33[A]	970.0[A]	254.10[A]	100.05[B]	16.69[B]	12.45[C]
T2	13.00[A]	187.33[A]	13.743[A]	28.80[A]	1233.3[A]	291.23[A]	147.83[A]	37.49[A]	31.46[A]
T3	12.50[A]	180.70[A]	13.753[A]	32.20[A]	1216.7[A]	286.40[A]	146.50[A]	38.35[A]	29.34[B]
Growth Parameter *Zea mays* (NON-AGRO)									
Treatment	Number of Leaves	Height (cm)	Diameter (mm)	Chlorophyll content (SPAD)	Fresh weight (Kg)	Dry weight (Kg)	Number of kernels	Kernel fresh weight (g)	Kernel dry weight (g)
T1	12.50[A]	179.62[A]	13.40[A]	19.867[A]	887.50[A]	170.39[B]	119.0[A]	36.34[A]	26.56[A]
T2	13.25[A]	182.62[A]	15.06[A]	24.033[A]	1037.50[A]	234.14[AB]	131.00[A]	32.47[B]	26.49[A]
T3	13.25[A]	182.95[A]	14.26[A]	23.533[A]	987.50[A]	246.00[A]	120.0[A]	32.63[B]	25.92[A]

Note: Different superscript letters within a column denote significant differences among rainfall treatments at p<0.05 (DMRT).

Significant differences were observed in the kernel-related parameters. The number of kernels differed significantly between treatments, with T2 recording the highest number (147.83±30.32 g), followed by T3 (146.50±20.65 g), while T1 recorded the lowest number (100.05±26.56 g). Kernel fresh weight was significantly higher in T2 (37.49±14.72 g) and T3 (38.35±12.34 g) than in T1 (16.69±10.89 g). Kernel dry weight also differed among treatments: T2 was highest (31.46±15.63 g), T3 was next (29.34±11.41 g), and T1 was lowest (12.45±6.31 g). These results indicate that normal (T2) and high (T3) rainfall improved kernel yield parameters, whereas low rainfall (T1) led to significantly lower kernel number and kernel weight.

Table 2 for the growth parameters of *Z. mays* (NON-AGRO) shows that similar trends were observed for the growth parameters. The number of leaves, plant height and chlorophyll content (SPAD) showed no significant differences between treatments. However, significant differences were observed in dry weight. Treatment T3 had the highest dry weight

(246.00±25.44 g), followed by T2 (234.14±29.37 g), while T1 had a significantly lower dry weight (170.39±31.65 g). In contrast, the fresh weight did not differ for all treatments.

Kernel-related parameters in the NON-AGRO showed slight fluctuations. The number of kernels showed no significant differences between the treatments. However, kernel fresh weight significantly, with T1 having the highest value (36.34±2.64 g), while T2 (32.47±4.16 g) and T3 (32.63±2.44 g) were significantly lower. Kernel dry weight, with all treatments showing similar values.

When comparing AGRO and NON-AGRO at different precipitation levels, the AGRO system performed better at normal (T2) and high (T3) precipitation levels. Number of kernels, kernel fresh weight and kernel dry weight were higher in the AGRO system compared to the NON-AGRO system at T2 and T3. Conversely, at low rainfall (T1), the NON-AGRO outperformed the AGRO in kernel fresh weight with 36.34 g compared to 16.69 g in the AGRO system. However, the total dry weight of the plants

remained lower in the NON-AGRO system under T1 compared to T2 and T3. These results suggest that the integration of *N. cadamba* into the AGRO system improves the performance and yield of *Z. mays* under normal and high rainfall conditions. At low rainfall, competition for resources in the AGRO system may have reduced yield performance.

The AGRO system showed better kernel yield parameters at T2 and T3, while the NON-AGRO system showed better kernel fresh weight at T1. These results emphasise the importance of rainfall patterns in determining the results of agroforestry integration on crop performance and yield.

Comparative Analysis of Growth and Yield Parameters of *Zea mays* Under Agroforestry and Non-Agroforestry Systems

Leaf number did not differ significantly between systems: AGRO, 12.83 ± 0.28 leaves; NON-AGRO, 13.00±0.43 leaves (p = 0.60). Stem diameter was also similar: AGRO, 13.60±0.24 mm; NON-AGRO, 14.23±0.83 mm (p = 0.27) (Table 3). These results indicate that the integration of agroforestry had no significant effect on the leaf number or stem diameter of *Z. mays* compared to monocropping.

Table 3. The effect of integration of *Neolamarckia cadamba* on growth performance and yield of *Zea mays*

Growth Performance						
Variable	*N. cadamba* x *Z. mays* (AGRO)	Only *Z. mays* (NON-AGRO)	n	t-value	dF	p
Number of leaves	12.83±0.28	13.00±0.43	3	-0.55	4	0.6087
Height (cm)	186.03±4.81	181.73±1.83	3	1.44	4	0.2221
Diameter (mm)	13.60±0.24	14.23±0.83	3	-1.28	4	0.2709
Chlorophyll content (SPAD)	29.44±1.44	22.47±2.31	3	2.74	4	0.0263
Fresh weight (g)	1109.2±71.82	970.83±76.37	3	2.29	4	0.0843
Dry Weight (g)	277.24±11.65	216.84±23.47	3	2.59	4	0.0452
Number of kernels	131.46±27.20	123.33±6.65	3	0.50	4	0.6418
Kernel fresh weight (g)	30.85±12.26	33.81±2.18	3	-0.41	4	0.7011
Kernel dry weight (g)	24.42±10.41	26.33±0.34	3	-0.32	4	0.7672

Note: Significantly different were detected at p<0.05 with (n = 4) using unpaired t-test

Chlorophyll content (SPAD) showed a significant difference between the two systems. AGRO cultivation recorded a significantly higher SPAD value of 29.44±1.44 compared to 22.47±2.31 in NON-AGRO cultivation (p = 0.0263). This result suggests that the integration of agroforestry positively influenced chlorophyll content, indicating an improved photosynthetic capacity of *Z. mays* in AGRO. No significant difference was observed in fresh weight between the two systems, where 1140±71.82 g) was recorded in AGRO compared to NON-AGRO (970.83±76.37 g) (p = 0.08). However, dry weight showed a significant difference between the systems, with AGRO having a higher mean value of 277.24±11.65 g compared to 216.84±23.47 g for NON-AGRO (p = 0.0452). This result indicates that the AGRO system improved biomass accumulation in *Z. mays*.

The number of kernels did not differ significantly between the systems, with AGRO having 131.46±27.20 kernels and NON-AGRO having 123.33±6.65 kernels (p = 0.64). Similarly, no significant difference was found kernel dry weight of the kernels, with values of 24.42±10.41 g for AGRO and 26.33±0.34 g for NON-AGRO (P = 0.76). These results indicate that kernel yield parameters did not differ significantly between AGRO and NON-AGRO.

Unpaired t-test analysis revealed that the AGRO system significantly improved the chlorophyll content (SPAD) and dry weight of *Z. mays* compared to the NON-AGRO system, while other growth and yield parameters, including the number of leaves, diameter, fresh weight and kernel-related variables, showed no significant differences.

DISCUSSION

The study found no significant differences in growth parameters, such as the number of leaves, plant height and stem diameter, between agroforestry (AGRO) and non-agroforestry (NON-AGRO). These observations are consistent with the results of Wamalwa *et al.* (2021), who reported similar growth responses in intercropped agroforestry trees, due to the minimal influence of light competition in the early growth stages. However, chlorophyll content (SPAD) was significantly higher in AGRO than in NON-AGRO (p = 0.0263). The higher SPAD under AGRO conditions may be attributed to the improved microclimatic conditions, including lower temperature stress and higher humidity favoured by the tree canopy. Similar patterns can be seen in maize alleys or border systems. Shade lowers the temperature of the canopy and the vapor pressure deficit. Litter improves infiltration and surface moisture. These benefits predominate in normal to wet seasons. In dry seasons, root competition can outweigh them, which explains the negative response under T1. This observation is supported by studies emphasising the role of agroforestry in enhancing photosynthetic capacity through a temperate microclimate and improved nutrient cycling (Mishra *et al.*, 2021).

A significant difference was also observed in plant biomass where dry weight of *Z. mays* was significantly higher in AGRO (277.24±11.65 g) than in NON-AGRO (216.84±23.47 g) (p = 0.0409). This result suggests that the presence of *N. cadamba* may have positively influenced nutrient availability through litter decomposition and nutrient cycling, which is a widely recognised advantage of agroforestry systems (Froufe *et al.*, 2020). While fresh weight had a higher mean value in the AGRO system, the difference was not statistically significant. Comparable results were reported by Dilla *et al.* (2018), where maize grown in agroforestry systems had higher biomass due to improved soil moisture and nutrient availability.

Kernel yield parameters gave contrasting results under different systems and rainfall conditions. In AGRO, number of kernels, fresh weight and dry weight were significantly increased under normal (T2) and high rainfall conditions (T3). This indicates that the AGRO system promotes kernel production under favourable moisture conditions, which is likely due to improved soil properties such as water retention and organic matter content, which are typical benefits of agroforestry systems (Ngaba *et al.*, 2023). Conversely, the NON-AGRO performed better than the AGRO in kernel fresh seed weight under low rainfall (T1). This result may be attributed to competition for water and nutrients between *Neolamarckia cadamba* and *Z. mays* under drought stress, as competition between trees and plants can be pronounced under water-limited conditions (Khatta *et al.*, 2023). Increasing the distance between *N. cadamba* and *Z. mays* can reduce below-ground competition. Light pruning during dry periods can reduce the trees' water consumption. Mulch helps to retain moisture in the soil. A small, targeted irrigation at the time of harvest and grain filling ensures yield with minimal water consumption. If water is very scarce, NON-AGRO or temporary irrigation in AGRO is advisable.

The significantly higher chlorophyll content and dry weight observed in the AGRO system are consistent with the concept that agroforestry can improve plant resilience and resource utilisation efficiency under normal and high rainfall conditions. Fahad *et al.* (2022) emphasised that trees integrated into agroforestry systems improve below-ground soil properties, such as nitrogen availability and organic carbon content, which can have a positive effect on plant growth. Under low rainfall (T1), the reduction in kernel yield in AGRO is consistent with evidence that water competition can outweigh microclimate benefits in tree crop systems during dry periods; mitigation through wider spacing, crown/pruning management, and small, well-timed irrigation is recommended (Kumar *et al.*, 2022).

The implications of these results are important for the management of agroforestry systems under different rainfall conditions. Under normal and high rainfall conditions, the integration of *N. cadamba* with *Z. mays* improves the overall growth and yield performance. This result demonstrates the potential of agroforestry to optimise agricultural productivity while contributing to ecosystem services such as improved soil health and climate resilience (Jose, 2009; Wamalwa *et al.*, 2021). However, under low rainfall conditions,

monocultures can provide better yield performance due to less competition for water resources. This highlights the importance of selecting appropriate agroforestry species and optimising management practices such as pruning and irrigation to minimise resource competition under drought stress (Bayala & Prieto, 2020)

The AGRO system improved the chlorophyll content and dry weight of *Z. mays* under favourable rainfall conditions, demonstrating the benefits of integrating *N. cadamba*. However, under water-limited conditions, the NON-AGRO system outperformed the AGRO system in kernel fresh weight. This emphasises the need for adaptive management strategies in agroforestry systems to improve resilience under changing environmental conditions.

This study used one soil (Nyalau; *Typic paleudults*), one site, and one season. Pots can restrict roots and alter lateral interactions. Tree age and spacing did not vary. We did not test fertiliser–water interactions. These constraints limit broad generalisation. Future work should include field plots across seasons, more soils, and a spacing–age gradient.

CONCLUSION

This study shows that the integration of *Neolamarckia cadamba* with *Zea mays* improves chlorophyll, biomass, and yield under normal and high rainfall, while low rainfall can shift the balance in favor of belowground competition. The results support agroforestry as a practical option under weather variability, with clear limits under drought. For farmers, the best use case is edge or alley cropping in normally wet seasons; in dry conditions, maintain wider spacing, retain mulch, and apply small, well-timed irrigation during whorls and grain fill. Policy makers should include maize–kelampayan designs in extension and consider establishment support and simple irrigation measures as part of climate-smart agriculture. Future research should test the effects of spacing and tree age across multiple seasons and soils, measure water balance and microclimate, and assess costs and returns to smallholder farmers. Practical recommendation such as introduces integration of maize and kelampayan when rainfall is normal or high could be switch to

wider spacing plus mulch and targeted irrigation when rainfall is low.

ACKNOWLEDGEMENTS

REFERENCES

Alam, M.M., Siwar, C., Jaafar, A., Talib, B. & Salleh, K. (2013). Agricultural vulnerability and adaptation to climatic changes in Malaysia: Review on paddy sector. *Political Economy: Taxation.* DOI: 10.12944/CWE.8.1.01

Bayala, J. & Prieto, I. (2019). Water acquisition, sharing and redistribution by roots: Applications to agroforestry systems. *Plant and Soil,* 453: 17–28. DOI: 10.1007/s11104-019-04173-z

Das, P., Singh, V., Johar, V., Deepaboli & Singh, A. (2024). Agroforestry as a contraption for controlling soil erosion and improving soil health: A review. *Pollution Research,* 43(1–2): 14–22. DOI: 10.53550/pr.2024.v43i01-02.014

Dilla, A., Smethurst, P., Barry, K., Parsons, D. & Denboba, M. (2018). Tree pruning, zone and fertiliser interactions determine maize productivity in the Faidherbia albida (Delile) A. Chev parkland agroforestry system of Ethiopia. *Agroforestry Systems,* 92(6): 1807–1817. DOI: 10.1007/s10457-018-0304-9

Erenstein, O., Jaleta, M., Sonder, K., Mottaleb, K. & Prasanna, B. (2022). Global maize production, consumption and trade: trends and R&D implications. *Food Security,* 14(5): 1295–1319. DOI: 10.1007/s12571-022-01288-7

Fahad, S., Chavan, S., Chichaghare, A.R., Uthappa, A.R., Kumar, M., Kakade, V., Pradhan, A., Jinger, D., Rawale, G., Yadav, D.K., Kumar, V., Farooq, T.H., Ali, B., Sawant, A., Saud, S., Chen, S. & Poczai, P. (2022). Agroforestry systems for soil health improvement and maintenance. *Sustainability,* 14(22): 14877. DOI: 10.3390/su142214877

Firdaus, R., Samsurijan, M., Singh, P., Yahaya, M.H., Latiff, A. & Vadevelu, K. (2018). Impak perubahan iklim ke atas pertanian berdasarkan model simulasi pertumbuhan tanaman (CGS). *Malaysian Journal of Society and Space,* 14(3): 67–79. DOI: 10.17576/GEO-2018-1403-05

Froufe, L., Schwiderke, D.K., Castilhano, A.C., Cezar, R., Steenbock, W., Seoane, C.E.S., Bognola, I.A. & Vezzani, F. (2019). Nutrient cycling from leaf litter in multistrata successional agroforestry systems and natural regeneration at Brazilian Atlantic Rainforest Biome. *Agroforestry Systems,* 94: 159–171. DOI: 10.1007/s10457-019-00377-5

Hooper, D., Chapin, F., Ewel, J., Hector, A., Inchausti, P., Lavorel, S., Lawton, J., Lodge, D., Loreau, M., Naeem, S., Schmid, B., Setälä, H., Symstad, A., Vandermeer, J. & Wardle, D. (2005). Effects of biodiversity on ecosystem functioning: A consensus of current knowledge. *Ecological Monographs,* 75: 3–35. DOI: 10.1890/04-0922

Jose, S. (2009). Agroforestry for ecosystem services and environmental benefits: An overview. *Agroforestry Systems,* 76: 1–10. DOI: 10.1007/s10457-009-9229-7

Khatta, A.N.M., Mekai, M.H.A., Kadir, A.M., Suhinin, O.A., Suhaidi, H., Abdullah, N., Nyen, K.P.K., Kimjus, K., Terhem, R. & Hassan, A. (2023). Acclimatisation of white laran (Neolamarckia cadamba Roxb. Bosser) and binuang (Octomeles sumatrana Miq.) seedlings to water-logged and water-stress conditions. *Forests,* 14(3): 500. DOI: 10.3390/f14030500

Kumar, Y., ManojKumar, S. & Behera, L. (2022). Tree root dynamics: An essential tool to combat root competition in agroforestry. *Ecology, Environment and Conservation,* 28(4): 1805–1811. DOI: 10.53550/eec.2022.v28i04s.057

Lorenz, K. & Lal, R. (2014). Soil organic carbon sequestration in agroforestry systems: A review. *Agronomy for Sustainable Development,* 34: 443–454. DOI: 10.1007/s13593-014-0212-y

Mishra, A., Sinha, B., Kumar, R., Barth, M., Hakkim, H., Kumar, V., Kumar, A., Datta, S., Guenther, A. & Sinha, V. (2020). Cropland trees need to be included for accurate model simulations of land-atmosphere heat fluxes, temperature, boundary layer height, and ozone. *The Science of the Total Environment,* 751: 141728. DOI: 10.1016/j.scitotenv.2020.141728

Ngaba, M.J.Y., Mgelwa, A.S., Gurmesa, G.A., Uwiragiye, Y., Zhu, F., Qiu, Q., Fang, Y., Hu, B. & Rennenberg, H. (2023). Meta-analysis unveils differential effects of agroforestry on soil properties in different zonobiomes. *Plant and Soil,* 496: 589–607. DOI: 10.1007/s11104-023-06385-w

Széles, A., Horváth, É., Simon, K., Zagyi, P. & Huzsvai, L. (2023). Maize production under drought stress: nutrient supply, yield prediction. *Plants,* 12(18): 3301. DOI: 10.3390/plants12183301

Tang, K. (2019). Climate change in Malaysia: Trends, contributors, impacts, mitigation, and adaptations. *The Science of the Total Environment,* 650(2): 1858–1871. DOI: 10.1016/j.scitotenv.2018.09.316

Wamalwa, D.S., Musyimi, D., Sikuku, P. & Odhiambo, D. (2021). Growth and gas exchange responses of maize and banana plants in an intercrop with agroforestry tree species in Vihiga County, Kenya. *Asian Journal of Agricultural and Rural Studies,* 6(3): 10–18. DOI: 10.9734/ajrcs/2021/v6i330119

Wang, H., Chen, B. & Shen, X. (2024). Extreme rainfall, farmer vulnerability, and labor mobility—evidence from rural China. *The Science of the Total Environment,* 919: 170866. DOI: 10.1016/j.scitotenv.2024.170866

Yin, X., Jabloun, M., Olesen, J., Öztürk, I., Wang, M. & Chen, F. (2015). Effects of climatic factors, drought risk and irrigation requirement on maize yield in the Northeast farming region of China. *The Journal of Agricultural Science,* 154: 1171–1189. DOI: 10.1017/S0021859616000150

Zomer, R., Neufeldt, H., Xu, J., Ahrends, A., Bossio, D., Trabucco, A., van Noordwijk, M. & Wang, M. (2016). Global tree cover and biomass carbon on agricultural land: The contribution of agroforestry to global and national carbon budgets. *Scientific Reports,* 6: 29987. DOI: 10.1038/srep29987

Influence of Temperature and Oxygen Injection on Population Growth of Marine Rotifers, *Brachionus plicatilis*

RIZAL ISMAIL[1], NORFAZREENA MOHD FAUDZI[1], CHING FUI FUI[1], KENNETH TEO[2], NAJAMUDDIN ABDUL BASRI[1], VUTTHICHAI ONIAM[3] & SITTI RAEHANAH MUHAMAD SHALEH[*1]

[1]Higher Institution Centre of Excellence (HICoE), Borneo Marine Research Institute, Universiti Malaysia Sabah, Kota Kinabalu, Sabah, Malaysia; [2]Modelling, Simulation and Computing Laboratory, Level 3, Block C, School of Engineering and Information Technology, Universiti Malaysia Sabah, Kota Kinabalu, Sabah, Malaysia; [3]Klongwan Fisheries Research Station, Academic Supporting Division, Faculty of Fisheries, Kasetsart University, Mueang, Prachuap Khiri Khan, 7700 Thailand
[*]Corresponding author: sittirae@ums.edu.my

ABSTRACT

Rotifers (*Brachionus plicatilis,* Brachionidae) are critical live feed for marine, crustaceans, and ornamental fish during their early developmental stages. This study investigated the effects of temperature and oxygen injection on rotifer population growth. A five-day experiment was conducted with nine treatments combining temperatures (26 °C, 28 °C, and 30 °C) and oxygen injection frequencies (0, 2, 4, and 6 times/day). Each treatment was triplicated, with 27 experimental jars containing 4 L of water, a filter, and aeration at 200 mL/min. Commercial *Nannochloropsis* sp. was used as feed through automated feeders. The results show significant effects of temperature and oxygen injection on population density, growth rate, and egg production ($p<0.01$). Statistical analysis was conducted using two-way ANOVA to assess the significance of main and interaction effects. The highest population density (308 individuals/mL) and growth rate (1.14 day^{-1}) were observed at 30 °C with 6 oxygen injections/day, followed by 256 individuals/mL with 4 injections/day. The lowest density (32 individuals/mL) and growth rate (0.62 day^{-1}) were recorded at 26 °C with 4 injections/day. Egg production was highest (27.09 ± 2.49%) at 30 °C with 6 injections/day. These findings indicate the critical role of temperature and oxygen injection frequency for optimizing rotifer production for aquaculture.

Keywords: Aquaculture, hatchery, live feed, mariculture, population growth, rotifer

INTRODUCTION

Due to its favorable nutritional profile, appropriate body size, relatively slow swimming behavior, and exceptional tolerance to a wide range of salinities, the marine rotifer *Brachionus plicatilis* is a zooplankton species that has been extensively studied. It is also vital to aquatic food webs and is heavily used extensively in aquaculture. *Brachionus plicatilis* is a perfect live feed for the early stages of growth of many marine fish and shellfish because of its capacity to stay suspended in the water column (Edward *et al.,*2020). According to Contente *et al.* (2024), the species is highly prized for its quick reproduction rate, ease of enrichment with essential fatty acids, and potential as a vector for delivering probiotics or antibiotics to target aquaculture species. *Brachionus. plicatilis* is currently used to feed over 60 marine finfish and 18 species crustaceans (Lubzens & Zmora, 2003; Yona, 2018).

Rotifers' development, reproduction, and population dynamics are greatly impacted by environmental factors as temperature and dissolved oxygen (DO). While temperature is essential for metabolic activity, reproduction, and survival (Nhinh *et al.,*2020), prior research has shown that DO influences rotifer feeding behaviour and growth performance (Koiso & Hino, 2006). Up to an ideal thermal threshold, higher temperatures often speed up metabolic rates, which encourages population expansion (Nhinh *et al.,*2020; Yoo *et al.,*2023). However, high temperatures can also cause DO levels to drop, which could reduce the productivity and health of rotifers (Chaturvedi & Misra, 2020).

Although much research has been done on the effects of temperature and DO separately on rotifer cultures, little is known about how these two variables interact, particularly how changes in the frequency of oxygen injections under various temperature regimes affect *B. plicatilis* growth and reproductive success. Given the rising need for scalable, highly efficient live feed production systems to service the burgeoning aquaculture industry, this constitutes a substantial knowledge gap.

By examining the combined impacts of temperature and oxygen enrichment frequency on the population expansion of *B. plicatilis*, this study seeks to close this gap. This study aims to determine the ideal environmental conditions for rotifer productivity by assessing these interdependent impacts. In addition to advancing our ecological knowledge of rotifer physiology, the results will offer valuable suggestions for enhancing the effectiveness of rotifer culture systems in commercial aquaculture environments. This work examines the combined impacts of temperature and DO regulation, providing fresh perspectives for improving rotifer cultivation in contrast to earlier research that mainly concentrated on single-factor influences.

MATERIALS AND METHODS

Rotifer Stock Culture

Rotifers, *Brachionus plicatilis*, L-strain had an average lorica length of 195.5 μm. They were sourced from the University Malaysia Sabah Crustacean Hatchery. They were cultured in a 100-liter conical tank preserved at a temperature of 28 °C. The initial stocking density was 10 rotifers/mL, and cultivation continued until the population density reached 100–150 rotifers/mL within 3 days. The culture salinity was set at 30‰. Concentrated microalgae (*Nannochloropsis* sp., Nano3600) were used as feed, supplied twice daily at 10.0×10^6 cells/mL. The rotifers were grown in batch culture, with water parameters such as temperature and dissolved oxygen (DO) monitored daily throughout the cultivation of the rotifer stock.

Experimental Design

Nine temperature and pure oxygen injection frequency combinations were evaluated using a factorial design (Table 1). Each experimental jar (4 L plastic jar) was filled with 3 L of seawater at 30‰ salinity and initially stocked with rotifers at a density of 10 rotifers/mL. The temperatures tested were 26 °C, 28 °C, and 30 °C. The oxygen injection frequencies were 0, 2, 4, and 6 times per day. The experimental jars were equipped with filters and aeration systems, with aeration regulated to 200 mL/min and maintained throughout the study. A water bath with submersible heaters was used to maintain the desired temperature levels. The experiment followed a batch culture method over five days. Daily measurements of water temperature (°C), dissolved oxygen (mg/L), and salinity (‰) were taken and recorded using a BLE-9100 Dissolved Oxygen Analyzer. The BLE-9100 Dissolved Oxygen Analyzer was calibrated prior to the start of the experiment following the manufacturer's recommended procedure, using a two-point calibration with air-saturated water (100% saturation) and sodium sulfite solution (0% saturation) as references. Calibration was conducted weekly to ensure accuracy in measurement throughout the experiment. The filters were cleaned every two days to remove debris and waste to maintain water quality.

Table 1. The combination of temperature (°C) and pure oxygen injection frequencies (POI) of each treatment

°C / Day⁻¹	26	28	30
0	(No injection, 26 °C)	(No injection, 28 °C)	(No injection, 30 °C)
2	(2, 26 °C)	(2, 28 °C)	(2, 30 °C)
4	(4, 26 °C)	(4, 28 °C)	(4, 30 °C)
6	(6, 26 °C)	(6, 28 °C)	(6, 30 °C)

Rotifer Diet Preparation

The concentrated microalgae paste was first diluted with filtered seawater and stored in one-liter plastic jars. To prevent the algae from settling at the bottom of the containers, the contents were mixed using a SOBO Aquarium Wave Maker, which was programmed to activate automatically at each feeding time. The jars were then stored in a styrofoam box containing ice packs to maintain a low temperature, preserving the quality of the microalgae throughout the experiment. The feeding process was fully automated and was carried out twice daily. In total, 100 mL of the diluted microalgae paste was dispensed into each experimental jar during each feeding. This feeding rate corresponded to an estimated density of 200,000 cells/rotifer.

Rotifer Counting

Every day at 0800 hours, 1 mL of rotifer culture was sampled from each experimental jar for counting. Acidic Lugol's solution was used to immobilise the rotifers before counting with a Sedgwick-Rafter counter. Empty loricae from dead rotifers were not included in the count. Every sample was counted three times. The mean value was recorded. The population growth rate (GR) of *B. plicatilis* was calculated using the formula: $G = \frac{1}{T}\ln(N_T - N_0)$. T is the period of culture days, N_0 is the initial number of rotifers, N_T is the total number after T days of culture. The egg percentage of rotifer (EP) was estimated using the formula: $EP = Nt / N \; x \; 100$. EP is the egg percentage of rotifer (%), N is the total number of *B. plicatilis*, Nt is the number of egg-bearing rotifer (Radhakrishnan *et al.,*2017).

Statistical Analysis

The Shapiro-Wilk test was used to determine whether the data were normal, and Levene's test was used to see whether the variances were homogeneous. The significance level was set at $p<0.05$. To assess both individual and interaction effects of the treatments, a two-way Analysis of Variance (ANOVA) was used to examine how temperature and oxygen injection frequency affected rotifer development characteristics.

Post hoc comparisons of treatment means were performed using Duncan's multiple range test to find significant changes between groups. The Statistical Package for Social Sciences (SPSS), Version 29.0.2.0, was used for all statistical analyses.

RESULTS

Population Growth

Based on the population growth curve (Figure 1), the population growth of *Brachionus plicatilis* varied significantly based on temperature and the frequency of pure oxygen injection. Across all treatments, population growth generally increased over time. However, higher temperatures (30 °C) and more frequent oxygen injections (6 times/day) led to the highest densities. Conversely, lower temperatures (26 °C) and the absence of oxygen injection resulted in the slowest growth.

At 26 °C, population growth remained low regardless of oxygen injection frequency. The treatment without oxygen injection showed the slowest and most stagnant growth. In contrast, even the highest oxygen injection frequency (six times/day) did not lead to substantial population increases compared to higher temperature treatments. Rotifers at 28 °C exhibited moderate growth, with the 6 times/day oxygen injection treatment indicating a noticeable increase from Day 2 before stabilising around Day 4. The 4 times/day treatment followed a similar trend but at a slightly lower rate, while the treatment without oxygen injection resulted in minimal growth.

The most rapid and highest population growth was observed at 30 °C, where rotifers with six oxygen injections per day reached the greatest density by Day 5, with a steep growth increase starting from Day 2. The 4 times/day treatment was followed closely, exhibiting steady but slightly lower growth, while the 2 times/day treatment showed a slower increase. At 30 °C, the absence of oxygen injection still led to some growth, but at a significantly lower rate compared to treatments with oxygen supplementation.
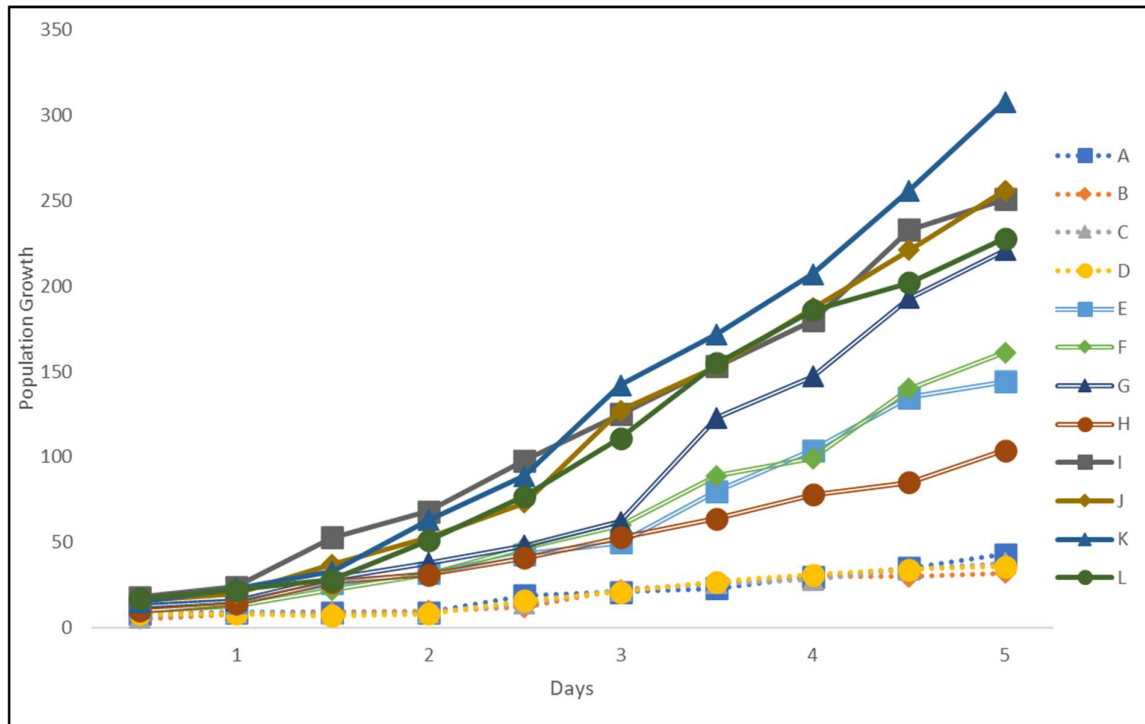
Figure 1. Growth curves of *Brachionus plicatilis* cultured under different combinations of temperature and oxygen injection frequencies: A (26 °C, 2 times/day), B (26 °C, 4 times/day), C (26 °C, 6 times/day), D (26 °C, no injection), E (28 °C, 2 times/day), F (28 °C, 4 times/day), G (28 °C, 6 times/day), H (28 °C, no injection), I (30 °C, 2 times/day), J (30 °C, 4 times/day), K (30 °C, 6 times/day), and L (30 °C, no injection).

Highest Population Density (HPD)

The highest population density (HPD) was observed on the fifth day (Table 2), revealing significant differences among all treatments. The HPD increased with higher temperatures and more frequent oxygen injections. At 30 °C, the HPD rose from 228 ± 26.69 rotifers/mL with no oxygen injection to 308 ± 17.14 rotifers/mL with six oxygen injections daily. In contrast, at 26 °C, the HPD remained consistently low across all POI levels, reaching a maximum of only 43±4.73 rotifers/mL at two oxygen injections per day. The effect of oxygen injection on HPD depends on temperature. Oxygen injection has minimal impact at lower temperatures (26 °C), but at higher temperatures (28 °C and 30 °C), it significantly enhances HPD.

Growth Rate (GR)

Growth rates followed a similar pattern, increasing with higher temperatures and more frequent oxygen injections. At 30 °C, the growth rate improved from 1.08±0.024 day⁻¹ with no oxygen injection to 1.14±0.012 day⁻¹ at six oxygen injections daily. Conversely, at 26 °C,

the growth rate remained consistently low, ranging from 0.62±0.018 day⁻¹ to 0.70±0.295 day⁻¹, regardless of the oxygen injection frequency (Table 2). Oxygen injection has a stronger effect on GR at higher temperatures (28 °C and 30 °C) than lower temperatures (26 °C), where it has a negligible effect.

Egg Percentage (EP)

Egg percentage (EP) followed a similar trend, with temperature and oxygen injection frequency (POI) significantly influencing EP (p<0.01) (Table 2). At 26 °C, egg percentage (EP) remained relatively low, ranging from 9.57% to 13.15%, and showed no correlation with oxygen injection. As the temperature increased to 28 °C, EP values improved overall (20.21% to 23.55%). However, no consistent trend was observed in response to oxygen injection. In contrast, at 30 °C, EP increased significantly with higher oxygen injection frequencies, reaching its peak 6 times per day (60.50±2.20%). Oxygen injection has a minimal on EP at lower temperatures (26 °C and 28 °C). However, at 30 °C, it significantly enhances EP, with the greatest effect at 6 times/day.

Table 2. Growth rate (GR, day^{-1}), highest population density (HPD, rotifer/ml) and egg percentage (EP, %) of *B. plicatilis* culture at different temperature (T, °C) and pure oxygen injection frequency (POI, times/day).

Parameters	T(°C)	POI (time/day)			
		0	2	4	6
GR (day^{-1})	26	0.70±0.295^{cd}	0.62±0.018^{cd}	0.67±0.014^{cd}	0.65±0.031^{cd}
	28	0.91±0.028^{c}	0.98±0.006^{bc}	1.00±0.005^{bc}	1.07±0.019^{e}
	30	1.08±0.024^{a}	1.10±0.020^{a}	1.10±0.017^{a}	1.14±0.012^{b}
HPD (rotifer/ml)	26	36±4.04^{f}	43±4.73^{f}	32±2.00^{f}	38±2.00^{f}
	28	105±3.31^{d}	144±4.04^{e}	161±4.16^{c}	221±19.13^{cd}
	30	228±26.69^{a}	251±24.56^{a}	256±20.60^{a}	308±17.14^{b}
EP (%)	26	12.98±2.44^{a}	13.15±4.63^{a}	10.37±4.68^{a}	9.57±3.82^{a}
	28	23.03±3.43^{b}	20.21±2.35^{b}	23.55±2.55^{b}	21.49±2.33^{b}
	30	29.33±4.04^{c}	42.00±2.64^{cd}	52.13±3.03^{cd}	60.50±2.20^{f}

Notes: Different letter superscripts indicate significance differences (Two-way ANOVA; $p<0.05$). Growth rate (GR, day^{-1}), highest population density (HPD, rotifer/ml) and egg percentage (EP, %) of *B. plicatilis* culture at different temperature (T, °C) and pure oxygen injection frequency (POI, times/day).

Interaction

Based on Table 3, the two-way ANOVA analysis revealed that temperature (T) and pure oxygen injection frequency (POI) had statistically significant effects on all measured parameters, including growth rate (GR), highest population density (HPD), and egg percentage (EP) of the rotifer *B. plicatilis*. For each parameter, the main effects of temperature and POI and their interaction were highly significant with p-values of 0.001. Temperature significantly influenced the GR of rotifers ($p = 0.001$), while POI also showed a significant effect on GR ($p = 0.001$). The interaction between temperature and POI showed a significant combined effect on GR ($p = 0.001$). This indicates that the response of the growth rate to one factor relies on the level of the other factor.

The HPD and EP showed a similar pattern, with temperature, POI, and their interactions being statistically significant ($p = 0.001$ in all cases). Given that the combined impacts of temperature and POI frequency are crucial in determining the development dynamics and reproduction of rotifers, these results imply that careful adjustment of these variables can lead to optimal rotifer output.

Table 3. Summary of two-way ANOVA (p-value) results analyzing the effects of temperature (T, °C), Pure oxygen injection interval (POI, time/day), and their interaction on growth rate (GR), highest population density (HPD), and egg percentage (EP)

Parameters	T(°C)	POI (time/day)	Interaction
GR	0.001	0.001	0.001
HPD	0.001	0.001	0.001
EP	0.001	0.001	0.001

DISCUSSION

This study shows *Brachionus plicatilis* reached its maximum population density (HPD) at 30 °C while receiving six oxygen injections daily. This result emphasizes how crucial it is to provide the perfect habitat for rotifer formation by maximising the temperature and oxygen supply. The lowest HPD, on the other hand, was recorded at 26 °C, underscoring the way that suboptimal temperatures hinder the dynamics of

rotifer populations. These findings are in line with earlier research that highlighted how important temperature is in affecting aquatic species' development, metabolism, and reproduction (Nhinh *et al.,* 2020). For instance, *B. calyciflorus* reached its maximal population growth at 27 °C, according to Nhinh *et al*. (2020), with growth being considerably slower at lower temperatures. In a similar vein, Yona (2018) discovered that although greater temperatures limited the lifetime of rotifers, they

also increased the reproduction rate. This shows an increase in population growth overall.

Temperature has a significant impact on reproductive output in addition to lifespan. In contrast to previous temperature treatments, rotifers cultivated at 30 °C in this study produced more eggs, which directly increased population expansion. Similarly, Yona (2018) found that although overall lifespans were shorter, reproductive periods varied with temperature, with higher reproductive rates happening at warmer temperatures. These results are consistent with the idea that higher temperatures raise metabolic rates, which speed up rotifer reproduction and senescence.

Another important element affecting rotifer growth and production was dissolved oxygen (DO). Maintaining aerobic respiration, metabolic activity, and effective food utilisation in rotifer cultures requires adequate DO levels (Ramaekers *et al.,*2022; Yang *et al.,*2024). Oxygen saturation must be kept within ideal levels to avoid hypoxic situations, particularly in dense cultures with high oxygen demand (Gerasimova & Sadchikov, 2022). However, as prior studies have demonstrated, overaeration can cause physical harm, foaming, and mechanical stress to fragile rotifers, especially those carrying eggs (Yoshimura *et al.,*1996). In order to overcome this, the current work used pure oxygen injection to effectively raise DO levels while reducing mechanical disruptions. This strategy worked because higher HPD and better reproductive outcomes were positively connected with more frequent oxygen injections.

Our findings are in line with those by Koiso and Hino (2006) and Yoo *et al.* (2023), who reported that a sudden reduction in DO can result in a significant decrease in rotifer feeding behaviour and reproductive success. Our results demonstrate that oxygen enrichment is particularly effective when combined with increased temperatures. The interaction between temperature and oxygen injection frequency was significant for all key variables HPD, GR, and EP (p = 0.001). Notably, oxygen injection had minimal impact at lower temperatures but became increasingly critical at higher temperatures, with greater metabolic demands. These results indicate that temperature directly influences the efficiency of oxygen utilisation by rotifers, suggesting that can more effectively convert available oxygen into reproductive output when cultured under thermally optimal conditions.

While the DO levels achieved in this study exceeded the general optimal recommendations (>6.0 mg/L; Yang *et al.,* 2024), not all treatments yielded proportional increases in GR or HPD. This indicates a potential threshold beyond which further oxygen enrichment does not confer additional reproductive or growth benefits. The interaction likely stems from a synergistic relationship wherein higher metabolic rates at elevated temperatures increase oxygen demand, and oxygen enrichment fulfils this requirement, leading to improved culture outcomes. However, beyond this synergistic range, further oxygenation may yield diminishing returns.

These effects can be explained by known physiological mechanisms in rotifers. Increased temperatures increase enzymatic activity, protein synthesis, and reproductive cycles. Simultaneously, sufficient DO ensures that aerobic respiration remains efficient, offering the necessary energy for heightened reproductive activity. Conversely, insufficient oxygen availability at high temperatures may lead to metabolic stress, reducing fecundity and potentially increasing mortality rates.

The results obtained have practical implications for large-scale aquaculture operations, particularly in the production of live feeds for marine hatcheries. The identification of 30 °C with six oxygen injections per day as an optimal condition offers aquaculture practitioners a reliable guideline for maximising rotifer output. However, the scalability of pure oxygen injection should be considered, as it may incur additional operational costs. Hatcheries aiming for cost-effective production must balance the benefits of higher rotifer yields against the expenses associated with oxygen supplementation. Moreover, integrating efficient oxygen delivery systems, such as fine diffusers or membrane oxygenation, could mitigate costs while improving culture performance.

While this study offers valuable insights into the effects of temperature and oxygen enrichment on *B. plicatilis* culture, further research is crucial to build on these findings. Future studies should focus on long-term culture

experiments to evaluate the cumulative effects of sustained high-temperature and oxygen enrichment on rotifer health, reproductive stability, and potential genetic adaptations over multiple generations. Additionally, investigating the effects of combining optimal physical conditions with targeted nutritional enrichment, such as the incorporation of essential fatty acids or probiotics, could provide further improvements in rotifer quality for aquaculture feed applications. Investigations into the selection or development of rotifer strains that show enhanced tolerance to high-density and high-productivity culture systems would also be beneficial for improving culture efficiency. Furthermore, it is essential to conduct economic feasibility assessments to determine the practicality and cost-effectiveness of implementing oxygen injection systems in commercial aquaculture hatcheries. Finally, future research should further explore the interactive effects of other abiotic factors, including salinity fluctuations, pH variation, and nutrient availability, to develop more comprehensive and robust best practices for rotifer culture management in diverse aquaculture settings.

CONCLUSION

This study demonstrated that temperature and pure oxygen injection (POI) significantly influenced rotifer production. Culturing rotifers at optimal temperatures, combined with POI, effectively enhanced population growth. However, further research is required to assess the nutritional quality of rotifers produced under these conditions.

ACKNOWLEDGEMENTS

REFERENCES

Chaturvedi, V. & Misra, S. (2020). Reductive metabolites of curcumin and their therapeutic effects. *Heliyon*, 6(5): 54-69. DOI: https://doi.org/10.1016/j.heliyon.2020.e05469

Contente, D. M. L., Díaz-Formoso, L., Feito, J. A., Hernández, P. E., Muñoz-Atienza, E., Borrero, J., Poeta, P. & Cintas, L. M. (2024). Genomic and Functional Evaluation of Two *Lacticaseibacillus paracasei* and Two *Lactiplantibacillus plantarum* Strains, Isolated from a Rearing Tank of Rotifers (*Brachionus plicatilis*), as Probiotics for Aquaculture. *Genes*, 15(1): 64. .DOI:https://doi.org/10.3390/genes15010064

Edward, L., Laxmilatha, P., Sreeramulu, K., Ranjith, L. & Megarajan, S. (2020). Influence of certain environmental parameters on mass production of rotifers: A review. *Journal of the Marine Biological Association of India*, 62(1): 49–53. DOI: https://doi.org/10.6024/jmbai.2020.62.1.2176-08

Gerasimova, T. N. & Sadchikov, A. P. (2022). The role of rotifer in water quality improvement in a fishpond. *Vestnik MGTU*, 25(2): 120–124. DOI: https://doi.org/10.21443/1560-9278-2022-25-2-120-124

Koiso, M. & Hino, A. (2006). Effect of sudden drop of dissolved oxygen on population growth and feeding in the rotifer *Brachionus plicatilis*. *Aquaculture Science*, 54(1), 37–45. DOI:https://doi.org/10.11233/aquaculturesci1953.54.37

Lubzens, E. & Zmora, O. (2003). Production and nutritional value of rotifers. In Støttrup, J. G. & McEvoy, L. A. (eds.) *Live feeds in marine aquaculture*. Oxford, UK, Blackwell Publishing. pp. 17–64. https://doi.org/10.1002/9780470995143.ch2

Nhinh, D. T., Hong, P. T. L., Hoai, T. D. & Van Van, K. (2020). Effects of temperature on population growth and resting egg production of freshwater rotifer (*Brachionus calyciflorus*). *Vietnam Journal of Agricultural Sciences*, 3(4): 798–805. DOI: https://doi.org/10.31817/vjas.2020.3.4.07

Radhakrishnan, K., Aanand, S., Rameshkumar, S. & Divya, F. (2017). Effect of feeding rate and feeding frequency in mass culture of *Brachionus plicatilis* in a semi-continuous method with a yeast-based diet. *Journal of Fisheries and Life Sciences*, 2(1): 40–44.

Ramaekers, L., Pinceel, T., Brendonck, L. & Vanschoenwinkel, B. (2022). Direct effects of elevated dissolved CO_2 can alter the life history of freshwater zooplankton. *Scientific Reports*, 12(1): 61-34. DOI: https://doi.org/10.1038/s41598-022-10157-2

Yang, D., Li, W. & Ma, X. (2024). Suitable acidified eggshell powder food promotes *Brachionus calyciflorus* growth and reproduction: From antioxidant capacity insight. *Aquaculture Nutrition*, 20(24): 1–10. DOI: https://doi.org/10.1155/2024/7875547

Yona, G. K. (2018). Effect of culture temperature on rotifers (*Brachionus plicatilis* sensu strictu) size and reproduction activities. *Tanzania Journal of Agricultural Sciences*, 17(1): 10–17.

Yoo, H. K., Kim, S. S., Lee, K. W., Lee, S. Y., Jung, M. M. & Woo, S. J. (2023). Determination of the optimal conditions for the mass culture of large-type rotifers (*Brachionus plicatilis*) at low temperatures. *Water*, 15(18): 3310. DOI: https://doi.org/10.3390/w15183310

Yoshimura, K., Ohmori, Y., Yoshimatsu, T., Tanaka, K. & Ishizaki, A. (1996). On the aeration method in high-density culture of rotifer *Brachionus rotundiformis. Nippon Suisan Gakkaishi*, 62(6): 897–902.

Bioactive Compound and Cytotoxic Analysis of *Premna oblongifolia* Merr. Ethanol Extract on Rat Bone Marrow-Derived MSC-like Cells

FILDZAH FILDZAH, SUHARTONO SUHARTONO, ROSNIZAR ROSNIZAR*

Department of Biology, Faculty of Mathematics and Natural Sciences, Universitas Syiah Kuala, Banda Aceh,
23111, Aceh, Indonesia
*Corresponding author: rosnizar@usk.ac.id

ABSTRACT

The use of natural products in regenerative medicine holds significant promise, especially in regions where traditional medicine is prevalent. This study investigates the bioactivity of the ethanol extract of green cincau leaves (*Premna oblongifolia* Merr.) (GCE) on bone marrow-derived mesenchymal stem cell-like cells (BM-MSCs). The leaves were extracted using the maceration method, and the bioactive compounds were analysed and detected by Gas Chromatography-Mass Spectroscopy (GC-MS). The cytotoxicity tests were conducted across a concentration range of 1–1200 μg/mL using WST-1 reagent, and cell viability was measured at 24, 48, and 72 h. The results of GC-MS indicated 28 bioactive compounds with the dominant groups being terpenoids and fatty acids. The most abundant compounds in GCE were phytol (19.06%), squalene (4.32%), Urs-12-en-28-oic acid, 3-hydroxy-, methyl ester, (3.beta.)- (6.23%) and 8,11,14-Eicosatrienoic acid, (Z,Z,Z)- (2.88%). The GCE maintained cell viability above 80% at all concentrations, indicating low cytotoxicity. Furthermore, Alizarin Red S staining revealed calcium deposit formation at 300 μg/mL, suggesting preliminary osteogenic activity. These findings suggest GCE may have potential for supporting BM-MSCs proliferation and demonstrates early osteogenic properties. Further investigation is recommended to explore its mechanism of action and therapeutic potential in differentiation applications.

Keywords: Cytotoxicity, green cincau, MSC-like cells, *Premna oblongifolia* Merr., regenerative medicine.

INTRODUCTION

Plant-based medicines are increasingly gaining attention due to their immunomodulatory effects (Shukla *et al*., 2022), lower risk of side effects, stability, and accessibility, making them viable alternatives to conventional pharmaceuticals in natural healthcare and chronic disease prevention (Dabas *et al*., 2023). According to the World Health Organisation (WHO), approximately 80% of the global population utilises herbal medicine as part of their primary healthcare approach. Additionally, about 25% of contemporary pharmaceuticals are sourced from plant materials largely due to the wide range of bioactive primary and secondary metabolites they produce (Turvey *et al*., 2022). Plants produce a diverse array of secondary metabolites, such as alkaloids, terpenoids, flavonoids, and phenolic compounds, each of which exhibit various biological activities (Bhatti *et al*., 2022).

The use of mesenchymal stem cells (MSCs) in regenerative treatments is one of the latest biomedical advancements. MSCs are multipotent cells that can differentiate into various cell types, including osteoblasts (Zainol Abidin *et al*., 2023), chondrocytes (Li *et al*., 2020) and adipocytes (Ebrahimi *et al*., 2023), making them promising candidates for regenerative medicine and tissue engineering. Bone marrow-derived MSCs particularly are widely studied due to their accessibility and differentiation potential (Asadi *et al*., 2022; Dzobo, 2021; Melo *et al*., 2020). However, ensuring their proliferation, survival, and regulated differentiation in vitro is a significant problem. Identifying bioactive compounds that can assist these processes is critical for developing MSC-based treatments.

Premna oblongifolia Merr. or commonly known as green cincau, is a verbenaceae family plant that is commonly used as a dessert component in Indonesia (Nurdin *et al*., 2018). Green cincau (GC) is known to contain bioactive

compounds that have the potential to have positive effects on health. Aryudhani (2011) reported that GC leaves contain several components of active compounds, including alkaloid compounds, phenol hydroquinone, flavonoids and tannins. These compounds have a wide range of biological activities, including antioxidant, anti-inflammatory, and antitumor activities (Jain *et al*., 2019). Previous studies have shown that GC extract has the potential to treat several degenerative diseases such as cholesterol (Astirani & R, 2012) and high blood pressure (Nurchairina and Aziza, 2020). However, research into its impact on stem cells, particularly MSCs, is currently restricted.

Despite all of the biological activity mentioned above, the cytotoxic effects of this extract on MSCs remain unknown. The use of plants in biomedical applications, a preliminary safety assessment of the chemicals contained is required which limits its potential application in stem cell research and treatment (Jain *et al*., 2018; Morais *et al*., 2010). In vitro cytotoxicity testing is a rapid and reduced costs when contrasted with animal studies approach of assessing the hazardous potential of a chemical (Aslantürk, 2018). Although plant-based medicines are believed to be safe and minimise side effects, extracts with high bioactivity can sometimes have harmful effects on cells at certain concentrations (Anlas *et al*., 2022).

Premna oblongifolia Merr has been used both as food and medicinal products, but no research on the content of phytochemical compounds has been conducted so far. This study contributes to investigating the chemical substances that are beneficial in the field of natural product-based regenerative medicine. Considering that several studies have reported the osteogenic potential of flavonoids, which are also contained in green cincau, in promoting the differentiation of MSCs into osteogenic cells. Therefore, based on this potential, we focused on osteogenesis differentiation as preliminary research on differentiation ability. Additionally, Cytotoxic testing on the ethanol extract of *P. oblongifolia* Merr. provides information on cytotoxicity levels and adds to the potential bioactivity of the extract specifically on MSCs, this may pave the way for its use in promoting osteogenic differentiation or other therapeutic applications. By addressing this gap, this study aimed to assess the cytotoxicity of ethanol extract of green

cincau leaves on bone marrow-derived MSC-like cells, providing baseline data that may inform future research on its application in stem cell-based treatments.

MATERIALS and METHODS

Preparation of Green Cincau Extract (GCE)

The leaves of *Premna oblongifolia* Merr. were collected from Lamseupeung village, Banda Aceh city (Indonesia) in March 2023. Plant identification was confirmed by Dr. Saida Rasnovi, S.Si., M.Si, taxonomist at the Herbarium of the Biology Department, Faculty of Mathematics and Natural Sciences, Universitas Syiah Kuala, and verified by the official identification letter (Letter No. 758/UN11.F8.4/TA.00.03/2025). The collected leaves were cleaned and dried at room temperature. The dried leaves were ground to a fine powder for extraction. Approximately 340 g of the powdered leaves was extracted using the maceration method with 96% ethanol as the solvent with 1:10 ratio for 3×24 hr. The extract was concentrated using a rotary evaporator to remove the solvent. The extraction yield of GCE was 6.97% (w/w), with approximately 23.7 g of concentrated extract. The concentrated extract was stored at 4°C until further use. For the analyses, the extract was diluted in ethanol to prepare a stock solution of 100 mg/ml. The working concentrations used for the cytotoxic experiments ranged from 1 to 1200 μg/ml.

Gas Chromatography-Mass Spectrometry (GC-MS)

The volatile compounds present in GCE were analysed using Gas Chromatography–Mass Spectrometry (GC-MS) (GCMS-QP2010, Shimadzu, Japan), employing a capillary column (30 m×0.25 mm ID×0.25 mm). Helium was used as the carrier gas at a constant flow rate of 1.0 mL/min. The injection volume was 1 μl, with the injector temperature set at 250°C in splitless mode. The temperature was programmed as follows: initial temperature at 50°C for 10 min, increased to 150°C at 5°C/min, then to 280°C at 10°C/min resulting in a total run time of approximately 59 min. Mass spectra of each chromatographic peak were analysed using GCMSsolution software (Shimadzu) and automated matching against reference spectrum libraries including the National Institute of

Standards and Technology (NIST) NIST17-1 version, W11main and FFNSC.

Collection, Isolation and Culture of BM-MSC like Cells

Male rats (150‑200 g) were euthanized via cervical dislocation, following ethical approval granted by the Committee of Veterinary Ethics, Faculty of Veterinary Medicine, Universitas Syiah Kuala (Reference number: 308/KEPH/VII/2024). Post-euthanasia, the femurs and tibias were excised, thoroughly rinsed with physiological saline to remove residual blood, and sterilized with 70% ethanol. Bone marrow was collected using the flushing method according to Lu *et al.* (2022). Briefly, a syringe filled with complete growth medium supplemented with 1% antibiotics and used to flush the marrow out of the bone cavity. The medium was prepared using Dulbecco's Modified Eagle's Medium (DMEM) high glucose with pyruvate and L-glutamine, supplemented with 15% fetal bovine serum (FBS) (Himedia, India), 1% antibiotic-antimycotic solution, and 1% non-essential amino acids (NEAA) (Sigma, USA). The cell suspension was centrifuged at 2000 rpm for 10 min. The pellet obtained was washed three times with phosphate-buffered saline (PBS) (Himedia, India) supplemented with 1% antibiotics (Sigma, UK). The number of cells were determined using a hemocytometer with 0.4% trypan blue staining (Sigma, USA) using this following equation (Abdul Aziz *et al*., 2022), Eq.(1):

$$Total\ cells\ (cell/mL) = \frac{Number\ of\ live\ cells\ on\ 4\ squares}{4} \times dilution\ factor \times 10^4\ Eq.(1)$$

The cells were seeded into 25 cm^2 culture flasks containing complete growth medium and incubated at 37°C with 5% CO_2. Non-adherent cells were removed on the fourth day of culture by washing with PBS, and the medium was replaced every three days. Cellular morphology was observed regularly using an inverted microscope (Olympus CKX41, Tokyo, Japan). When cell confluency reached 80%, subcultures were initiated using 0.25% Trypsin-EDTA (Gibco, USA).

Cytotoxicity Assay

The viability of cells was assessed using Cell Proliferation Reagent WST-1 (Roche, Mannheim, Germany) following manufacturer's instruction and as described by Gharbaran *et al*. (2021). Briefly, after incubating the MSC-like cells (1×10^4 cells/well) on 96-well plate for 24 hr at 37°C under 5% CO_2, the medium was replaced with complete medium (100 µl) containing 1% GCE with various concentrations (1, 5, 10, 20, 40, 80, 150, 300, 600 and 1200 µg/ml). The cells were incubated in three exposure times, namely 24, 48 and 72 hr. After the cells were exposed to the extract for a predetermined time, the medium was replaced with medium containing 10 µl WST-1 and incubated for 3 hr. 70 µl of the medium was transferred into a 96-well plate with flat bottom, and the absorbance was measured at 450 nm using a microplate reader (EZ Read 400 Biochrom, UK). The percentage of cell viability can be determined using the following formula (Widiandani *et al*., 2023), Eq. (2):

$$Cell\ viability\ (\%) = \frac{Abs.treatment - Abs.blank}{Abs.control - Abs.blank} \times 100\%\ \ Eq.(2)$$

Cell Differentiation

0.055×10^6 cells/well at third passage were seeded in 24-well plate and allowed to reach 80% confluence. Cells were then treated either in GCE medium which was growth medium supplemented with GCE at the concentration of 0, 150, 300, and 600 µg/ml or in osteogenic medium consist of growth medium supplemented with 0.1 µM dexamethasone (GLPBIO, USA), 10 mM β-glycerophosphate (Sigma-Aldrich, USA) and 50 µM ascorbic acid (Merck, Germany) (Bochon *et al*., 2021). Morphological examination using a microscope was carried out on days 3, 7, 11 and 14.

Alizarin Red Staining (ARS)

Staining of mineralisation was done with ARS after 14 days of treatment. Cells were washed with PBS twice and fixed in 10% formaldehyde for 30 min at room temperature. Then, the cells were stained with 2% ARS (Merck, Darmstadt, Germany) for 30 min and rinsed twice with PBS to remove any remaining staining. The cells were observed and captured by inverted microscope (Olympus CKX41, Tokyo, Japan).

Data Analysis

All experiments were done in triplicate and data were expressed as means ± Standard deviation (SD). Data were analysed using One Way

Analysis of Variance (ANOVA). P<0.05 was considered as significant difference.

RESULTS and DISCUSSION

Chemical Composition of GCE

According to the analysis of GC-MS shown in Figure 1, there were 28 peaks of different compounds in the sample (Table 1). The chromatogram was dominated by two consecutive peaks (6th and 7th peaks) as 2,4,6,8-Tetramethyl-1,3,5,7,2,4,6,8-tetraoxatetrasilocane which identified as siloxane compound. It should be noted that this compound may represent artifacts from laboratory equipment or column bleeding during GC-MS analysis rather than true plant metabolites. Siloxane has been reported as a common laboratory contaminant in GC-MS studies (English, 2022; McMaster, 2008). Therefore, in line biological significance of these compounds should be interpreted with caution. Thus, these siloxane peaks were not considered genuine metabolites of *P. oblongifolia* and were excluded from our biological interpretation.
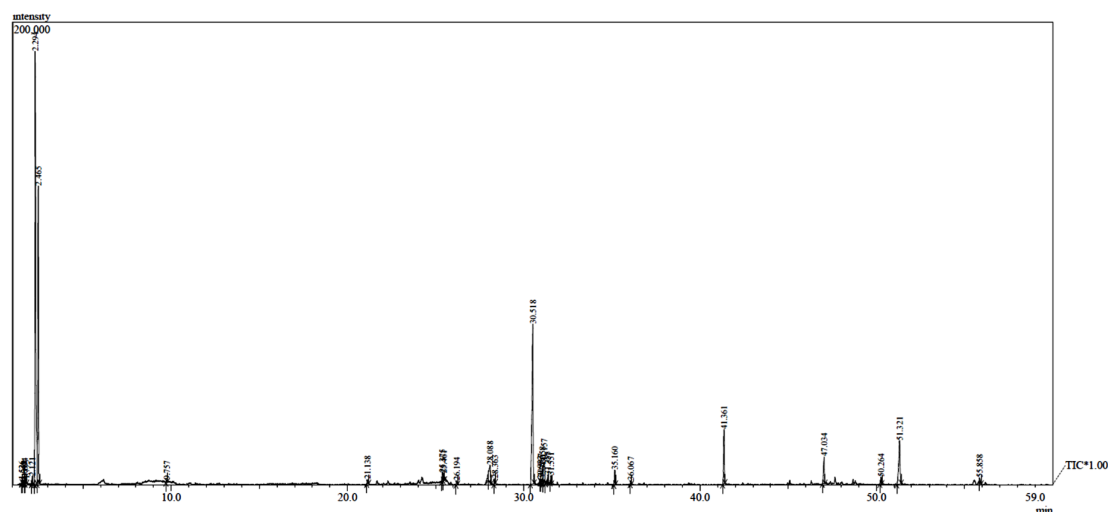
Figure 1. GC-MS chromatogram of green cincau ethanol extracts

After neglecting these artefacts, the most abundant and biologically relevant compounds were terpenoids (23%) and fatty acids (19%) (Figure 2). The chemical structures of the major identified phytochemicals are shown in Figure 3. The existence of terpenoids is particularly important, as this class of natural compounds is increasingly recognised for its potential in the osteoporosis treatment including bone health (Zhuo *et al*., 2022). In addition, certain terpenes have been identified as bioactive agents capable of directly influencing the fate and function of mesenchymal stromal cells (MSCs) (Mazzone *et al*., 2025). This may provide a convincing explanation for their role in the biological activities we have observed.
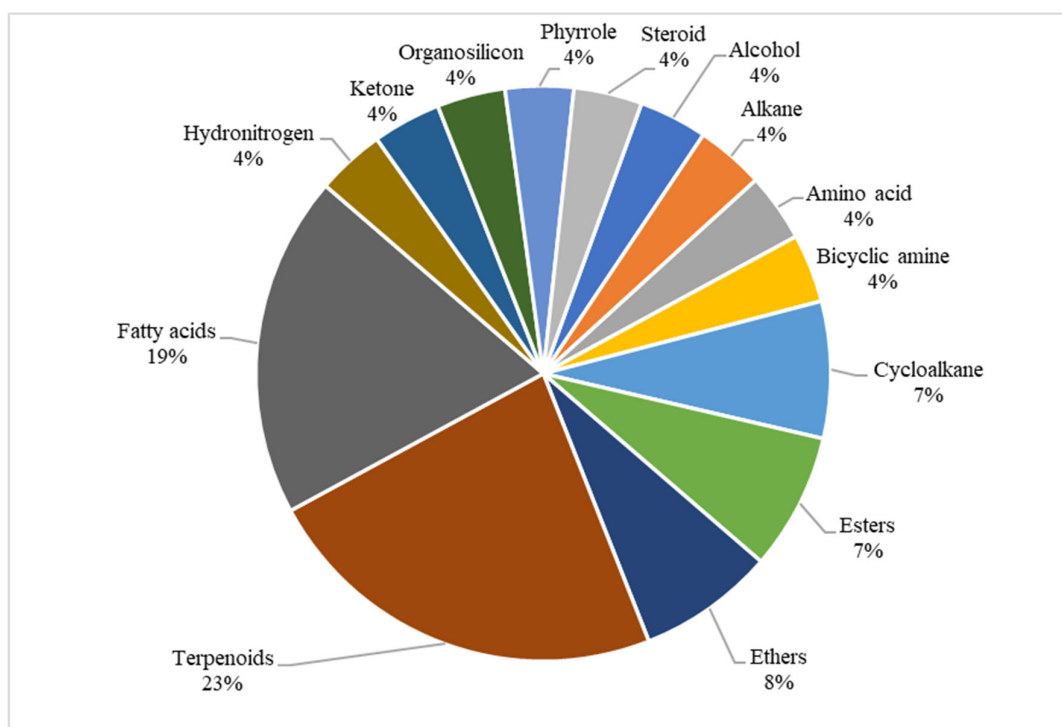
Figure 2. The group of chemical compounds found in GCE

The predominant compounds identified were phytol (19.06%), urs-12-en-28-oic acid, 3-hydroxy-, methyl ester, (3.beta.)- (6.23%), and squalene (4.32%). Other terpenoids identified include neophytadiene (0.7%), Olean-12-en-28-oic acid, 3-hydroxy-, methyl ester, (3.beta.)-(0.62%), and Cyclopentane, 1-ethenyl-3-ethyl-2-methyl- (0.38%). The identified fatty acids include hexadecanoic acid (2.49%), 8,11,14-(Z,Z,Z)-eicosatrienoic acid (2.88%), 7,10,13-(Z,Z,Z)-hexadecatrienoic acid (0.77%), 8-methylnonanoic acid (0.51%), and undecanoic acid, ethyl ester (0.35%).

Importantly, these specific compounds exhibit documented activity, providing a reasonable mechanistic link to the observed biocompatibility and osteogenic potential. The most abundant metabolite, Phytol (19.06%), shows direct relevance to mesenchymal stem cell (MSC) biology. In addition to its established anti-inflammatory and antioxidant properties (Naikwadi *et al*., 2022; Ren *et al*., 2023), the compound has been shown to promote osteoblast differentiation in mouse mesenchymal stem cells (C3H10T1/2) (Sanjeev *et al*., 2020). Its ability to activate the PI3K/Akt signalling pathway (Wang *et al*., 2017) is significant, as this pathway is a crucial regulator of cell survival and differentiation and indicates a key mechanistic pathway through which it can enhance MSC commitment to the osteogenic lineage.

Furthermore, the presence of urs-12-en-28-oic acid, 3-hydroxy-, methyl ester, (3.beta.)-(6.23%) provides a potent association with osteogenic mechanisms. While these compounds exhibit the known activities including antibacterial and anti-inflammatory (Sujatha *et al*., 2017), their significant role in bone regeneration should be highlighted. Structurally similar ursolic acid compounds have been demonstrated to upregulate the key osteogenic marker significantly including Runx2, Osterix, ALP, and Osteopontin (D. E. Lee *et al*., 2023), while protecting osteoblasts from oxidative stress through the IER3/Nrf2 pathway (S. Lee, 2019). This dual role in promoting the bone formation and ensuring cell survival positions these derivatives as important bioactive components contributing to the extract's osteogenic potential.

Squalene (4.32%) is known for its strong antioxidant properties. According to Du *et al*. (2024), the compound has been reported to protect cell membranes from free radical damage and improve lipid stability. Picón and Skouta

(2023) added that this compound also plays a role in regulating lipid peroxidation contributing to its protective effect against oxidative damage. In line with these findings, this function is very important because oxidative stress is a major factor that disrupts cellular energy metabolism, which is a determining factor in directing MSC differentiation (Yan *et al.*, 2021). By reducing oxidative damage, squalene helps maintain metabolic homeostasis. Importantly, squalene has been identified as a component in olive oil fraction that specifically enhances osteoblast differentiation over adipogenesis in MSCs (Casado-Díaz *et al.*, 2019), indicating an active role in cell fate determination beyond mere cell protection.

In conclusion, the presence of these combined metabolites indicates varied biological activities. Through important pathways, phytol functions as a differentiation signal; derivatives of ursolic acid regulate the genetic program of bone formation; and squalene optimises the oxidative and metabolic conditions for cell function. *P. oblongifolia* extract's biological activity is supported by a strong mechanistic hypothesis due to this synergistic combination of phytochemicals, which also makes it a possible candidate for more study in the area of bone regenerative therapy.

Table 1. Phytochemical components identified in green cincau ethanol extract by GC-MS analysis

No	Name of compound	RT[a]	MF[b]	MW[c]	PA[d](%)	Classification	Function
1	Butane, 1,1'-[(1-methylethylidene)bis(oxy)]bis-	1.526	$C_{11}H_{24}O_2$	188	0.12	Ether	Unknown
2	Silane, trimethyl-	1.642	$C_3H_{10}Si$	74	0.29	Organosilicon	Unknown
3	3-Hexanol	1.694	$C_6H_{14}O$	102	0.3	Alcohol	Antifungal (Naqvi *et al.*, 2022)
4	1-Aminoisopropane-1-carboxylic acid-D3	1.775	$C_4H_6D_3NO_2$	106	0.34	Amino acid	Unknown
5	Hydrazine, 1,2-dimethyl-	2.121	$C_2H_8N_2$	60	0.42	Hydronitrogen	Pharmaceutical and agricultural applications (Ramaro *et al.*, 2024)
6	2,4,6,8-Tetramethyl-1,3,5,7,2,4,6,8-tetraoxatetrasilocane	2.294	$C_4H_{16}O_4Si_4$	240	35.35	Siloxane	Unknown
7	2,4,6,8-Tetramethyl-1,3,5,7,2,4,6,8-tetraoxatetrasilocane	2.465	$C_4H_{16}O_4Si_4$	240	18.13	Siloxane	Unknown
8	1-Ethyl-2-methylcyclohexane	9.757	C_9H_{18}	126	0.19	Cycloalkane	Unknown
9	1,2,5-Trimethyl-1H-pyrrole	1.138	$C_7H_{11}N$	109	0.39	Phyrrole	Unknown
10	Neophytadiene	5.375	$C_{20}H_{38}$	278	0.7	Diterpenoid	Antimicrobial and anti-inflammatory (Tawfeeq *et al.*, 2024) and neuroprotective activities (Gonzalez-Rivera *et al.*, 2023)
11	Phytone	5.461	$C_{18}H_{36}O$	268	0.4	Ketone	Antibacterial (Al-Shaar *et al.*, 2025); analgesic, and anti-inflammatory activities (Nasrollahi *et al.*, 2022)
12	3-Methylene-7,11-dimethyl-1-dodecene	6.194	$C_{15}H_{28}$	208	0.25	Alkene	Unknown
13	Hexadecanoic acid	8.088	$C_{16}H_{32}O_2$	256	2.49	Fatty acid	Anti-inflammatory agent, antimicrobial, antioxidant (Ferdosi *et al.*, 2021), cell proliferation (Chen *et al.*, 2010)
14	Undecanoic acid, ethyl ester	8.363	$C_{13}H_{26}O_2$	214	0.35	Fatty acid ester	Antioxidant (Uka *et al.*, 2022)

		RT	MF	MW	PA		
15	Phytol	0.518	$C_{20}H_{40}O$	296	19.06	Diterpenoid	Induces cell differentiation (Sanjeev *et al.*, 2020), antioxidant, anti-inflammatory (Naikwadi *et al.*, 2022)
16	Isobutyrate <2,4-hexadienyl->	0.933	$C_{10}H_{16}O_2$	168	0.1	Ester	Unknown
17	7-Azabicyclo[4.1.0]heptane, 3-methyl-	0.967	$C_7H_{13}N$	111	0.23	Bicyclic amine	Unknown
18	1,9-Cyclohexadecadiene	1.058	$C_{16}H_{28}$	220	1.66	Cycloalkadiene	Unknown
19	8,11,14-Eicosatrienoic acid, (Z,Z,Z)-	1.157	$C_{20}H_{34}O_2$	306	2.88	Fatty acid	Antimicrobial (Naikwadi *et al.*, 2022)
20	7,10,13-Hexadecatrienoic acid, (Z,Z,Z)-	1.355	$C_{16}H_{26}O_2$	250	0.77	Fatty acid	Antibacterial, antioxidant,antitumor, immunostimulant (Saha *et al.*, 2024)
21	8-Methylnonanoic acid	1.551	$C_{10}H_{20}O_2$	172	0.51	Fatty acid	Unknown
22	Hexanedioic acid, bis(2-ethylhexyl) ester	5.16	$C_{22}H_{42}O_4$	370	1.03	Diester	Antimicroba (Ferdosi *et al.*, 2021; Wulandari *et al.*, 2024)
23	Ethanamine, 2,2'-oxybis[N,N-dimethyl-	6.067	$C_8H_{20}N_2$	160	0.2	Ether	Unknown
24	Squalene	1.361	$C_{30}H_{50}$	410	4.32	Triterpenoid	Skin emollient, antioxidant (Kumar *et al.*, 2021), cytoprotective activity (Das *et al.*, 2008) and metabolism-enhancing activity (Ganbold *et al.*, 2020)
25	Gamma.-Sitosterol	7.034	$C_{29}H_{50}O$	414	2.28	Steroid	Antioxidant, anti-bacterial and prophylatic activies and antidiabetic (Namuga *et al.*, 2024)
26	Olean-12-en-28-oic acid, 3-hydroxy-, methyl ester, (3.beta.)-	0.264	$C_{31}H_{50}O_3$	470	0.62	Triterpenoid	Unknown
27	Urs-12-en-28-oic acid, 3-hydroxy-, methyl ester, (3.beta.)-	1.321	$C_{31}H_{50}O_3$	470	6.23	Triterpenoid	Unknown
28	Cyclopentane, 1-ethenyl-3-ethyl-2-methyl-	5.858	$C_{10}H_{18}$	138	0.38	Triterpenoid	Unknown

Note: a: RT=Retention time;b: MF=Molecular formula; c: MW=Molecular weight; d: PA=Peak area;
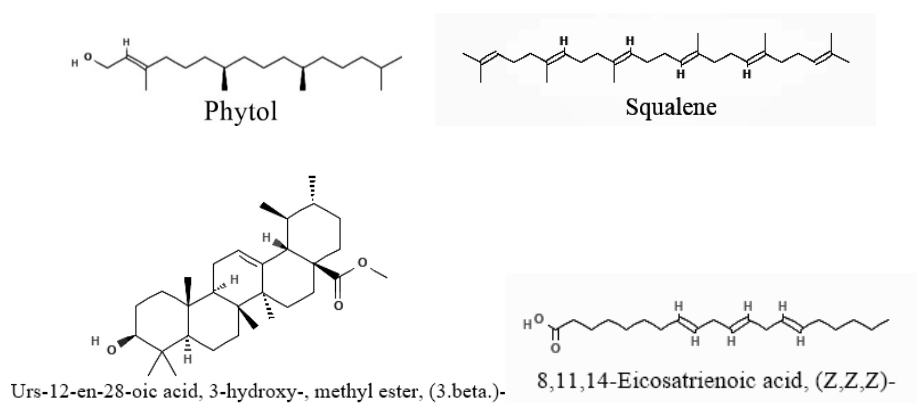
Figure 3. Chemical structure of the main phytochemical components discovered in the ethanol extract of green cincau
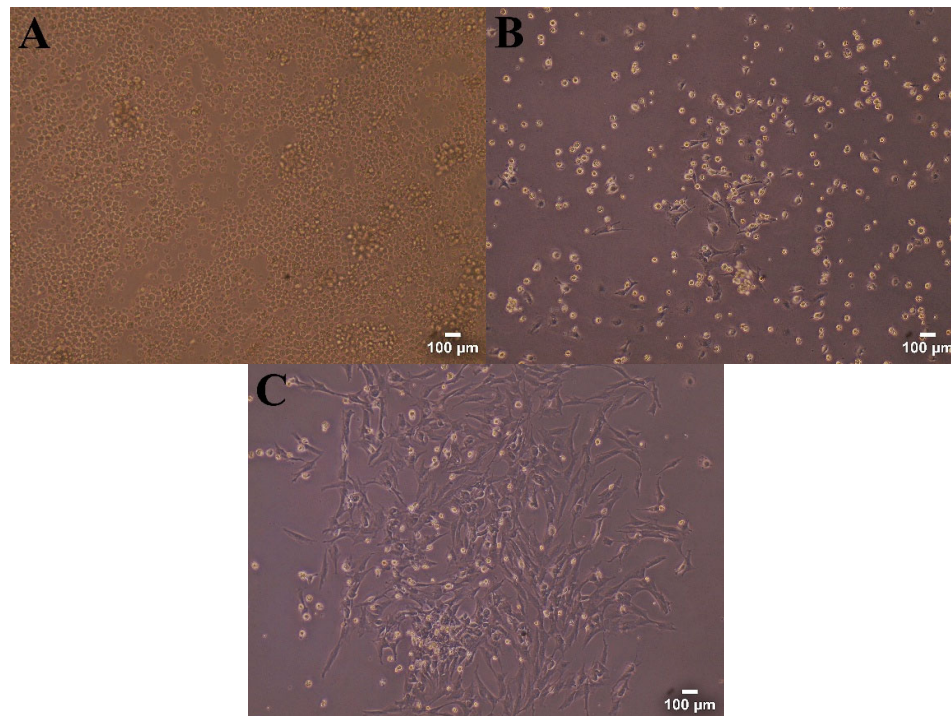
Figure 4. Cell morphology on primary isolation. (A) Cells remained spherical on the second day. (B) Spindle-shaped cells began to develop on the fifth day. (C) MSC-like cells formed colonies on the eighth day. Magnification: 100X; scale bar: 100µm.

Primary Culture of Bone Marrow MSC-like Cells

Isolation of MSC-like cells from rat bone marrow was carried out using the flushing method, in which bone marrow was extracted from the femur and tibia of adult rats. The total number of cells isolated from each mouse was approximately 3.152×10^8 cells. The primary cell in this study initially showed heterogeneous morphology as shown in Figure 4A. According to Chong *et al*. (2018), primary isolation from bone marrow (BM-MSC) can be contaminated with hematopoietic cells during the bone marrow collection process and can be mixed with peripheral blood or lipids, causing a mixture of cell types and potential contamination. However, as the passages proceed, the non-adherent hematopoietic cells will disappear (Baustian *et al*., 2015; Rennerfeldt *et al*., 2019).

On the early day of culture (Figure 4A) most cells still were mononuclear. Some cells began to adhere to the culture surface, while others have not yet adhered and formed separate deposits on the surface of the culture vessel. Joujeh *et al*. (2021) stated that spindle-shape morphology increased since day three of primary culture, which in this study appeared on the fifth day (Figure 4B). The cells exhibited fibroblast-like appearance and started to form colonies on the eighth day (Figure 4C). Primary cells reached confluence on day 27. This duration was shorter than the study conducted by Pissarra *et al*. (2022) where it took 35-56 days for the cells to reach confluence.

Effect of GCE on Cellular Viability

Cytotoxic examination was performed using the WST-1 method. The principle of WST-1 is based on the conversion of WST-1 tetrazolium salt into a coloured dye by the mitochondrial dehydrogenase enzyme (Gharbaran *et al*., 2021). Cell viability was evaluated after treatment with 10 different concentrations of GCE (1-1200 µg/ml) for 24, 48, and 72 hr. The findings revealed that as the concentration of the extract increased the percentage of cell viability remained relatively constant across most concentrations, however, as the exposure duration of the extract increased, the percentage of viability showed a decreasing trend (Figure 5). Statistical analysis indicated that GCE concentrations demonstrated no significant cytotoxic activity ($p > 0.05$) at any specific time point, although the variation in viability with exposure duration was considerable ($p < 0.05$).

Detailed observation of the data revealed a time-dependent and biologically significant decline in viability. Cell viability decreased by 21%, 29%, and 27% after 48 hr of exposure to GCE concentrations of 80, 600, and 1200 µg/ml, respectively. After 72 hr of exposure to the extract at 300 µg/ml concentration, viability decreased by more than 20%. It is important to note that while cell viability reduced as exposure duration increased, it remained above 70-80% across all tested conditions. Moreover, a standard half-maximal inhibitory concentration (IC_{50}) could not be calculated for any exposure time because the cell viability did not fall below 50%, even at the highest concentration of 1200 µg/ml. This result indicates that the IC_{50} value for GCE is definitively greater than 1200 µg/ml. Based on established toxicity categories, such as that of Saputri *et al*. (2019), this places GCE in the "no significant cytotoxicity" classification ($IC_{50} > 1000$ µg/ml). The decrease in viability observed with longer exposure may be due to the cumulative action of bioactive chemicals, which can result in the accumulation of toxic metabolites and initiate cellular stress responses. The duration of exposure in cytotoxic is crucial since it influences the amount of cell damage and the efficiency of the cytotoxic substance (Byrne and Maher, 2019). Prolonged exposure of extracts may result in higher toxicity, but shorter intervals may not result in meaningful cellular reactions. Other factors that are suspected to influence the results are the proportion of bioactive chemicals extracted in plant extracts may vary depending on the extraction solvent and technique used (Anlas *et al*., 2022).

Based on the results, it can be concluded that in the concentration range of 1-1200 µg/ml and incubation times of 24, 48, and 72 hr of GCE did not exhibit severe toxicity. The inability to calculate an IC_{50} within this range confirms its low cytotoxic potential. Nevertheless, the time-dependent declines in viability of 20-30% indicate that the claim of GCE being completely non-toxic requires caution. Hence, while GCE has a favourable safety profile for possible use as an active ingredient, particularly in situations involving shorter periods, its effects on prolonged exposure require further investigation.
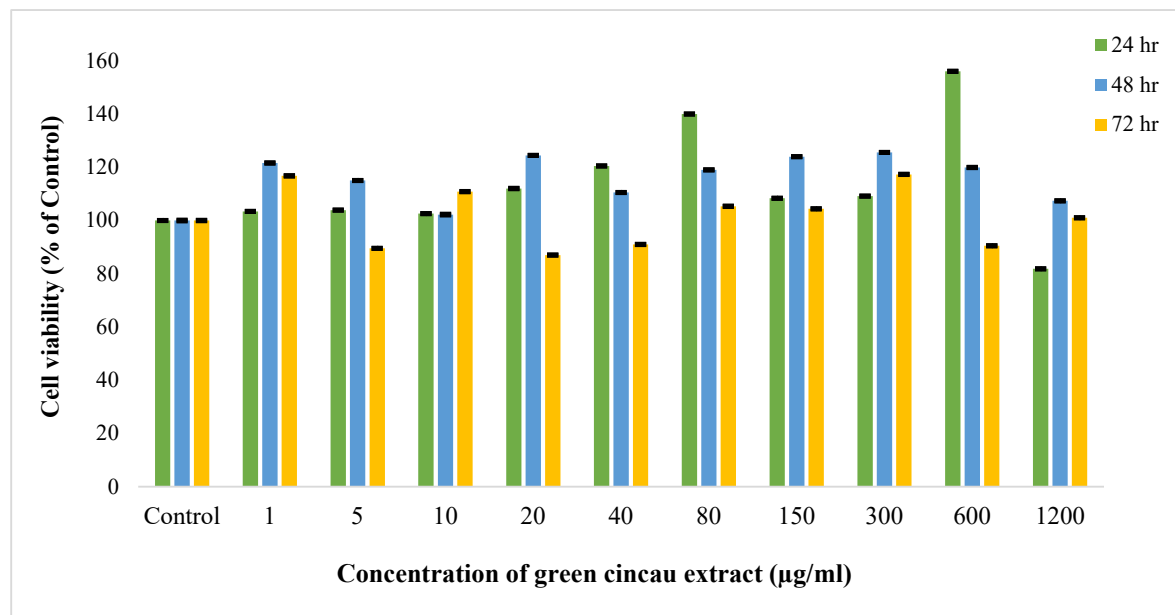
Figure 5. Percent cell viability of BMMSC-like cells were measured at 24, 48, and 72 hr after treatment with varying concentration of GCE by WST-1 assay. Data were presented as mean ± standar deviation (n=3).

The Effect of GCE on Cell Differentiation

The observation of cell morphology development during the differentiation process with treatment using GCE (Figure 6) at different concentrations (150, 300, and 600 µg/ml) as well as positive control (K+) and negative control (K-) on the third day showed cell morphology resembling fibroblasts with relatively uniform distribution. There was no morphological difference in the positive control treatment with other treatment groups until day 14. Calcium deposit examination was conducted on day 14 based on Hanna *et al*. (2018), Ca^{2+} deposits begin to accumulate at the end of the second week and become increasingly dense. Alizarin Red S (ARS) is a staining standard commonly used for the detection and quantification of mineralisation, which is a marker of osteoblast differentiation (Liu *et al*., 2021).

The osteogenic medium-treated group showed orange to red stains (Figure 7B), which are most likely ARS that binds to calcium ions, allowing visualisation of mineralised structures in the tissue. The mixture of ingredients used to induce osteocyte differentiation was dexamethasone, ascorbic acid and β-glycerophosphate. The combination of these ingredients is commonly used in osteogenic differentiation studies (Azizsoltani *et al*., 2018; Colter *et al*., 2001; Harsoyo *et al*., 2020). Dexamethasone triggers Runx2 expression and activity through activation of FHL2/β-catenin, TAZ, and MKP-1 pathways to support the osteogenic pathway (Bella *et al*., 2021; Langenbach and Handschel, 2013). Ascorbic acid stimulates the formation of type I collagen (Col1). β-GP contains the inorganic phosphate required for the production of hydroxyapatite, the main mineral component of bone (Freeman *et al*., 2016; Langenbach and Handschel, 2013). The positive control indicated that the osteogenic pathway was successfully activated, although not optimally.

The GCE treatment group with a concentration of 300 µg/ml showed indications of possible mineral deposition through red staining (Figure 7D). In addition, the fibroblastic-like characteristics on the cell morphology still showed. The phytol content in GCE could potentially contribute to this process, based on literature report that has been conducted by Sanjeev *et al*. (2020), treatment with phytol enhanced osteoblast differentiation in C3H10T1/2 cells by promoting Runx2 expression, a process linked to the downregulation of Smad7 through miR-21a activity.

Treatments with other GCE concentrations (150 and 600 µg/ml) displayed relatively stable shape, this is thought to be due to the presence of several bioactive ingredients of GCE that function as antioxidants which may support the differentiation of damaged stem cells. The substances that may function as antioxidants and anti-inflammatories include neophytadiene (Tawfeeq *et al*., 2024), phytone (Nasrollahi *et al*., 2022), hexadecanoic acid (Ferdosi *et al*., 2021), undecanoic acid, ethyl ether (Uka *et al*., 2022), phytol (Naikwadi *et al*., 2022), 7,10,13-hexadecatrienoic acid, (Z,Z,Z)- (Saha *et al*., 2024), squalene (Kumar *et al*., 2021) and Gamma.-Sitosterol (Namuga *et al*., 2024). However, it is crucial to acknowledge that the evidence for the differentiation in this study is still preliminary. Qualitative morphological findings and ARS staining indicate mineral deposition at 300 µg/ml, but cannot be considered final confirmation. These findings require to be validated using quantitative approaches such as measuring alkaline phosphatase (ALP) activity, analysing mineralisation quantitatively, and using qPCR to assess the expression of osteogenic marker genes Runx2 and Osteocalcin. In a result, while GCE has the potential to influence osteogenic differentiation, further research is essential to provide solid evidence.
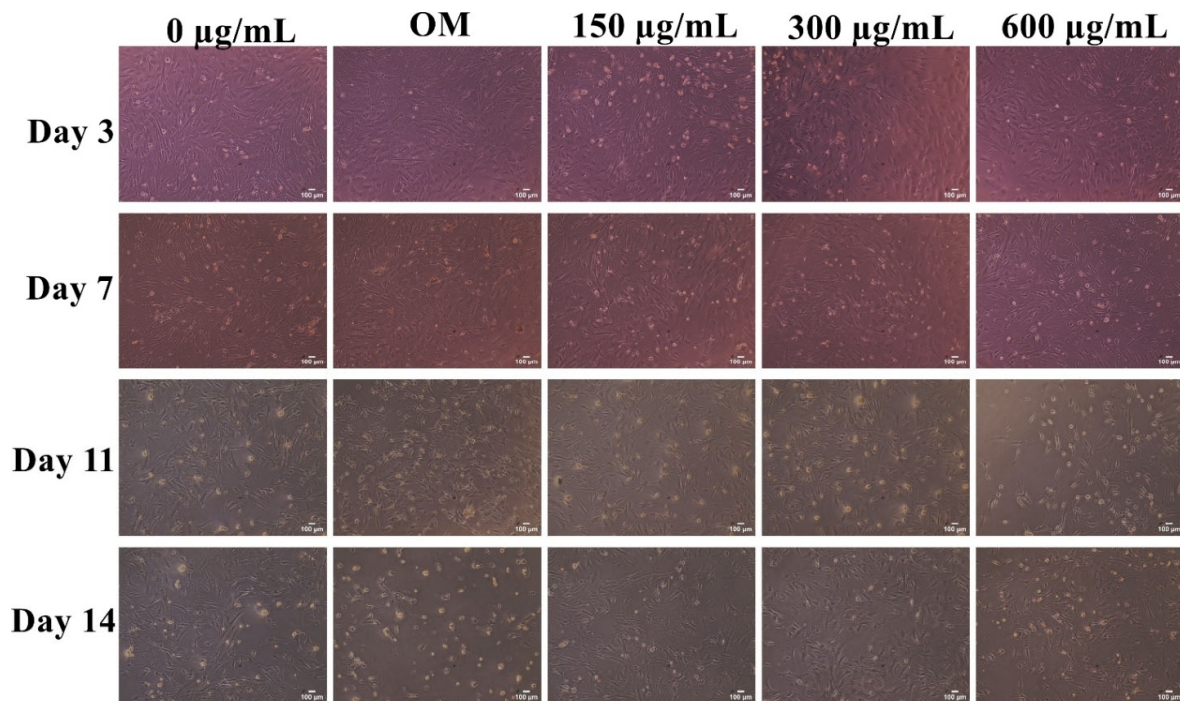
Figure 6. Morphological details of MSC-like cells during the differentiation process up to day 14. Notes: (1) horizontal rows represent morphological changes on days three to 14 in each treatment (2) vertical columns represent treatments consisting of negative control (0 µg/ml), osteogenic medium (OM), 3 treatments of GCE with 3 different concentrations of 150, 300, and 600 µg/ml. Magnification: 100X; scale bar: 100 µm.
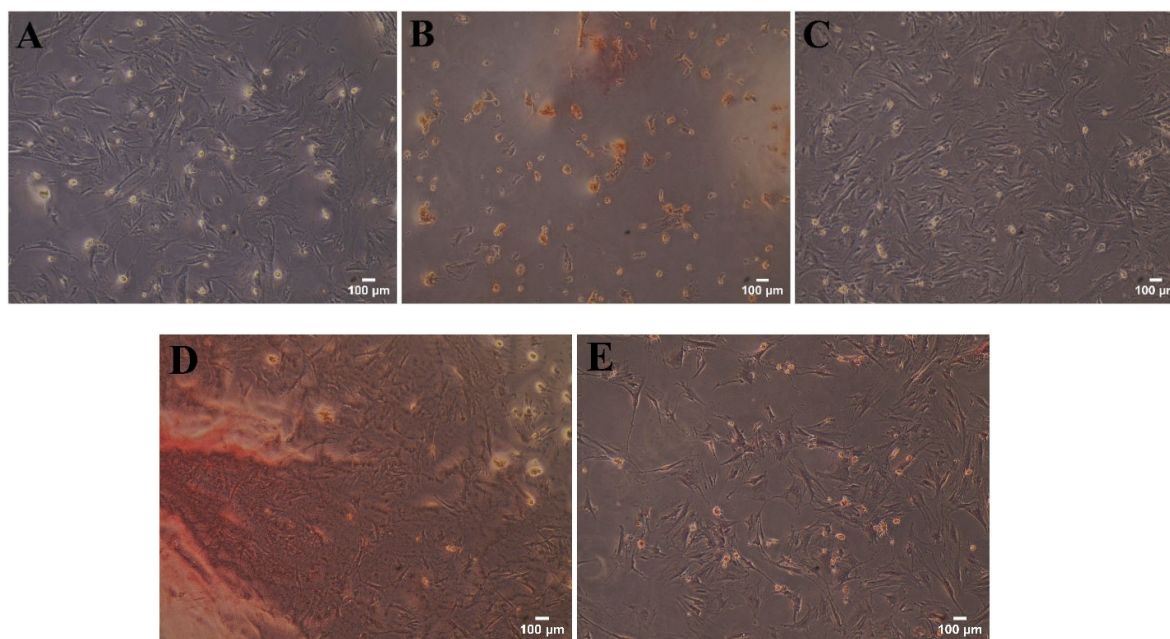
Figure 7. Cell staining using Alizarin Red S on day 14. Notes: (A) Negative control (0 μg/ml), (B) osteogenic medium (OM) is the positive control treatment, (C, D, E) GCE treatment with 3 different concentrations of 150, 300, and 600 μg/ml, respectively. Magnification: 100X; scale bar: 100 μm.

Study Limitations

This study has several limitations that should be acknowledged. First, the finding of siloxane compounds as the predominant peaks was a major issue of the phytochemical study. Siloxane compounds may represent artefacts from laboratory equipment or column bleeding during GC-MS analysis rather than actual plant metabolites. This is an initial shortcoming that future studies will need to address using other method such as Nuclear Magnetic Resonance (NMR) spectroscopy to identify the most important active compounds in *P. oblongifolia*. Second, the cytotoxic assays were performed in triplicates (n = 3). Although commonly used in preliminary screening, this can limit statistical robustness. Future studies are recommended to use a larger sample size (n ≥ 6) to increase the reliability of statistical analysis. Finally, the differentiation study was limited to qualitative Alizarin Red S staining. Future studies should include a longer time study (21-28 days) to monitor the full progression of mineralization and quantitative assessments such as ARS quantification, alkaline phosphatase activity assays, and qPCR analysis of osteogenic markers (Runx2, osteocalcin, osteopontin) to provide more robust evidence of differentiation.

CONCLUSION

The bioactive profile of the *Premna oblongifolia* extract is primarily composed of terpenoids and fatty acids, with Phytol, Urs-12-en-28-oic acid, 3-hydroxy-, methyl ester, (3.beta.)-, and squalane identified as the most abundant compounds. This preliminary investigation indicates that the ethanol extract of *P. oblongifolia* Merr. exhibits low cytotoxic potential on MSC-like cells and demonstrates potential for maintaining cell viability. Notably, cell viability remained above acceptable levels across tested concentrations up to 1200 μg/ml, though time-dependent effects were observed. However, to completely ascertain its therapeutic promise, more comprehensive research incorporating quantitative differentiation analyses, mechanistic studies, and in vivo validation remains necessary.

ACKNOWLEDGEMENTS

Universitas Syiah Kuala for supporting the research.

REFERENCES

Abdul Aziz, M. W. H., Basri, D. F., Masre, S. F., & Ghazali, A. R. (2022). Fatty acids and terpenoids from Canarium odontophyllum Miq. leaf and their antioxidant and cytotoxic effects on uvb-induced immortalized human keratinocytes cells (hacat). *Malaysian Applied Biology*, 51(3):79–87. DOI: 10.55230/mabjournal.v51i3.2377

Al-Shaar, M., Mando, H., & Alkhatib, R. (2025). In silico antioxidant activity of six volatile constituents in Capsella bursa-pastoris. *Jordan Journal of Pharmaceutical Sciences*, 18(1): 230–244. DOI: 10.35516/jjps.v18i1.2537

Anlas, C., Bakirel, T., Koca-Caliskan, U., Donmez, C., Ustun-Alkan, F., & Ustuner, O. (2022). In Vitro Cytotoxicity and Genotoxicity Screening of Cuscuta Arvensis Beyr. and Achillea Wilhelmsii C. Koch. *Journal of Research in Veterinary Medicine*, 41(2): 143–149. DOI: 10.30782/jrvm.1161358

Aryudhani, N. (2011). *Mekanisme aktivitas antitumor bubuk daun cincau hijau (Premna oblongifolia Merr.) pada Mencit C3H yang ditransplantasi sel tumor payudara*, (Master thesis), IPB University, Bogor.

Asadi, F., Ayoobi, F., Arababadi, M. K., Arababadi, Z. K., & Yousefi-Ahmadipour, A. (2022). Aqueous extract of Achillea millefolium significantly affects mesenchymal stem cell renewal and differentiation in a dose dependent manner. *Journal of Stem Cells and Regenerative Medicine*, 18(2): 29–35. DOI: 10.46582/jsrm.1802006

Aslantürk, Ö. S. (2018). In vitro cytotoxicity and cell viability assays: principles, advantages, and disadvantages. *In Genotoxicity - A Predictable Risk to Our Actual World* (pp. 1–18). InTech. DOI: 10.5772/intechopen.71923

Astirani, A. E., & R, H. M. (2012). Pengaruh pemberian sari daun cincau hijau (Premna Oblongifolia Merr) Terhadap kadar kolesterol HDL dan kolesterol LDL tikus Sprague Dawley dislipidemia. *Journal of Nutrition College*, 1(1): 265–272.

Azizsoltani, A., Piri, K., Behzad, S., Soleimani, M., Nekouei, M., Mahmoudi, Z., & Kazemi, A. (2018). Ethyl acetate extract of licorice root (Glycyrrhiza glabra) enhances proliferation and osteogenic differentiation of human bone marrow mesenchymal stem cells. *Iranian Journal of Pharmaceutical Research*, 17(3): 1057–1067.

Baustian, C., Hanley, S., & Ceredig, R. (2015). Isolation, selection and culture methods to enhance clonogenicity of mouse bone marrow derived mesenchymal stromal cell precursors. *Stem Cell Research and Therapy*, 6(1): 1–13. DOI: 10.1186/s13287-015-0139-5

Bella, E. Della, Buetti-Dinh, A., Licandro, G., Ahmad, P., Basoli, V., Alini, M., & Stoddart, M. J. (2021). Dexamethasone induces changes in osteogenic differentiation of human mesenchymal stromal cells via sox9 and pparg, but not runx2. *International Journal of Molecular Sciences*, 22(9). DOI: 10.3390/ijms22094785

Bhatti, M. Z., Ismail, H., & Kayani, W. K. (2022). Plant secondary metabolites: therapeutic potential and pharmacological properties. In *Secondary Metabolites - Trends and Reviews*. IntechOpen. DOI: 10.5772/intechopen.103698

Bochon, K., Zielniok, K., Gawlak, M., Zawada, K., Zarychta-Wiśniewska, W., Siennicka, K., Struzik, S., Pączek, L., & Burdzińska, A. (2021). The effect of L-Ascorbic Acid and serum reduction on tenogenic differentiation of human mesenchymal stromal cells. *International Journal of Stem Cells*, 14(1): 33–46. DOI: 10.15283/ijsc20023

Byrne, H. J., & Maher, M. A. (2019). Numerically modelling time and dose dependent cytotoxicity. *Computational Toxicology*, 12. DOI: 10.1016/j.comtox.2019.100090

Casado-Díaz, A., Dorado, G., & Quesada-Gómez, J. M. (2019). Influence of olive oil and its components on mesenchymal stem cell biology. *World Journal of Stem Cells*, 11(12): 1045–1064. DOI: 10.4252/wjsc.v11.i12.1045

Chen, D. F., Li, X., Xu, Z., Liu, X., Du, S. H., Li, H., Zhou, J. H., Zeng, H. P., & Hua, Z. C. (2010). Hexadecanoic acid from buzhong yiqi decoction induced proliferation of bone marrow mesenchymal stem cells. *Journal of Medicinal Food*, 13(4): 967–975. DOI: 10.1089/jmf.2009.1293

Chong, P. P., Selvaratnam, L., Abbas, A. A., & Kamarul, T. (2018). Factors influencing the successful isolation and expansion of aging human mesenchymal stem cells. *Open Life Sciences*, 13(1): 279–284. DOI: 10.1515/biol-2018-0034

Colter, D. C., Sekiya, I., & Prockop, D. J. (2001). Identification of a subpopulation of rapidly self-

renewing and multipotential adult stem cells in colonies of human marrow stromal cells. *Proceedings of the National Academy of Sciences*, 98(14): 7841–7845. DOI: 10.1073/pnas.141221698

Dabas, A., Yadav, P., Geetanjali, & Singh, R. (2023). Role of herbal medicine in boosting immune system. In *Role of Herbal Medicines*, 389–401. DOI: 10.1007/978-981-99-7703-1_19

Das, B., Antoon, R., Tsuchida, R., Lotfi, S., Morozova, O., Farhat, W., Malkin, D., Koren, G., Yeger, H., & Baruchel, S. (2008). Squalene selectively protects mouse bone marrow progenitors against cisplatin and carboplatin-induced cytotoxicity in vivo without protecting tumor growth. *Neoplasia*, 10(10): 1105. DOI: 10.1593/neo.08466

Du, X., Ma, X., & Gao, Y. (2024). The physiological function of squalene and its application prospects in animal husbandry. *Frontiers in Veterinary Science*, 10. DOI: 10.3389/fvets.2023.1284500

Dzobo, K. (2021). Recent trends in multipotent human mesenchymal stem/stromal cells: learning from history and advancing clinical applications. *OMICS: A Journal of Integrative Biology*, 25(6): 342–357. DOI: 10.1089/omi.2021.0049

Ebrahimi, F., Pirouzmand, F., Cosme Pecho, R. D., Alwan, M., Yassen Mohamed, M., Ali, M. S., Hormozi, A., Hasanzadeh, S., Daei, N., Hajimortezayi, Z., & Zamani, M. (2023). Application of mesenchymal stem cells in regenerative medicine: A new approach in modern medical science. *Biotechnology Progress*, 39(6). DOI: 10.1002/btpr.3374

English, C. (2022). *Understanding the Origins of Siloxane Ghost Peaks in Gas Chromatography*. Retrieved October 1, 2025, from https://www.chromatographyonline.com/view/understanding-the-origins-of-siloxane-ghost-peaks-in-gas-chromatography

Ferdosi, M. F. H., Khan, I. H., Javaid, A., Saeed, H. M., Butt, I., & Munir, A. (2021). GC-MS analysis and bioactive components of flowers Bergenia ciliata, a weed of rock crevices in Pakistan. *Pakistan Journal of Weed Science Research*, 27(4): 527–535. DOI: 10.28941/pjwsr.v27i4.1012

Freeman, F. E., Stevens, H. Y., Owens, P., Guldberg, R. E., & McNamara, L. M. (2016). Osteogenic differentiation of mesenchymal stem cells by mimicking the cellular niche of the endochondral template. *Tissue Engineering - Part A*, 22(19–20):

1176–1190. DOI: 10.1089/ten.tea.2015.0339

Ganbold, M., Ferdousi, F., Arimura, T., Tominaga, K., & Isoda, H. (2020). New amphiphilic squalene derivative improves metabolism of adipocytes differentiated from diabetic adipose-derived stem cells and prevents excessive lipogenesis. *Frontiers in Cell and Developmental Biology*, 8(11): 1–14. DOI: 10.3389/fcell.2020.577259

Gharbaran, R., Shi, C., Onwumere, O., & Redenti, S. (2021). Plumbagin induces cytotoxicity via loss of mitochondrial membrane potential and caspase activation in metastatic retinoblastoma. *Anticancer Research*, 41(10): 4725–4732. DOI: 10.21873/anticanres.15287

Gonzalez-Rivera, M. L., Barragan-Galvez, J. C., Gasca-Martínez, D., Hidalgo-Figueroa, S., Isiordia-Espinoza, M., & Alonso-Castro, A. J. (2023). In Vivo neuropharmacological effects of neophytadiene. *Molecules*, 28(8): 3457. DOI: 10.3390/molecules28083457

Hanna, H., Mir, L. M., & Andre, F. M. (2018). In vitro osteoblastic differentiation of mesenchymal stem cells generates cell layers with distinct properties. *Stem Cell Research and Therapy*, 9(1): 1–11. DOI: 10.1186/s13287-018-0942-x

Harsoyo, A., Suparto, I. H., Yuniadi, Y., Boediono, A., & Sajuthi, D. (2020). Differentiation of cardiomyocytes and identification of cardiac conduction system connexins derived from bone marrow mesenchymal stem cells of macaca nemestrina. *HAYATI Journal of Biosciences*, 27(4): 337–344. DOI: 10.4308/hjb.27.4.337

Jain, C., Khatana, S., & Vijayvergia, R. (2019). Bioactivity of secondary metabolites of various plants: A review. *International Journal of Pharmaceutical Sciences and Research*, 10(2): 494–504. DOI: 10.13040/IJPSR.0975-8232.10(2).494-04

Jain, M. R., Bandyopadhyay, D., & Sundar, R. (2018). Scientific and regulatory considerations in the development of in vitro techniques for toxicology. In *In Vitro Toxicology*, 165–185. DOI: 10.1016/B978-0-12-804667-8.00009-2

Joujeh, D., Ghrewaty, A., Soukkarieh, C., Almarrawi, A., & Darwicha, J. A. N. (2021). An optimized protocol for mouse bone marrow mesenchymal stromal cells isolation and culture. *Cellular Therapy and Transplantation*, 10(3–4): 61–70. DOI: 10.18620/ctt-1866-8836-2021-10-3-4-61-70

Kumar, R., Kumar, B., Kumar, A., Kumar, A., & Singh, M. (2021). GC-MS analysis of phytocomponents in the methanol extract of Premna latifolia Roxb. *Pharmacognosy Research*, 14(1): 19–23. DOI: 10.5530/pres.14.1.4

Langenbach, F., & Handschel, J. (2013). Effects of dexamethasone, ascorbic acid and β-glycerophosphate on the osteogenic differentiation of stem cells in vitro. *Stem Cell Research & Therapy*, 4(5): 117. DOI: 10.1186/scrt328

Lee, D. E., Park, K. H., Hong, J.-H., Kim, S. H., Park, K.-M., & Kim, K. H. (2023). Anti-osteoporosis effects of triterpenoids from the fruit of sea buckthorn (Hippophae rhamnoides) through the promotion of osteoblast differentiation in mesenchymal stem cells, C3H10T1/2. *Archives of Pharmacal Research*, 46(9–10): 771–781. DOI: 10.1007/s12272-023-01468-9

Lee, S. (2019). Protective effects of ursolic acid on osteoblastic differentiation via activation of IER3/Nrf2. *Journal of Dental Hygiene Science*, 19(3): 198–204. DOI: 10.17135/jdhs.2019.19.3.198

Li, T., Liu, B., Chen, K., Lou, Y., Jiang, Y., & Zhang, D. (2020). Small molecule compounds promote the proliferation of chondrocytes and chondrogenic differentiation of stem cells in cartilage tissue engineering. *Biomedicine and Pharmacotherapy*, 131(5): 110652. DOI: 10.1016/j.biopha.2020.110652

Liu, M., Ding, H., Wang, H., Wang, M., Wu, X., Gan, L., Cheng, L., & Li, X. (2021). Moringa oleifera leaf extracts protect BMSC osteogenic induction following peroxidative damage by activating the PI3K/Akt/Foxo1 pathway. *Journal of Orthopaedic Surgery and Research*, 16(1): 1–14. DOI: 10.1186/s13018-021-02284-x

Lu, Y., Han, Y., Zhou, L., Shi, G., Bai, L., Wang, K., & Qin, C. (2022). A comparative study of mouse bone marrow mesenchymal stem cells isolated using three easy-to-perform approaches. *FEBS Open Bio*, 12(12): 2154–2165. DOI: 10.1002/2211-5463.13493

Mazzone, V., Alessio, N., Aprile, D., Galano, G., De Rosa, R., Schiraldi, C., Di Bernardo, G., & Galderisi, U. (2025). Terpenes: natural compounds found in plants as potential senotherapeutics targeting senescent mesenchymal stromal cells and promoting apoptosis. *Stem Cell Research & Therapy*, 16(1): 231. DOI: 10.1186/s13287-025-04310-9

McMaster, M. C. (2008). *GC/MS: a practical user's guide*. John Wiley & Sons, Inc. DOI: 10.1002/9780470228357

Melo, F. G., Ocarino, N. M., Reis, A. M. S., Gimeno, E. J., Massone, A. R., Melo, M. M., Botelho, A. F. M., Stehmann, J. R., & Serakides, R. (2020). The Solanum glaucophyllum Desf. extract reduces mineralized matrix synthesis in osteogenically differentiated rat mesenchymal stem cells in vitro. *Journal of Animal Physiology and Animal Nutrition*, 104(5): 1256–1266. DOI: 10.1111/jpn.13366

Morais, J. M., Papadimitrakopoulos, F., & Burgess, D. J. (2010). Biomaterials/tissue interactions: possible solutions to overcome foreign body response. *The AAPS Journal*, 12(2): 188–196. DOI: 10.1208/s12248-010-9175-3

Naikwadi, P. H., Phatangare, N. D., & Mane, D. V. (2022). Ethanopharmacological anti-inflammatory study of phytol in pet ether extract of Woodfordia floribunda Salisb. *Annals of Phytomedicine: An International Journal*, 11(2). DOI: 10.54085/ap.2022.11.2.52

Namuga, C., Muwonge, H., Nasifu, K., Sekandi, P., Sekulima, T., & Kirabira, J. B. (2024). Hoslundia opposita vahl; a potential source of bioactive compounds with antioxidant and antibiofilm activity for wound healing. *BMC Complementary Medicine and Therapies*, 24(1): 1–16. DOI: 10.1186/s12906-024-04540-z

Naqvi, S. F., Khan, I. H., & Javaid, A. (2022). Detection of compounds and efficacy of n-butanol stem extract of Chenopodium Murale L. Against Fusarium oxysporum F.Sp. Lycopersici. *Bangladesh Journal of Botany*, 51(4): 663–668. DOI: 10.3329/bjb.v51i4.63483

Nasrollahi, I., Talebi, E., & Bashardoost, Z. (2022). In-vitro study of chemical composition , antimicrobial and antioxidant properties of Adiantum capillus-veneris L . essential oil. *In Press*, *July*. DOI: 10.20944/preprints202207.0214.v1

Nurchairina, & Aziza, N. (2020). Pengaruh konsumsi Premna oblongifolia meer terhadap tekanan darah pada lansia dengan hipertensi di wilayah kerja puskesmas tanjung bintang lampung selatan tahun 2018. *Jurnal Ilmiah Keperawatan Sai Betik*, 16(1): 39. DOI: 10.26630/jkep.v16i1.1889

Nurdin, S. U., Le Leu, R. K., Aburto-Medina, A., Young, G. P., Stangoulis, J. C. R., Ball, A. S., & Abbott, C. A. (2018). Effects of dietary fibre from

the traditional indonesian food, green cincau (Premna oblongifolia Merr.) on preneoplastic lesions and short chain fatty acid production in an Azoxymethane rat model of colon cancer. *International Journal of Molecular Sciences*, 19(9): 2593. DOI: 10.3390/ijms19092593

Picón, D. F., & Skouta, R. (2023). Unveiling the therapeutic potential of squalene synthase: deciphering its biochemical mechanism, disease implications, and intriguing ties to ferroptosis. *Cancers*, 15(14): 3731. DOI: 10.3390/cancers15143731

Pissarra, M. F., Torello, C. O., Saad, S. T. O., & Lazarini, M. (2022). Evaluation of different protocols for culturing mesenchymal stem cells derived from murine bone marrow. *Hematology, Transfusion and Cell Therapy*, 44(4): 560–566. DOI: 10.1016/j.htct.2021.02.005

Ramaro, K. D. R., Razali, Z., Somasundram, C., Kunasekaran, W. thiran, & Jin, T. L. (2024). Effects of drying methods on the antioxidant properties of Piper betle leaves. *Molecules*, 29(8): 1–14. DOI: 10.3390/molecules29081762

Ren, X. M., Chang, R. C., Huang, Y., Amorim Amato, A., Carivenc, C., Grimaldi, M., Kuo, Y., Balaguer, P., Bourguet, W., & Blumberg, B. (2023). 2,4-Di-tert-butylphenol induces adipogenesis in human mesenchymal stem cells by activating retinoid x receptors. *Endocrinology (United States)*, 164(4): 1–11. DOI: 10.1210/endocr/bqad021

Rennerfeldt, D. A., Raminhos, J. S., Leff, S. M., Manning, P., & Van Vliet, K. J. (2019). Emergent heterogeneity in putative mesenchymal stem cell colonies: Single-cell time lapsed analysis. In *PLoS ONE*, 14(4). DOI: 10.1371/journal.pone.0213452

Saha, S., Paul, S., Jana, R., Bhowmik, A., Jana, M., Panigrahi, S., Sengupta, D., Das, S., Mondal, T., Chatterjee, A., & Khanra, R. (2024). Assessment of antioxidant and antimicrobial activities, along with the quantification of diverse phytoconstituents using GC-MS and HPTLC of the methanolic extract of Raphanussativus leaves. *African Journal of Biomedical Research*, 6(10): 4134–4147. DOI: 10.53555/AJBR.v27i3S.3126

Sanjeev, G., Sidharthan, D. S., Pranavkrishna, S., Pranavadithya, S., Abhinandan, R., Akshaya, R. L., Balagangadharan, K., Siddabathuni, N., Srinivasan, S., & Selvamurugan, N. (2020). An osteoinductive effect of phytol on mouse mesenchymal stem cells (C3H10T1/2) towards osteoblasts. *Bioorganic and Medicinal Chemistry Letters*, 30(11): 127-137. DOI: 10.1016/j.bmcl.2020.127137

Saputri, M. V., Carabelly, A. N., & Firdaus, I. W. A. K. (2019). Toxicity test of the mixed mouthwash of Mauli banana stem and basil leaf against fibroblast cell study In Vitro. *Dentino: Jurnal Kedokteran Gigi*, 4(2), 151–155.

Shukla, M. K., Singh, S. K., Pandey, S., Gupta, P. K., Choudhary, A., Jindal, D. K., Dua, K., & Kumar, D. (2022). Potential immunomodulatory activities of plant products. *South African Journal of Botany*, 149: 937–943. DOI: 10.1016/j.sajb.2022.04.055

Sujatha, P., Evanjaline, M. R., Muthukumarasamy, S., & Mohan, V. R. (2017). Determination of bioactive components of Barleria courtallica NEES (acanthaceae) by gas chromatography–mass spectrometry analysis. *Asian Journal of Pharmaceutical and Clinical Research*, 10(6): 273. DOI: 10.22159/ajpcr.2017.v10i6.18035

Tawfeeq, A. A., Tawfeeq, T. A., Naqqash, Z. A. . Al, & Kamal, Z. A. (2024). Phytochemical investigation and GC-MS analysis of Tribulus terrestris L. cultivated in Iraq. *Obat: Jurnal Riset Ilmu Farmasi Dan Kesehatan*, 2(5): 22–29. DOI: 10.61132/obat.v2i5.594

Turvey, T., Loggenberg, S. R., & Lall, N. (2022). Introduction. In *Medicinal Plants for Cosmetics, Health and Diseases* (pp. 1–9). CRC Press. DOI: 10.1201/9781003108375-1

Uka, E., Eghianrunwa, Q. A., & Akwo, V. D. (2022). GC-MS analysis of bioactive compounds in ethanol leaves extract of Sphenocentrum jollyanum and their biological activities. *International Journal of Scientific Research in Engineering and Management (IJSREM)*, 6(1): 1–29. DOI: 10.55041/IJSREM11414

Wang, J., Hu, X., Ai, W., Zhang, F., Yang, K., Wang, L., Zhu, X., Gao, P., Shu, G., Jiang, Q., & Wang, S. (2017). Phytol increases adipocyte number and glucose tolerance through activation of PI3K/Akt signaling pathway in mice fed high-fat and high-fructose diet. *Biochemical and Biophysical Research Communications*, 489(4): 432–438. DOI: 10.1016/j.bbrc.2017.05.160

Widiandani, T., Tandian, T., Zufar, B. D., Suryadi, A., Purwanto, B. T., Hardjono, S., & Siswandono. (2023). In vitro study of pinostrobin propionate and pinostrobin butyrate: Cytotoxic activity against breast cancer cell T47D and its selectivity index. *Journal of Public Health in Africa*, 14: 97–102. DOI: 10.4081/jphia.2023.2516

Wulandari, A. P., Nafisa, Z. K., Herlina, T., Maharani, R., Darmawan, G., Parikesit, A. A., & Zainul, R. (2024). Metabolite profiling of potential bioactive fractions from ethanol extract of Boehmeria nivea flowers by GC–MS/MS analysis. *Phytomedicine Plus*, 4(2): 100557. DOI: 10.1016/j.phyplu.2024.100557

Yan, W., Diao, S., & Fan, Z. (2021). The role and mechanism of mitochondrial functions and energy metabolism in the function regulation of the mesenchymal stem cells. *Stem Cell Research & Therapy*, 12(1): 140. DOI: 10.1186/s13287-021-02194-z

Zainol Abidin, I. Z., Johari, A. N., Yazid, M. D., Zainal Ariffin, Z., Eziwar Dyari, H. R., & Zainal Ariffin, S. H. (2023). Osteogenic potential and bioactive profiles of Piper sarmentosum ethanolic extract-treated stem cells. *Pharmaceuticals*, 16(5). DOI: 10.3390/ph16050708

Zhuo, Y., Li, M., Jiang, Q., Ke, H., Liang, Q., Zeng, L.-F., & Fang, J. (2022). Evolving roles of natural terpenoids from traditional chinese medicine in the treatment of osteoporosis. *Frontiers in Endocrinology*, 13(5): 1–18. DOI: 10.3389/fendo.2022.901545

Physicochemical Properties of Pili (*Canarium ovatum*) Nut Oils Extracted Using Different Extraction Solvents

AEMELDA NASTIYANA ADIN[1], YEE LIN CHANG[1], 'AISYAH AMINI AMIN[1], JABI TANANAK[2], NUR HANISAH AZMI[3], JAU SHYA LEE[4], HASMADI MAMAT[4], NOOR ATIQAH AIZAN ABDUL KADIR[3], MUHAMAD HANIF RAWI[4], YUS ANIZA YUSOF[5,6], BANGUN PRAJANTO NUSANTORO*[7] & YANTY NOORZIANNA ABDUL MANAF*[8,9]

[1]Faculty of Food Science and Nutrition, Universiti Malaysia Sabah, Jalan UMS, 88400 Kota Kinabalu, Sabah, Malaysia; [2]Lagud Sebrang Agriculture Research Centre, Sabah Agriculture Department, Peti Surat No. 197, 89908 Tenom, Sabah, Malaysia; [3]Nutrition in Community Engagement (NICE) Living Laboratory, Universiti Malaysia Sabah, Jalan UMS, 88400 Kota Kinabalu, Sabah, Malaysia; [4]Food Security Research Laboratory, Faculty of Food Science and Nutrition, Universiti Malaysia Sabah, Jalan UMS, 88400 Kota Kinabalu, Sabah, Malaysia; [5]Halal Products Research Institute, Universiti Putra Malaysia, 43400 UPM Serdang, Serdang, Selangor, Malaysia; [6]Faculty of Engineering, Universiti Putra Malaysia, 43400 UPM Serdang, Serdang, Selangor, Malaysia; [7]Department of Food and Agricultural Product Technology, Gadjah Mada University, Jl. Flora 1, Yogyakarta 55281, Indonesia; [8]Halal Research Group, Faculty of Food Science and Nutrition, Universiti Malaysia Sabah, Jalan UMS, 88400 Kota Kinabalu, Sabah, Malaysia; [9]Halal Service and Research Centre, Faculty of Food Science and Nutrition, Universiti Malaysia Sabah, Jalan UMS, 88400 Kota Kinabalu, Sabah, Malaysia.
*Corresponding author: yanty.manaf@ums.edu.my; bpnusantoro@ugm.ac.id

ABSTRACT

There is still lack of information on pili (*Canarium ovatum*) nut oil from Sabah, Malaysia. Therefore, the objective of this research was to investigate the physicochemical properties of pili nut oils obtained from Soxhlet extraction by using different extraction solvents such as petroleum ether, hexane, acetone and ethanol. The extracted pili nut oils were assessed for colour, refractive index, slip melting, and cloud point; iodine, free fatty acid, peroxide, p-anisidine, totox values; carotene content, thermal behaviour, fatty acid composition, and triacylglycerol profile. The highest oil yields were obtained by extraction using petroleum ether and hexane. The physical and chemical properties of oil are found to be significantly differed with different extraction solvents. The major triacylglycerols of pili nut oils were palmitoyl–di–oleoyl glycerol (PPO) and di-palmitoyl–oleoyl glycerol (PPO) with oleic and palmitic were the most predominant fatty acids. All extracted pili nut oils were below than the permitted range of free fatty acid content, peroxide and totox values (maximum 10 meq O_2/kg) for cooking oils. The pili nut oil extracted with petroleum ether contained the highest (~ 110 ppm) β-carotene. Among the extraction solvents, petroleum ether was the best in terms of oil yield, quality, and β-carotene content.

Keywords: Pili nut oil, properties, solvent extraction

INTRODUCTION

Pili (*Canarium ovatum*) is a member of the Burseraceae family. Many of the literatures focused on pili nut oil from the Philippines. Kakuda *et al.* (2000) extracted pili nut oil using Soxhlet method which petroleum ether as a solvent. They found that the pili nut contained higher amount of saturated fatty acids than unsaturated fatty acids. The polyunsaturated fatty acids were less than 11%. Other researches using Soxhlet extraction with petroleum ether as solvent also found that pili nut was light yellowish in colour with oleic stearic, palmitic, linoleic, and linolenic acids as the major fatty acids (Pham & Dumandan, 2015; Millena *et al.,* 2018; Millena *et al.,* 2023). Other study conducted by Zarinah *et al.,* (2014) extracted pili nut oil using cold press method and the physicochemical properties were determined for roasted and unroasted pili nut. The percentage of oil yield and iodine value were not significantly different between roasted and unroasted pili nuts. However, the percentage of free fatty acid and peroxide value showed a significant different. Both samples had a high proportion of

oleic acid and fully melted at 25 °C and were claimed to be free of trisaturated triacylglycerols.

Extraction of oil using Soxhlet technique could produces a higher oil yield than most other extraction techniques, albeit taking longer to complete (López-Bascón & Luque de Castro, 2020). This method also can use different extraction solvents such as hexane, acetone, etc. The sample is dried before the extraction process because it can increase the oil yield, decrease the moisture content, and deactivate enzymes that encourage the lipid oxidation. Additionally, it promotes the breakdown of cell tissue, which facilitates the solvent's easy penetration of flake (Keneni *et al.,* 2020). The aim of this study was to extract the pili nut oil using Soxhlet technique with different extraction solvents to assess the pili nut oil's physical, chemical, and quality properties.

Researching the physicochemical properties of pili nut oil is crucial for assessing its quality, stability, and potential for diverse applications. Detailed characterization of parameters such as refractive index, melting behaviour, oxidative stability, and fatty acid profile provides essential insights into its functional and nutritional value. Such knowledge not only guides the optimization of processing, storage, and utilization practices but also strengthens the positioning of pili nut oil as a unique and value-added specialty oil for the food, nutraceutical, and cosmetic industries.

MATERIALS & METHODS

Materials

The dried pili nut was gifted by the Lagud Sebrang Agriculture Research Centre, Sabah Agriculture Department in Tenom, Sabah, Malaysia. Analytical and general grade chemicals were used in this research. All physicochemical analysis was carried in triplicate.

Oil Extraction

Oil was extracted using Soxhlet method (AOAC, 2023). A 150 g of dried and crushed pili nuts were put in cellulose thimble, and the oil was extracted for 8 hr using petroleum ether (60 °C) in a Soxhlet extractor. A rotary evaporator (Tokyo Rakakikal Co., Ltd., Tokyo, Japan) was used to recover the oil. After an hour at 60 °C in the oven, the extracted oil was put into an air tight bottle and kept at -20 °C. The similar method was repeated using different solvents (hexane, acetone and ethanol). Prior to analysis, the oil was left at room temperature (25 °C) for 1 hour before heated at 60 °C until it was totally molten.

Determination of Oil Yield

The oil yield was determined according to AOAC (2023) using specific equation, Eq. (1):

$$\text{Percentage of oil yield (w/w)} = W_{Oil}/W_{Sample} \times 100\% \qquad \text{Eq.(1)}$$

W_{Oil} is the weight of extracted oil and W_{Sample} is the weight of the pili nut powder.

Determination of Colour

The colour of the oil samples was measured using a colorimeter using the Hunter Lab system, where a* value ranges from negative (green) to positive (red), and L* value is the lightness of colour from 0 (black) to 100 (white) in the tristimulus colour coordinate system. It can be either positive (yellow) or negative (blue) for b* value (PORIM, 1995).

Determination of Refractive Index (RI), Slip Melting Point (SMP), Cloud Point (CP), Totox Value, Carotene Content, Iodine Value (IV), Free Fatty Acid (FFA), Peroxide Value (PV), and p-Anisidine Value (p-AV)

The refractive index (RI), slip melting point (SMP), cloud point (CP), Totox value, carotene content, iodine value (IV), free fatty acid (FFA), peroxide value (PV), and p-anisidine value (p-AV) of the extracted oil samples were determined according to the official methods of the American Oil Chemists' Society (AOCS, 2000).

Determination of Fatty Acid (FA) Composition

Fatty acid composition was determined by esterifying the oil into methyl esters (FAME) by dissolving 50 mg of oil in 0.8 ml of hexane and 0.2 ml of a 1 M solution of sodium methoxide (AOCS, 2000). The FAME subsequently analysed using a gas chromatograph (GC) with a

flame ionization (FID) was used as a detector. The polar capillary column (RTX-5; 0.32 mm × 30 m length x 0.25 µm thickness) was used. The temperature of the oven was set at 50 °C (for 1 min) and increased to 200 °C at a flow rate of 8 °C/min. The temperatures of the injector and detector were kept at 200 °C throughout the analysis. With a split ratio of 58:1, the flow rate of the helium as a carrier gas was maintained at 1.0/min. The peaks were identified using a FAME standard (Supelco, Bellefonte, PA). The partial area divided by the entire peak area was used to determine the percentage of FA (Yanty *et al.,* 2018).

Determination of Triacylglycerol (TAG) Composition

A high-performance liquid chromatography with a refractive index as a detector was used to determine TAG composition. A column (RP-18; 5 µm × 12.5 cm length × 4 mm i.d.; Merck, Darmstadt, Germany) and the mobile phase of acetone/acetonitrile (63.5:36.5 v/v) was used. The flow rate was maintained at 1.5 ml/min with the oven temperature was maintained at 30 °C. A 1 ml of 5% (w/w) oil in chloroform were used as an injector volume. The individual peaks were identified by comparing their retention time TAG standards, and the relative percentage of individual TAGs was reported as the relative proportion of the TAGs (Yanty *et al.,* 2013).

Determination of Thermal Behaviour

The differential scanning calorimeter was used to measure thermal behaviour of extracted oil samples using a method of Yanty *et al.* (2014). Nitrogen gas (purity: 99.99%) was used as the purge gas at a pressure of 20 psi and a flow rate of 100 ml/min. An empty aluminium sample pan was used as a reference. A sample pan containing 3 to 5 mg of oil was sealed and put inside the sample chamber of the device. An oil sample was heated from -60 – 60 °C at a rate of 5 °C/min, kept at 60 °C isothermally for 2 min, and then cooled from 60 – -60 °C at a rate of 5 °C/min. The onset, peak, and offset (end) temperatures were recorded for heating and cooling thermograms. The temperature at which the melting and crystallisation process begins, the temperature at which the majority of the TAG has melted and crystallised, and the temperature at which the oil has completely melted and crystallised were all indicated by these values from the heating and cooling thermograms.

Statistical Analysis

A Statistical Package for Social Sciences (SPSS) software (Version 28) using one-way analysis of variance (ANOVA) with a confidence level of 95% was used to determine the significant difference among mean scores of the data.

RESULTS & DISCUSSION

Oil Yield

The oil yield of pili nut oils extracted using different extraction solvents are shown in Table 1. Pili nut oil extracted using petroleum ether (69.60%) and hexane (68.85%) as the extraction solvents showed the highest oil yield. However, there was no significant difference ($p<0.05$) in oil yield between the two extraction solvents. The lowest oil yield obtained through extraction of oil using acetone (60.27%) as extraction solvent. The differences in oil yield obtained using different extraction solvents may be attributed to their polarity. Petroleum ether and hexane are non-polar solvents, whereas acetone and ethanol are polar solvents. Generally, non-polar solvents produce higher oil yields because lipids are largely non-polar, and their solubility decreases in highly polar solvents, where excessive polarity may lead to solvolysis and reduced lipid recovery (Isaac *et al*., 2023). However, in some cases, polar solvents can promote oil release by interacting with ester groups of triglycerides through hydrogen bonding and by facilitating cell membrane disruption, which enhances the release of intracellular oil (Wang *et al*., 2023). In addition, polar solvents may lower surface tension at the phase boundary, thereby improving phase separation. Overall, the present results are consistent with the principle of "like dissolves like," whereby non-polar solvents exhibit stronger hydrophobic interactions with lipids, leading to higher extraction yields (Wang *et al*., 2023).

Table 1. Oil yield of pili nut oils using different extraction solvents.

Extraction Solvent	Oil Yield (%)
Petroleum Ether	69.60±0.94[a]
Hexane	68.85±1.25[a]
Acetone	60.27±0.70[c]
Ethanol	64.86±0.10[b]

Each values represent average of triplicates ± standard deviation. Different superscripted letters in the column indicate significant difference (p<0.05) between the samples.

Physical Properties of Oils

The colour, refractive index, slip melting point, and cloud point of extracted pili nut oil using different extraction solvents are shown in Table 2. Based on the results, the colour of the oil showed a significant difference between the solvents used. The pili nut oil extracted with ethanol showed a higher value for all colour parameters [lightness (L*), redness (a*) and yellowness (b*)]. The oil had a value of 25.92 (L*), -1.91 (a*) and 28.68 (b*). On the other hand, hexane as an extraction solvent showed the lowest value for colour parameter among all solvents. The oil had L*, a* and b* of 9.51, -1.14 and 9.38, respectively. The redness (a*) showed a negative value which indicated greenness of colour. The differences of the intensity of the colour of extracted oils were due to the concentration of pigments such as carotenoids, etc. Visually, all extracted pili nut oils in this study were yellow in colour.

Refractive index (RI) is to analyse light rays traversing through materials medium (Sarkar *et al.*, 2015). RI is usually used to identify the possible chances of rancidity development in oil. A higher value of RI can increase the chance of the oxidation of oil that can cause rancidity. It is the basic value for the degree of unsaturation, chain length of fatty acids and degree of conjugation (Awuchi *et al.*, 2018). According to Table 2, there were significant different of RI values of extracted oils. The highest (1.47) RI value is oil extracted with hexane and ethanol while lowest (1.45) is extracted with acetone.

Due to the large number of different triglycerides, oils and fats do not have exact melting points (Shin & Lee, 2022). Particularly in baked goods, the slip melting point of fats and oils affects the incorporation of air, mouthfeel, rheology, shelf life and other quality criteria. Based on Table 2, the slip melting point (SMP) of extracted oil using acetone as an extraction solvent showed a significant higher compared to those of other extracted oils. SMP could be affected with the differences in carbon number or length of fatty acid (Tian *et al.*, 2024). Therefore, saturated fatty acid with high carbon number will result in a higher melting point which need more heat energy to break the bond between fatty acids (Shin & Lee, 2022). Since saturated fatty acid tend to solidify at higher temperatures, a high SMP indicates a larger percentage of saturated fatty acid in the oil (Sarkar *et al.*, 2015). The cloud point is the temperature when the oils start to become cloudy as the temperature reduce. However, there were not much different between all extracted pili nut oils.

Table 2. Physical properties of pili nut oil using different extraction solvents.

Parameter		Petroleum ether	Hexane	Acetone	Ethanol
	L*	13.27 ± 0.16[c]	9.51 ± 0.03[d]	14.50 ± 0.02[b]	25.92 ± 0.12[a]
Colour	a*	-1.63 ± 0.12[c]	-1.14 ± 0.04[b]	-1.34 ± 0.19[a]	-1.91 ± 0.19[c]
	b*	16.52 ± 0.14[c]	9.38 ± 0.08[d]	18.14 ± 0.12[b]	28.68 ± 0.77[a]
Refractive index		1.46 ± 0.00[b]	1.47 ± 0.00[a]	1.45 ± 0.00[c]	1.47 ± 0.00[a]
Slip melting point (°C)		18.50 ± 0.50[b]	19.17 ± 0.29[b]	24.33 ± 0.58[a]	18.67 ± 1.15[b]
Cloud point (°C)		23.17 ± 0.29[c]	24.27 ± 0.25[bc]	24.27 ± 0.25[ab]	24.83 ± 1.04[a]

Each value in the table represents the mean ± standard deviation of three replicates. Different superscripted letters in the row indicate significant difference (p<0.05) between the samples.

Thermal Behaviour Profiles

The heating and cooling thermograms of extracted pili nut oil using different extraction solvents are shown in Figure 1 and Figure 2, respectively. Based on Figure 1, the extracted oil had similar trend in term of heating profiles especially for oil extracted using petroleum ether, hexane and acetone as a solvent. There were two major peaks which were 0.80 °C and 5.33 °C (petroleum ether), 2.41 °C and 6.25 °C (hexane), 0.14 °C and 4.40 °C (acetone) and 1.16 °C and 5.74 °C (ethanol) with a shoulder peak at 11.77 °C, 11.35 °C, 10.50 °C and 10.09 °C, respectively. The end-set of melting point for each solvent was 26.70 °C (petroleum ether), 23.50 °C (hexane), 26.27 °C (acetone) and 24.77 °C (ethanol). The trend and temperature in the heating profile of this pili nut oils extracted with different solvent could be affected by the degree of unsaturation of fatty acids (Yanty *et al.,* 2018).

The cooling thermograms of pili nut oils extracted using different extraction solvents are shown in Figure 2. All of oils extracted using different extraction solvents showed similar cooling profiles. The oil samples extracted with hexane had a major peak (at around 2.66 – -0.02 °C) with a shoulder peak at around -0.58 – -11.80 °C. In addition, all oil samples had two minor peaks at around -26.49 – -33.49 °C and -45.18 – -55.45 °C. The oil extracted using hexane had the highest (4.49 °C) and acetone had the lowest (3.81 °C) onset temperatures. The oil extracted using hexane had the highest (-55.45 °C) and acetone had the lowest (-45.16 °C) endset temperatures. These findings could be caused by the concentration of the triacylglycerol molecules which crystallise at higher temperature regions and thus show a slightly different at the onset point of crystallisation. In addition, the major peak in the cooling curve associated with solidification of major triacylglycerol (Van Wetten *et al.,* 2014).
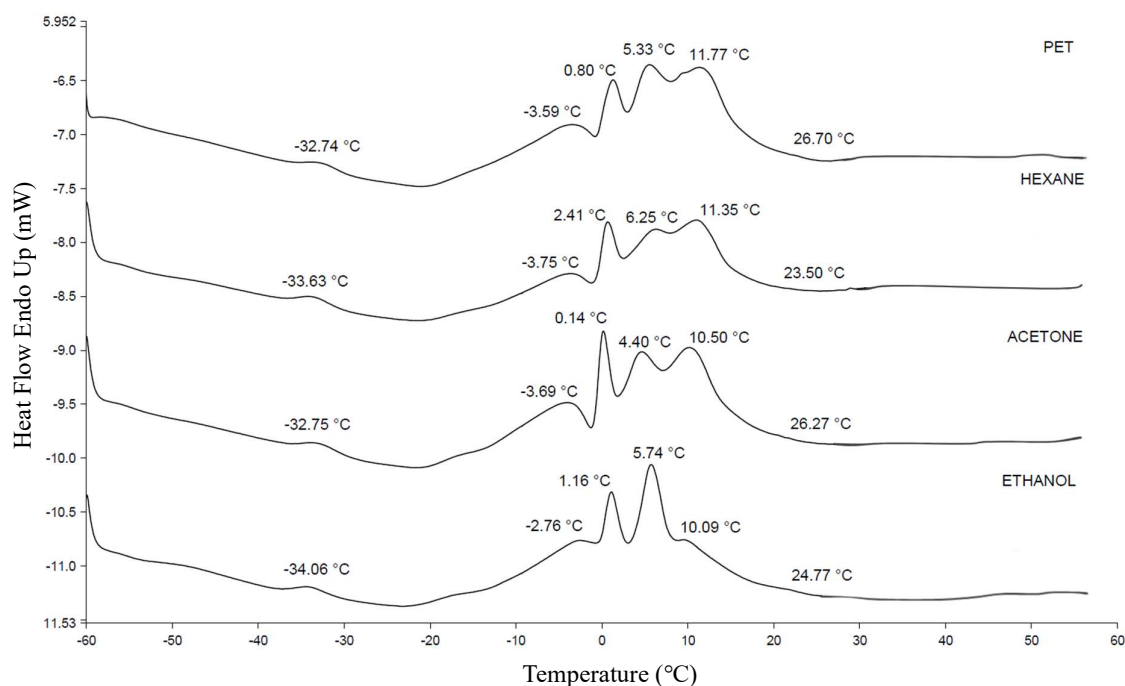
Figure 1. Heating thermogram of pili nut oils extracted with different extraction solvents PET: Petroleum ether.
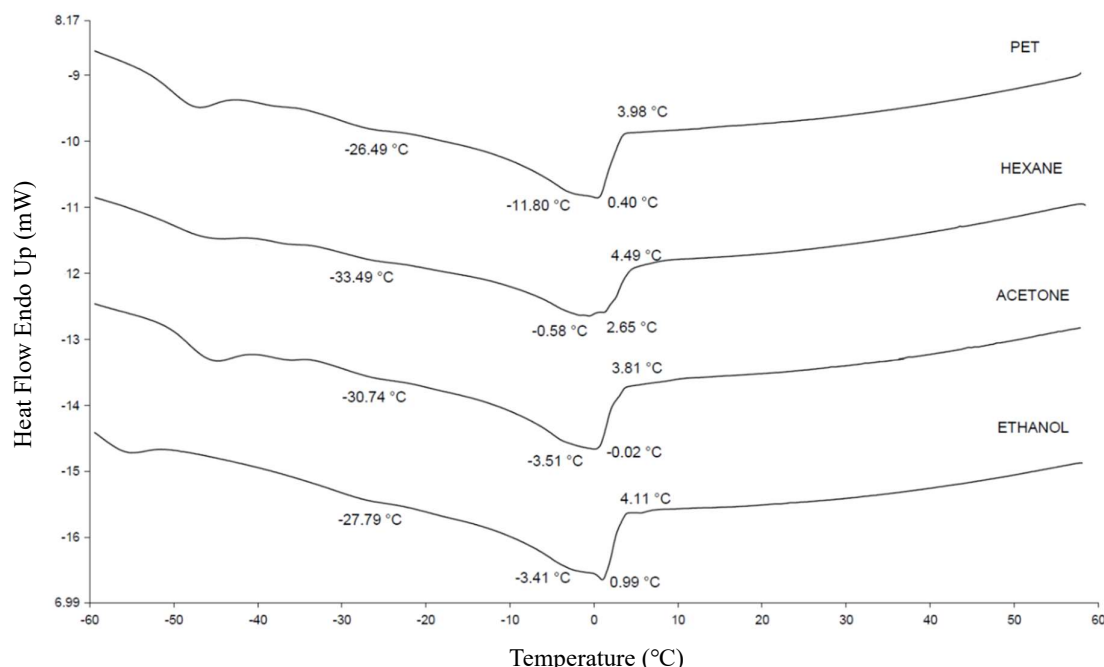
Figure 2. Cooling thermogram of pili nut oils extracted with different extraction solvents PET: Petroleum ether

Chemical Properties of Oils

The chemical properties of pili nut oil extracted using different solvents are shown in Table 3. Iodine value (IV) is the measurement of the total unsaturated fatty acid present in edible oils. This analysis is important to predict whether the oils have high unsaturated or saturated lipids which is important to human health (Pulassery *et al.,* 2022).

The IV of extracted pili nut oils showed a significant different between all extraction solvents which petroleum ether had the highest IV. It might be due to higher unsaturated fatty acid content obtained through extraction using petroleum ether as compared to other oil samples. It is reported that oils with high iodine value was more prone to oxidation (Norazlina *et al.,* 2021).

Free fatty acid (FFA) is widely recognized as a highly important component and is associated with both the commercial value and quality of edible oils. In general, oils and fats are hydrolysed in order to produce free fatty acids (Mahesar *et al.,* 2014). The pili nut oil extracted using petroleum ether had the highest FFA (1.46%) than those of other oil samples.

However, there was no significant different between pili nut oil extracted using acetone, hexane and ethanol. In the food industry, frying oil with FFA more than 2% are either thrown away or replace with fresh oil to reduce the content of FFA (Dunford, 2016). Therefore, FFA of all extracted oils were in the range.

Table 3 shows the peroxide value (PV) of pili nut oil using different extraction solvents. PV is an indicator to oxidation of oil. The result showed that the PV of pili nut oil extracted using ethanol (0.91 meq O_2/kg) had the lowest value as compared to other extraction solvents. Peroxide value less than 10 meq O_2/kg indicate that the oil is in a good quality while the value between 30 and 40 meq O_2/kg indicates that the oil is rancid. In this study, all oil samples were in a good quality (below 10 meq O_2/kg).

p-Anisidine value (p-AV) measures the secondary oxidation of the oils by determining the amount of aldehyde in animal fats and vegetable oils. PV is highly related to p-AV to assess the rancidity of the oil (Abdulkarim *et al.,* 2007). Extracted pili nut oil using ethanol as extracted solvent (4.00 meq O_2/kg) showed the highest p-AV while petroleum ether (1.24 meq O_2/kg) showed the lowest p-AV among all

extraction solvents (Table 3). The p-AV should be less than 10 meq O_2/kg for indication of good quality oil (Tesfaye *et al.,* 2017). All samples of the pili nut oil in this study showed lower values than 10 meq O_2/kg which indicate it is a good quality of oil. Totox value is directly related to the PV and p-AV, indicating the lipid's primary and secondary oxidation. Totox value of pili nut oils showed no significant different between extraction solvents used.

Carotene content (expressed as β-carotene) is an important source of pro-vitamin A and it is a micronutrient antioxidant regulating vital metabolism in our body (Tesfaye *et al.,* 2017). According to Table 3, the oil sample extracted using petroleum ether (109.51 ppm) showed the highest value of carotene content while oil samples extracted using acetone showed the lowest value (61.25 ppm) of carotene content. Manaf *et al.* (2024) reported that the carotene content of pili nut oil extracted using petroleum ether had a lower value (66.22 ppm) as compared to this study. According to Ignaczak *et al.* (2023), polyunsaturated fatty acid is positively related to the concentration of carotene. However, the present research showed a higher carotene value than the past research reported by Manaf *et al.* (2024), even though the same method and extraction solvent used. This may be due to the increased susceptibility of the oil to lipid peroxidation, as the conjugated double bonds of polyunsaturated fatty acids readily undergo reactions with free radicals, particularly peroxyl radicals, resulting in a higher oxidation rate compared to oils extracted with other solvents (Mordi *et al.,* 2020).

Table 3. Chemical properties of pili nut oil using different extraction solvents.

Parameter	Petroleum Ether	Hexane	Acetone	Ethanol
Iodine value (g I_2/100 g)	96.44 ± 0.00^a	59.48 ± 0.96^c	67.91 ± 0.62^b	61.74 ± 1.33^c
Free fatty acid (%)	1.46 ± 0.29^a	0.69 ± 0.03^b	0.52 ± 0.26^b	0.66 ± 0.04^b
Peroxide value (meq O_2/kg)	2.53 ± 0.23^a	2.24 ± 0.43^a	2.07 ± 0.23^a	0.91 ± 0.15^b
p-Anisidine value (meq O_2/kg)	1.24 ± 0.22^d	2.88 ± 0.02^c	2.38 ± 0.02^b	4.00 ± 0.29^a
Totox value	6.31 ± 0.53^{ab}	7.37 ± 0.87^a	6.51 ± 0.44^{ab}	5.83 ± 0.15^b
Carotene (ppm as β-carotene)	109.51 ± 0.00^a	101.18 ± 0.00^b	61.25 ± 0.00^d	96.64 ± 0.00^c

Each value in the table represents the mean ± standard deviation of three replicates. Different superscripted letters in the row indicate significant difference (p<0.05) between the samples.

Fatty Acid Composition

The fatty acid composition of pili nut oil extracted using different extraction solvents are shown in Table 4. According to Table 4, all extracted oils had eleven fatty acids from C12 to C20. The fatty acids of pili nut oils were lauric (ranging from 0.03 – 0.05 %), myristic (ranging from 0.03 – 0.04%), followed by palmitic (ranging from 30.10 – 30.87%), palmitoleic (ranging from 0.39 – 0.43%), margaric (ranging from 0.12 – 0.13%), stearic (ranging from 7.92 – 9.13%), oleic (ranging from 51.18 – 51.44%), linoleic (ranging from 7.85 – 8.63%), linolenic (ranging from 0.54 – 0.69%), arachidic (ranging from 0.22 – 0.23%) and eicosenoic (ranging from 0.11 – 0.15%) acids. The oil with the highest (40.25%) saturated content was obtained through acetone extraction.

The result was agreeable with the highest SMP (Table 2) value of this oil. The ratio of saturated and unsaturated fatty acids among all oil samples were approximately 1:1. Therefore, these oils were a semi-solid state at room temperature (25 °C). This result was comparable to fatty acid composition of pili nut oil extracted with petroleum ether and palm oil which had a

ratio of 1:1 on its saturated and unsaturated fatty acids (Marikkar *et al.,* 2018; Manaf *et al.,* 2024). Therefore, the pili nut oil has the potential to become a palm oil substitute for commercial uses. In addition, pili nut oil also has the potential to undergo fractionation process due to ratio of saturated and unsaturated (1:1) fatty acids. The olein part can be used for liquid or cooking purposes and the stearin part can be used for shortening production.

Triacylglycerol Composition

The triacylglycerol composition of pili nut oil extracted using different extraction solvents is shown in Table 5. According to Table 5, the dominant triacylglycerol compositions of pili nut oil extracted using different extraction solvents were POO (ranging from 29.42 – 28.54%), PPO (ranging from 18.65 – 17.62%) and OOO (ranging from (11.99 – 9.00%). According to Adin *et al.* (2024), pili nut oil extracted from mechanical press extraction also contained POO (28.01%) and PPO (20.58%) as the major triacylglycerol molecules. Among all extraction solvent used, pili nut oil extracted using acetone contained the highest amount of PPO (18.65%) and the lowest amount of PPO (12.57%) was found in the oil extracted using hexane. The triacylglycerol composition is mainly related to fatty acid composition as the triacylglycerol is formed from several fatty acids. Therefore, the predominant TAG in pili nut oil was formed from the major fatty acids which were oleic and palmitic acid (Table 4). As mentioned earlier, the oil extracted using acetone contained more saturated fatty acid which was palmitic acids (Table 4) as the most dominant and higher SMP (Table 2) compared to those of other extraction solvents.

Table 4. The fatty acid composition of pili nut oil extracted using different solvents.

Fatty acid	Petroleum Ether	Hexane	Acetone	Ethanol
Lauric acid (C12:0)	0.04±0.00[c]	0.05±0.00[a]	0.03±0.00[d]	0.04±0.00[b]
Myristic acid (C14:0)	0.03±0.00[c]	0.04±0.00[b]	0.04±0.00[a]	0.04±0.00[a]
Palmitic acid (C16:0)	30.10±0.00[d]	30.37±0.00[b]	30.87±0.01[a]	30.19±0.05[c]
Palmitoleic acid (C16:1)	0.39±0.00[c]	0.39±0.00[c]	0.40±0.00[b]	0.43±0.00[a]
Margaric acid (C17:0)	0.13±0.00[a]	0.12±0.00[b]	0.12±0.00[b]	0.13±0.00[ab]
Stearic acid (C18:0	9.13±0.00[a]	9.05±0.00[b]	8.95±0.01[c]	7.92±0.01[d]
Oleic acid (C18:1)	51.40±0.00[b]	51.18±0.00[c]	50.20±0.02[d]	51.44±0.00[a]
Linoleic acid (C18:2)	7.85±0.00[d]	7.96±0.00[c]	8.49±0.01[b]	8.63±0.00[a]
Linolenic acid(C18:3)	0.55±0.00[c]	0.56±0.00[b]	0.54±0.00[d]	0.69±0.00[a]
Arachidic acid (C20:0)	0.23±0.00[a]	0.23±0.00[a]	0.22±0.00[b]	0.22±0.00[b]
Eicosenoic acid (C20:1)	0.14±0.00[b]	0.15±0.00[a]	0.13±0.00[c]	0.11±0.00[d]
Saturated fatty acid	39.67±0.00[c]	39.86±0.00[b]	40.25±0.02[a]	38.54±0.05[d]
Unsaturated fatty acid	60.34±0.00[b]	60.24±0.00[c]	59.76±0.02[d]	61.30±0.00[a]

Each value in the table represents the mean ± standard deviation of three replicates. Different superscripted letters in the row indicate significant difference (p<0.05) between the samples.

Table 5. Triacylglycerol (TAG) composition of pili nut oil extracted using different extraction solvents.

TAG	Percentage (%)			
	Petroleum Ether	Hexane	Acetone	Ethanol
LnLnL	1.20±0.56[a]	2.87±2.00[a]	1.90±0.03[a]	1.40±0.66[a]
LnLL	0.93±0.09[a]	2.24±1.67[a]	0.57±0.16[a]	0.61±0.19[a]
LLL	0.74±0.00 [a]	4.40±3.93[a]	0.65±0.04[a]	1.32±0.30[a]
PLnL	0.46±0.00[a]	2.80±3.10[a]	0.43±0.03[a]	0.83±0.33[a]
OLL	1.29±0.01[a]	3.82±2.34[a]	0.79±0.21[a]	1.39±0.28[a]
PLL	2.53±0.01[a]	4.52±2.28[a]	2.43±0.18[a]	2.82±0.30[a]
OOL	3.36±0.07[ab]	4.90±1.57[a]	2.73±0.06[b]	3.27±0.41[ab]
POL	7.59±0.12[a]	6.33±0.29[b]	6.44±0.07[b]	6.31±0.20[b]
PPL	4.48±0.02[ab]	6.07±1.24[a]	4.11±0.01[b]	4.32±0.13[b]
OOO	11.29±0.21[ab]	9.00±2.09[b]	11.65±0.11[ab]	11.99±0.45[a]
POO	28.54±0.32[a]	14.66±9.20[b]	29.42±0.30[a]	26.01±2.08[ab]
PPO	17.62±0.02[b]	12.57±4.19[c]	18.65±0.12[a]	17.52±1.31[b]
PPP	0.47±0.03[a]	0.91±0.70[a]	0.47±0.02[a]	0.29±0.13[a]
OOS	7.73±0.06[a]	8.31±1.29[a]	7.75±0.01[a]	8.17±0.46[a]
POS	8.75±0.08[a]	9.77±2.42[a]	8.90±0.01[a]	9.55±0.64[a]
PPS	0.38±0.01[a]	0.58±0.23[a]	0.40±0.06[a]	0.45±0.56[a]
SSO	1.61±0.01[b]	3.28±0.57[a]	1.60±0.08[b]	1.59±0.52[b]
Unknown	1.03±0.00[b]	4.94±2.84[a]	1.10±0.08[b]	1.84±1.19[ab]

O: oleic; P: palmitic; S: stearic; L: linoleic; Ln: linolenic. Each value in the table represents the mean ± standard deviation of three replicates. Different superscripted letters in the row indicate significant difference ($p<0.05$) between the samples.

CONCLUSION

Pili nut oil (*Canarium ovatum*) may become a new potential source of edible oil that is rich in oleic and palmitic acids. Petroleum ether and hexane were the most suitable extraction solvents due to high oil yield (~70%) obtained from this study. The extracted oils were semisolid form in room temperature (25 °C) but they had different SMP values. The oil extracted using petroleum ether had the lowest SMP value, which contained the lowest amount of saturated fatty acid (palmitic acid) and the highest source of β-carotene. Therefore, this study concluded that extraction of pili nut oil using a petroleum ether as an extraction solvent was the best in terms of the quality.

ACKNOWLEDGEMENTS

REFERENCES

Abdulkarim, S.M., Long, K., Lai, O.M., Muhammad, S.K.S. & Ghazali, H.M. (2007). Frying quality and stability of high-oleic *Moringa oleifera* seed oil in comparison with other vegetable oils. *Food Chemistry*, 105(4): 1382–1389. DOI: 10.1016/j.foodchem.2007.05.013.

Adin, A., Gawai, A.A., Josli, I.C., Nakolas, L., Amin, A.A., Linton, J., Azmi, N.H., Yin, F.H., Arshad, S., Nusantoro, B.P., Wasoh, H. & Manaf, Y.N.A. (2024). Physicochemical and quality characteristics of pili (*Canarium ovatum*) nut oil obtained from mechanical press extraction. *Transactions on Science and Technology*, 11(4-2): 1–6.

Association of Official Analytical Chemists (AOAC). (2023). *Official Methods of Analysis*. 22nd Edition. Rockville, United State of America.

The American Oil Chemists' Society (AOCS). (2000). *Official Methods and Recommended Practices of the American Oil Chemists' Society.* Champaign, United State of America.

Awuchi, C.G., Ikechukwu, A.O. & Gonzaga, A. (2018). Effects of repeated deep frying on refractive index and peroxide value of selected vegetable oils. *International Journal of Advanced Academic Research*, 4(4): 106–116.

Dunford, N.T. (2016). *Edible Oil Quality. Robert M. Kerr Food & Agricultural Products Center Food Technology Fact Sheet 405-744-6071.*

https://extension.okstate.edu/factsheets/edible-oil-quality.html. Downloaded on 1 May 2025.

Ignaczak, A., Salamon, A., Kowalska, J., Marzec, A. & Kowalska, H. (2023). Influence of pre-treatment and drying methods on the quality of dried carrot properties as snacks. *Molecules,* 28(17): 6407. DOI: 10.3390/molecules28176407.

Isaac, I.O., Enengedi, I.S. & Abdulazeez, I.A. (2023). Quality assessment of *Vitellaria paradoxa* seed oil obtained under different extraction conditions and solvents. *Sustainable Chemistry and Pharmacy,* 35: 101–176. DOI: 10.2139/ssrn.4446435.

Kakuda, Y., Jahaniaval, F., Marcone, M.F., Montevirgen, L., Montevirgen, Q. & Umali, J. (2000). Characterization of pili nut *(Canarium ovatum)* oil: Fatty acid and triacylglycerol composition and physicochemical properties. *Journal of The American Oil Chemists' Society,* 77(9): 991–997. DOI: 10.1007/s11746-000-0156-8.

Keneni, Y.G., Bahiru, L.A. & Marchetti, J.M. (2020). Effects of different extraction solvents on oil extracted from jatropha seeds and the potential of seed residues as a heat provider. *Bioenergy Research,* 14: 1207–1222. DOI: 10.1007/s12155-020-10217-5.

López-Bascón, M.A. & Luque De Castro, M.D. (2020). *Soxhlet Extraction.* In Poole, C.F. (eds.) *Liquid-Phase Extraction.* Spain, Elsevier. pp. 327–354).

Mahesar, S.A., Sherazi, S.T.H., Khaskheli, A.R., Kandhro, A.A. & Uddin, S. (2014). Analytical approaches for the assessment of free fatty acids in oils and fats. *Analytics Methods,* 6(14): 4956–4963. DOI: 10.1039/c4ay00344f.

Manaf, A., Lin, C.Y., Josli, I.C., Tananak, J., Adin, A., Amin, A.A., Kadir, A., Siew, C.K., Lee, J.S., Muhamad, H.R. & Nusantoro, B.P. (2024). Physicochemical properties of pili *(Canarium ovatum)* nut oil from Sabah, Malaysia. *Transactions on Science and Technology,* 11(4): 228–234.

Marikkar, J.M.M., Yanty, N.A.M., Paciulli, M., Miskandar, M.S. & Chiavaro, E. (2018). Composition and thermal properties of quaternary mixtures of palm oil:palm stearin:soybean oil:cocoa butter. *Italian Journal of Food Science,* 30(4): 740–751.

Millena, C.G. & Sagum, R.S. (2018). Physicochemical characterization and fatty acid profiling of different Philippine pili nut *(Canarium ovatum)* varieties. *Journal of American Oil Chemist Society,* 95: 325–336. DOI: 10.1002/aocs.12028.

Millena, C.G., Baloloy, K.A., Doma, N.G. & Hernan, P.B. (2023). Effect of maturity on physicochemical and fatty acid profile of Philippine pili *(Canarium ovatum).* *Philippine Journal of Science,* 152(1): 159–171. DOI:10.56899/152.01.11.

Mordi, R.C., Ademosun, O.T., Ajanaku, C.O., Olanrewaju, I.O. & Walton, J.C. (2020). Free radical mediated oxidative degradation of carotenes and xanthophylls. *Molecules,* 25(5): 1038. DOI: 10.3390/molecules25051038.

Norazlina, M.R., Tan, Y.S., Hasmadi, M. & Jahurul, M.H.A. (2021). Effect of solvent pre-treatment on the physicochemical, thermal profiles and morphological behavior of *Mangifera pajang* seed fat. *Heliyon,* 7(9): 1–6. DOI: 10.1016/j.heliyon.2021.e08073.

Palm Oil Research Institute of Malaysia (PORIM). (1995). *Methods of Test for Palm Oil and Palm Oil Product.* Bangi, Malaysia.

Pham, L.J. & Dumandan, N.G. (2015). Philippine Pili: Composition of the lipid molecular species. *Journal of Ethnic Foods,* 2(4): 147–153. DOI: 10.1016/j.jef.2015.11.001.

Pulassery, S., Abraham, B., Ajikumar, N., Munnilath, A. & Yoosaf, K. (2022). Rapid iodine value estimation using a handheld Raman spectrometer for on-site, reagent-free authentication of edible oils. *ACS Omega,* 7(11): 9164–9171. DOI: 10.1021/acsomega.1c05123.

Sarkar, A., Pandey, J.P., Singh, A., Tiwari, L. & Kumar, A. (2015). Novel method of using refractive index as a tool for finding the quality of aqueous enzymatic extracted algae oil. *Advances in Applied Science Research,* 6(4): 50–60.

Shin, K.S. & Lee, J.H. (2022). Melting, crystallization, and in vitro digestion properties of fats containing stearoyl-rich triacylglycerols. *Molecules,* 27(1), 191. DOI: 10.3390/molecules27010191.

Tesfaye, B., Abebaw, A. & Reddy, M.U. (2017). Determination of cholesterol and β- carotene content in some selected edible oils. *International Journal of Innovative Science and Research Technology,* 2(7): 14–17.

Tian, W., Yan, X., Zeng, Z., Xia, J., Zhao, J., Zeng, G., Yu, P, Wen, X. & Gong, D. (2024). Enzymatic interesterification improves the lipid composition, physicochemical properties and rheological behavior of *Cinnamomum camphora* seed oil, *Pangasius bocourti* stearin and perilla seed oil blends. *Food Chemistry,* 430: 137026. DOI: 10.1016/j.foodchem.2023.137026.

Van Wetten, I. A., Van Herwaarden, A. W., Splinter, R., & Van Ruth, S. M. (2014). Oil Analysis by FastDSC. *Procedia Engineering*, 87: 280–283. DOI: 10.1016/j.proeng.2014.11.662.

Wang, Y., Su, Y., Shehzad, Q., Yu, L., Tian, A., Wang, S., Ma, L., Zheng, L. & Xu, L. (2023). Comparative study on quality characteristics of *Bischofia olycarpa* seed oil by different solvents: Lipid composition, phytochemicals, and antioxidant activity. *Food Chemistry,* 202(17): 100588. DOI: 10.1016/j.fochx.2023.100588.

Yanty, N.A.M., Dollah, S., Marikkar, J.M.N., Miskandar, M.S., Desa, M.N.M. & Nusantoro, B.P. (2018). Physicochemical properties and thermal behavior of binary blends of *Madhuca longifolia* seed fat and palm oil as a lard substitute. *Journal of Advanced Agricultural Technologies,* 5(3): 202–208. DOI: 10.18178/joaat.5.3.202-208.

Yanty, N.A.M., Marikkar, J.M.N. & Shuhaimi, M. (2013). Effect of fractional crystallization on the composition and thermal properties of engkabang *(Shorea macrophylla)* seed fat and cocoa butter. *Grasas Y Aceites,* 64(5): 546–553. DOI: 10.3989/gya.023213.

Yanty, N.A.M., Marikkar, J.M.N., Nusantoro, B.P., Long, K. & Ghazali H.M. (2014) Physicochemical characteristics of papaya (*Carica papaya* L.) seed oil of the Hong Kong/Sekaki variety. *Journal of Oleo Science,* 63(9): 885–892. DOI: .5650/jos.ess13221.

Zarinah, Z., Maaruf, A.G., Nazaruddin, Wong, W.W.W. & Xuebing. (2014). Extraction and determination of physico-chemical characteristics of pili nut oil. *International Food Research Journal*, 21(1): 297-301.

Thermal, Structural and Biodegradability Properties of Bio-Based Kenaf/PMMA Composites Reinforced with Chitosan

NURQISTINA NABILAH ABDUL RAHAMAN[1], NOR HANUNI RAMLI[2] & NURJANNAH SALIM*[1,3]

[1]Faculty of Industrial Sciences and Technology, Universiti Malaysia Pahang Al Sultan Abdullah, Lebuh Persiaran Tun Khalil Yaacob, 26300 Kuantan, Pahang, Malaysia; [2]Faculty of Chemical and Process Engineering Technology, Universiti Malaysia Pahang Al Sultan Abdullah, 26300 Kuantan, Pahang, Malaysia; [2]Advanced Intelligent Materials Centre, Universiti Malaysia Pahang Al Sultan Abdullah, Lebuh Persiaran Tun Khalil Yaacob, 26300 Kuantan, Pahang, Malaysia
*Corresponding email address: njannah@umpsa.edu.my

ABSTRACT

This study investigates the incorporation of chitosan into kenaf/poly(methyl methacrylate) (PMMA) hybrid composites to enhance thermal, physical, and biodegradability properties. Kenaf fibers were alkali-treated, ground, and mixed with PMMA, while chitosan was incorporated at 10 g and 20 g concentrations in PMMA. The composites were fabricated via hot pressing method and characterized using Fourier Transform Infrared Spectroscopy (FTIR), Scanning Electron Microscopy (SEM), Energy Dispersive X-ray Spectroscopy (EDX), Thermogravimetric Analysis (TGA), water absorption and soil burial analyses. FTIR spectra revealed intensified –OH and –NH stretching peaks (~3351 cm^{-1}), indicating strong hydrogen bonding and compatibility between chitosan and the PMMA matrix. SEM micrographs showed improved fiber–matrix adhesion with reduced void formation in the 20 g chitosan composite. TGA results demonstrated enhanced thermal stability, with char residue increasing from 1.43% (0 g chitosan) to 2.07% (20 g chitosan) and degradation temperatures shifting toward higher ranges. Water absorption tests showed a reduction of up to 28% in moisture uptake in chitosan-modified samples compared to the control. Soil burial analysis confirmed improved biodegradability, with weight loss increasing by nearly 35% after 30 days for the highest chitosan-loaded sample. EDX analysis further confirmed successful chitosan incorporation with increased oxygen and carbon elemental signals. Overall, chitosan significantly improved the interfacial bonding, thermal stability, durability, and environmental responsiveness of the kenaf/PMMA hybrid composites, making them viable candidates for sustainable applications such as biodegradable panels and green furniture.

Keywords: Bio-based Filler, Chitosan, Kenaf Fiber, PMMA Composite

INTRODUCTION

In recent years, the incorporation of bio-based fillers into polymer composites has gained increasing attention due to growing environmental concerns and the need to reduce dependency on petroleum-based materials (Salim & Sarmin *et al.*, 2023). Natural fiber-reinforced composites, particularly those utilizing lignocellulosic fibers such as kenaf, jute, hemp, and flax, are widely studied for their biodegradability, renewability, and satisfactory mechanical properties (Salim & Sarmin, 2023; Salim *et al.*, 2024; Sharma *et al.*, 2025). However, the hydrophilic nature of these fibers and the incompatibility with hydrophobic polymer matrices like PMMA often result in poor interfacial adhesion, which affects the overall performance of the composites (Akil *et al.*, 2011; Jawaid & Khalil, 2011).

Kenaf fiber has been extensively studied for composite reinforcement owing to its excellent strength-to-weight ratio, cost-effectiveness, and environmental benefits. Yet, its tendency to absorb moisture and degrade under humid or thermal conditions remains a challenge. To address this, various surface treatments, compatibilizers, and hybridization strategies have been explored (Bledzki & Gassan, 1999). For example, alkali treatment is a common method used to clean fiber surfaces and increase roughness for better matrix adhesion.

Poly(methyl methacrylate) (PMMA) is a widely used thermoplastic polymer known for its excellent optical clarity, good weather resistance, and ease of processing, which make it attractive in applications ranging from biomedical devices to automotive components (Kim *et al.*, 2023; Lin *et al.*, 2023). However, neat PMMA suffers from inherent drawbacks such as brittleness, relatively low impact strength, and limited thermal stability, restricting its broader utilization in high-performance or structural applications (Lin *et al.*, 2023; Sosiati *et al.*, 2022). To overcome these limitations, reinforcement with natural fibers or functional additives has been explored to enhance toughness, thermal resistance, and environmental performance.

Chitosan, a derivative of chitin, has gained attention as a valuable additive in this context. It possesses unique functional properties, including antimicrobial activity, biocompatibility, and excellent film-forming ability, which make it an ideal candidate for incorporation into polymer blends and bio-composites. A study by (Du *et al.*, 2014) showed that adding chitosan to PLA composites improved moisture barrier properties and delayed the onset temperature of degradation (Ilyas *et al.*, 2022) further reported that chitosan enhanced both thermal stability and mechanical strength when used as a coating agent on natural fibers in polyester matrices.

Studies by Ilyas *et al.* (2021) and Sarmin *et al.* (2023) have provided a foundational understanding of chitosan's interaction with different polymers. Chitosan's polar functional groups are capable of forming hydrogen bonds and even ionic interactions with certain matrix components, thus improving compatibility and interfacial adhesion. This interaction is particularly important in systems where the base polymer is non-polar, such as PMMA, and the reinforcement is polar, such as kenaf fiber.

This study contributes to the growing body of work on sustainable polymer composites by demonstrating that chitosan not only enhances the thermal and structural integrity of kenaf/PMMA composites but also accelerates biodegradability, offering a balanced pathway between durability and environmental responsibility. Unlike previous studies that examined chitosan primarily as a coating or barrier additive, our work integrates it directly into the composite matrix, showing its dual role as both a reinforcing and eco-functional filler.

A study by Akil *et al.* (2011) investigated the use of chitosan in kenaf/polypropylene composites and found that the incorporation of chitosan not only reduced water uptake but also improved tensile strength and thermal stability. However, research specifically focusing on chitosan's role in kenaf/PMMA systems remains limited. Furthermore, investigations that link chitosan's functional effects to biodegradability performance via soil burial testing are rare, despite their importance for sustainable material development.

Therefore, this study contributes to the current body of knowledge by exploring the combined effects of kenaf fiber and chitosan in a PMMA matrix, aiming to produce a composite that is both high-performing and environmentally responsible. The evaluation of thermal, morphological, and biodegradability characteristics provides new insights into the design of future green composite materials. This study contributes to the growing body of work on sustainable polymer composites by demonstrating that chitosan not only enhances the thermal and structural integrity of kenaf/PMMA composites but also accelerates biodegradability, offering a balanced pathway between durability and environmental responsibility.

METHODOLOGY

Preparation of Kenaf/PMMA/Chitosan Hybrid Composite

The main materials used in this work are kenaf fibers, Poly(methyl methacrylate) (PMMA), and chitosan. In this context, the kenaf fibers undergo alkaline treatment with 6% NaOH for six hours in room temperature to improve their properties through the effective removal of lignin and hemicellulose, which are elements in a fiber that may reduce its strength and compatibility with the polymer matrix. After treatment, the fibers were dried at 50 ºC in oven for 24 hours to remove the moisture. Finally, the materials were milled into powder form with size of 250 μm and mix properly with PMMA. The composite was prepared by thoroughly mixing the kenaf fiber powder (60 g) with PMMA (60

g) and adding 10 g and 20 g of chitosan to observe the effect on the properties of the composites. The formulation was selected based on previous study reporting effective reinforcement of bio-based composites with 10–20 wt.% chitosan (Ilyas *et al*., 2022), which demonstrated significant improvements in interfacial bonding and thermal stability and based on the preliminary trials in this study

indicated that higher chitosan content beyond 20 wt.% led to poor dispersion and agglomeration. A composite without chitosan was also prepared as a control sample. The composition of the composites is shown in Table 1. Proper blending was necessary for uniform distribution of the materials to achieve maximum performance characteristics in the final product.

Table 1. Composition of the sample preparation

Sample	Kenaf powder (g)	PMMA powder (g)	Chitosan powder (g)
1	60	60	0
2	60	60	10
3	60	60	20

The hot press method was used to mold the composite samples once the materials were well mixed. This involved placing the blended mixture into a mold and applying heat for 100 °C and a pressure of 10 MPa for 15 minutes. Hot pressing is important, as it ensures better interfacial bonding of kenaf fiber with PMMA along with chitosan, which leads to good mechanical properties and good structural

integrity of the final composite material. The hot-pressed samples were then allowed to cool and were subjected to various tests in order to study their physical, thermal, and biodegradability properties. This systematic approach in the preparation of materials ensures improved performance characteristics of the composites as in Figure 1.
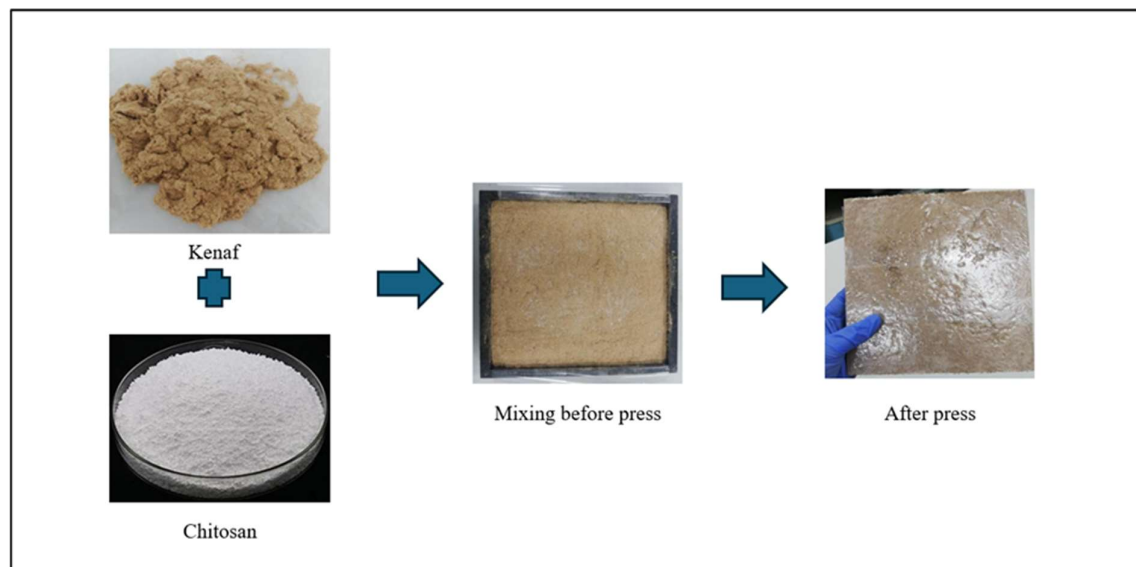
Figure 1. The process of making composites

Characterization and Testing of Properties of the Kenaf/PMMA/Chitosan Hybrid Composite

Water Absorption

The water absorption test was conducted with three replicate to assess the moisture resistance

of the composites by measuring the amount of water absorbed over time. This test is crucial for understanding how well the composite can withstand humid environments, which is vital for its durability in practical applications (Sosiati *et al*., 2022). The water absorption percentage can be calculated using the formula Eq. (1):

$$Water\ Absorption\ (\%) = ((wf - wi)/wi) \times 100\% \quad Eq.\,(1)$$

Where *wf* is the final weight after immersion, and *wi* is the initial weight. Samples with the size of 50 mm × 50 mm × 3 mm were immersed in water at intervals of up to 24 hours, with absorption percentages calculated after each two hours.

Soil Burial Test

The soil burial test evaluated the degradation behavior of kenaf/PMMA/chitosan hybrid composites in natural soil conditions. Uniformly sized samples of 50 mm × 50 mm × 3 mm were oven-dried at 60 °C for 24 hours to remove moisture and weighed precisely. Prepared local soil area, free of debris, was used as the burial medium, with maintained moisture and a temperature of 25–30 °C to simulate real-life conditions (Samir *et al.*, 2022). Samples were buried at a 40 mm depth, ensuring exposure to active microbial decomposition while preventing cross-contamination as in Figure 2. After 14 days, samples were retrieved, washed with distilled water, dried again, and reweighed. The extent of biodegradation was calculated using the formula Eq.(2):

$$Weight\ Loss\ (\%) = ((wo - wt)/wo) \times 100\% \qquad Eq.(2)$$

Where *wo* is the initial dry weight, and *wt* is the dry weight after burial. The weight loss reflected the material's degradation due to microbial activity.
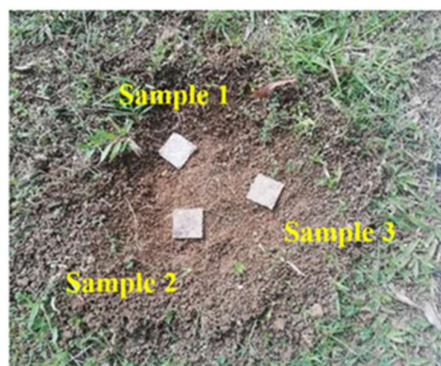
Figure 2. The position of samples for the soil burial test

Scanning Electron Microscopy (SEM)

Scanning Electron Microscopy (SEM) is a high-resolution imaging technique used to analyze the surface morphology, composition, and crystalline structure of materials. In this study, a Joel SEM was employed to examine the kenaf/PMMA/chitosan hybrid composite. Samples were coated with a thin layer of gold using a sputter coater to prevent electrostatic charging and placed in a vacuum chamber for imaging. SEM achieved magnifications ranging from a few times to hundreds of thousands, providing detailed insights into the microstructure. Coupled with Energy-Dispersive X-ray Spectroscopy (EDX), SEM enables elemental composition analysis by detecting characteristic X-rays emitted from the sample.

Thermogravimetric Analysis (TGA)

Thermogravimetric Analysis (TGA) is a technique used to evaluate a material's thermal behavior by measuring weight changes as a function of temperature. In this study, a Hitachi STA7000 analyzer was used to analyze the thermal stability of kenaf/PMMA hybrid composites with chitosan. Samples were heated from 30 to 700 °C at a rate of 10 °C/min under a 10 mL/min air flow, generating TGA curves that provided insights into decomposition temperatures, thermal stability, and volatile component content.

RESULTS AND DISCUSSION

Water Absorption

The water absorption characteristics of kenaf/PMMA hybrid composites with varying chitosan content were evaluated for 24 hours

(Figure 3). As expected, all samples showed a gradual increase in water absorption with time however, significant differences were observed

in the overall absorption levels based on chitosan loading.
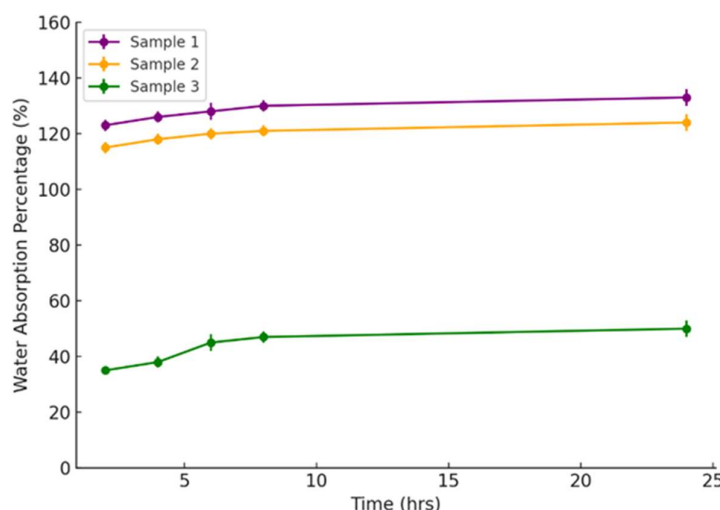
Figure 3. The graph shows the water absorption property of Kenaf/PMMA/Chitosan hybrid composite.

Sample 1, the control composite without chitosan, exhibited the highest water uptake, reaching approximately 135% after 24 hours. Sample 2, with 10 g of chitosan, showed a slightly reduced water absorption of about 130%, while Sample 3, with 20 g of chitosan, demonstrated a substantially lower absorption rate of around 52%.

This trend demonstrates the positive role of chitosan in mitigating water absorption. The observed reduction in water uptake with increasing chitosan content can be attributed to improved interfacial bonding between the kenaf fibers and the PMMA matrix. Chitosan, with its film-forming ability and reactive amine and hydroxyl groups, enhances the matrix–filler interface by filling micro-voids and reducing capillary pathways for water penetration. As supported by SEM analysis (Figure 5), the presence of chitosan contributed to a more compact and homogeneous morphology, which effectively minimized water ingress.

These findings are in agreement with prior studies. For instance, Srivastava *et al*. (2024) reported a similar reduction in water absorption in chitosan-reinforced bamboo fiber composites, attributing it to better fiber-matrix adhesion (Srivastava *et al*., 2024). Similarly, Ahmadzadeh *et al*. (2018) developed PLA/CNT/chitosan composite fibers using electrospinning. They

found that low-content chitosan (~7 wt%) enhanced mechanical strength and water resistance. Furthermore, Ilyas *et al*. (2022) reported that chitosan incorporation can reduce porosity and micro-crack formation in fiber matrices, leading to improved barrier properties and delayed moisture ingress.

The current results reinforce these previous observations and provide additional evidence that chitosan acts not only as a bio-based filler but also as an effective compatibilizer. Its multifunctional role improves interfacial integrity, reduces fiber hydrophilicity, and imparts greater dimensional stability under humid or wet conditions.

Overall, the integration of chitosan, particularly at 20 g loading, significantly enhances the composite's water resistance, making it possible for outdoor or humid-environment applications. The reduction in water uptake without compromising biodegradability or other functional properties positions this material as a promising candidate in the field of sustainable biocomposites.

Soil Burial

The biodegradability of the kenaf/PMMA/Chitosan hybrid composites was assessed through a soil burial test, and the

resulting weight loss percentages are presented in Figure 4. After a predetermined burial period, the results indicated a clear trend: increased chitosan content corresponded with greater weight loss, suggesting enhanced biodegradability.
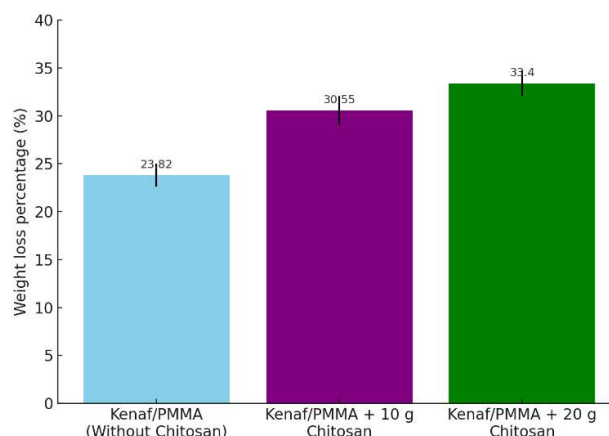
Figure 4. The graph shows the weight loss percentage of Kenaf/PMMA/Chitosan hybrid composite samples with different

The control sample exhibited a weight loss of 23.82%, whereas sample 2 with 10 g of chitosan showed a higher weight loss of 30.55%. The sample 3 with 20 g of chitosan recorded the highest degradation rate at 33.4%. This progressive increase in weight loss can be attributed to the biodegradable nature of chitosan, which enhances the overall microbial accessibility and degradation of the composite matrix when exposed to soil environments.

The results are in strong agreement with findings from Mokhothu & John, (2017) and Thomas *et al*. (2021), who reported that the incorporation of natural, biodegradable fillers such as starch, chitosan, and cellulose derivatives into synthetic polymer matrices significantly improved the degradation behavior of hybrid composites. In particular, Râpă *et al*. (2016) found that PLA-based composites containing chitosan experienced higher microbial colonization and structural breakdown during soil burial testing due to the biopolymer's susceptibility to enzymatic hydrolysis and microbial attack.

The enhancement in biodegradability is likely due to the increased hydrophilicity and availability of functional groups (–OH and –NH_2) introduced by chitosan, which promotes microbial adhesion and enzymatic activity. Furthermore, the improved dispersion and interfacial bonding between the kenaf fibers and PMMA matrix may have led to more uniform degradation, as voids and microcracks formed during degradation could propagate more readily in a compact composite structure containing chitosan.

Moreover, the increased weight loss of the chitosan-enhanced samples also reflects a shift in material balance toward more eco-friendly constituents. While PMMA is not inherently biodegradable, the synergistic effect of kenaf and chitosan which are both rich in cellulose and polysaccharides contributed to a composite system that is more susceptible to environmental degradation mechanisms.

These findings underscore the dual benefit of chitosan inclusion not only improves the composite's mechanical and barrier properties as shown in the water absorption and thermal tests, but it also advances the environmental degradability properties, aligning with the growing demand for sustainable materials. Such characteristics make the kenaf/PMMA/chitosan system a promising candidate for short-term or semi-durable applications where post-use degradation is desirable, such as in packaging, agricultural mulch films, or temporary construction panels.

Scanning Electron Microscopy (SEM) Analysis

Figure 5 presents SEM micrographs of the fracture surfaces of the kenaf/PMMA hybrid

composites at 500x magnification. These images provide insight into the fiber–matrix interfacial morphology and the dispersion quality of chitosan within the composite system.

Kenaf/PMMA without chitosan	Kenaf/PMMA + 10 g chitosan	Kenaf/PMMA + 20 g chitosan
Sampel 1:	Sample 2:	Sample 3:
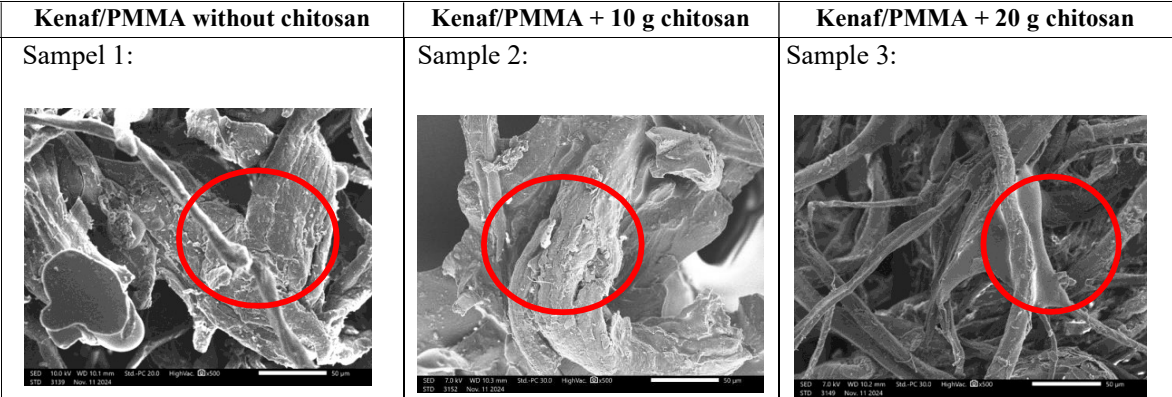
Figure 5. The SEM images of Kenaf/PMMA/Chitosan hybrid composite samples at 500x magnification.

Sample 1 exhibits poor interfacial adhesion, as evidenced by the presence of noticeable voids, fiber pull-outs, and gaps between the kenaf fibers and the PMMA matrix. The absence of compatibilizing agent in this sample likely contributed to insufficient bonding, leading to weak stress transfer efficiency across the fiber–matrix interface. Such features are commonly associated with mechanical failure initiation and water permeation pathways.

In contrast, Sample 2 shows a marked improvement in surface morphology. The interface between the fiber and matrix appears more cohesive, with fewer visible voids and more embedded fibers, suggesting enhanced compatibility. The presence of chitosan likely improved wettability and interfacial interaction, forming a more integrated structure through hydrogen bonding and physical entanglement between the amine and hydroxyl groups of chitosan and the PMMA matrix.

Sample 3 demonstrates the most uniform and compact morphology. The fibers are well-encapsulated, and the surface appears smoother and denser, with minimal voids or discontinuities. This suggests that the higher chitosan content facilitated a more effective matrix-fiber network formation, reducing interfacial defects and enhancing structural integrity.

These observations are in agreement with prior studies by Popyrina *et al.* (2024) who reported that adding chitosan to natural fiber composites significantly reduced interfacial porosity and improved fiber adhesion. Similarly, Sarmin *et al.* (2023) observed that chitosan inclusion in jute fiber/epoxy composites enhanced fiber dispersion and matrix encapsulation, resulting in superior mechanical and water resistance properties. Moreover, Amaregouda *et al.* (2024) found that chitosan's ability to interact through hydrogen bonding contributed to the formation of a robust interface in starch-based biocomposites.

The enhanced fiber–matrix adhesion seen in chitosan-containing samples supports the improved performance noted in water absorption and thermal analysis. The reduction of microvoids not only limits water ingress but also delays the onset of degradation mechanisms under environmental exposure. Thus, SEM analysis confirms the crucial role of chitosan in improving the microstructural integrity of the kenaf/PMMA hybrid composites.

EDX Analysis

The Energy Dispersive X-ray (EDX) spectra of the composite samples, as shown in Figure 6, reveal the elemental compositions of the kenaf/PMMA composite without chitosan (Sample 1) and with 10 g chitosan (Sample 2). The primary elements detected were carbon (C) and oxygen (O), which are consistent with the organic nature of the matrix and reinforcing fiber components.

Sample 1 exhibited a carbon mass percentage of 47.48% and oxygen at 52.52%, indicating a relatively oxygen-rich environment due to the

presence of hydroxyl groups from cellulose and PMMA's ester functionalities. In contrast, Sample 2 showed an increase in carbon content to 50.25% and a corresponding decrease in oxygen to 49.75%.
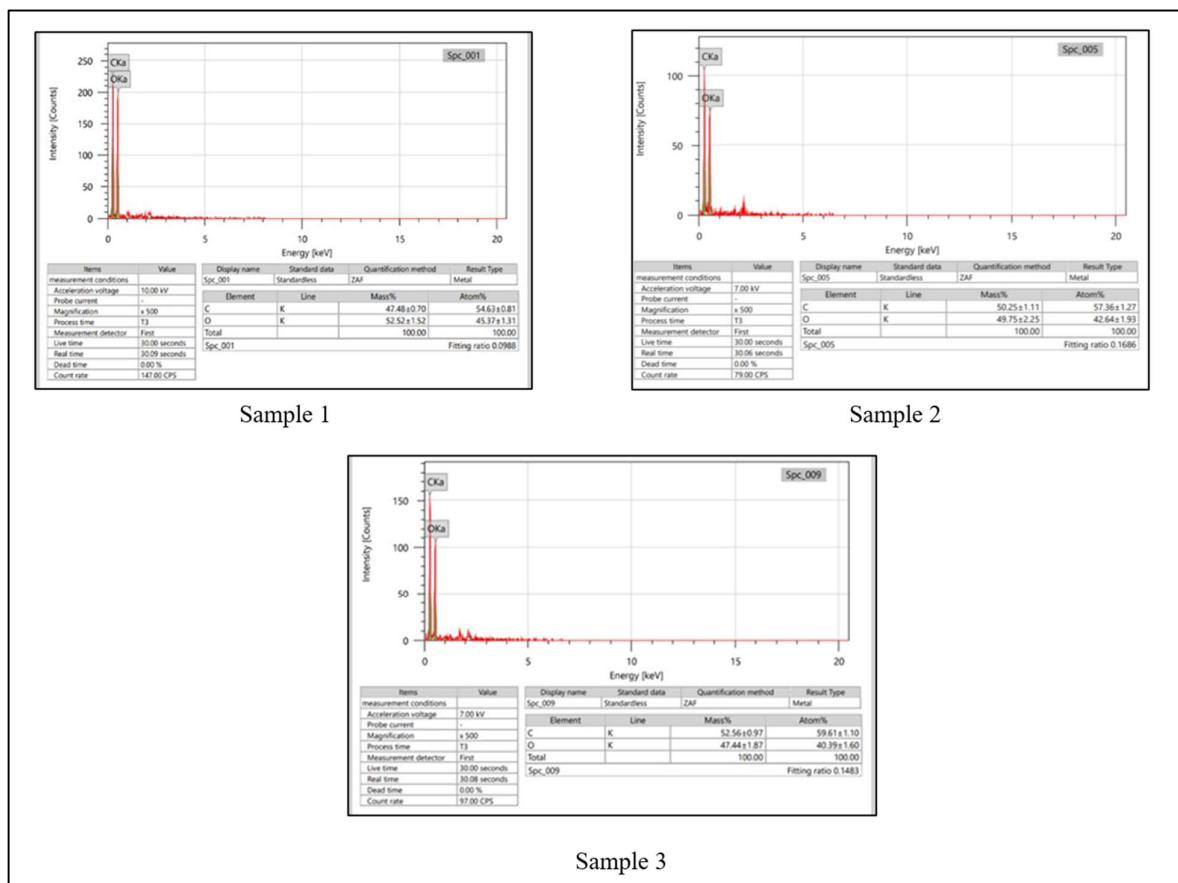
Figure 6. The energy spectra of Kenaf/PMMA/Chitosan hybrid composite samples at 500x magnification

This shift suggests the successful incorporation of chitosan into the composite matrix, as chitosan has a higher C:N ratio and a lower oxygen content compared to cellulose. The reduced oxygen percentage and enhanced carbon concentration in Sample 2 align with findings by Manyatshe *et al*. (2022), who reported similar elemental shifts upon the incorporation of chitosan into lignocellulosic matrices, attributing them to the partial substitution of hydroxyl groups with amino functionalities from chitosan (Manyatshe *et al*., 2022).

Moreover, the increased carbon content may also indicate improved compatibility and bonding between the chitosan and PMMA, enhancing the composite's homogeneity. This is in agreement with observations by Rajamuneeswaran *et al*. (2015), who emphasized the role of chitosan in improving the matrix-fiber interface due to its polar functional groups, which interact effectively with both the filler and polymer matrix (Rajamuneeswaran *et al*., 2015).

The fitting ratio values (0.0986 for Sample 1 and 0.1666 for Sample 2) further support the improved matrix-filler interaction in the presence of chitosan. A higher fitting ratio typically suggests a better signal-to-noise ratio and can be interpreted as a more homogeneous elemental distribution. Overall, the EDX results confirm the successful integration of chitosan into the kenaf/PMMA matrix and point to an enhanced interfacial interaction that likely contributes to improved composite properties, which will be further corroborated by SEM and thermal analysis results.

FTIR

The Fourier Transform Infrared Spectroscopy (FTIR) spectra of the kenaf/PMMA composites with and without chitosan (Figure 7) reveal significant insights into the chemical interactions between the matrix and filler components.
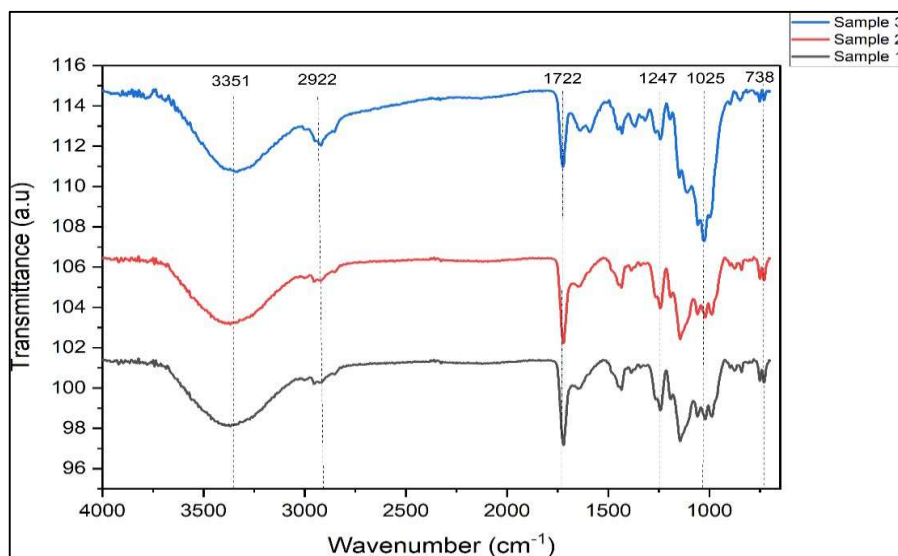
Figure 7. FTIR spectra of Kenaf/PMMA/Chitosan hybrid composite samples with varying amounts of chitosan (0, 10 g, and 20 g).

Characteristic absorption bands are observed at 3351, 2922, 1722, 1247, 1025, and 738 . The broad peak at 3351 cm^{-1} corresponds to the –OH and –NH stretching vibrations, typically associated with hydrogen bonding in hydroxyl and amine groups. This band becomes more intense and defined in Samples 2 and 3, suggesting the presence of chitosan, which is rich in hydroxyl and amino groups. This indicates enhanced hydrogen bonding interactions between chitosan and the kenaf/PMMA matrix. Similar results were reported by Wang *et al*. (2018), where the addition of chitosan to lignocellulosic matrices introduced stronger intermolecular bonding, as evidenced by amplified –OH bands (Wang *et al*., 2018).

The absorption at 2922 cm^{-1} is attributed to the aliphatic –CH stretching of the PMMA matrix and kenaf fibers. This band remains consistent across all samples, confirming the presence of the polymeric backbone and reinforcing fiber structures.

A strong peak at 1722 cm^{-1}, characteristic of C=O stretching in the ester group of PMMA, is observed in all samples. However, the slight shift and increased sharpness in Samples 2 and 3 suggest possible hydrogen bonding or dipole–dipole interactions between chitosan and the carbonyl groups of PMMA. This supports the hypothesis of chemical compatibility between the chitosan filler and PMMA matrix.

The bands at 1247 and 1025 cm^{-1} are associated with C–O–C stretching vibrations, indicative of PMMA and cellulose structure. These peaks become more prominent in chitosan-modified samples, further implying improved molecular interactions and potentially enhanced dispersion of chitosan within the matrix.

Finally, the 738 cm^{-1} band represents out-of-plane C–H bending, commonly associated with PMMA. This region does not show a major shift, but its relative intensity decreases in Samples 2 and 3, possibly due to the increasing dominance of chitosan's spectral features.

Overall, the FTIR results confirm that chitosan was successfully integrated into the kenaf/PMMA matrix, forming hydrogen bonds and possibly ionic interactions that enhance interfacial compatibility. These findings are consistent with the improved structural integrity observed in the SEM and EDX results. As noted

by Rachtanapun *et al*. (2012), such interactions can significantly improve the mechanical, thermal, and barrier properties of bio-based composites.

TGA

The TGA curves (Figure 8) reveal the thermal degradation behavior over 100–700 °C and Table 2 shows the interpolated onset (T_5%), maximum (T_max), and final (T_{95}%) degradation temperatures together with the total weight loss and char residue for kenaf/PMMA/Chitosan hybrid composites.

Sample 1 (Kenaf/PMMA without chitosan) exhibited a two-step degradation pattern. The initial degradation temperature (T_5%) occurred at approximately 250 °C, corresponding to the volatilization of low molecular weight compounds and hemicellulose decomposition. The maximum degradation temperature

(T_max) was around 382 °C, associated with cellulose decomposition and PMMA backbone scission, followed by a final degradation temperature (T_{95}%) near 480 °C. The overall weight loss reached 98.6%, leaving a char residue of 1.43% at 693.8 °C, indicating limited thermal resistance and char formation.

Upon incorporation of 10 g chitosan (Sample 2), the composite showed delayed degradation. The onset temperature shifted to ~280 °C, while T_max increased to 396 °C and the final degradation temperature was extended to 492 °C. The total weight loss was slightly reduced to 98.5%, with a char residue of 1.47% at 694.0 °C. This indicates that chitosan contributed to improved thermal resistance, attributed to its nitrogen content, which promotes char formation. These findings align with Hu *et al*. (2013), who demonstrated that chitosan-based flame retardants accelerate char yield and improve thermal stability in polymer systems.
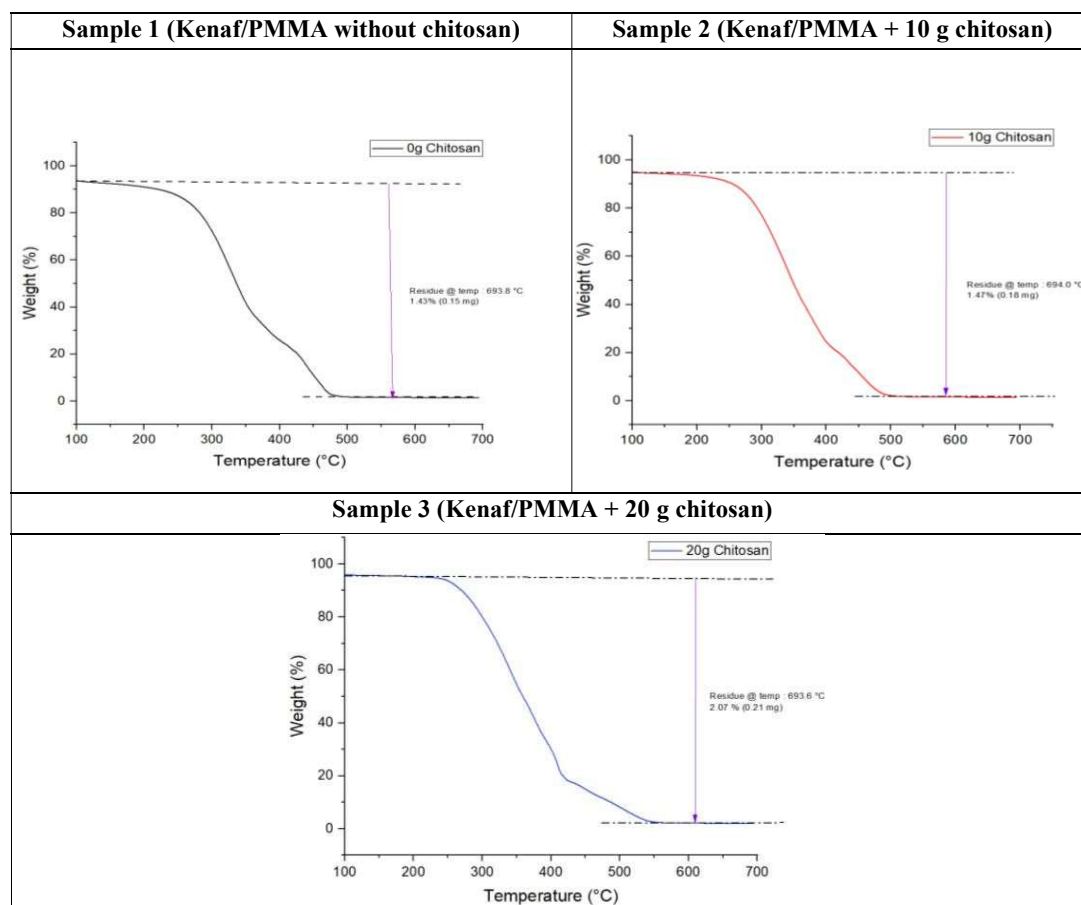
Figure 8. TGA curves of Kenaf/PMMA/Chitosan hybrid composite samples at different chitosan composition.

Table 2. The interpolated onset ($T_5\%$), maximum (T_max), and final ($T_{95}\%$) degradation temperatures together with the total weight loss and char residue for kenaf/PMMA/Chitosan hybrid composites.

Sample	Onset Temp $T_5\%$ (°C)	Maximum Temp T_max (°C)	Final Temp $T_{95}\%$ (°C)	Total Weight Loss (%)	Char Residue at 700 °C (%)
Sample 1	250	382	480	98.6	1.43
Sample 2	280	396	492	98.5	1.47
Sample 3	300	406	503	97.9	2.07

Sample 3 (20 g chitosan) showed the most significant improvement, with an onset temperature of ~300 °C, T_max at 406 °C, and a final degradation temperature of ~503 °C. The total weight loss was reduced to 97.9%, leaving a char residue of 2.07% at 693.6 °C. The increased residue confirms enhanced carbonaceous char yield with higher chitosan loading, consistent with the role of nitrogenous groups in catalyzing char formation. Similar effects have been reported by Wang *et al*. (2018) in lignocellulose–chitosan composites, where interfacial bonding and nitrogen-induced char formation improved thermal stability and dimensional integrity.

The improved thermal stability observed in Samples 2 and 3 can also be attributed to stronger interfacial interactions between chitosan and the polymer matrix, as supported by FTIR analysis. The formation of hydrogen bonds and possible ionic interactions between amino groups in chitosan and ester groups in PMMA restrict chain mobility, thereby delaying thermal chain scission and raising decomposition onset temperatures (Grząbka-Zasadzińska *et al*., 2017).

In summary, interpolation of the TGA data confirms that chitosan incorporation systematically increases the onset, maximum, and final degradation temperatures while reducing overall weight loss and increasing char residue. These results demonstrate that chitosan not only reinforces interfacial adhesion but also acts as a thermal stabilizer through its char-promoting effect, making kenaf/PMMA–chitosan composites more resistant to high-temperature degradation.

CONCLUSION

This study successfully demonstrated the incorporation of chitosan as a bio-based filler into kenaf/PMMA hybrid composites to enhance their thermal, physical, and environmental properties. The primary objective was to evaluate the effect of chitosan addition on interfacial bonding, thermal stability, water resistance, and biodegradability. The elemental analysis via EDX confirmed the homogeneous dispersion and interaction of chitosan within the kenaf/PMMA matrix, as evidenced by increased carbon and oxygen content correlating with chitosan incorporation. FTIR analysis further revealed the formation of hydrogen bonding and potential ionic interactions between the functional groups of chitosan and PMMA, indicating good interfacial compatibility and chemical integration. Thermal analysis by TGA demonstrated that chitosan addition significantly enhanced the thermal stability of the composites. An increase in char residue and a shift in degradation temperatures were observed with higher chitosan content, supporting its role in thermal resistance improvement due to its nitrogen-rich structure that promotes char formation. Chitosan also contributed to reduced water absorption, attributed to its semi-crystalline structure and compatibility with the PMMA matrix, which limited water ingress. This suggests improved durability and potential for application in humid environments. Moreover, soil burial tests confirmed increased biodegradability with chitosan addition, aligning with the environmental objective of developing a more eco-friendly composite. While the present work demonstrates significant improvements in thermal stability, interfacial bonding, and biodegradability, mechanical properties such as tensile, flexural, and impact strength were not evaluated. These are essential parameters for assessing practical applicability of bio-based composites. Future work will focus on systematically investigating the mechanical performance of kenaf/PMMA/Chitosan hybrid composites to complement the current findings and provide a more comprehensive understanding of their application potential

REFERENCES

Ahmadzadeh, S., Azadmard, D.S., Valizadeh, H., & Peighambardoust, S. H. (2018). Production of chitosan–gallic acid nanogel and its application in sunflower oil oxidative stability. *Iranian Journal of Biosystems Engineering*, 49(1): 121-128.

Akil, H., Omar, M. F., Mazuki, A. A. M., Safiee, S., Ishak, Z. A. M., & Bakar, A. A. (2011). Kenaf fiber reinforced composites: A review. *Materials & Design*, 32(8-9): 4107-4121.

Amaregouda, Y., & Kamanna, K. (2024). Carboxymethyl cellulose/starch-based films incorporating chitosan nanoparticles for multifunctional food packaging. *Cellulose*, 31(4): 2413-2427.

Bledzki, A. K., & Gassan, J. (1999). Composites reinforced with cellulose based fibres. *Progress in polymer science*, 24(2): 221-274.

Du, Y., Wu, T., Yan, N., Kortschot, M. T., & Farnood, R. (2014). Fabrication and characterization of fully biodegradable natural fiber-reinforced poly (lactic acid) composites. *Composites Part B: Engineering*, 56: 717-723.

Grząbka-Zasadzińska, A., Amietszajew, T., & Borysiak, S. (2017). Thermal and mechanical properties of chitosan nanocomposites with cellulose modified in ionic liquids. *Journal of Thermal Analysis and Calorimetry*, 130(1): 143-154.

Hu, S., Song, L., Pan, H., & Hu, Y. (2013). Effect of a novel chitosan-based flame retardant on thermal and flammability properties of polyvinyl alcohol. *Journal of thermal analysis and calorimetry*, 112(2): 859-864.

Ilyas, R., Sapuan, S., Harussani, M., Hakimi, M., Haziq, M., Atikah, M., Nurazzi, N. (2021). Polylactic acid (PLA) biocomposite: Processing, additive manufacturing and advanced applications. *Polymers*, 13(8): 1326.

Ilyas, R. A., Aisyah, H. A., Nordin, A. H., Ngadi, N., Zuhri, M. Y. M., Asyraf, M. R. M., Abral, H. (2022). Natural-fiber-reinforced chitosan, chitosan blends and their nanocomposites for various advanced applications. *Polymers*, 14(5): 874.

Jawaid, M., & Khalil, H. P. S. A. (2011). Cellulosic/synthetic fibre reinforced polymer hybrid composites: A review. *Carbohydrate polymers*, 86(1): 1-18.

Kim, D., Lim, J., Jung, D., Oh, W., Kyeong, J., Kwon, S. H., & Lee, S. G. (2023). Thermal and mechanical properties of polymeric materials for automotive applications using molecular dynamics simulation. *Materials Today Communications*, 36: 106529.

Lin, H.-N., Peng, T.-Y., Kung, Y.-R., Chiou, Y.-J., Chang, W.-M., Wu, S.-H., Lin, C.K. (2023). Effects of the methyl methacrylate addition, polymerization temperature and time on the MBG@PMMA core-shell structure and its application as addition in electrospun composite fiber bioscaffold. *Ceramics International*, 49(5): 7630-7639.

Manyatshe, A., Cele, Z. E. D., Balogun, M. O., Nkambule, T. T. I., & Msagati, T. A. M. (2022). Lignocellulosic derivative-chitosan biocomposite adsorbents for the removal of soluble contaminants in aqueous solutions–preparation, characterization and applications. *Journal of Water Process Engineering*, 47: 102654.

Mokhothu, T. H., & John, M. J. (2017). *Bio-based fillers for environmentally friendly composites*. Wiley Publisher. pp. 243-270.

Popyrina, T. N., Khavpachev, M. A., Ivanov, P. L., Monakhova, K. Z., Kuchkina, I. O., Evtushenko, Y. M., & Zelenetskii, A. N. (2024). Morphology and Physical-Chemical Properties of Composite Materials Based on Polyolefins and Chitosan. *Polymer Science, Series C*, 66(1): 46-54.

Rachtanapun, P., & Suriyatem, R. (2012). Moisture sorption isotherms of soy protein isolate/carboxymethyl chitosan blend films. *Journal of Agricultural Science and Technology.* 2(1A): 50.

Rajamuneeswaran, S., Jayabal, S., Kalyana Sundaram, S., Balaji, N. S., & Ramkumar, P. (2015). Effect of chitosan particle addition on the tensile and flexural strength of coir fiber reinforced polyester composites. *Applied Mechanics and Materials*, 813: 30-33.

Râpă, M., Miteluţ, A. C., Tănase, E. E., Grosu, E., Popescu, P., Popa, M. E., Vasile, C. (2016). Influence of chitosan on mechanical, thermal, barrier and antimicrobial properties of PLA-biocomposites for food packaging. *Composites Part B: Engineering*, 102: 112-121.

Salim, N., & Sarmin, S. N. (2023). Biocomposites as Structural Components in Various Applications. In Abu, Z.Y., Mohd S.S., Junidah, L (eds). *Cellulose*. CRC Press. pp. 105-117

Salim, N., Sarmin, S. N., & Roslan, R. (2024). Effect of interfacial bonding characteristics of chemically treated of various natural fibers reinforced polymeric matrix composites. In Krishnasamy, S., Hemath Kumar, M., Parameswaranpillai, J., Mavinkere Rangappa, S., Siengchin, S. (eds). *Interfacial Bonding Characteristics in Natural Fiber Reinforced Polymer Composites. Composites Science and Technology.* Springer. pp.317-337.

Samir, A., Ashour, F. H., Hakim, A. A. A., & Bassyouni, M. (2022). Recent advances in biodegradable polymers for sustainable applications. *Materials Degradation*, 6(1): 68.

Sarmin, S. N., Jawaid, M., Ismail, A. S., Hashem, M., Fouad, H., Midani, M., & Salim, N. (2023). Effect of chitosan filler on the thermal and viscoelasticity properties of bio-epoxy/date palm fiber composites. *Sustainable Chemistry and Pharmacy*, *36*, 101275.

Sharma, H., Arora, G., Singh, M. K., Rangappa, S. M., Bhowmik, P., Kumar, R., Siengchin, S.

(2025). From composition to performance: Structural insights into polymer composites. *Next Materials*, 8: 100852. DOI:10.1016/j.nxmate.2025.100852

Sosiati, H., Al-Giffary, F., Adil, F. A., Kamiel, B. P., Adi, R. K., & Yusuf, Y. (2022). The properties of kenaf/carbon/PMMA hybrid composites by adding chitosan nano and microparticles. *Materials Today: Proceedings*, 66: 2908-2913.

Srivastava, S., Sarangi, S. K., & Singh, S. P. (2024). Water absorptivity and porosity investigation of nano bio-silica, hemp, and bamboo fibre-reinforced chitosan Bio-composite Material. *Silicon*, 16(11): 4723-4728. DOI:10.1007/s12633-024-03027-3

Thomas, S. K., Parameswaranpillai, J., Krishnasamy, S., Begum, P. M. S., Nandi, D., Siengchin, S., Sienkiewicz, N. (2021). A comprehensive review on cellulose, chitin, and starch as fillers in natural rubber biocomposites. *Carbohydrate Polymer Technologies and Applications*, 2: 100095.

Wang, Z., Yan, Y., Shen, X., Qian, T., Wang, J., Sun, Q., & Jin, C. (2018). Lignocellulose-Chitosan-Multiwalled Carbon Nanotube Composites with Improved Mechanical Strength, Dimensional Stability and Fire Retardancy. *Polymers*, 10(3): 341.

Effect of Drying Pre-Treatment on Nutritional Composition, Fatty Acid Profile, and Antioxidant Properties of Bambangan (*Mangifera pajang*) Seed and Its Fat

NORAZLINA MOHAMMAD RIDHWAN[*1], KHOR BI SHUANG[1], HASMADI MAMAT[1], MD JAHURUL HAQUE AKANDA[2], NORLIZA JULMOHAMMAD[1], MARIAH AQILAH MOHD AFFANDY[1] & NORAIDAH HAINI[3]

[1] Food Security Research Laboratory, Faculty of Food Science and Nutrition, Universiti Malaysia Sabah, 88400 Kota Kinabalu, Sabah, Malaysia; [2] Department of Agriculture, School of Agriculture, University of Arkansas, 1200 North University Dr., M/S 4913, Pine Bluff, AR 71601; [3]Chemistry Laboratory, Forest Research Centre, Sabah Forestry Department, Mile 14, 90175, Sandakan, Sabah.
*Corresponding author: azlina_ridhwan@ums.edu.my

ABSTRACT

This study investigates the effects of five different drying methods (sun, oven, cabinet, microwave, and freeze-drying) on the nutritional composition, fatty acid profile, and antioxidant properties of bambangan seed powder and its extracted fat. Proximate analysis revealed that freeze drying preserved the highest crude fat content (6.94%), while sun drying resulted in higher crude fiber levels (4.51%). Cabinet drying achieved the lowest moisture content (5.57%), thereby enhancing shelf stability. Fatty acid profiling showed stearic (37.29 - 44.68%) and oleic acids (38.71 - 45.53%) as dominant in bambangan seed fat, with freeze drying and cabinet drying retaining higher saturated fatty acids, whereas oven drying and microwave drying promoted unsaturated fatty acid. Total phenolic content (62.43 - 83.90 mg GAE/g) and ferric reducing antioxidant power (102.41 - 129.52 mM/100g) were highest in freeze drying samples, particularly in seed powder, indicating superior retention of antioxidant compounds. A strong positive correlation ($r>0.800$) between TPC and FRAP was observed. Freeze drying is the most effective method for preserving nutritional and bioactive components, followed closely by cabinet drying, which offers a practical balance between quality retention and processing feasibility.

Keywords: Antioxidant activity, drying methods, fatty acid profile, *Mangifera pajang*, phenolic content

INTRODUCTION

Underutilized plant species are used because they are considered less important than staple foods in terms of global production and market value (Gosh *et al.*, 2023). However, many of these underutilized foods have high nutrient density and can be grown with minimal agricultural inputs. In addition, fruit by-products, such as seeds and peels, are naturally rich in antioxidants due to their phenolic components. The peel and seed of the bambangan fruit (*Mangifera pajang*) are rich in antioxidants and phytochemicals such as polyphenols, flavonoids, carotenoids, and anthocyanins, which help neutralize free radicals and have the potential for nutraceutical and functional food applications (Jahurul *et al.*, 2019a & 2019b). Bambangan seeds contain 7.67 - 11.00% fat, 3.08 - 4.10 % protein, and 38.68 - 72.90% carbohydrates, making them a nutritious food source (Jahurul *et al.*, 2018a; Norazlina *et al.*, 2021). The seeds are a potential ingredient for nutraceutical and functional foods. Due to their nutritional content and antioxidant properties, bambangan seeds can be used in the development of functional foods by incorporating them into foods, which can enhance their health-promoting properties (Kalsum & Mirfat, 2014; Jahurul *et al.*, 2018b).

However, post-harvest preservation is essential to maintain their quality, and drying is a common method used for this purpose. While various drying processes have been extensively studied in other fruits, their effects on the composition of bambangan seeds are still unexplored. Drying is a common preservation technique that reduces moisture content and transforms perishable fruits and vegetables into

stable, shelf-stable powders suitable for functional food applications (Lalita & Jiradech, 2016; Abebe & Gesessew, 2021; Fernandes *et al*., 2025). While drying improves storage, transportation, and year-round availability, it can also significantly impact the retention of bioactive compounds and nutrients. Common drying methods include sun drying (SD), oven drying (OD), cabinet drying (CD), microwave drying (MD), and freeze-drying (FD). Each method differs in heat transfer mechanisms, energy efficiency, and effects on food matrices.

Among these, SD is cost-effective and widely used in tropical regions such as Malaysia (Nazirah *et al*., 2024). The drying process is through natural solar radiation and ambient air flow. OD and CD offer reliable moisture reduction at relatively low cost. OD uses hot air convection in a controlled chamber to uniformly remove moisture, whereas CD employs a controlled chamber with forced air circulation and adjustable airflow. MD provides faster drying rates and more uniform energy distribution (Özkan *et al.,* 2018). This is achieved by electromagnetic waves that generates internal heating through molecular vibration of water, promoting rapid moisture removal while minimizing nutrient and antioxidant loss due to shorter exposure time. FD is often considered the most effective method for preserving nutrients and bioactive components (Lalita & Jiradech, 2016). It involves freezing the sample followed by sublimation of ice under vacuum, bypassing the liquid phase. This process is gentle, preserving heat-sensitive compounds, resulting in a porous, lightweight product with excellent rehydration properties.

Given the growing demand for high-quality, nutrient-rich foods, improving drying methods has become a key focus in food processing research. Although numerous studies have reported the effects of various drying methods on the quality of fruits and vegetables (Özkan *et al*., 2018; Adugna *et al*., 2020; Abebe & Gesessew, 2021; Sundar *et al*., 2024), there is a lack of research on the drying behavior of bambangan seed and its implications for functional food development. This study addresses that gap by evaluating how different drying techniques influence the nutritional and antioxidant properties of bambangan seed and its fat. Specifically, it aims to assess the effects of the five drying methods (SD, OD, CD, MD, and FD)

on the proximate composition, fatty acid content, TPC, and antioxidant capacity of bambangan seed and its fat. This study reports the effects of different drying methods on the nutritional composition and antioxidant properties of bambangan seed and its fat, offering valuable insights for optimizing its processing into value-added functional ingredients.

MATERIALS AND METHODS

Materials

Ripe bambangan fruits were collected from Tuaran, Sabah (Malaysia). Chemicals and reagents used for the analyses included ferric chloride, gallic acid, hexane (analytical grade), n-hexane (GC-grade), hydrochloric acid, Kjedahl tab, methanol (analytical and LC-MS grade), sodium carbonate, sulphuric acid, sodium hydroxide, sodium acetate trihydrate and 2,4,5-tripridyl-s-triazine (TPTZ) were sourced from Sigma (USA) and were of the highest purity available.

Preparation of Bambangan Seed Powder (BSP) from Various Drying Methods

The peel and flesh of the bambangan fruit (Figure 1) were manually removed using a stainless-steel household knife. The seeds were thoroughly rinsed with distilled water to remove residual flesh and then cut into uniform pieces (1 cm × 2 cm × 0.2 cm). The seeds were dried according to the method described by Banerjee *et al.* (2016), Dorta *et al.* (2012), and Jahurul *et al.* (2019). The dried seeds were ground into powder form using a grind mill (MX898M, Panasonic, Malaysia) and sieved to obtain uniform particle size (<250 μm). The drying treatments applied were as follows:

Sun Drying (SD) Treatment

The seeds were spread in a single layer on stainless steel trays and covered with a fine mesh to protect them from insects and debris. Drying was conducted under ambient outdoor temperature (28-35 ℃) for 72 hours with 8 hours of direct sun exposure per day. Samples were turned twice daily to ensure uniform drying and prevent fungal growth.

Cabinet Drying (CD) Treatment

Drying was conducted using a cabinet dryer (TD-1200, Thermoline, AUS) at a set temperature of 60 °C for 24 hours. Seed pieces were placed in a single layer on the stainless-steel trays. The drying continued until the samples reached constant weight

Oven Drying (OD) Treatment

Samples were dried in a convection oven (Binder ED 115, Binder, Germany) at 60 °C for 24 hours. Seed samples were spread evenly in a single layer on aluminum trays. The oven provided natural air circulation, and samples were not disturbed during the process. Moisture content was monitored to ensure drying was complete once constant weight was obtained.

Microwave Drying (MD) Treatment

Drying was carried out in a domestic microwave oven (Samsung ME9114, South Korea; 900 W maximum power). Seed pieces were arranged in a single layer on a microwave-safe glass plate and exposed to microwave energy at 180 W (20% power level) for 10 minutes. The seeds were turned manually at the 5-minute mark to improve drying uniformity. The microwave had no rotating turntable. Drying was stopped once the sample reached constant weight based on pre-calibrated moisture testing.

Freeze Drying (FD) Treatment

Fresh seed samples were frozen at –20 °C for 24 hours before being freeze-dried in a freeze dryer (Alpha 2-4 LSC plus, CHRIST, Germany) at –40 °C under a vacuum of 0.04 mbar for 48 hours. Dried samples were stored in airtight containers at 4 °C until analysis. Freeze-dried samples were not ground until analysis to minimize oxidation.

(a) Bambangan fruit   (b) Bambangan cross section

Figure 1. Picture of bambangan fruit (a) and its seed cross-section (b)

Extraction of Bambangan Seed Fat (BSF)

The crude BSF was extracted using Soxhlet extraction, following the AOAC (2003) official analysis method with slight modification. 80.00 ± 0.01 g of BSP was extracted in the Soxhlet extractor, using hexane as a solvent at a 1:5 (w/v) ratio, for 8 hours (40 °C). The residual solvent in the extracted BSF was evaporated at 40 °C using a rotary evaporator (4001, HEIDOLPH LABORTA, Germany). The fat was dried in an oven (Binder ED 115, Binder, Germany) at 40 °C for 2 hours. The weight of the extracted BSF was recorded to determine the total fat yield.

Proximate Analysis

The proximate analysis of BSP, including moisture, ash, fat, protein, crude fiber, and carbohydrates, was determined according to the official method of the Association of Official Analytical Chemists (AOAC, 2016). The moisture content was determined using the oven (Binder ED 115, Binder, Germany) drying method (official AOAC method 984.25). In contrast, the fat and ash content were determined using the standard methods of Soxhlet extraction and ashing. The protein content was calculated by determining the nitrogen content and multiplying it by the conversion factor of 6.25. Crude fibre was determined by acid and alkali digestion. The total carbohydrate content was

calculated by difference by subtracting the combined percentages of moisture, ash, fat, protein, and fibre from 100 %.

Fatty Acid Composition of BSF

The fatty acid analysis was conducted following the IUPAC 2.301 method. For the preparation of samples, 0.50 ± 0.01 g of BSF was dissolved in 2.5 ml n-hexane and 0.5 ml of 2N potassium hydroxide in methanol. The resulting mixture was vortexed for 1 minute at 1200 rpm, followed by 10 10-minute settling period. The transparent upper layer was then extracted for analysis. The fatty acid methyl ester (FAMEs) profiles of the blends were analyzed using a DB-23 column (30 m x 0.32µm x 0.25: ID) in a gas chromatography (GC), equipped with a flame ionization detector (GC-2-10, Shimadzu, Japan). Fatty acids were identified under the following conditions: an initial temperature of 90 °C (maintained for 5 minutes), increased at 8 °C/ minute to 185 °C (maintained for 1 minute), and then increased at 2 °C/minute to a final temperature of 250 °C (maintained for 5 minutes). The injector and detector temperatures were set at 250 °C using a split mode (1:20). The elution of the fatty acid methyl ester was determined based on the standard.

Determination of Total Phenolic Content (TPC) and Ferric-Reducing Antioxidant Power (FRAP)

The TPC in BSP and BSF was determined following the Follin-Ciocalteau and FRAP assay described by Jahurul *et al*. (2018b) and Khairy *et al*. (2015). FRAP was measured using the TPTZ reagent and expressed as mmol Fe(II)/100g. Methanol:hexane partitioning was utilized to extract phenolics from seed powder and BSF. The methanolic extract of BSP and BSF was prepared prior to analysis. A total of 2.50 ± 0.01 g of BSF was dissolved in 5 ml of hexane and 5 ml of 60% methanol. The resulting mixture was thoroughly stirred for 1 minute using a vortex. Subsequently, the mixture was centrifuged at 3500 rpm for 10 minutes at 4 °C. The supernatant was collected for further analysis. The TPC of BSP and BSF was expressed as Gallic Acid Equivalents (GAE) per gram of fresh weight. For FRAP, the antioxidant activity of the extracts was assessed based on a calibration curve generated using $FeSO_4 \cdot 7H_2O$. The results were expressed as the concentration of

antioxidants with ferric-reducing ability per gram of bambangan seed extract (µM/g).

Statistical analysis

Analyses were performed in triplicate, with results expressed as means ($\pm$) and standard deviations (SD). SPSS version 29 was used for statistical analysis. A one-way ANOVA was used to test for differences between means, followed by a Tukey's test for comparison. Pearson correlation was used to measure the relationship between TPC and FRAP, with a significance of $p < 0.05$.

RESULTS AND DISCUSSION

Effect of Drying Methods on the Proximate Compositions of Bambangan Seeds

The proximate analysis in Table 1 revealed that the moisture, crude fat, and crude fiber content were significantly ($p < 0.05$) affected by the drying methods. Moisture content was lowest in cabinet drying (CD) (5.57%) and highest in sun drying (SD) (8.63%), indicating that CD is highly effective in moisture removal due to the controlled temperature and consistent air circulation. Moisture content is a crucial parameter that influences the quality and shelf life. The results showed CD exhibited a consistent heating effect, effectively eliminating humid air from the seed surface and facilitating moisture loss, resulting in the lowest moisture content. The lower moisture content is due to controlled heat and air circulation. In contrast, SD prolonged exposure to ambient conditions may result in less effective drying and moisture reabsorption from the environment. However, the slightly high moisture in FD (7.40%) is acceptable given the preservation of heat-sensitive compounds.

These values are generally lower than the 8.90% reported moisture by Jahurul *et al*. (2018a), possibly due to differences in variety, growing conditions, or post-harvest treatment. The results obtained in this study are in agreement with those of Siddiqui *et al*. (2024), who reported that controlled drying environments such as CD and OD effectively reduce moisture content and improve drying efficiency. FD, while resulting in slightly higher moisture content than CD or OD, is known to

preserve heat-sensitive compounds and maintain structural integrity. A trend similarly observed in studies by Mina *et al*. (2024) on carrot slices. In addition, the moisture content found here is consistent with the value of 6.13% reported by Norazlina *et al*. (2020) for bambangan seeds. Compared to other tropical fruit seeds such as jackfruit (10.78%) and avocado (13.09 – 15.10%) (Egbuonu *et al*., 2018; Ejiofor *et al*., 2018), bambangan seeds exhibit relatively low moisture levels, which may contribute to better shelf stability and reduced microbial risk.

Crude fat content was highest in freeze drying (FD) (6.9%), followed by CD (6.70%) and SD (6.18%). Oven drying (OD) (5.17%) yielded the lowest crude fat. The high fat retention in FD samples promotes the ability of the method to preserve thermolabile and volatile lipids without using high temperatures. The fat loss observed in OD samples was presumably due to oxidation or volatilization of fats under prolonged heating. These results align with the findings of Dadhaneeya *et al*. (2023), who reported that FD preserved more lipids in dragon fruit due to the absence of high-temperature exposure, which helps retain sensitive compounds. Similarly, Belwal *et al*. (2022) reported significant lipid degradation in plant-based products subjected to hot air drying. In addition to expressing the fat content as a percentage of the proximate composition, the actual fat yield was determined based on 80 g of the dried seed powder used for extraction. The total fat extracted ranged from 4.14 g (OD) to 5.55 g (FD), corresponding to a fat yield of 5.17% to 6.94% of the lowest and highest fat mass, respectively. Crude fiber content was highest in SD (4.51%), while FD (2.13%) resulted in the lowest fiber content. The higher fiber content in SD samples resulted from the partial degradation or removal of non-fiber components, concentrating the fiber fraction.

On the other hand, FD may retain more intact cellular structures, resulting in slightly lower measurable crude fiber after defatting. This observation aligns with Dadhaneeya *et al*. (2023), who reported that FD preserves cell wall integrity, potentially affecting fiber determination. Ash content showed no significant differences, which is consistent with the general understanding that minerals are non-volatile and resist degradation during thermal processing (Silva *et al*., 2020). However, CD and MD yielded slightly higher ash content

compared to OD, FD, and SD. This variation may be due to differences in heat intensity and exposure duration, where rapid dehydration in CD and MD could lead to greater retention of inorganic matter. Siddiqui *et al*. (2024) similarly reported that while ash content generally remains stable, drying conditions can influence the retention of specific minerals depending on the food matrix and method used.

Protein content is better preserved in SD and FD due to the lower temperatures involved. The chemical reaction between amino acids and reducing sugars typically occurs at elevated temperatures and leads to loss of available protein through complex formation, thus minimizing thermal denaturation and Maillard reactions. In contrast, CD, OD, and MD, which involve high temperatures, showed reduced protein levels. This trend is in line with Siddiqui *et al*. (2024), who emphasized that high-temperature drying methods can lead to protein denaturation and compromised nutritional quality. Although the protein content of the bambangan seed is lower than that of other fruit seeds such as avocado and rambutan, it still offers high-quality protein, as evidenced by its rich amino acid profile (Jahurul *et al*., 2018b). Carbohydrates represented the largest nutrient fraction in bambangan seeds, ranging from 74.82% to 80.00%. This high carbohydrate content plays a key role in influencing the functional and sensory characteristics of the seed-based product, including texture, sweetness, and energy density. Carbohydrates contribute to desirable qualities such as mouthfeel and palatability, which are essential for consumer acceptance in food applications.

Oven Drying (OD) (80.00%) samples had the highest carbohydrate content, likely due to the concentration effect following the removal of other components during drying. SD (74.82%) samples exhibited the lowest carbohydrate content, possibly due to slower dehydration and partial sugar degradation. While prolonged heat exposure can concentrate carbohydrates, excessive heat may alter their structure and digestibility (Siddiqui *et al*., 2024). Overall, CD was effective in reducing moisture content, FD was optimal for fat retention, and SD contributed to higher fiber content, albeit with higher residual moisture, possibly reducing microbial safety. The choice of drying methods should

therefore be tailored to the desired nutritional properties of the final product.

Table 1. Effect of drying on the proximate composition of bambangan seed on a dry basis

Proximate composition	Sun Drying	Cabinet Drying	Oven Drying	Microwave Drying	Freeze Drying (FD)
Moisture (%)	8.63±0.30[a]	5.57±0.45[c]	7.19±0.12[b]	7.49±0.0[b]	7.40±0.13[b]
Fat (%)	6.18±0.06[c]	6.70±0.05[b]	5.17±0.06[d]	6.07±0.05[c]	6.94±0.02[a]
Fat (g per 80 g of dried seeds)	4.94±0.17[c]	5.36±0.09[b]	4.14±0.36[d]	4.86±0.27[c]	5.55±0.33[a]
Ash (%)	2.20±0.37[a]	2.57±0.15[a]	2.45±0.14[a]	2.52±0.22[a]	2.32±0.03[a]
Protein (%)	3.75±0.06[a]	2.87±0.04[c]	2.96±0.06[c]	2.87±0.01[c]	3.34±0.01[b]
Fibre (%)	4.51±0.26[a]	3.06±0.08[b]	2.30±0.15[c]	2.59±0.36[b, c]	2.13±0.05[c]
Carbohydrate (%)	74.82±0.37[d]	79.26±0.06[b]	80.00±0.42[a]	78.60±0.25[b, c]	77.88±0.13[c]

Data are mean value ± standard deviation. Different letter(s) within the row are significant differences according to One-way ANOVA ($p<0.05$).

Effect of Drying Pretreatment on Fatty Acid Compositions of BSF

Nine fatty acids were identified in bambangan seed fat (BSF) (Table 2), with stearic acid (37.29 - 44.68%) and oleic acid (38.71 - 45.53%) being predominant, followed by palmitic, linoleic, and arachidic acids. Long-chain saturated fatty acids (SFAs), such as lignoceric acid, were detected only in SD, CD, OD, and FD samples, with FD and CD showing higher levels of stearic acid. In contrast, oleic and linoleic acid concentrations were lower in heat-based treatments, with CD exhibiting the lowest values. This suggests that prolonged heat exposure likely accelerates oxidation of unsaturated fatty acids (USFAs), resulting in fat degradation (Mokhtar *et al*., 2018). FD samples exhibited nearly equal proportions of stearic (41.49%) and oleic (42.49%) acids, whereas CD samples exhibited a stearic acid (44.68%) dominance, indicating a shift toward a more saturated profile. This is reflected in the total SFA content, which was highest in CD, followed by FD.

On the other hand, OD, MD, and SD samples retained higher USFA concentrations (Figure 2). This variation in fatty acid profiles likely arises from oxidative degradation of USFAs, which generates volatile by-products and reduces nutritional value (Wang *et al*., 2020). These findings are consistent with Hurtado-Ribeira *et al*. (2023a), who reported significant changes in fat integrity due to drying and defatting techniques in BSF. Their study found that OD preserved fat stability better than FD, while FD caused increased free fatty acid levels due to enhanced lipolysis. They also noted that thermal drying reduced both moisture and free fatty acid levels, thereby improving fat stability. This supports the current findings, where CD and FD, despite contrasting thermal mechanisms, led to higher SFA and lower USFA contents, reflecting modified fat quality.

Moreover, Hurtado-Ribeira *et al*. (2023b) also reported that freeze-drying combined with mechanical pressing, although efficient for fat extraction, increased free fatty acid and moisture content, potentially compromising fat stability. This aligns with our observation that FD samples retained some USFAs but showed signs of oxidative deterioration. Compared to mango seed fat, which contains 6.67 – 7.71% palmitic acid, 42.27 – 48.23% stearic acid, 32.91 – 41.41% oleic acid, and 5.51 – 5.97% linoleic acid (Jahurul *et al*., 2018c; Jin *et al*., 2017), BSF fat exhibits a higher oleic acid and lower stearic acid content. These differences demonstrates the influence of both botanical origin and post-harvest processing on fatty acid profiles.

Table 2. Effect of drying on the fatty acid composition of bambangan seed fat.

Fatty acid (%)	Sun Drying	Cabinet Drying	Oven Drying	Microwave Drying	Freeze Drying
Saturated fatty acids (SFAs)					
Palmitic (C_{16})	7.74 ± 0.03^a	$8.17 \pm 0.02^{c,d}$	8.13 ± 0.02^c	8.23 ± 0.00^d	7.86 ± 0.05^b
Stearic (C_{18})	38.60 ± 0.00^c	44.68 ± 0.01^e	37.29 ± 0.05^a	37.80 ± 0.00^b	41.49 ± 0.01^d
Arachidic (C_{20})	1.83 ± 0.02^a	2.38 ± 0.01^c	1.93 ± 0.02^b	$1.87 \pm 0.03^{a,b}$	$1.87 \pm 0.03^{a,b}$
Behenic (C_{22})	0.31 ± 0.00^a	0.41 ± 0.01^d	0.34 ± 0.00^c	$0.32 \pm 0.00^{a,b}$	$0.33 \pm 0.00^{b,c}$
Lignoceric (C_{24})	0.53 ± 0.03	0.84 ± 0.00	0.65 ± 0.00	-	0.57 ± 0.00
Unsaturated fatty acids (USFAs)					
Oleic ($C_{18:1}$)	45.53 ± 0.02^e	38.71 ± 0.02^a	45.07 ± 0.02^d	44.03 ± 0.03^c	42.49 ± 0.01^b
Linoleic ($C_{18:2}$)	5.07 ± 0.01^b	4.51 ± 0.01^a	6.08 ± 0.01^d	6.82 ± 0.01^e	5.14 ± 0.00^c
Linolenic ($C_{18:3}$)	0.23 ± 0.02^a	0.21 ± 0.00^a	0.32 ± 0.00^c	0.28 ± 0.00^b	0.27 ± 0.04^b
Paullinic acid ($C_{20:1}$)	0.14 ± 0.00^c	0.93 ± 0.00^a	0.15 ± 0.00^d	0.14 ± 0.00^c	0.13 ± 0.02^b

Data are mean value ± standard deviation. Different letter(s) within the row are significant differences according to One-way ANOVA ($p<0.05$).
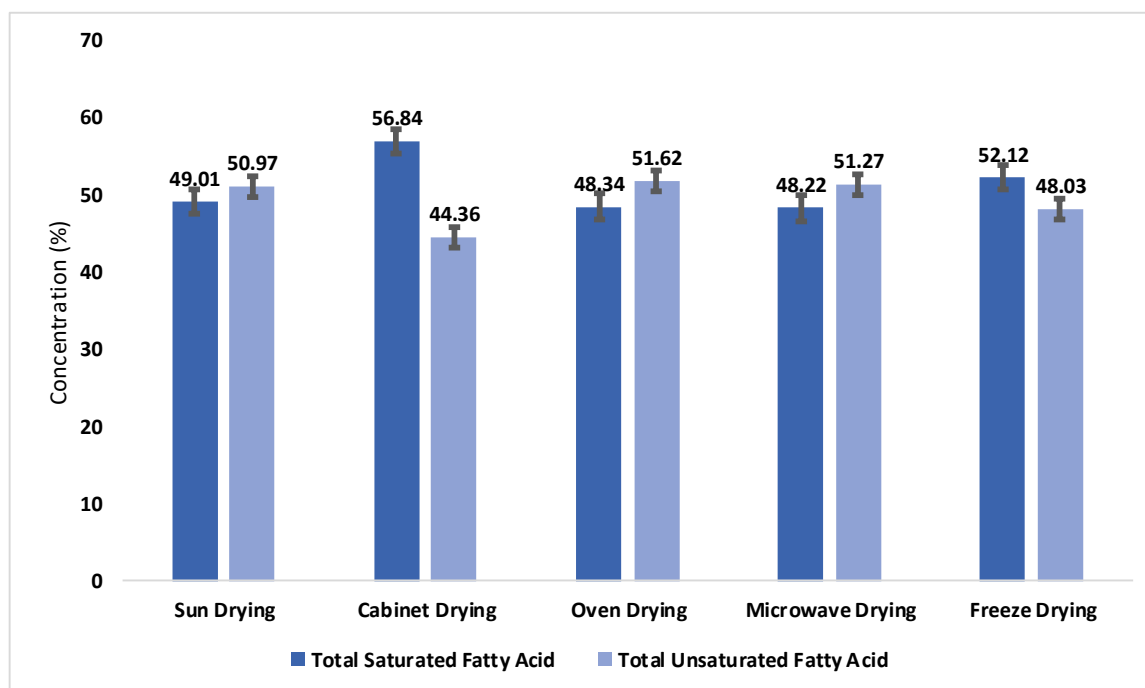
Figure 2. Effect of drying method on total saturated fatty acid and unsaturated fatty acids of bambangan seed fat

Effect of Drying Pretreatment on the Phenolic Content and FRAP

Polyphenolic compounds are key contributors to the antioxidant capacity of fruits and vegetables, protecting against oxidative stress (Borlace *et al*., 2024). In this study, FD samples exhibited the highest phenolic content, with values of 83.90 mg GAE/g for BSP and 62.43 mg GAE/g for BSF. CD retained moderate phenolic levels, whereas OD, MD, and SD led to significantly ($p<0.05$) lower TPC values (Table 3). The reduced TPC in MD samples was due to the rapid and intense heat exposure, causing degradation or polymerization of thermolabile compounds. Similarly, SD resulted in low TPC,

attributed to enzymatic degradation and potential microbial activity during prolonged exposure to ambient conditions (Mansour, 2016; Zeidvand *et al.*, 2024). OD, although more economical, showed limited phenolic retention, especially compared to FD, which is known for preserving heat-sensitive bioactives. Across all treatments, TPC values were consistently lower in BSF than BSP, indicating that Soxhlet extraction may degrade some heat-sensitive phenolics (Jouki *et al.*, 2014). The Soxhlet method requires prolonged heating (8 hours at 40 °C), which can promote oxidation or polymerisation of sensitive compounds, contributing to the lower antioxidant levels observed in BSF. In future work, the use of gentler extraction methods, such as enzyme-assisted, cold-press or supercritical CO_2 methods, could help to better preserve antioxidants and unsaturated fatty acids.

These findings are in line with recent studies. An investigation on *Capparis spinosa* L. (caper fruit) reported that FD was most effective in preserving phenolic content and antioxidant activity (Babaei Rad *et al.*, 2025). In addition, a study on *Moringa oleifera* leaf waste found that tray drying, a method comparable to CD, preserved more phenolics and flavonoids than SD, with strong correlation to antioxidant activity (Irwansyah *et al.*, 2020). Research on agarwood (*Aquilaria malaccensis*) also concluded that controlled drying techniques (dehydrator and air-drying) were better than SD for retaining phenolic compounds (Delica-Balagot *et al.*, 2024), reinforcing the advantage

of CD and FD over uncontrolled methods. The ferric reducing antioxidant power (FRAP) values also followed a similar trend and were significantly different across drying methods (p<0.05). FD yielded the highest antioxidant activity (129.52 ± 0.67 mmol Fe (II)/100 g extract), followed by CD, SD, OD, and MD.

Notably, BSF samples had lower FRAP (73.62 - 102.41 mM/100g) values than BSP (116.86 - 129.52 mM/100g), supporting the hypothesis that the fat matrix undergoes greater oxidative degradation during drying and extraction, especially under thermal conditions. A strong positive correlation (r>0.800) between TPC and FRAP in BSP confirms the central role of phenolics as contributors to antioxidant activity. Across drying methods, BSP consistently retained more phenolic and antioxidant compounds than BSF. This can be explained by the inherently higher concentration of polyphenolics in the seed powder matrix, which offers greater protection compared to the fat fraction that is more prone to oxidative deterioration. FD proved most effective in preserving antioxidant properties in both BSP and BSF. However, the high energy demands and operational costs limit its scalability for industrial applications. Cabinet drying, which demonstrated moderate yet stable retention of bioactive compounds, presents a more viable alternative for large-scale processing due to its balance between performance and cost-efficiency.

Table 3. Effect of drying on the antioxidant parameters of bambangan seed powder (BSP) and bambangan seed fat (BSF).

Drying methods	BSP		BSF	
	Total phenolic contents (mg GAE/g)	FRAP values (mM/100g)	Total phenolic Contents (mg GAE/g)	FRAP values (mM/100g)
Sun Drying	79.27±0.01[a]	117.17±1.63[b]	48.45±1.24[b]	86.70±0.11[c]
Cabinet Drying	80.43±0.38[b]	126.44±0.31[c]	56.12±0.19[d]	94.23±0.61[d]
Oven Drying	79.18±0.22[a]	116.89±3.13[a]	45.62±0.14[a]	85.29±0.04[b]
Microwave Drying	79.27±1.32[b]	116.86±1.92[a]	54.70±6.67[c]	73.62±0.57[a]
Freeze Drying	83.90±0.09[c]	129.52±0.67[d]	62.43±0.11[e]	102.41±0.06[e]

Data are mean value ± standard deviation. BKP: bambangan kernel powder, BKF: bambangan kernel fat, GAE: gallic acid equivalent. Different letters (a-e) within the column are significant differences according to One-way ANOVA (*p<0.05*).

CONCLUSIONS

This study examined the effects of different drying methods on the nutritional composition, fatty acid profile, and antioxidant properties of bambangan (*Mangifera pajang*) seed powder (BSP) and bambangan seed fat (BSF). FD was the most effective method for preserving nutrients, phenolic compounds, and antioxidant capacity, followed closely by CD. Both FD and CD caused minimal thermal degradation, resulting in better retention of fat and protein content. Although SD yielded the highest crude fibre content and is economically viable, it showed reduced antioxidant activity and total phenolic content. OD and MD were less favourable due to greater nutrient losses caused by prolonged or intense heat exposure. The BSF was found to be rich in stearic and oleic acids, indicating its potential as a functional fat source. A strong positive correlation between total phenolic content and antioxidant capacity (FRAP) supports the use of bambangan seed-derived products as natural antioxidant ingredients. These results demonstrate that bambangan seeds can serve as a nutrient ingredient for functional food development, particularly when processed using FD or CD to retain nutritional and bioactive properties. Further research is recommended to optimize drying parameters and evaluate the performance of BSP and BSF in food formulations, including their sensory attributes and shelf-life stability. This will contribute to the value-added utilization of bambangan seeds as a functional component in food applications.

ACKNOWLEDGEMENTS

REFERENCES

Akeemana, C., Wickramasinghe, I. & Wanniarachchi, T.V. (2022). Effect of drying and frying pre-treatment on nutrient profile, antioxidant capacity, cooking time, and sensory acceptability of easy to cook jackfruit. *Applied Food Research*, *2*(2*)*, 100234. https://doi.org/10.1016/j.afres.2022.100234

Abebe, D. & Gesessew, K. (2021). Effect of pretreatment and drying methods on the quality of acnhote (*Coccinia abyssinica* (Lam.) Flour. *Journal of Food Quality,* 2021(1), 1-14. https://doi.org/10.1155/2021/3183629

Adugna, M.B., Yetenayet, T., Tarekegn, B.E. & Sirawdink, F.F. (2020). Effect of predrying treatment and drying temperature on proximate composition, mineral contents, and thermophysical properties of anchote (*Coccinia abyssinica* (Lam.) Cogn.) flour. *Food Science and Nutrition,* 8 (10), 5532-5544. https://doi.org/10.1002/fsn3.1860

AOAC International. (2016). *Official methods of analysis of AOAC International* (20th ed.). Washington, DC: AOAC International.

AOAC, *Official Methods of Analysis*. (2003). Association of Analytical, Washington, DC, USA, 17 edition.

Babaei Rad, S., Mumivand, H., Mollaei, S. & Khadivi, A. (2025). Effects of drying methods on phenolic compounds and antioxidant activity if *Capparis spinosa* L. fruits. *BMS Plant Biology,* 25: 133. https://doi.org/10.1186/s12870-025-06110-y

Belwal, T., Cravotto, C., Prieto, M. A., Venskutonis, P. R., Daglia, M., Devkota, H. P. & Cravotto, G. (2022). Effects of different drying techniques on the quality and bioactive compounds of plant-based products: a critical review on current trends. *Drying Technology*, 40(8), 1539–1561. https://doi.org/10.1080/07373937.2022.2068028

Borlace, G.N., Sringam, P., Thongkham, E. & Aiemsaard, J. (2024). Antioxidant activity and antibacterial effects of *Boesenbergia rotunda* extract against *Staphylococcus pseudintermedius* isolates from canine superficial pyoderma. *Songklanakarin Journal of Science and Technology,* 46(4), 355-361.

Banerjee, J., Patti, A. F., Vijayaraghavan, R., Singth, R., MacFarlane, D. & Arora, A. (2016). Effect of drying methods and extraction time-temperature regime on mango kernel lipids. *International Journal of Food and Nutritional Science,* 3(2): 1-10.

Delica-Balagot, K., Halasan, H.G.M., Martinez, C.M.J., Collera, J.J.A., Balagot, K.W.M., Kamantigue, E.C., Semano, F.B. & Lapuz, R.B. (2024). Effect of drying methods on the phenolic

compounds and antioxidant activity of leaf of agarwood (*Aquilaria malaccencis* Lam.). *Phillipines Journal of Science,* 153, 1217-1225

Dadhaneeya, H., Kesavan, R.K., Inbaraj, B.S., Sharma, M., Kamma, S., Nayak, P. & Sridhar, K. (2023). Impact of different drying methods on the phenolic composition, in vitro antioxidant activity, and quality attributes of dragon fruit slices and pulp. *Foods*, 12 (7), 1387. https://doi.org/10.3390/foods12071387

Dorta, E., Lobo, M. G. & González, M. (2012). Using drying treatments to stabilise mango peel and seed: Effect on antioxidant activity. *LWT - Food Science and Technology*, 45(2): 261-268. https://doi.org/10.1016/J.LWT.2011.08.016

Egbuonu, A. A. C., Opara, I. C., Onyeabo, C. & Uchenna, N. O. (2018). Proximate, functional, Antinutrient and antimicrobial properties of avocado pear (*Persea americana*) seeds. *Journal of Nutritional Health & Food Engineering,* 8(1). DOI: 10.15406/jnhfe.2018.08.00260

Ejiofor, N., Ezeagu, I., Ayoola, M. & Umera, E. (2018). Determination of the Chemical Composition of Avocado (*Persea Americana*) Seed. *Advances in Food Technology and Nutritional Sciences,* 2, 51-55. DOI:10.17140/AFTNSOJ-SE-2-107

Fernandes, S.S., Peraza, C.C., Marasca, N.S. & Egea, M.B. (2025). Effect of drying methods on the nutritional composition, technofunctional properties, and phytochemicals of kumquat (*Fortunella margarita*). *Journal of Food Composition and Analysis,* 13: 107618. https://doi.org/10.1016/j.jfca.2025.107618

Ghosh, S., Sarkar, T. & Chakraborty, R. (2023). Underutilized plan sources: A hidden treasure of natural colors. *Food Bioscience,* 52: 102361. https://doi.org/10.1016/j.fbio.2023.102361

Hurtado-Ribeira, R., Villanueva-Bermejo, D., Rodríguez García-Risco, M., Hernández, M. D., Sánchez-Muros, M. J., Fornari, T., Vázquez, L. & Martin, D. (2023). Evaluation of the interrelated effects of slaughtering, drying, and defatting methods on the composition and properties of black soldier fly (Hermetia illucens) larvae fat. *Current Research in Food Science*. https://doi.org/10.1016/j.crfs.2023.100633

Hurtado-Ribeira, R., Hernández, D. M., Villanueva-Bermejo, D., García-Risco, M. R., Hernández, M. D., Vázquez, L., Fornari, T. & Martin, D. (2023b). The Interaction of Slaughtering, Drying, and Defatting Methods Differently Affects Oxidative

Quality of the Fat from Black Soldier Fly (*Hermetia illucens*) Larvae. *Insects*, *14*(4), 368. https://doi.org/10.3390/insects14040368

Iwansyah, A. C., Manh, T. D., Andriana, Y., Aiman bin Hessan, M., Kormin, F., Cuong, D. X., Xuan Hoan, N., Thai Ha, H., Thi Yen, D., Thinh, P. V., The Hai, L. & Ngoc Minh, T. (2020). Effects of various drying methods on selected physical and antioxidant properties of extracts from *Moringa oliefera* leaf waste. *Sustainability*, 12(20): 8586. https://doi.org/10.3390/su12208586

Jouki, M., Mortazavi, S.A., Yazdi, F.T. & Koocheki, A. (2014). Optimization of extraction, antioxidant activity and functiona properties of quince seed mucilage by RSM. *International Journal of Biological Macromolecules,* 66: 113-124. DOI: 10.1016/j.ijbiomac.2014.02.026

Jahurul, M.H.A., Zaidul, I.S.M., Leykey, B., Sharifudin, M.S., Siddiquee, S., Hasmdi, M., Sahena, F., Mansoor, A.H., Lee, J.S. & Jinap, S. (2019a). Valuable components of bambangan fruit (Mangifera pajang) and its co-products: A review. Food Research International, 115, 105-115. DOI: 10.1016/j.foodres.2018.08.017

Jahurul, M., Ying, L., Amir, H., Azzatul, F., Sharifudin, M., Hasmadi, M., Lee, J., Mansoor, A., Jumardi, R., Matanjun, P., Firoz Khan, M. & Zaidul, I. (2019b). Effects of drying methods on the characteristics of rambutan (*Nephelium lappaceum L.*) seed fat: An optimisation approach. *Engineering Reports,* 1(3). https://doi.org/10.1002/eng2.12050

Jahurul, M.H.A., Soon, Y., Sharifudin, M.S., Hasmadi, M., Mansoor, M., Zaidul, I.S.M., Lee, J.S., Ali, M.E., Ghafoor, K., Zzaman, W., & Jinap, S. (2018a). Bambangan (*Mangifera pajang*) kernel fat: a potential new cocoa butter alternative. *International Journal of Food Science and Technology,* 53(7): 1689-1697.

Jahurul, M. H. A., Leykey, B., Sharifudin, M. S., Hasmadi, M., Zaidul, I. S. M., Jinap, S. (2018b). Optimization of fat yield of bambangan (*Mangifera pajang*) kernel using response surface methodology and its antioxidant activities. *Journal of Food Measurement and Characterization,* 12: 1427–1438. DOI: 10.1007/s11694-018-9758-8

Jahurul, M.H.A., Zaidul, I.S.M., Sahena, F., Sharifudin, M.S., Norulaini, N.N., Eaqub, M.A., Hasmadi, M., Ghafoor, K., Wahidu, Z., Omar, A.K.M. 2018c. Physicochemical properties of cocoa butter replacers from supercritical carbon dioxide extracted mango seed fat and palm oil mid

fraction blends. *International Food Research Journal, 25*(1), 143-149.

Jin, J., Wang, Y., Su, H., Warda, P, Xie, D. & Liu, Y. 2017. Oxidative stabilities of mango kernel fat fractions produced by three-stage fractionation. *International Journal of Food Properties,* 20 (11): 2817-2829.https://doi.org/10.1080/10942912.2016.1253096

Khairy. H, L., Yang, T. A. & Saadoon. A, F. (2015). Study on color and antioxidant properties of rambutan seed fat as cocoa butter alternative. *International Journal on Advanced Science, Engineering and Information Technology,* 5(2): 90.DOI: 10.18517/ijaseit.5.2.487

Kalsum, H. Z. U., & Mirfat, A. H. S. (2014). Proximate composition of Malaysian underutilised fruits. *Journal of Tropical Agriculture and Food Science,* 42(1): 63–72.

Lalita, S. & Jiradech, M. (2016). Effect of drying methods on dietery fiber content in dried fruit and vegetable from non-toxic agricultural field. *International Journal of GEOMATE,* 11 (28): 2896-2900. DOI: 10.21660/2016.28.1372

Mina,Z.P., Kaseke, T., Fadiji, T., Silue, Y. & Fawole, O.A. (2024). Combined oven/frozen drying as a cost and energy-efficint drying method for preserving quality attributes and volatile compounds of carrot slices. *Frontiers in Horticulture,* 3: 1447957. DOI: 10.3389/fhort.2024.1447957

Mokhtar, S.M., Swailam, H.M. & Embaby, H. (2018). Physicochemical properties, nutritional value and techno-functional properties of goldenberry (*Physalis peruviana)* waste powder concise title: composition of goldenberry juice waste. *Food Chemistry,* 248: 1-7.

Mansour, R. (2016). Effects of drying process on total phenolics, and flavonoids content of *Thyme vulgaris* extract. *International Journal of ChemTech Research.* 9(5): 632-63.

Nazirah, M., Khairee, M.S., Hasmadi, M., Md Shafiquzzaman, S., Mphd Hafiz, A.M. & Moha Sani, S. (2024). Comparative study of drying methods on seaweeds (*Kappahycus* sp., and *Padina* sp.) based on their phytochemical and polysaccharaide content located in Sabah. *Borneo Journal of Resource Science and Tehcnology, 14* (1): 112-122. https:doi.org/10.33736/bjrst.6089.2024

Norazlina, M.R., Jahurul, M.H.A., Hasmadi, M., Sharifudin, M.S., Patricia, M., Mansoor, A.H. & Lee, J.S. (2020). characteristics of bambangan kernel fat fractions produced by solven fractionation and their potential industrial applications. *Journal of Food Processing and Preservation,* 44(6), e14446.https://doi.org/10.1016/j.lwt.2021.112556

Norazlina, M.R., Tan, Y.S., Hasmadi, M. & Jahurul, M.H.A. (2021). Effect of solvent pre-treatment on the physicochemical, thermal profiles and morphological behavior of *Mangifera pajang* seed fat. *Heliyon,* 7, e08073. https://doi.org/10.1016/j.heliyon.2021.e08073

Özkan Karabacak, A., Suna, S., Tamer C.E. & Çopur, Ö.U. (2018). Effects of oven, microwave and vacuum drying on drying characteristics, colour, total phenolic content, and antioxidant capacity of celery slices. *Quality Assurance and Safety of Crops & Foods, 10*(2), 193-205.DOI: 10.3920/QAS2017.1197

Mohamad, S., Mohd Said, F., Abdul Munaim, M., Mohamad, S. & Wan Sulaiman, W. (2019). Proximate composition, mineral contents, functional properties of Mastura variety jackfruit (*Artocarpus heterophyllus*) seeds and lethal effects of its crude extract on zebrafish (*Danio rerio*) embryos. *Food Research, 3*(5), 546-555. DOI: 10.26656/fr.2017.3(5).095

Sagar, V.R. & Suresh Kumar, P. (2010). Recent advances in drying and dehydration of fruits and vegetables: a review. *Journal of Food Science and Technology, 47,* 15–26. doi: 10.1007/s13197-010-0010-8

Siddiqui, S.A., Ucak, I., Jain, S., Elsheikh, W., Redha, A.A., Kurt, A. & Toker, O.S. (2024). Impact of drying on techno-functional and nutritional properties of food proteins and carbohydrates - A comprehensive review. *Drying Technology,* 42, 592-611. doi: https://doi.org/10.1080/07373937.2024.2303580

Silva, J.S., Ortiz, D.W., Garcia, L.G.C., Asquieri, E.R., Becker, F.S. & Damiani, C. (2020). Effect of drying on nutritional composition, antioxidant capacity and bioactive compounds of fruits co-products. *Food Science and Technology,* 40, 810-816.https://doi.org/10.1590/fst.21419

Sundar, S., Singh, B. & Kaur, A. (2024). Microwave roasting effects on phenolic, tocopherol, fatty acid and phytosterol profiles, physicochemical, oxidative and antioxidant properties of hemp seed

oil. *Food Chemistry Advances,* 4: 100596. https://doi.org/10.1016/j.focha.2023.100596

Qixing, J., Zhengran, M., Shuoshuo, W., Yanshun, X., Fengyu, T., Xueqin, X. & Wenshui, X. (2014). Effect of temperature on protein compositional of big head carp (*Aristichtys nobilis*) muscle and exudates. *Food Science and Technology Research*, 20(3): 655-661.https://doi.org/10.3136/fstr.20.655

Wang, D., Javed, H.U., Shi, Y., Naz, S., Ali, S. & Duan, C.Q. (2020). Impact of drying method on the evaluation of fatty acids and their derived volatile compounds in 'Thomson Seedless' Raisins. *Molecules.* 25: 608. https://doi.org/10.3390/molecules25030608

Zeidvand, S., Movahhed, S., Chenarbon H.A., Rajaei, P. (2024). Encapsulation of felty germander (*Teucrium polium* L.) extract using the freeze-drying method. *Food Science & Nutrition,* 12: 4899-4913. https://doi.org/10.1002/fsn3.4136

Brown Banana Leaf (*Musa x paradisiaca*) Improve *Betta splendens* Hatching, Larvae, Survival and Growth Performance While Affecting its Sex Ratio

NOR IZATY ASRA-ASWADI[1], IVAN CHONG CHU KOH[2], MUHAMMAD YAZED ABDUH[1], MOHD AZRUL-LOKMAN[3] & NOR HAKIM NORAZMI-LOKMAN*[1]

[1]Aquaculture Innovation and Empowerment Research Interest Group, Faculty of Fisheries and Aquaculture Sciences, Universiti Malaysia Terengganu, 21300 Kuala Nerus, Terengganu, Malaysia; [2]Institut Penyelidikan Marin Borneo, Universiti Malaysia Sabah, 88400 Kota Kinabalu, Sabah; [1]Faculty of Food Science and Agrotechnology, Universiti Malaysia Terengganu, 21300 Kuala Nerus, Terengganu, Malaysia
*Corresponding author: lokhakim@umt.edu.my

ABSTRACT

The effectiveness of brown banana leaf (BBL) *Musa x paradisiaca* as a culture media for rearing *Betta splendens* larvae was investigated. Larvae (n=630, 3 days old, 6 replicates) were reared in 7 rearing medium; C1 (no leaf, control), C2 (0.7 g brown catappa leaf, positive control), T1 (0.7 g; Treatment 1), T2 (0.8 g; Treatment 2), T3 (0.9 g, Treatment 3), T4 (1.0 g, Treatment 4) and T5 (1.1 g, Treatment 5) of BBL per litre of rearing water respectively. Throughout the 80 days trial period, larvae were first fed microworms twice daily for two weeks, then Artemia for another two weeks, followed by ad libitum feeding of commercial feed twice daily. Water quality was monitored every two days, and water was changed every two weeks. The hatching rate, survival, growth parameters and sex ratio were determined after 80 days. There were significant differences (P<0.05) in all the parameters observed. The highest hatching and survival rates were found in treatment C2 (95.86%; 95.56%) and T5 (95.63%; 95.56%). For treatment T1, T2, T3 and T4, the hatching (HR) and survival rate (SR) was 85.75±7.31% (HR), 68.89±13.11% (SR); 75.54±2.04% (HR),76.67±15.64% (SR); 89.76±0.587% (HR), 74.44±22.08% (SR) and 92.63±2.23% (HR), 61.11±6.56% (SR) respectively. The lowest percentage of hatching rate was shown by C1 at 68.08±1.089% while the lowest survival rate was shown by T4. The highest specific growth rate (SGR) was T3 (6.00±0.34% day^{-1}) (weight) and T5 (3.45±0.10% day^{-1}) (length). The SGR for C2, TI, T2 and T4 was recorded at 5.837±0.34, 5.857±0.5, 5.81±0.429 and 5.612±0.243 % day^{-1} respectively. The sex ratios were skewed in 2 treatments; T1 (12 male: 19 female) and T5 (19 male: 9 female) with the rest showing no significant difference to the 50:50 (M:F) ratio. Hatching rate, SGR and sex ratio was not recorded for C1 as all larvae reached 100% mortalities after two weeks of the rearing trials. Based on the result, it is safe to conclude that BBL is a good and safe alternative/replacement to catappa leaf for usage in the aquaculture industry.

Keywords: Larvae culture, Ornamental fish, Phytochemicals

INTRODUCTION

Ornamental fish industry is a global multimillion dollar business (dos Anjos *et al*., 2009) worth USD15 to USD30 billion per year (Evers *et al*., 2019). The Siamese fighting fish (*Betta splendens* Regan, 1910) is one of the popular ornamental species among aquarists and hobbyists especially in Southeast Asia. Based on a simple search across online forums and marketplaces, the price of a single *B. splendens* can reach up to USD 30, depending on the variety. There is no reliable source of information on the exact pricing, as it is highly subjective and market driven. However, a study by Rahmatulloh *et al.* (2023) reported that in Palembang, Indonesia, the highest recorded price for *B. splendens* could reach approximately USD 2,000. In Malaysia, it was reported that the trade value of this species reached RM9.4 million in 2023 (BERNAMA, 2024). Despite its long history in scientific study and commercial culture, *B. splendens* still lacks standardized and effective husbandry and larval nutritional protocols, with only limited peer-reviewed literature available on these aspects (Lichak *et al*., 2022 and Murray *et al*., 2024).

The larvae and juveniles of *B. splendens* are known to be very sensitive and fragile. High mortalities can occur when the rearing environment fails to meet the species' water quality requirements (Kajimura *et al.*, 2023). Nutrition, pathogen, water quality, and stress are aspect that contributes to larval survival (Herath & Atapaththu, 2012). One of the key factors influencing *B. splendens* culture is water quality, as this species prefers slightly acidic conditions (Watson *et al.*, 2019). Farmers commonly use catappa leaves (*Terminalia catappa*) in the rearing medium as they are considered eco-friendly due to their high content of phenolic compounds and tannins (Annegowda *et al.*, 2010), which lower water pH and create a calmer environment resembling the fish's natural habitat (Ashraf & Bengtson, 2007). In addition, catappa leaves are known for their antimicrobial properties, which help protect fish from pathogens (Chitmanat *et al.*, 2003; Neelavathi *et al.*, 2013). However, since the plant grows mainly in coastal areas (Mallik *et al.*, 2013), farmers and breeders especially those where their farm location are far from coastal areas used brown banana leaf (*Musa spp.*), a much more accessible plant that can be found almost everywhere as an alternative to Catappa leaf in *B. splendens* cultivation.

Banana plant is a species that has many cultivars (Calberto *et al.*, 2015), are traded and consumed worldwide. According to Kema *et al.* (2021), in Southeast Asia, banana plants are abundant and being grown in backyards or home gardens for domestic consumption. Aside from its major use as food (banana fruit) for humans and animal farming, several literatures have reported that other portions of this plant have the potential to be utilized in aquaculture as a natural treatment to assist/increase productivity. In Vietnam, farmers used banana leaf from various cultivars as feed for fish cultured in ponds (Dongmeza *et al.*, 2009). In Rohu (*Labeo rohita*) aquaculture, banana peels and banana peel flour from *M. acuminata* were given as feed and have showed a positive impact on growth performance, increment in survival rate, and increase immunity against *Aeromonas hydrophila* (Giri *et al.*, 2016). There is also a report on the application of banana leaf as substrate in breeding *B. splendens* where the percentage of fry survival is higher compared to rigifoam and polythene (Rajapakshe *et al.*, 2020).

Till date, no study has been systematically done to explore and optimize the potential of brown banana leaf and ensure the safety and efficiency of its usage in ornamental fish culture despite being used by local fish farmers and breeders for quite some time. Previous studies are mostly focused on the benefits as an ingredient in fish feed but not its usage as a rearing medium especially in *B. splendens* larvae culture. Therefore, this study was carried out to determine the effects of brown banana leaf rearing medium on survivability, growth performance, and sex ratio of *B. splendens* larvae thus confirming whether banana leaf can be a good, safe, and sustainable alternative to Catappa leaf.

MATERIALS & METHODS

Location and Ethics Statement

These experiments were conducted at the Quality and General Analysis Laboratory and the Ornamental Fish Breeding Unit Hatchery of the Faculty of Fisheries and Aquaculture Sciences (FSPA), Universiti Malaysia Terengganu and at a private hatchery in Kampung Sungai Deraka, Kuantan, Pahang. Moral and ethical aspect of the research such as animal handling and minimum number of fish needed for valid statistical analysis complied with the Research Ethics Guidelines of Universiti Malaysia Terengganu (2014).

Sample Preparation

Samples of brown banana leaf (BBL) (*Musa x paradisiaca*) were collected from nearby locations at Kuala Nerus (5.3679° N, 103.0472° E), Terengganu (2 km radius from the university campus). The collected samples were transported to the laboratory for taxonomic verification. The leaves were washed with distilled water to remove dirt and other contaminants before being used. Fertilized eggs and larvae used in this experiment were obtained from routine breeding of FSPA hatchery broodstocks.

Experimental Design

A total of five treatments and two controls (6 replicates each) were set in this study. They were: C1 (no leaf), C2 (0.7 g brown catappa leaf (BCL)), T1 (0.7 g BBL), T2 (0.8 g BBL), T3 (0.9

g BBL), T4 (1.0 g BBL) and T5 (1.1 g BBL) per 1 L of rearing water. The concentrations were determined based on the acute lethal toxicity levels of *Musa × paradisiaca* and *T. catappa* extracts on fish, as reported by Yunus *et al.* (2019) and Aswadi (2023). Stock rearing water were prepared by immersing BCL and BBL in leaf form according to the dose of each treatment in freshwater (unchlorinated municipal tap water) for one day prior to usage. This rearing water was then used for the rearing of broodstock and larvae.

To measure the hatching rate in each treatment, 9 pairs of *B. splendens* broodstocks obtained from the hatchery stock were reared in each rearing medium treatment (Total n: 63 pairs, male (3.55±0.06 g in weight; 4.02±0.04 cm in total length) and female (2.10±0.08 g in weight; 3.58±0.06 cm in total length)) using a 2 L plastic aquarium. The aquarium was arranged randomly, and a plastic board were used as a partition to avoid the pairs from seeing other breeding pairs which might influence their breeding behaviour. Observation on the hatching rate was made 48 hours after fertilization of each pairs occurred. Hatching rate (%) was calculated by using the formula: the number of larvae hatched/ number of eggs laid multiplied with 100. Photos of the bubble nest containing eggs was captured and the number of eggs was counted using ImageJ software.

For survival, growth, and sex ratio observation, 630 larvae aged three days after hatch (from the breeding trials) were used in this rearing trial. They were randomly selected and distributed evenly (15 larvae per treatment) into 3 litres plastic tanks each containing the specified amount of BBL and BCL.

For the first two weeks of the experiment, larvae were given microworms that were cultured in the hatchery (twice daily), followed by *Artemia* (Bio-Marine, USA) (twice daily) for the next two weeks. Ad libitum feeding using commercial feed (Sanyu Betta, 30% crude protein) was done twice daily as soon as the larvae reach one month old. Water quality (DO, pH, total ammonia and temperature) were measured every two days and 70% water change was done every two weeks throughout the 80 days rearing trial. The water quality parameters throughout this experiment were maintained as follows: temperature (28 ± 2°C); dissolved oxygen (6.5 ± 0.2 mg/L); pH (7.25 ± 0.30) and total ammonia (0.12 ± 0.1 mg/L) (Norazmi-Lokman *et al.*, 2020).

Survival and Growth Rate

Total numbers of mortality in treatments were counted and recorded every day throughout the 80 days of the experiment. The survival rate was calculated by dividing the total number of fish at the end of the experiment with the total number of fish at the start of the experiment and was them multiplied with 100. Growth rate criteria such as total length and total weight were measured during the initial (day 0) and final day (day 80) of the experiment. The fish were starved overnight and anesthetized before weight and length measurements were taken. Length of the fish was measured using standard ruler meanwhile growth was measured using Savio Mini Digital Scale. Then, mean total length, mean weight gain, body weight gain and specific growth rate were calculated using the following formulas (Mandal *et al.*, 2010):
   a) Mean total length gain (mm)
      = Final total length-Initial total length
   b) Mean weight gain (g)
      = Final body weight- Initial body weight
   c) Body weight gain (%)
      = [(Final body weight – Initial body weight]/ Initial body weight] x 100
   d) Specific growth rate (SGR) length (mm %/day)
      = [(Ln (Final length) – Ln (Initial length))/ Number of days] x 100
   e) Specific growth rate (SGR) weight (g %/day)
      = [(Ln (Final weight) – Ln (Initial weight))/ Number of days] x 100

Sex Ratio

Identification of sex in *B. splendens* for each treatment was carried out by observing commonly known secondary sex characteristics of the species such as their body size, body coloration and the size of fins at the end of the experiment (Day 80) (Table 1).

Table 1. Secondary characteristics in differentiation of male and female

Characteristics	Male	Female
Colour	Brightly coloured	Subdued in colour
Fins	Long and flowing	Short
Body shape	Slim and narrow	Short and wider
Opercular membrane	Large and visible without flaring	Small and only visible during flaring
Ovipositor spot	Do not have	Have egg spot between ventral and anal fins

Data Analysis

Statistical analysis was performed using SPSS software version 25. The results were expressed as mean ± standard deviation (SD). All data taken were subjected to normality test using a Shapiro-Wilk's test and for equality of variance using a Levene's test. Kruskal Wallis H test leading to median post hoc test were run to assess the survival rate meanwhile hatching rate and growth performances were conducted using One Way Analysis of Variance (ANOVA) and followed by Tukey post hoc test. In order to determine the sex ratio significant for each treatment, Chi-Square tests were used. All P values less than 0.05 were considered statistically significant (Laerd, 2022).

RESULTS

Total Hatching Rate

Hatching rates of eggs was significantly different (P<0.05) among treatments at 48 hours after observation (Figure 1). The highest hatching rate was observed in those of C2 (0.7 g/L BCL) (95.86±0.66%) and T5 (1.1 g/L BBL) (95.63±0.74%) while C1 (0.8 g BBL) had the lowest percentage of hatching rate (68.08±1.089%). For treatment T1, T2, T3 and T4, the hatching rate was 85.75±7.31%, 75.54±2.04%, 89.76 ± 0.587% and 92.63 ± 2.23% respectively. The statistical analysis also showed that all treatments containing leaf (C2, T1, T2, T3, T4 and T5) had significantly higher hatching rates compared to treatment without leaf (C1).
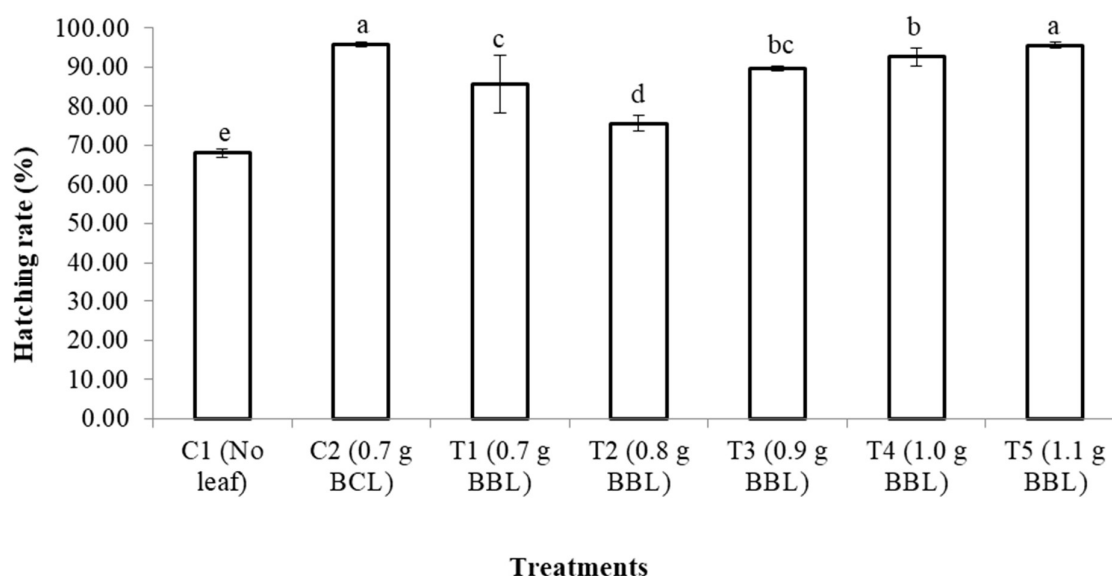

Figure 1. Hatching rates of *Betta splendens* after 48 hours in C1 (control, no leaf), C2 (0.7 g brown Catappa leaf, BCL) as positive control, T1: 0.7 g, T2: 0.8 g, T3: 0.9 g, T4: 1.0 g and T5: 1.1 g of brown banana leaf (BBL). Data are presented as mean ± SD (n= 9). Bars with different letters are significantly different (P < 0.05).

Survival rate and growth performance

The survival rate, SGR (weight and length) of larvae reared in 0.7 g BCL and different weight of BBL after 80 days of experiment is presented in Table 2. After 80 days of the experiment, survival rate and SGR were significantly different (P<0.05) among the treatments. However, no result was recorded for C1 (control, no leaf) as all larvae reached 100% mortalities after two weeks of the rearing trials. The results showed that C2 (0.7 g BCL) (95.56%) and T5 (1.1 g BBL) (95.56%) had the highest larval survival. Meanwhile, T4 (1.0 g BBL) (61.11%) had the lowest survival rate compared to other BBL treatments. The obtained result indicated SGR (weight) was significantly lower in larvae reared in T4 (1.0 g of BBL) compared to other treatments. This is in contrast with SGR length where the result showed T4 (1.0 g BBL) and T5 (1.1 g BBL) were the highest meanwhile C2 (0.7 g BCL) was the lowest among treatments.

Table 2. The survival rate and SGR (weight and length) of *Betta splendens* in C2 (0.7 g brown catappa leaf, BCL) as positive control, T1: 0.7 g, T2: 0.8 g, T3; 0.9 g, T4: 1.0 g and T5: 1.1 g of brown banana leaf (BBL) after 80 days of experimental period. Data are expressed as the mean ± SD (n=30). Values with different superscript are significantly different (P<0.05).

Treatments	Survival rate (%)	SGR weight (g %/day)	SGR length (mm %/day)
C2 (0.7 g BCL)	95.56±3.44[a]	5.837±0.341[a]	3.260±0.232[a]
T1 (0.7 g BBL)	68.89±13.11[b]	5.857±0.500[a]	3.383±0.150[bc]
T2 (0.8 g BBL)	76.67±15.64[b]	5.810±0.429[a]	3.392±0.194[bc]
T3 (0.9 g BBL)	74.44±22.08[b]	5. 997±0.342[a]	3.334±0.151[ab]
T4 (1.0 g BBL)	61.11±6.56[b]	5.612±0.243[b]	3.428±0.102[c]
T5 (1.1 g BBL)	95.56±3.44[a]	5.929±0.188[a]	3.451±0.104[c]

Sex ratio

The sex ratios in each treatment after 80 days of the rearing trials are as shown in Table 3. In C2 (0.7 g BCL) (positive control), the sex ratio was 50% male and 50% female while a slightly skewed sex ratio was observed in T1 (0.7 g BBL) toward female population with 61.3% female and T5 (1.1 g BBL) toward male population with 67.9% male. For treatments T2, T3, and T4, the proportions of males were 46.4%, 55.2%, and 55.0%, respectively. Nevertheless, chi-square analysis indicated that the sex ratios did not deviate significantly from the expected 1:1 ratio observed in the control group (T2).

Table 3. Sex ratio of *Betta splendens* in 0.7 g brown Catappa leaf (BCL) and different weight of brown banana leaf (BBL) after 80 days of experimental period.

Treatments	Sexual maturity (%)		χ^2	df	P
	Male	Female			
C2 (0.7 g BCL)	50	50			
T1 (0.7 g BBL)	38.7	61.3			
T2 (0.8 g BBL)	46.4	53.6			
T3 (0.9 g BBL)	55.2	44.8			
T4 (1.0 g BBL)	55.9	44.1			
T5 (1.1 g BBL)	67.9	32.1	14.385	5	0.013

DISCUSSION

Evidently it can be seen in this study, the absence of any brown leaf in the rearing water of *B. splendens* larvae leads to the collapse of the culture. After two weeks, all the fish in C1 treatment dies while treatments containing Catappa and banana leaf showed a significant and positive result in terms of hatching, survival and growth rates. A unique observation on the skewness of the sex ratio of fishes reared in water containing BBL was discovered.

The highest hatching rates were observed in C2 (0.7 g BCL, positive control) and T5 (1.1 g BBL). Previous studies have reported that fish egg hatchability increases when the fertilized eggs were treated with plants. For instance, when fennel (*Foeniculum vulgara)* was administered at a dosage of 150mg/kg to convict cichlid (*Cichlasoma nigrofasciatum*), it led to a hatching rate of 92.33±1.63% (Sotoudeh & Yeganeh, 2017). Similarly, the use of ginseng root (2 g/kg) in rainbow trout (*Oncorhynchus mykiss*) resulted in hatching rates of 85.2±7.01 (Kadak *et al*., 2019).

Previous studies of phytochemical in plant showed that hydrolysable tannin had a positive impact in stimulating rohu (*Labeo rohita*) immunological parameters (Prusty *et al*., 2007) and boosted carbohydrate accumulation and digestion in grass carp (*Ctenopharyngodon idellus)* (Yao *et al*., 2019). In striped bass (*Morone saxatilis*) larvae, tannic acid was added into feed which led to increases in growth rates and survival rates (Ashraf & Bengtson, 2007). According to Shirmohammadli *et al*, (2018), the hatching and survival percentage in eggs treated with tannic acid (hydrolysable tannin) was much higher compared to clay suspension treatment and the eggs also showed lower fungal contamination. As phytochemicals (tannins, flavonoids and saponins) are known to be present in the culture water of this study (Aswadi, 2023; Norazmi-Lokman & Aswadi, 2023), it can be said that this was the contributing factor to the excellent performance of survival and hatching rate observed in this study. Nevertheless, further investigation is needed to determine the mechanism of tannin on fertilized eggs and how it contributes to the favourable hatching rate.

Environmental conditions are known to have significant impact on reproduction particularly during the embryonic and larval development stages (Baumgartner *et al,* 2008). Within the realm of environmental factors, pH is a parameter that is routinely observed and assessed, particularly when it comes to the development of eggs and the performance of fish larvae (dos Santos *et al*., 2020). The ideal pH values for the embryonic and larval development stages vary depending on the species. For instance, in Pacu (*Piaractus mesopotamicus*), common carp, (*Cyripinus carpio*) (Sapkale *et al*., 2011), Chum salmon (*Oncorhynchus keta*) (Bell *et al*., 1969) and rainbow trout, (*Oncorhynchus mykiss*) (Hagenmaier, 1974), the optimal pH levels were found to be 9, 7.5, 7.5-8.0, and 6.5 respectively.

The variation in the ideal pH levels is associated with the activity of hatching enzymes, specifically chorionase. This activity is primarily influenced by both the fish species and the water's pH (Bell *et al*., 1969; Hagenmaier, 1974). Fertilized fish eggs possess a chorion and plasma membrane that together create a protective and resilient barrier (egg hardening). This barrier serves to safeguard the developing embryo from external environmental conditions (Marimuthu *et al*., 2019). Prior to hatching, fish embryos develop specialized hatching glands that subsequently produce hatching enzymes. These enzymes play a crucial role in breaking down the eggshell during the hatching process (Jezierska *et al*., 2009). However, if fertilized eggs exposed to highly acidic or alkaline pH conditions, it could lead to damage by causing the eggshells to become excessively hard. This in turn, hinders the functioning of hatching enzymes and the embryo, resulting in unsuccessfully embryo hatching and the mortality of larvae (Peterson & Martin-Robichaud, 1983; Kareem *et al*., 2017). According to Marimuthu *et al,* (2019), fertilized eggs and early life of African catfish, *C. gariepinus* were low under extreme pH at both acidic and alkaline concentrations.

The complete dataset of water quality parameters, including pH, recorded throughout this study is available in Norazmi-Lokman and Aswadi (2023). In the current study, the pH of the rearing water of the treatments with highest hatching rate C2, and T5 was 6.60±0.13 and 6.59±0.16 respectively which is also the optimum pH for *B. splendens*. There was a difference in the pH value of each treatment

where the pH value decreases with the increment of BBL usage. These conditions were foreseen because the presence of tannins in BBL can lead to reduction in the pH of the water in the culture. It is therefore suggested that the rearing water needs to be slightly acidic (6.5 to 6.65) to obtain hatching rates of more than 90% in *B. splendens* production.

Stressful condition encountered by fish in captivity such as water replacement might result in high mortality of fish larvae. *Betta splendens* is a species adapted to blackwater environments with a preferred pH range of 5.6 to 6.8. Providing appropriate water conditions for rearing is crucial to ensure the sustainable production of this species. Cultivating blackwater fishes in captivity using clear water has been associated with the occurrence of larval deformities and increased mortality in fish larvae, as observed in studies by Sung & Abol-Munafi (2019) and Ramos *et al.* (2020).

This current study shows that the use of BBL reduces mortality of *B. splendens* larvae. The highest survival rate for cultured *B. splendens* larvae was recorded at the end of the experiment in two groups: C2 (0.7 g BCL, positive control) and T5 (1.1 g BBL). It is well known that *T. catappa* promotes higher survival rate of *B. splendens*. Previously, it has been demonstrated that rearing *B. splendens* in *T. catappa* leaves leads to an increase survival rate, as supported by research conducted by Chansue & Assawongkasem, (2008) and Nugroho *et al*. (2016). The findings from this study, which indicate that the survival rates of larvae reared in BBL and BCL are similar, strongly suggest that BBL can serve as a suitable substitute for BCL in the rearing of *B. splendens* larvae and juvenile. This observation aligns with an acute-lethal toxicity assessment where similar BBL concentrations were found to be non-toxic and shows no adverse impact on *B. splendens* survival rates (Aswadi, 2023). However, a higher amount of BBL is needed to get the same result as those observed in BCL treatment.

Generally, it is established that using plant extracts enhances the survival rate of fish in comparison to control treatments (without plant extract). It shows that survival rate was higher in all treatments with leaf extract compared to in control treatment where 100% mortality occurred after two weeks of experiment. In immersion studies involving pandanus leaf (*Pandanus amaryllifolius*), lemongrass (*Cymbopogon citratus*) and horse radish (*Moringa oleifera*) with Nile tilapia (*O. niloticus*) and African catfish (*C. gariepinus*), it was found that they exhibited a greater survival rate in comparison to control treatment (Sopiah *et al*., 2018; Doctolero *et al*., 2021). Besides that, oral administration in hybrid catfish (*Clarias microcephalus x C. gariepinus*), African catfish (*C. gariepinus*), tilapia (*O. mossambicus*) and goldfish (*Carasius auratus*) fed with asthma weed (*Euphorbia hirta*), mulberry leaf meal (*Morus alba*), Bermuda grass (*Cynodon dactylon*), beal (*Aegle marmelos*), winter cherry (*Withania somnifera*), ginger (*Zingiber officinale*) and neem (*Azadirachta indica*) also showed higher survival rates than in control treatment (Immanuel *et al*., 2009; Kumar *et al*., 2013; Olaniyi *et al*., 2016; Panase *et al*., 2018). The authors suggested that the outcomes observed might be attributed to the presence of phytochemicals in these plants, which could have potentially assisted the fish in the treatment groups in coping with stressful conditions and improving their overall well-being. However, the mode of action of these plants on the survival of fish is not yet understood and needs further study.

Phytochemicals in plants are acknowledged as immunostimulatory agents due to their ability to stimulate immunes system in fish (Makled *et al*., 2020; Rosidah & Pratiwy, 2022). The immune system in fish comprises both innate immunity and adaptive immunity which work together in synergy to provide protection against pathogens and these phytochemicals have been shown to affect both immune pathways (Secombes & Wang, 2012; Ahmadifar *et al*., 2021). Immunostimulators enhance innate immunity by increasing the activity of phagocytic cell, lysozyme, the complement systems, and lymphocyte (Sakai, 1999). Jatropha (*Jatropha vernicosa*), Sage (*Salvia officinalis*) and garlic (*Allium sativum*) which are rich in flavonoids, saponins, coumarin and essential oils, have been documented to possess the capability to defend against bacterial infection by enhancing phagocytosis and lysozyme activity in yellowtail fish (*Seriola rivoliana*), Nile tilapia (*O. niloticus*) and European sea bass (*Dicentrarchus labrax*) (Reverter *et al*., 2014; Abdellatief *et al*., 2018; Serradell *et al*., 2020; Silva-Jara *et al*., 2020).

Phytochemicals might additionally strengthen innate immunity by obstructing virus transcription and diminishing its replication within host cells, potentially leading to higher survivability (Citarasu, 2010). This has been reported in grass carp (*Ctenopharyngodon idella*) and Asian sea bass (*Lates calcarifer*), where phytochemicals have been suggested to function as inhibitors against reovirus and nervous necrosis virus (Chen *et al*., 2017; Islam *et al*., 2021).

In adaptive immunity, a complex network of cells, genes, proteins, and cytokines are involved in the reactions, which encourage the host to react to antibodies and antigens (Uribe *et al*., 2011; Rosales & Uribe-Querol, 2017). The identification of antigen (proteins located on the pathogen's surface) in fish relies on the major histocompatibility complex (MHC) molecules, which are glycoprotein receptors encoded by genes within the MHC (Abbas *et al*., 2019). Subsequent to this recognition, T lymphocyte (T cells) release cytokines which later stimulate B lymphocytes (B cells) to generate antibodies for the purpose of neutralizing and eliminating the pathogens (Salinas *et al*., 2011). Research conducted on Bangkal (*Nauclea subdita*), Stinging neetle (*Urtica dioica*) and fennel (*Radix bupleuri*) which contain flavonoids, sterols, tannins, alkaloids, and phenolics, has shown that they contributed to the up-regulation of immune gene expression levels such as major histocompatibility complex class II (MHC2), IkappaB kinase (IKK α), cytokines interleukin (IL)-8, IL-1β and IL-6 associated with higher survival rate in rainbow trout (*Oncorhynus mykiss*) and hybrid grouper (*Epinephelus lanceolatus x E. fuscoguttatus*) (Reverter *et al*., 2014; Zou *et al*., 2019; Mehrabi *et al*., 2020). Hence, it is proposed that the phytochemicals found in BBL in the current study may exhibit a similar interaction, potentially contributing to the enhanced survival rate observed in *B. splendens* larvae.

In the present study, 80 days of BBL immersion enhanced growth performance specifically specific growth rate (SGR) with better values found in fish with inclusion level of T5 (1.1 g of BBL). Growth performance in current study may be related to the phytochemicals in the plant extracts that affecting growth-related genes such as growth hormone (GH) and insulin-like growth factor,

(IGF) in the aquatic animals (Ahmadifar *et al*., 2021). Once the pituitary gland releases growth hormone, its role is to activate the liver by attaching to the growth hormone receptor (GHR). This activation prompts the liver to produce and secrete IGFs such as insulin-like growth factor, 1 (IGF-1) and insulin-like growth factor, 2 (IGF-2) (Carnevali *et al*., 2005). After that, IGFs act on target cells to induce proliferation and differentiation and eventually promotes growth in fish body (Guo *et al*., 2018). In studies of beluga sturgeon (*Huso huso*), zebrafish (*Danio rerio*), rohu (*Labeo rohita*) and tilapia (*O. mossambicus*) showed that expression levels of GH, IGF-1 and IGF-2 increases (Kamboh & Zhu, 2013; Midhun *et al*., 2016; Safari *et al*., 2020; Ahmadifar *et al*., 2022). The authors suggested that flavonoids and tannins are responsible in raises the concentration of IGF-1 by up regulating the binding of GH and liver GHR and thus enhancing the growth performances. It is suggested that tannin and flavonoids in the BBL may enhanced the growth rate by upregulating these genes of *B. splendens* in the present study. These phytochemicals may improve fish growth performances by activating a series of function with up-regulating/stimulates the growth-related genes.

Sex determination is one of significant parts in the maintenance of fish populations. In ornamental fishes, when one sexual category displays dazzling colouration or higher growth rate, the phenotypic sex manipulation becomes essential (Uguz *et al*., 2003; Cogliati *et al*., 2010). This is the same condition occurring in male *B. splendens* where they are more desired which lead to high market demand meanwhile female commonly demand for breeding purposes. Commonly, phenotypic sex manipulation uses steroid which give rise to the public concerns (Katare *et al*., 2015) as they cause environmental and public health problems (Pattiasina *et al*., 2021). Thus, it is required to strive to get adequate male so that it is economically cost-effective and environmentally friendly.

In the present study, the sex ratio of *B. splendens* was skewed from the expected 1:1 expected ratio. The highest concentration treatment T5 (1.1 g BBL) produces the highest number of male (19 male: 9 female), meanwhile lowest treatment T1 (0.7 g/L BBL) produces the highest number of female (12 male: 19 female) after 80 days of exposure. It seems that higher

concentration in immersion of plant extract seems to influence the total of male population. In the present study, the highest concentration (T5, 1.1 g/L BBL) produces the highest number of males. Similar result was found in study of African catfish (*C. gariepinus*) and guppy (*Poecilia reticulata*) showed increases in male percentage in the highest dose (9 g/30 L) and (0.15 g/L) respectively after immersion in the puncture vine, *Tribulus terrestris* extract (Cek *et al.*, 2007; Turan & Cek, 2007). The authors suggested that this may be due to the phytochemical released by the plant extract where the higher the concentration the higher the amount of phytochemical released.

Phytochemicals might affect sex ratio by interacting with the endogenous hormone. Phytochemicals might instigate biological responses in fish such as estrogenic effects and disruption in aromatase expression/activity (CYP19) and are considered as endocrine disrupting chemicals (EDCs) (Ng *et al.*, 2006; Cheshenko *et al.*, 2008). Ribeiro *et al*, (2012) stated that phytochemical compounds achieve their effects by blocking and binding or deactivating oestrogen receptor sites which affecting the sex hormone bioavailability by promoting the production of hormone-binding globulin. This has been reported in African catfish (*C. gariepinus*), Nile tilapia (*O. niloticus*) and zebrafish (*Danio rerio*), (Mukherjee *et al.*, 2015; Gabriel *et al.*, 2017; Nian *et al.*, 2017; Syarifuddin *et al.*, 2019; Gharaei *et al.*, 2020; Wokeh & Orose, 2020; Aziz *et al.*, 2022).

There were two possible scenarios suggested by Sirotkin & Harrath (2014) on the expression of phytochemicals in endocrine modulation. Firstly, the phytochemicals in plants are capable of controlling endocrine systems (estrogenic and androgenic activity) due to their molecular structure that is similar with estradiol (17- β-estradiol) (Younes & Honma, 2011; Rearick *et al.*, 2014). In addition, the action of estrogens is activated by binding to the estrogen receptors (Matthews *et al.*, 2000). Since the molecular structure of saponins and flavonoids is similar to androgens and estrogens (D' Arrigo *et al.*, 2021), they have the capacity to compete, mimic and replace endogenous estrogens at binding sites on estrogen receptor sites (Pilsakova *et al.*, 2010). This was reported in a study where puncture vine (*Tribulus terrestris*) extract raises testosterone level in convict cichlid (*Cichlasoma nigrofasciatum*) due to the presence of estradiol glycosides (saponins) which acted as inductors (Yeganeh *et al.*, 2017). Besides that, saponins from plant extract also acted as mediators in which they facilitated the production of androgens from estradiol thereby raising testosterone levels (Tadayon *et al.*, 2018).

Another possible scenario is where saponins and flavonoids inhibit the aromatase activity by blocking the biosynthesis and action of estrogen (Berrino *et al.*, 2001; Pilsakova *et al.*, 2010; Ribeiro *et al.*, 2012). Khumpirapang *et al.* (2021) reported that flavonoids caused sex reversal of *B. splendens* by producing 95% male larvae. In *B. splendens*, sex determination and gonad differentiation occurred in the early stages of life cycle. However, the possibility of sex reversal is present because ovarian differentiation begins earlier than formation of testicular tissues (Omeje, 2016). When cholesterol is converted into estradiol-17-β through the enzymatic action of aromatase, sexual differentiation into ovarian cells occurs (Nakamura *et al.*, 1998; Nagahama 2002). Thus, when phytochemicals block the aromatase activity, this leads to a reduction of estrogen biosynthesis in cells which resulting to testicular development instead of the ovary development (Dabrowski *et al.*, 2005). This scenario was supported by Khumpirapang *et al*, (2021) where flavonoids had significant effect on sex reversal of *B. splendens* by producing 95% of male larvae. It can be concluded that these scenarios may took place and influence the male population in our study.

CONCLUSION

In conclusion, the main objective of this study was to demonstrate the effect of (BBL) in *B. splendens* aquaculture was successfully achieved. The findings of this study reveal that BBL has the same effects as BCL where these two treatments have the highest hatching and survival rate. In *B. splendens* larvae culture, BBL treated fish has better growth performance compared to BCL where the highest SGR weight was in T3 (0.9 g BBL) and SGR length in T5 (1.1 g BBL). Based on observation of hatching rate, survival rate and growth performances, the findings of this work indicated that culture water with 1.1 g/L of BBL is the most optimum for *B. splendens*. Furthermore, the immersion of BBL has presented that it is effective in earning the

preferred gender population. Specifically, higher male population of *B. splendens* can be obtained by T5 treatment (1.1 g BBL) meanwhile a higher female population in T1 treatment (0.7 g BBL). It is safe to conclude that BBL is a good and safe alternative/ replacement to Catappa leaf. Other than that, the water quality does not give a negative impact during the immersion of BBL in any treatments. The knowledge and methods developed in this study will succour further enhancement in *B. splendens* breeding and larvae culture. However, further studies are required to determine the mechanism underlying influences of BBL in physiology and reproductive behaviour in *B. splendens*. Additional study is also required to provide conclusive evidence regarding BBL efficacy to be used as sex reversal agent in *B. splendens* culture. Nevertheless, this study has opened a path toward a BBL application in this species.

ACKNOWLEDGMENTS

REFERENCES

Abbas, A.K., Lichtman, A.H. & Pillai, S. (2019). *Basic immunology E-book: functions and disorders of the immune system*. Sixth Edition. Philadelphia: Elsevier.

Abdellatief, S.A., Abdel Rahman, A.N. & Abdallah, F.D. (2018). Evaluation of immunostimulant activity of Spirulina platensis (*Arthrospira platensis*) and Sage (*Salvia officinalis*) in Nile tilapia (*Oreochromis niloticus*). *Zagazig Veterinary Journal,* 46, 25-36. DOI: https://doi.org/10.21608/zvjz.2018.7621

Ahmadifar, E., Pourmohammadi Fallah, H., Yousefi, M., Dawood, M.A.O., Hoseinifar, S.H., Adineh, H., Yilmaz, S., Paolucci, M. & Doan, H.V. (2021). The gene regulatory roles of herbal extracts on the growth, immune system, and reproduction of fish. *Animals,* 11(8), 2167. DOI: https://doi.org/10.3390/ani11082167

Annegowda, H.V., Nee, C.W., Mordi, M.N., Ramanathan, S., & Mansor, S.M. (2010). Hydrolysed extracts of *Terminalia catappa* L. leaf. *Asian Journal of Plant Sciences, 9(8)*, 479–485. DOI: https://doi.org/10.3923/ajps.2010.479.485

Ashraf, M. & Bengtson, D.A. (2007). Effect of tannic acid on feed intake, survival and growth of striped bass (*Morone saxatilis*) larvae. *International Journal of Agriculture and Biology,* 9, 751-754. DOI: https://doi.org/10.30574/wjarr.2023.17.1.1157

Aswadi, N.I.A. (2023). *Elucidating the potential of banana leaf (Musa x paradisiaca) in siamese fighting fish (Betta splendens) production.* (Master Thesis), Universiti Malaysia Terengganu, Malaysia.

Aziz, M.A., Mostary, M.M., Sume, I.J., Uddin, M.H., Khan, M.G.Q., Alam, M.S. & Islam, M. S. (2022). The efficacy of using pine (*Pinus massoniana*) pollen as an alternative to synthetic steroids in producing monosex male Nile tilapia (*Oreochromis niloticus*, L.). *Aquaculture, Fish and Fisheries,* 2(5), 375-383. DOI: https://doi.org/10.1002/aff2.59

Baumgartner, G., Nakatani, K., Gomes, L.C., Bialetzki, A., Sanches, P.V. & Makrakis, M.C. (2008). Fish larvae from the upper Paraná River: do abiotic factors affect larval density? *Neotropical Ichthyology*, 6, 551-558. DOI: https://doi.org/10.1590/S1679-62252008000400002

Bell, G.R., Hoskins, G.E. & Bagshaw, J.W. (1969). On the structure and enzymatic degradation of the external membrane of the salmon egg. *Canadian Journal of Zoology,* 47, 146-148. DOI: https://doi.org/10.1139/z69-028

BERNAMA. (2024). DOF committed to support high-potential ornamental fish industry. https://bernama.com/en/news.php?id=2310154. Downloaded on 13 October 2025.

Berrino, F., Bellati, C., Secreto, G., Camerini, E., Pala, V., Panico, S., Allegro, G. & Kaaks, R. (2001). Reducing bioavailable sex hormones through a comprehensive change in diet: the diet and androgens (DIANA) randomized trial. *Cancer Epidemiology Biomarkers & Prevention*, 10(1), 25-33. https://aacrjournals.org/cebp/article/10/1/25/164016/Reducing-Bioavailable-Sex-Hormones-through-a

Calberto, G., Staver, G. C. & Siles, P. (2015). An assessment of global banana production and suitability under climate change scenarios. In Elbehri, A. (ed.) *Climate change and food systems: Global assessments and implications for*

food security and trade. Food Agriculture Organization of the United Nations (FAO). pp. 266-291.

Carnevali, O., Cardinali, M., Maradonna, F., Parisi, M., Olivotto, I., Polzonetti-Magni, A.M., Mosconi, G. & Funkenstein, B. (2005). Hormonal regulation of hepatic IGF-I and IGF-II gene expression in the marine teleost *Sparus aurata*. *Molecular Reproductive and Development: Incorporating Gamete Research,* 71(1), 12-18. DOI: https://doi.org/10.1002/mrd.20122

Cek, S., Turan, F. & Atik, E. (2007). The effects of Gokshura, *Tribulus terrestris* on sex reversal of guppy, *Poecilia reticulata*. *Pakistan Journal of Biological Sciences,* 10, 718-725. DOI: https://doi.org/10.3923/pjbs.2007.718.725

Chansue, N. & Assawawongkasem, N. (2011). The in vitro antibacterial activity and ornamental fish toxicity of the water extract of Indian almond leaves (*Terminalia catappa Linn*.). *KKU Veterinary Journal,* 18(1), 36-45. http://www.allnaturalpetcare.com/Natural_Aquariums/Indian_Almond_Leaves-Guppies_Bettas_Goldfish.pdf

Chen, X., Hu, Y., Shan, L., Yu, X., Hao, K. & Wang, G.X. (2017). Magnolol and honokiol from *Magnolia officinalis* enhanced antiviral immune responses against crass carp reovirus in *Ctenopharyngodon idella* kidney cells. *Fish & Shellfish Immunology,* 63, 245-254. DOI: https://doi.org/10.1016/j.fsi.2017.02.020

Cheshenko, K., Pakdel, F., Segner, H., Kah, O. & Eggen, R. I. L. (2008). Interference of endocrine disrupting chemicals with aromatase CYP19 expression or activity, and consequences for reproduction of teleost fish. *General and Comparative Endocrinology,* 155, 31-62. DOI: https://doi.org/10.1016/j.ygcen.2007.03.005

Chitmanat, C., Tongdonmuan, K., Khanom, P., Pachontis, P. & Nunsong, W. (2003). Antiparasitic, antibacterial, and antifungal activities derived from a *Terminalia catappa* solution against some tilapia (*Oreochromis niloticus*) pathogens. In Franz, C., Mathe, A., Craker, L.E. and Gardner, Z.E. (eds.) *Acta Horticulturae. III WOCMAP Congress on Medicinal and Aromatic Plants—Volume 4: Targeted Screening of Medicinal and Aromatic Plants, Economics & Law.* Chiang Mai, Thailand. pp. 179-182. DOI: https://doi.org/10.17660/ActaHortic.2005.678.25

Citarasu, T. (2010). Herbal biomedicines: A new opportunity for aquaculture industry. *Aquaculture International,* 18, 403-414. DOI: https://doi.org/10.1007/s10499-009-9253-7

Cogliati, K.M., Corkum, L.D. & Doucet, S.M. (2010). Bluegill coloration as a sexual ornament: evidence from ontogeny, sexual dichromatism, and condition dependence. *Ethology,* 116, 416-428. DOI: https://doi.org/10.1111/j.1439-0310.2010.01755.x

D'Arrigo, G., Gianquinto, E., Rossetti, G., Cruciani, G., Lorenzetti, S. & Spyrakis, F. (2021). Binding of androgen-and estrogen-like flavonoids to their cognate (non) nuclear receptors: a comparison by computational prediction. *Molecules*, 26(6), 1613. DOI: https://doi.org/10.3390/molecules26061613

Dabrowski, K., Gustavo, R. & Mary, A. G. A. (2005). Use of phytochemicals as an environmentally friendly method to sex reverse Nile tilapia. In: Burright, J. Flemming, C. and Egna, H. (eds.) *Twenty-Second Annual Technical Report*. Oregon State University, Aquaculture CRSP. pp. 287-303.

Doctolero, J.S., Estrella, E.S. & Vera Cruz, E.M. (2021). Influence of water immersion using guava (*Psidium guajava*), lemon-grass (*Cymbopogon ciratus*) and horse radish (*Moringa oleifera*) aqueous leaves extract on the nursing of Nile tilapia (*Oreochromis niloticus*). *International Journal of Zoology and Animal Biology,* 4(1), 000279. DOI: https://doi.org/10.23880/izab-16000279

Dongmeza, E., Steinbronn, S., Francis, G., Focken, U. & Becker, K. (2009). Investigations on the nutrient and antinutrient content of typical plants used as fish feed in small scale aquaculture in the mountainous regions of Northern Vietnam. *Animal Feed Science and Technology, 149*(1-2), 162-178. DOI: https://doi.org/10.1016/j.anifeedsci.2008.04.012

dos Anjos, H.D.B., Amorim, R.D.S., Siqueira, J.A. & dos Anjos, C.R. (2009). Ornamental fish export of the state of Amazonas, Amazon basin, Brazil. *Boletim do Instituto de Pesca*, 35(2), 259-274. http://www.pesca.sp.gov.br/sumario35_2.php

dos Santos, J. A., Soares, C. M. & Bialetzki, A. (2020). Effects of pH on the incubation and early development of fish species with different reproductive strategies. *Aquatic Toxicology,* 219, 105382. DOI: https://doi.org/10.1016/j.aquatox.2019.105382

Evers, H. G., Pinnegar, J. K. & Taylor, M.I. (2019). Where are they all from? Sources and sustainability in the ornamental freshwater fish trade. *Journal of Fish Biology,* 94(6), 909-916. DOI: https://doi.org/10.1111/jfb.13930

Gabriel, N.N., Qiang, J., Ma, X.Y., He, J., Xu, P. & Omoregie, E. (2017). Sex-reversal effect of dietary *Aloe vera* (Liliaceae) on genetically improved farmed Nile tilapia fry. *North American Journal of Aquaculture*, 79(1), 100-105. DOI: https://doi.org/10.1080/15222055.2016.1236046

Gharaei, A., Jorjani, H.E., Harijani, J.M. & Miandare, H.K. (2020). Effects of *Tribullus terrestris* extract on masculinization, growth indices, sex detemination reversal and steroid hormones level in Zebra fish (*Danio rerio*). *International Aquatic Research*, 12(1), 22-29. DOI: https://doi.org/10.22034/IAR(20).2020.670992

Giri, S.S., Jun, J.W., Sukumaran, V. & Park, S.C. (2016). Dietary administration of banana (*Musa acuminata*) peel flour affects the growth, antioxidant status, cytokine responses, and disease susceptibility of rohu, *Labeo rohita*. *Journal of Immunology Research,* 2016, 4086591. DOI: https://doi.org/10.1155/2016/4086591

Guo, H., Lin, W., Hou, J., Wang, L., Zhang, D., Wu, X., Li, L. & Li, D. (2018). The protective roles of dietary selenium yeast and tea polyphenols on growth performance and ammonia tolerance of juvenile Wuchang bream (*Megalobrama amblycephal*a). *Frontiers in Phycology,* 9, 1371. DOI: https://doi.org/10.3389/fphys.2018.01371

Hagenmaier, H.E. (1974). The hatching process in fish embryos IV. The enzymological properties of a highly purified enzyme (chorionase from the hatching fluid of the rainbow trout. *Salmo gairdneri* Rich.). *Comparative Biochemistry and Physiology,* 49, 313-324. DOI: https://doi.org/10.1016/0305-0491(74)90166-7

Herath, S. & Atapaththu, K. (2012). Effects of different live feeds on growth performance of fighter fish (*Betta Splendens*) larvae. The 2nd International Symposium, 25-27 May 2012. South Eastern University of Sri Lanka. pp. 129-131. http://ir.lib.seu.ac.lk/handle/123456789/2844

Immanuel, G., Uma, R., Iyapparaj, P., Citarasu, T., Punitha Peter, S., Michael Babu, M. & Palavesam, A. (2009). Dietary medicinal plant extracts improve growth, immune activity and survival of tilapia *Oreochromis mossambicus*. *Journal of Fish Biology,* 74(7), 1462-1475. DOI: 10.1111/j.1095-8649.2009.02212.x

Islam, S.I., Mou, M.J., Sanjida, S. & Mahfuj, S. (2021). An in-silico approach fro identifying phytochemical inhibitors against nervous necrosis virus (NNV) in asian sea bass by targeting capsid protein. *Genetics of Aquatic Organism,* 6(2), GA487. DOI: 10.4194/GA487

Jezierska, B., Ługowska, K. & Witeska, M. (2009). The effects of heavy metals on embryonic development of fish (a review). *Fish Physiology and Biochemistry*, 35(4), 625-640. DOI: https://doi.org/10.1007/s10695-008-9284-4

Kadak, A.E., Bilen, S., Ozdemir, R.C. & Sonmez, A.Y. (2019). Effect of ginseng root (Araliaceae sp.) extracts on sperm quality parameters and reproductive performance in rainbow trout (*Oncorhynchus mykiss*). *Israeli Journal of Aquaculture-Bamidgeh*, 71, 20992. DOI: http://dx.doi.org/10.46989/001c.20992

Kajimura, M., Takimoto, K. & Takimoto, A. (2023). Acute toxicity of ammonia and nitrite to Siamese fighting fish (*Betta splendens*). *BMC Zoology.* 8(25). DOI: https://doi.org/10.1186/s40850-023-00188-3

Kamboh, A.A. & Zhu, W.Y. (2013). Effect of increasing levels of bioflavonoids in broiler feed on plasma anti-oxidative potential, lipid metabolites, and fatty acid composition of meat. *Poultry Science*, 92(2), 454-461. DOI: https://doi.org/10.3382/ps.2012-02584

Kareem, O.K., Ajani, E.K., Akintunde, M.A., Olanrewaju, A.N. & Oduntan, O.B. (2017). Effect of different fertilization and egg de-adhesion methods on hatching and survival of *Clarias gariepinus* (Burchell 1822) fry. *Journal of Fisheries Sciences.com*, 11(1), 21-27. DOI: http://dx.doi.org/10.21767/1307-234X.1000103

Katare, M.B., Basavaraja, N., Joshi, H.D. & Archana, C. (2015). Effect of letrozole on masculinization of Siamese fighting fish (*Betta splendens*). *Journal of Applied and Natural Science*, 7(1), 425-433. DOI: https://doi.org/10.31018/jans.v7i1.627

Kema, G.H., Drenth, A., Dita, M., Jansen, K., Vellema, S. & Stoorvogel, J.J. (2021). Fusarium wilt of banana, a recurring threat to global banana production. *Frontiers in Plant Science, 11*, 628888. DOI: https://doi.org/10.3389/fpls.2020.628888

Khumpirapang, N., Sassa-Deepaeng, T., Suknuntha, K., Anuchapreeda, S. & Okonogi, S. (2021). Masculinizing effects of chrysin-loaded poloxamer micelles on Siamese fighting

fish. *Veterinary Sciences*, 8(12), 305. DOI: https://doi.org/10.3390/vetsci8120305

Kumar, S., Raman, R.P., Pandey, P.K., Mohanty, S., Kumar, A. & Kumar, K. (2013). Effect of orally administered azadirachtin on non-specific immune parameters of goldfish *Carassius auratus* (Linn. 1758) and resistance against *Aeromonas hydrophila*. *Fish Shellfish Immunology,* 34, 564-573. DOI: https://doi.org/10.1016/j.fsi.2012.11.038

Laerd. (2022). Statistics Laerd. Available at: htttps://statistics.laerd.com.

Lichak, M. R., Barber, J. R., Kwon, Y. M., Francis, K. X. & Bendesky, A. (2022). Care and use of Siamese fighting fish (*Betta splendens*) for research. *Comparative Medicine*, *72*(3), 169-180. DOI: https://doi.org/10.30802/AALAS-CM-22-000051

Makled, S.O., Hamdan, A.M. & El-Sayed, A.F.M. (2020). Growth promotion and immune stimulation in nile tilapia, *Oreochromis niloticus*, fingerlings following dietary administration of a novel marine probiotic, *Psychrobacter maritimus* S. *Probiotics and Antimicrobial Proteins,* 12(2), 365-374. DOI: https://doi.org/10.1007/s12602-019-09575-0

Mallik, J., Al, F.A. & Kumar, B.R. (2018). A Comprehensive review on pharmacological activity of *Terminalia catappa* (Combretaceae) - An update. *Asian Journal of Pharmaceutical Research and Development*, 1(2), 65–70.

Mandal, S.C., Sahu, N.P., Kohli, M.P.S., Das, P., Gupta, S.K. & Munilkumar, S. (2010). Replacement of live feed by formulated feed: effect on the growth and spawning performance of Siamese fighting fish (*Betta splendens*, Regan, 1910). *Aquaculture Research,* 41(11), 1707-1716. DOI: https://doi.org/10.1111/j.1365-2109.2010.02564.x

Marimuthu, K., Palaniandya, H. & Muchlisin, Z.A. (2019). Effect of different water pH on hatching and survival rates of African catfish *Clarias gariepinus* (Pisces: Clariidae). *Aceh Journal of Animal Science,* 4(2), 80-88. DOI: https://doi.org/10.13170/ajas.4.2.13574

Matthews, J., Celius, T., Halgren, R. & Zacharewski, T. (2000). Differential estrogen receptor binding of estrogenic substances: a species comparison. *The Journal of Steroid Biochemistry and Molecular Biology*, 74(4), 223-234. DOI: https://doi.org/10.1016/S0960-0760(00)00126-6

Mehrabi, Z., Firouzbakhsh, F., Rahimi-Mianji, G. & Paknejad, H. (2020). Immunity and growth improvement of rainbow trout (*Oncorhynchus mykiss*) fed dietary nettle (*Urtica dioica*) against experimental challenge with *Saprolegnia parasitica*. *Fish & Shellfish Immunology,* 104, 74-82. DOI: https://doi.org/10.1016/j.fsi.2020.05.050

Midhun, S.J., Arun, D., Edatt, L., Sruthi, M., Thushara, V., Oommen, O.V., Kumar, V.S. & Divya, L. (2016). Modulation of digestive enzymes, GH, IGF-1 and IGF-2 genes in the teleost, Tilapia (*Oreochromis mossambicus*) by dietary curcumin. *Aquaculture International,* 24, 1277-1286. DOI: https://doi.org/10.1007/s10499-016-9984-1

Mukherjee, D., Ghosal, I. & Chakraborty, S.B. (2015). Production of monosex Nile tilapia, Oreochromis niloticus using seed of *Mucuna pruriens*. *IOSR Journal of Pharmacy and Biological Sciences*, 10, 55-59. DOI: 10.9790/3008-10145559

Murray, C.A., Markham, O.I., Wood, A.L. & Dimaggio, M. A. (2024). Developing efficient feeding and weaning protocols for Betta splendens informed by larval digestive physiology. *Aquaculture*, *587*, 740884. DOI: https://doi.org/10.1016/j.aquaculture.2024.740884

Nagahama, Y. (2002). Endocrine regulation of gametogenesis in fish. *International Journal of Developmental Biology*, 38(2), 217-229. DOI: https://pubmed.ncbi.nlm.nih.gov/7981031/

Nakamura, M., Kobayashi, T., Chang, X.T. & Nagahama, Y. (1998). Gonadal sex differentiation in teleost fish. *Journal of Experimental Zoology*, 281(5), 362-372. DOI: https://doi.org/10.1002/(SICI)1097-010X(19980801)281:5%3C362::AID-JEZ3%3E3.0.CO;2-M

Neelavathi, P., Venkatalakshmi, P. & Brindha, P. (2013). Antibacterial activities of aqueous and ethanolic extracts of *Terminalia catappa* leaves and bark against some pathogenic bacteria. *International Journal of Pharmacy and Pharmaceutical Sciences*, 5(1), 114–120.

Ng, Y., Hanson, S., Malison, J.A., Wentworth, B. & Barry, T.P. (2006). Genistein and other isoflavones found in soybeans inhibit estrogen metabolism in salmonid fish. *Aquaculture,* 254, 658-665. DOI: https://doi.org/10.1016/j.aquaculture.2005.10.039

Nian, C.T., Tumbokon, B.L.M. & Serrano, A.E. (2017). *Pinus tabulaeformis* pollen as replacement for 17-alpha-methyltestosterone in the diet of *Oreochromis niloticus* larvae for sex reversal and growth. *Israeli Journal of Aquaculture-Bamidgeh*, 69, 1-8. DOI: http://dx.doi.org/10.46989/001c.21042

Norazmi-Lokman, N. H., Baderi, A. A., Zabidi, Z. M. & Diana, A.W. (2020). Effects of different feeding frequency on Siamese fighting fish (*Betta splenden*) and Guppy (*Poecilia reticulata*) juveniles: Data on growth performance and survival rate. *Data in Brief*, *32*, 106046. DOI: https://doi.org/10.1016/j.dib.2020.106046

Norazmi-Lokman, N.H. & Aswadi, N.I.A. (2023). Raw data on the phytochemical content of banana leaf (*Musa x paradisiaca*) and *Betta splendens* rearing water containing Brown Banana leaf (*Musa x paradisica*) along with main water quality data of the rearing water, Mendeley Data, V4. DOI: https://doi.org/10.17632/9rh4tdwy57.4

Nugroho, R.A., Manurung, H., Saraswati, D., Ladyescha, D. & Nur, F.M. (2016). The effects of *Terminalia catappa L*. leaves extract on the water quality properties, survival and blood profile of ornamental fish (*Betta sp.*) cultured. *Biosaintifika: Journal of Biology & Biology Education,* 8(2), 240-247. DOI: https://doi.org/10.15294/biosaintifika.v8i2.6519

Olaniyi, C.O., Adebowale, T.T. & Mustapha, R.O. (2016). Effect of mulberry leaf meal on growth and reproductive performance of African catfish. *CIBTech Journal of Zoology*, 5(2), 20-24.

Omeje, V.O. (2016). *Effect of Pawpaw (Carica papaya) seed meal on the reproductive, endocrine and immune system of Mozambique tilapia (Oreochromis mossambicus)* (PhD thesis), Stellenbosch University, South Africa.

Panase, P., Kamee, B., Moungmor, S., Tipdacho, P., Matidtor, J. & Sutthi, N. (2018). Effects of *Euphorbia hirta* plant leaf extract on growth performance, hematological and organosomatic indices of hybrid catfish, *Clarias macrocephalus× C. gariepinus*. *Fisheries science,* 84(6), 1025-1036. DOI: https://doi.org/10.1007/s12562-018-1234-1

Pattiasina, B., Pattinasarany, M., Manuputty, M. & Kokmesa, E. (2021). Masculinization of beta fish larvae *Betta splendens* through the different treatment immersion of honey solution and larval age. *IOP Conference Series: Earth and Environmental Science*, 797, 012016. DOI: 10.1088/1755-1315/797/1/012016

Peterson, R.H. & Martin-Robichaud, D.J. (1983). Embryo movements of Atlantic salmon (*Salmo salar*) as influenced by pH, temperature, and state of development. *Canadian Journal of Fisheries and Aquatic Sciences*, 40(6), 777-782. DOI: https://doi.org/10.1139/f83-100

Pilsakova, L., Riecanský, I. & Jagla, F. (2010). The physiological actions of isoflavone phytoestrogens. *Physiological Research*, 59(5), 651. DOI: https://doi.org/10.33549/physiolres.931902

Prusty, A.K., Sahu, N., Pal, A., Reddy, A. & Kumar, S. (2007). Effect of dietary tannin on growth and haemato-immunological parameters of *Labeo rohita* (Hamilton) fingerlings. *Animal Feed Science and Technology,* 136(1-2), 96-108. DOI: https://doi.org/10.1016/j.anifeedsci.2006.08.023

Rahmatulloh, M.R., Elfitasari, T. & Windarto, S. (2023). Marketing Analysis of Betta Fish (*Betta sp.*) Cultivation in Semarang City. *IOP Conference Series: Earth and Environmental Science*, 1224(1), 012008. DOI: https://doi.org/10.1088/1755-1315/1224/1/012008

Rajapakshe, W. & Srikrishnan, R. (2020). Evaluation of growth performance and breeding habits of fighting fish (*Betta splendens*) under 3 diets and shelters. *Fisheries Science,* 3(2), 50-65. doi: 10.18331/SFS2017.3.2.6

Ramos, F.M., Abe, H.A., Couto, M.V.S.D., Paixão, P.E.G., Martins, M.L., Carneiro, P.C.F., Maria, A.N. & Fujimoto, R.Y. (2020). *Terminalia catappa* improves growth performance and survival of the Amazon leaf fish (*Monocirrhus polyacanthus*) larvae submitted to handling stress. *Aquaculture Research,* 51(11), 4805-4808. DOI:https://doi.org/10.1111/are.14783

Rearick, D.C., Fleischhacker, N.T., Kelly, M.M., Arnold, W.A., Novak, P.J. & Schoenfuss, H.L. (2014). Phytoestrogens in the environment, I: occurrence and exposure effects on fathead minnows. *Environmental Toxicology and Chemistry*, 33(3), 553-559. DOI: https://doi.org/10.1002/etc.2461

Reverter, M., Bontemps, N., Lecchini, D., Banaigs, B. & Sasal, P. (2014). Use of plant extracts in fish aquaculture as an alternative to chemotherapy: current status and future perspectives. *Aquaculture,* 433, 50-61. DOI: https://doi.org/10.1016/j.aquaculture.2014.05.048

Ribeiro, C., Urbatzka, R., Castro, L.F.C., Carrola, J., Fontainhas-Fernandes, A., Monteiro, R. A., Rocha, M. & Rocha, M.J. (2012). In vitro exposure of Nile tilapia (*Oreochromis niloticus*) testis to estrogenic endocrine disrupting chemicals: mRNA expression of genes encoding steroidogenic enzymes. *Toxicology Mechanisms and Methods*, 22(1), 47-53. DOI: https://doi.org/10.3109/15376516.2011.593053

Rosales, C. & Uribe-Querol, E. (2017). Phagocytosis: A fundamental process in immunity. *BioMed Research International, 2017*, 9042851. DOI: https://doi.org/10.1155/2017/9042851

Rosidah, W.L. & Pratiwy, F.M. (2022). A mini-review: Potential utilization of *Morinda citrifolia* for health and growth of fish. *International Journal of Fisheries and Aquatic Studies,* 10(2), 133–137.

Safari, R., Hoseinifar, S.H., Imanpour, M.R., Mazandarani, M., Sanchouli, H. & Paolucci, M. (2020). Effects of dietary polyphenols onmucosal and humoral immune responses, antioxidant defense and growth gene expression in beluga sturgeon (*Huso huso*). *Aquaculture,* 528, 735494. DOI: https://doi.org/10.1016/j.aquaculture.2020.735494

Sakai, M. (1999). Current research status of fish immunostimulants. *Aquaculture*, 172(1-2), 63-92. DOI: https://doi.org/10.1016/S0044-8486(98)00436-0

Salinas, I., Zhang, Y.A. & Sunyer, J.O. (2011). Mucosal immunoglobulins and B cells of teleost fish. *Developmental & Comparative Immunology,* 35(12), 1346-1365. DOI: https://doi.org/10.1016/j.dci.2011.11.009

Sapkale, P., Singh, R. & Desai, A. (2011). Optimal water temperature and pH for development of eggs and growth of spawn of common carp (*Cyprinus carpio*). *Journal of Applied Animal Research,* 39(4), 339-345. DOI: https://doi.org/10.1080/09712119.2011.620269

Secombes, C.J. & Wang, T. (2012). The innate and adaptive immune system of fish. In *Infectious disease in aquaculture*. England: Woodhead. pp. 3-68.

Serradell, A., Torrecillas, S., Makol, A., Valdenegro, V., Fernández-Montero, A., Acosta, F., Izquierdo, M. & Montero, D. (2020). Prebiotics and phytogenics functional additives in low fish meal and fish oil based diets for European sea bass (*Dicentrarchus labrax*): Effects on stress and immune responses. *Fish & Shellfish Immunology,* 100, 219-229. DOI: https://doi.org/10.1016/j.fsi.2020.03.016

Shirmohammadli, Y., Efhamisisi, D. & Pizzi, A. (2018). Tannins as a sustainable raw material for green chemistry: A review. *Industrial Crops and Products,* 126, 316-332. DOI: https://doi.org/10.1016/j.indcrop.2018.10.034

Silva-Jara, J., Angulo, C., Macias, M.E., Velazquez, C., Guluarte, C. & Reyes-Becerril, M. (2020). First screening report of immune andprotective effect of non-toxic *Jatropha vernicosa* stem bark against *Vibrio parahaemolyticus* in Longfin yellowtail *Seriola rivoliana* leukocytes. *Fish & Shellfish Immunology,* 101, 106-114. DOI: https://doi.org/10.1016/j.fsi.2020.03.048

Sirotkin, A.V. & Harrath, A.H. (2014). Phytoestrogens and their effects. *European Journal of Pharmacology*, 741, 230-236. DOI: https://doi.org/10.1016/j.ejphar.2014.07.057

Sopiah, S., Rosidah, R., Lili, W., Iskandar, I. & Suryadi, I.B. (2018). The effectivity of pandanus leaf extract for the treatment of sangkuriang catfish juvenile *Clarias gariepinus* infected by *Aeromonas hydrophila*. *Jurnal Akuakultur Indonesia*, 17(2), 120-129. DOI: https://doi.org/10.19027/jai.17.2.120-129

Sotoudeh, A. & Yeganeh, S. (2017). Effects of supplementary fennel (*Foeniculum vulgare*) essential oil in diet on growth and reproductive performance of the ornamental fish, Convict cichlid (*Cichlasoma nigrofasciatum*). *Aquaculture Research,* 48(8), 4284-4291. DOI: https://doi.org/10.1111/are.13249

Sung, Y.Y. & Abol-Munafi, A. B. (2019). *Terminalia catappa* leaf extract is an effective rearing medium for larviculture of gouramis. *Journal of Applied Aquaculture*, 1-11. DOI: https://doi.org/10.1080/10454438.2019.1614509

Syarifuddin, Y.N., Sri, A., Yenny, R. & Rahem, F. A. (2019). Masculinization of tilapia (Oreochromis niloticus) by immersion method using methanol extract of pasak bumi roots (Eurycoma longifolia jack). *Russian Journal of Agricultural and Socio-Economic Sciences*, 93(9), 79-87. DOI: http://dx.doi.org/10.18551/rjoas.2019-09.08

Tadayon, M., Shojaee, M., Afshari, P., Moghimipour, E. & Haghighizadeh, M.H. (2018). The effect of hydro-alcohol extract of *Tribulus terrestris* on sexual satisfaction in postmenopause women: A double-blind randomized placebo-controlled trial. *Journal of Family Medicine and Primary Care,*

7(5), 888-892. DOI: https://doi.org/10.4103%2Fjfmpc.jfmpc_355_17

Turan, F. & Cek, S. (2007). Masculinization of African catfish (*Clarias gariepinus*) treated with gokshura (*Tribulus terrestris*). *Israeli Journal of Aquaculture Bamidgeh,* 59, 224-229. DOI: http://dx.doi.org/10.46989/001c.20528

Uguz, C., Iscan, M. & Toganand, I. (2003). Developmental genetics and physiology of sex differentiation in vertebrates. *Environmental Toxicology and Pharmacology,* 14, 9-16. DOI: https://doi.org/10.1016/S1382-6689(03)00005-X

Uribe, C., Folch, H., Enríquez, R. & Moran, G.V.J.M. (2011). Innate and adaptive immunity in teleost fish: a review. *Veterinarni medicina,* 56(10), 486-503. DOI: 10.17221/3294-VETMED.

Watson, C.A., DiMaggio, M., Hill, J.E., Tuckett, Q.M. & Yanong,R.P. (2019). Evolution, culture, and care for *Betta splendens*. EDIS, FA212, 1–5. DOI: https://doi.org/10.32473/edis-fa212-2019.

Wokeh, O.K. & Orose, E. (2021). Use of dietary phytochemicals as control for excessive breeding in Nile tilapia (*Oreochromis niloticus*): A review. *GSC Biological and Pharmaceutical Sciences*, 17(2), 152-159. DOI: https://doi.org/10.30574/gscbps.2021.17.2.0336

Yao, J., Chen, P., Apraku, A., Zhang, G., Huang, Z. & Hua, X. (2019). Hydrolysable Tannin Supplementation Alters Digestibility and Utilization of Dietary Protein, Lipid, and Carbohydrate in Grass Carp (*Ctenopharyngodon idellus*). *Frontiers in Nutrition,* 6(183). DOI: https://doi.org/10.3389/fnut.2019.00183

Yeganeh, S., Sotoudeh, A. & Movaffagh, A.N. (2017). Effects of *Tribulus terrestris* extract on growth and reproductive performance of male convict cichlid (*Cichlasoma nigrofasciatum*). *Turkish Journal of Fisheries and Aquatic Sciences,* 17(5), 1003-1007. DOI: 10.4194/1303-2712-v17_5_15

Younes, M. & Honma, N. (2011). Estrogen receptor β. *Archives of pathology & laboratory medicine*, 135(1), 63-66. DOI: https://doi.org/10.5858/2010-0448-RAR.1

Zou, C., Su, N., Wu, J., Xu, M., Sun, Z., Liu, Q., Chen, L., Zhou, Y., Wang, A. & Ye, C. (2019). Dietary *Radix bupleuri* extracts improves hepatic lipid accumulation and immune response of hybrid grouper (*Epinephelus lanceolatus*♂×*Epinephelus fuscoguttatus*♀). *Fish & Shellfish Immunology,* 88, 496-507. DOI: https://doi.org/10.1016/j.fsi.2019.02.052

Physicochemical and Antioxidant Properties of Copper-Amaranth Leaf Purees Using Viscozyme-L Enzymatic Liquefaction

SITI FARIDAH MOHD AMIN[*1,2], KHARIDAH MUHAMMAD[1], YUS ANIZA YUSOF[3], AHMAD HAZIM ABDUL AZIZ[2] & NOR QHAIRUL IZZREEN MOHD NOOR[2]

[1]Faculty of Food Science and Technology, Universiti Putra Malaysia, 43400 UPM Serdang, Selangor, Malaysia; [2] Food Security Research Laboratory, Faculty of Food Science and Nutrition, Universiti Malaysia Sabah, 88400 Kota Kinabalu, Sabah, Malaysia; [3]Faculty of Engineering, Universiti Putra Malaysia, 43400 UPM Serdang, Selangor, Malaysia.
*Corresponding Author: faridah@ums.edu.my

ABSTRACT

This study evaluated the effect of cell wall-degrading enzyme (Viscozyme® L) on the physicochemical properties and antioxidant activity of copper-amaranth (*Amaranthus Viridis* Linn.) leaf purees. The purees were liquefied with varying concentrations of Viscozyme® L (0–3% v/w) over different incubation times (30 minutes to 24 hours). It was observed that treatment with 1% Viscozyme® L (v/w) at pH 5 for 3 hours, followed by incubation at 45 °C, resulted in a significant increase in total soluble solids (°Brix), acidity, and total chlorophyll content. The enzyme-treated purees exhibited higher DPPH (13.52 mM (TE)/g fresh weight), and FRAP (6.04 mM (TE)/g fresh weight) values, as well as in reducing sugar (118.43 mg/mL), soluble dietary fibre (4.32%) content and greener colour (-0.35) values, as compared to non-enzyme treated purees (0.13 mg/g, 9.47 mM (TE)/g and 3.72 mM (TE)/g fresh weight, and 12.75 mg/mL, 0.60%, and -0.28, respectively). These findings demonstrate that treatment with Viscozyme® L enzymes can effectively improve the nutritional and functional quality of vegetable-based purees, with potential applications in the processing of green vegetable juices.

Keywords: Amaranth; cell wall-degrading enzyme; chlorophyll content; Viscozyme® L

INTRODUCTION

Slender amaranth *(Amaranthus viridis* Linn.*)* is one of Malaysia's most popular green leafy vegetables (Amin *et al.*, 2006; Akbar *et al.*, 2017). Amaranth has nutritional values similar to those of spinach but significantly higher than those of other vegetables, such as cabbage (Akbar *et al.*, 2017). Amaranth is also high in vitamins, minerals, dietary fibre, polyphenols, flavonoids, anthocyanins, and chlorophylls (Wargovich, 2000; Dias and Ryder, 2011). Green amaranth leaves are higher in flavonoid content (1.5 mg CE/g FW) and antioxidant activity (61 µmol TE/g FW) than spinach (0.70 mg CE/g FW and 16 µmol TE/g FW, respectively) (Isabelle *et al.*, 2010; Mavhungu, 2011; Jiménez-Aguilar and Grusak, 2015). Despite all the health benefits of green leafy vegetables, their application in food processing is often limited due to chlorophyll degradation that occurs during thermal processing, acidification or enzymatic treatment, which causes discolouration (Östbring *et al.*, 2014) and

reduction in antioxidant activity. To address this issue, researchers explored to stabilise the magnesium ion in the porphyrin ring of chlorophyll by replacing the magnesium ion in its central porphyrin ring with divalent cations, such as copper (Cu), to form metallo-chlorophyll complexes (Humphrey, 2004). These metal-chlorophyll derivatives are more resistant to acid and heat and retain the green colour of the vegetable during processing (Leunda *et al.*, 2000).

The enzymatic treatment approach offers an environmentally friendly alternative, with higher extraction efficiency and yield while minimising solvent and energy requirements compared to conventional methods (Puri *et al.*, 2012). Furthermore cell wall membrane must be disrupted for chlorophyll extraction in vegetables, and the chlorophyll pigments can be separated from their associated proteins (Pocock *et al.*, 2004) using enzymes. Consequently, enzymatic treatment of vegetables is a good technique for reducing the viscosity (Urlaub,

2002), facilitates easy pressing, and improves yield, clarity, filterability, flavour and colour in fruit and vegetable juice (Godfrey *et al*., 1996; Galante *et al*., 1998; Uhlig, 1998; Kashyap *et al*., 2001; Tochi *et al*., 2009). According to Chong and Wong (2015), enzyme liquefaction is more effective than adding water to the puree in reducing viscosity,, as it requires more energy to remove the additional water during spray drying (Grabowski *et al*., 2006). Several studies have reported the use of enzymatic liquefaction as a pre-treatment in juice processing and spray drying such as in carrots (Stoll *et al*., 2003), pineapple (Wong *et al*., 2015), mango (Sakhale *et al*., 2016) and cabbage (Buckenhüskes *et al*., 1990). However, there are scarce reports on the enzymatic liquefaction of green leafy vegetables.

Few studies have found that enzyme types and concentrations, temperature, and time influence the liquefaction process (Lee *et al*., 2006; Liew Abdullah *et al*., 2007) in several plants. According to Kotcharian *et al*. (2004), the cell wall structure and viscosity of carrot puree were altered by enzymatic cell wall degradation utilising the pectolytic (Rohapect AP) and cellulolytic (Rohament PL) enzymes. Chong and Wong (2015) demonstrated that liquefaction of sapodilla puree with 0.5% (v/w) Pectinex Ultra SP-L and Celluclast 1.5 L at 40 °C for 1.5 h had a better reduction in viscosity before spray drying. Özkan and Bilek (2015) reported a similar observation that optimum conditions for chlorophyll extracted from spinach pulp were using 8% Pectinex Ultra SP-L at 45 °C for 30 min. Meanwhile, Sun *et al*. (2007) required up to 8 hours using Viscozyme® L enzyme at 37 °C to increase antioxidant activity, yield, soluble solid content, and colour of asparagus macerates.

In this research, multi-enzymatic complexes such as Viscozyme® L, which contain cellulases, arabinases, hemicellulases, glucanases and xylanases, cause the cell walls to rupture, facilitating the extraction of valuable compounds from vegetable tissues (Dueñas *et al*., 2007). Therefore, the range of all liquefaction parameters should be carefully selected to obtain the lowest viscosity of amaranth puree and increase the antioxidant activity and chlorophylls in the enzyme-treated puree. Therefore, this study aimed to determine the effects of Viscozyme® L concentrations and liquefaction time on the physicochemical properties of Cu-amaranth puree.

MATERIALS AND METHODS

Materials

Fresh green amaranth (characterised by slender leaves) was purchased from a local market in Kuala Lumpur, Malaysia. All reagents and solvents were analytical grade and purchased from Sigma Chemical Co. (St. Louis, MO, USA). Viscozyme® L was purchased from Novozymes Inc. (Copenhagen, Denmark). This commercial enzyme is a multi-enzyme complex containing cellulases, hemicellulases, pectinases, arabanase, β-glucanase and xylanase from *Aspergillus niger* with a declared activity of ≥100 FBG/g. The optimum conditions are pH 3.3 to 5.5 and temperature 25 to 55±1 °C.

Preparation of Enzyme-Treated Cu-amaranth Puree

Fresh amaranth leaves with stalks were washed, cleaned with running tap water, and chopped to remove the roots. It was then homogenised in a Waring blender for 5 min at high speed to form amaranth purees. The amaranth purees were further treated with 210 ppm of copper sulfate at pH 6 and heated at 80 °C for 15 min, as described in our previous publication by Siti Faridah *et al*. (2021), to form Cu-amaranth puree. For enzymatic treatment, 300 g of Cu-amaranth puree was thawed at 4 °C and individually treated with different concentrations of Viscozyme® L (0-3.0% v/w) under fixed conditions (45 °C for 24 h at pH 5). The pH of the mixtures was adjusted with a 1% (v/v) citric acid solution and 1% NaOH solution (if necessary). The optimum enzyme concentrations were selected based on the purees with the highest chlorophyll content, the highest antioxidant activity, and the lowest viscosity. The same procedure was repeated for the effect of incubation time (0.5-24 h) using an optimised Viscozyme® L concentration at pH 5 and incubated at 45 °C. The non-enzyme-treated Cu-amaranth puree was also prepared as a control and set under the same conditions. At the end of the incubation, all samples were heated for 5 min at 90 °C to inactivate the enzyme. The samples were then strained through a plastic nylon strainer with a fine sieve of 0.4 mm mesh size, packaged in aluminium laminated polyethene

pouches, and stored at -20 °C until further analyses.

Apparent Viscosity

The RheolabQC rheometer (Anton Paar Physica, Gmbh, Germany) was used to evaluate the apparent viscosity of the enzyme-treated Cu-amaranth puree at room temperature (24 ± 1 °C) at 160 rpm using a concentric cylinder and spindle no. 3. A measuring cup with dimension of 52.6 mm in diameter, 75 mm in height, and 150 mL was filled with an aliquot of the enzyme-treated puree. The viscosity of the mixture was measured in millipascal-seconds (mPa.s).

Spectrophotometric Measurement of Total Chlorophyll Content

The chlorophyll content of the enzyme-treated Cu-amaranth puree was determined using the method described by Dere *et al.* (1998) and Siti Faridah *et al.* (2021). Briefly, 1 g of Cu-amaranth puree was ground with 100% acetone using a mortar and pestle until the residue was colourless. Then, the extract was transferred into a centrifuge tube covered with aluminium foil and repeatedly washed with 50 mL (100% acetone). The mixture was then centrifuged ($3500 \times g$, 10 min), and the absorbances of the extracted chlorophylls in the supernatant were measured using a UV-Vis spectrophotometer (Shimadzu, Japan) at 662 and 645 nm against 100% acetone as a blank. The equation, Eq. (1) from Costache *et al.* (2012) was used to quantify the total chlorophyll content (mg/g fresh weight).

Total chlorophyll content (TCC) = ($16.26A_{645}$ + $7.790A_{642}$) × Dilution factor/1000 Eq.(1)

Antioxidant Activity Assay

The enzyme-treated Cu-amaranth purees were dried at 45 °C for 24 h in a convection oven (Venticell 111, MMM Group, Munich, Germany) and then ground into a fine powder using a Pulverisette 14 rotor mill (Fritsch, GmbH, Oberstein, Germany). Each powder (0.25 g) was extracted with 10 mL of 80% methanol at 40 °C for 24 h. The samples were then cooled to room temperature (27 ± 2 °C) and centrifuged at $3500 \times g$ for 15 min. The

supernatant was collected in an airtight glass vial for further analysis (Li *et al.*, 2008).

Free Radical 2,2-diphenyl-1-picrylhydrazyl (DPPH) Assay

The antioxidant activities of the enzyme-treated Cu-amaranth extracts were measured using the DPPH assay as outlined by Brand-Williams *et al.* (1995). Briefly, 0.1 mL of amaranth puree extract was mixed with a 3.9 mL aliquot of 0.1 mM methanolic DPPH solution (prepared using 80% v/v methanol). The mixture was vortexed for 15 seconds and left in the dark for 15 min at room temperature. The absorbance was read at 515 nm using a UV-Vis spectrophotometer (Shimadzu, Japan) with 80% methanol (v/v) as the blank. The FRAP values were expressed as mM of Trolox Equivalents (TE) per gram fresh weight.

Ferric Reducing Antioxidant Power (FRAP) Assay

The FRAP assay was conducted as outlined by Benzie and Strain (1996) with slight modifications. In brief, 2.85 mL of FRAP reagent and 150 µL of Cu-amaranth puree extract were combined, and the mixture was kept in the dark at room temperature for 30 minutes. The absorbance of the reaction mixture was recorded at 593 nm. Trolox was used to construct a standard curve, and the results were represented as mM of Trolox Equivalents (TE) per gram of fresh weight.

Total Soluble Solids (TSS) and pH

The TSS content was measured using a portable hand refractometer (Atago®, Japan) with a 0-32 ºBrix scale. The pH value was measured using a digital pH meter (Jenway, model 3505, UK).

Colour Measurement

A HunterLab Ultra-Scan Colorimeter (Sphere Spectrocolorimeter, Hunter Association Inc., Reston, USA), in the reflectance mode and with illuminant D65, was used to determine a* (+a* = red, -a* = green) and b* (+b* = yellow, -b* = blue). The ratio - a*/b* was used as a measure of variation in green colour as described by Guzmán *et al.* (2002).

Reducing Sugar Measurement by 3,5–dinitrosalicylic Acid (DNS) Method

The activity of the cell wall-degrading enzymes on the enzyme-treated Cu-amaranth purees was determined by measuring reducing sugars released (as glucose equivalents) using a modified 3,5-dinitrosalicylic acid (DNS) method (Saqib and Whitney, 2011). The absorbance was measured at 540 nm using a UV-Vis spectrophotometer (Shimadzu, Japan). Quantification was based on the standard curve (0.03 to 0.25 mg/mL) of D-(+)-glucose (≥99.5%, Sigma G8270) and the results were expressed as mg glucose equivalent in mL of sample (mg/mL).

Total Dietary Fibre Analysis

The soluble (SDF), insoluble (IDF) and total (TDF) dietary fibres were determined using the enzymatic-gravimetric method according to Lee *et al*. (1992). Dried samples (duplicate 1 g) were then subjected to sequential enzymatic digestion and protein digestion in three incubation steps: (i) heat-stable alpha-amylase (or termamyl) (1500 - 3000 units/mg protein; Sigma Chemical Co.) at 98 to 100 ºC for 30 min; (ii) amyloglucosidase (5000 - 8000 units/mL; Sigma Chemical Co.) at 60 ºC for 30 min, pH 4.0 - 4.7; and (iii) protease (7 - 15 units/mg protein; Sigma Chemical Co.) at 60 ºC for 30 min. Each sample was suspended in 40 mL MES/ TRIS buffer (pH 8.2). The enzyme digestate was then filtered using acid-washed celite on a Fibretec system E1023 filtration unit (Tecator, Sweden). After filtration, the remaining residue was the IDF, and the filtrate was the SDF. The IDF was washed with 10 mL of 95% ethanol and 10 mL of acetone. For SDF, the filtrate was precipitated with four volumes of 95% ethanol at 60 ºC before filtering. The SDF was then washed with two portions of 15 mL ethanol (78%, 95%) and 15 mL acetone. TDF, IDF and SDF residue values were all corrected for undigested protein, ash and blank.

Statistical Analyses

All the experiments were performed in triplicate. MINITAB (version 16) statistical software was used for one-way analysis of variance (ANOVA) and Tukey's test was carried out to determine the significant differences among means at the 5% level. Data were reported as mean ± standard deviation.

RESULTS AND DISCUSSION

Effect of Viscozyme® L Concentration

The viscosities of enzyme-treated Cu-amaranth purees with different concentrations (0-3%) of Viscozyme® L incubated at pH 5 and 45°C for 24 h are shown in Figure 1. The untreated Cu-amaranth puree (0% Viscozyme® L) exhibited the highest viscosity due to the presence of undigested compounds, including pulp fibre (hemicellulose and cellulose), protein, and pectin (Roslan *et al*., 2020). In contrast, as the viscosity of Cu-amaranth puree decreased, an increase in the enzyme concentration was observed. It was due to the synergistic effects of pectolytic, cellulolytic, and hemicellulolytic enzymes in the Viscozyme® L, which break down vegetable cell walls, reduce water retention, and release free water into the system (Schweiggert *et al*., 2008). According to Norjana and Noor Aziah (2012), the viscosity of Cu-amaranth puree is reduced due to the presence of free water. However, increasing the enzyme concentration to above 1% of the Viscozyme® L concentration showed no significant effect (p > 0.05) on reducing the viscosities of the purees. It may be due to the complete breakdown of complex polysaccharides into soluble substances, indicating that 1% Viscozyme® L is appropriate for cell wall hydrolysis of Cu-amaranth purees. Thus, 1% of Viscozyme® L was selected as a suitable concentration for cell wall hydrolysis of Cu-amaranth purees. Additionally, to prevent high manufacturing costs, the consumption of enzymes for enzymatic liquefaction should be maintained to a minimum (Chong and Wong, 2015).
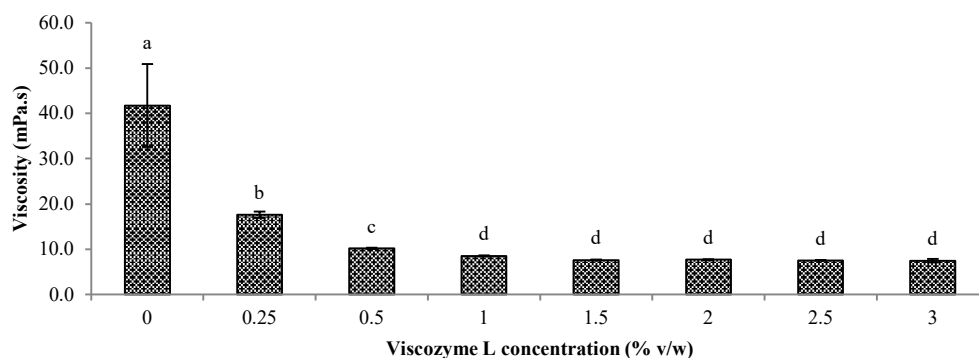
Figure 1. Viscosity of Cu-amaranth purees at pH 5 and 45 ºC for 24 h with different concentrations (0 - 3% v/w) of Viscozyme L. Each value is expressed as mean ± standard deviation (n = 3) of triplicate analysis. Bars with different lowercase letters indicate significant differences (p<0.05) by Tukey's HSD test.

The antioxidant activities (DPPH and FRAP) and total chlorophyll content (TCC) of Cu-amaranth purees after 24 h of enzymatic liquefaction at 45 °C and pH 5 were measured in response to the different concentrations of Viscozyme® L, as shown in Table 1. Cu-amaranth, enzymatically treated with 1% Viscozyme® L, significantly (p<0.05) contained the highest TCC (0.40 mg/g FW) as compared to other purees. A similar observation has been reported for the highest DPPH and FRAP values (10.65 and 5.83 mM (TE)/g FW, respectively) after liquefaction with 1% Viscozyme® L. However, DPPH and FRAP values were not significantly improved at concentrations above 1% Viscozyme® L. According to Puri *et al.* (2012), various enzymes, including cellulases, pectinases, and hemicellulases, interfere with the structural integrity of the plant cell wall. These enzymes hydrolysed the cell wall components, increasing their permeability and producing higher bioactive extraction yields. Furthermore, the formation of metallo-chlorophyll derivatives with metals such as copper has been reported to exhibit high antioxidant activity (Wrolstad *et al.*, 2005).

A similar finding was reported by Sun *et al.* (2007) that liquefaction of asparagus with 1% Viscozyme® L (v/w) at 37 °C and 2 h incubation time gave higher antioxidant activity than control juice (1.4 and 1.2 mM (TE)/L juice, respectively). Koley *et al.* (2011) also showed that enzymatic processing using Viscozyme® L improved the antioxidant activity (FRAP) of Chinese apples (*Zizyphus mauritiana* Lamk).

Table 1. Effect of Viscozyme® L concentration on the antioxidant activities and total chlorophyll content of Cu-amaranth purees.

Viscozyme® L concentration (% v/w)	Antioxidant activity (mM (TE)/g fresh weight)		Total chlorophyll content (mg/g fresh weight)
	DPPH	FRAP	
0.00	9.47 ± 0.07[b]	3.72 ± 0.04[e]	0.13 ± 0.00[e]
0.25	10.06 ± 0.06[ab]	4.23 ± 0.10[de]	0.24 ± 0.01[d]
0.50	10.20 ± 0.59[ab]	4.26 ± 0.09[d]	0.21 ± 0.00[d]
1.00	10.65 ± 0.64[a]	5.83 ± 0.24[a]	0.40 ± 0.00[a]
1.50	10.26 ± 0.12[ab]	5.49 ± 0.19[ab]	0.34 ± 0.02[b]
2.00	10.29 ± 0.48[ab]	4.90 ± 0.27[c]	0.25 ± 0.01[cd]
2.50	10.03 ± 0.07[ab]	5.48 ± 0.04[ab]	0.29 ± 0.05[bc]
3.00	10.27 ± 0.45[ab]	5.06 ± 0.27[bc]	0.31 ± 0.01[b]

Values are the means ± standard deviations of triplicate analyses. [a-e] Different superscript lowercase letters indicate significant differences (p<0.05) within column.

Meanwhile, Hong *et al.* (2013) reported that DPPH radical scavenging activity and total polyphenols of green tea extract treated with Viscozyme® L were significantly higher than those treated with other commercial enzymes (Econase, Pectinex Ultra SP-L, Celluclast, and Rapidase PAC).

Effect of Incubation Time

Figure 2 represents the viscosities of Cu-amaranth purees treated with 1% (v/w) Viscozyme® L at pH 5 and 45 °C for 0.5 - 24 h. A rapid decline in viscosity was observed after 2 hours of incubation, but it gradually increased as the incubation time increased from 12 hours to 24 hours. A slight increase in the viscosity of Cu-amaranth purees might be due to the evaporation of free water in the puree as exposed for a longer time at 45 °C.

The TSS of the puree increased from 2 to 4 °Brix after liquefaction with 1% Viscozyme® L for 3 hours. Similarly, Yusof and Ibrahim (1994) reported that using an enzyme for soursop liquefaction significantly increased its total soluble solid content from 6.8 to 7.3 °Brix within the first hour of incubation. This may be due to the breakdown of cell wall polymers into oligomeric and monomeric soluble solids (Stoll *et al.*, 2003), resulting in an increased TSS and decreased viscosity (Sharma *et al.*, 2005). According to Sakhale *et al.* (2016), the enzymatic liquefaction process on Kesar mango pulp not only increases the overall yield of juice but also improves the quality features of the extracted juice. However, the pH values of the enzyme-treated Cu-amaranth purees were lower than those of the control (non-enzymatically treated) puree. Enzymatic degradation of polysaccharides and pectin, which releases carboxyl groups and galacturonic acid, may be caused by the slight decrease in pH (Gurrieri *et al.*, 2000; Hesham and Manal, 2015).

Meanwhile, the effect of incubation time on the antioxidant activities and total chlorophyll content (TCC) of Cu-amaranth purees was examined (Table 2). An increase in the DPPH and FRAP values 13.52 and 6.04 mM (TE)/g FW, respectively and TCC (0.33 mg/g FW) were observed during the initial 3 hours of incubation with 1% Viscozyme® L. These results agreed with the findings of Li *et al.* (2006), who reported that cell wall-degrading enzymes disrupted the integrity of cell walls, thereby resulting in the efficient extraction of chlorophyll derivatives. Furthermore, degradation of cell-wall polysaccharides resulted in the release of phenolic compounds that contribute to higher antioxidant activity as measured by DPPH and FRAP (Shin & Lee, 2021).

Enzymatic treatment at 3 hours is selected because, according to Umsza-Guez *et al.* (2011), liquefying puree for an extended time at high temperatures is not recommended, as it would negatively affect the enzyme's activity. Additionally, sensitive components in the puree might be overexposed to heat, light, and oxygen. Furthermore, lower enzyme concentration and time are preferable for low-cost operation.
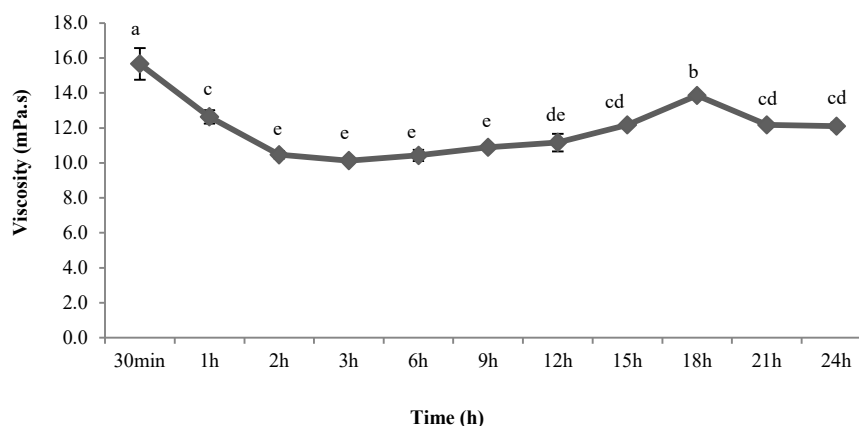

Figure 2. Effect of incubation time (h) on the viscosity (mPa.s) of Cu-amaranth purees with 1% (v/w) Viscozyme® L at pH 5 and 45 ℃. Each value is expressed as mean ± standard deviation (n=3) of triplicate analysis. Bars with different lowercase letters indicate significant differences (p<0.05) by Tukey's HSD test

Table 2. Effect of incubation time on the antioxidant activities and total chlorophyll contents of enzymatically treated Cu-amaranth purees.

Incubation time (h)	Antioxidant activity (mM (TE)/g fresh weight)		Total chlorophyll content (mg/g)
	DPPH	FRAP	
30min	10.38 ± 0.62^c	3.30 ± 0.04^e	0.23 ± 0.00^d
1h	10.75 ± 0.58^{bc}	5.51 ± 0.05^{ab}	0.30 ± 0.01^b
2h	10.54 ± 0.11^c	5.16 ± 0.24^b	0.30 ± 0.00^b
3h	13.52 ± 0.11^a	6.04 ± 0.24^a	0.33 ± 0.00^a
6h	13.63 ± 0.29^a	3.60 ± 0.14^{de}	0.33 ± 0.00^a
9h	12.61 ± 1.42^{ab}	3.56 ± 0.34^{de}	0.28 ± 0.00^c
12h	12.69 ± 1.40^{ab}	4.19 ± 0.27^c	0.30 ± 0.00^b
15h	9.86 ± 0.13^c	4.06 ± 0.16^{cd}	0.30 ± 0.00^b
18h	10.53 ± 0.31^c	4.22 ± 0.14^c	0.28 ± 0.00^c
21h	10.58 ± 0.16^c	4.10 ± 0.10^{cd}	0.28 ± 0.02^c
24h	10.39 ± 0.16^c	4.16 ± 0.08^c	0.28 ± 0.00^c

Values are the means ± standard deviations of triplicate analyses. [a-e] Different superscript lowercase letters indicate significant differences ($p<0.05$) within column. *with 1% (v/w) Viscozyme® L at pH 5 and 45 °C.

Physicochemical Characteristics of Non-Enzyme and Enzyme-Treated Puree

Enzyme-treated Cu-amaranth purees possessed higher total soluble solids (TSS), lightness (L*), a* and b* values, reducing sugar, and soluble dietary fibre (SDF) content as compared to the control (non-enzyme treated) puree as presented in Table 3. An increase in TSS might be due to the degradation of middle lamella and cell wall pectin present in the puree by cellulase, hemicellulase, and pectinase activity in Viscozyme® L, which forms soluble materials such as acid and neutral sugars (Chauhan *et al*., 2017). Similar findings on the physicochemical improvements in TSS, reducing sugar and lightness value are reported in sugar palm (Arsad *et al*., 2015), apricot (Bashir *et al*., 2021), and pear (Amobonye *et al*., 2022).

The a*/b* value of enzyme-treated puree was greener (-0.35) than the control (non-enzymatically treated) puree (-0.28). It may be due to cell wall-degrading enzymes, which facilitate the extraction of chlorophylls and impart green colour to the puree. Meanwhile, enzyme-treated Cu-amaranth purees have higher reducing sugar contents (118.43 mg/mL) than the control puree (12.75 mg/mL).

Table 3. Physicochemical characteristics of non-enzymatically and enzymatically treated Cu-amaranth purees

	Non enzyme-treated	Enzyme-treated *
TSS (°Brix)	2.00 ± 0.15^b	4.00 ± 0.20^a
pH	5.17 ± 1.78^a	4.56 ± 0.34^b
L*	18.20 ± 0.08^a	18.85 ± 0.06^a
a*/b*	-0.28 ± 0.01^b	-0.35 ± 0.01^a
b*	19.53 ± 0.22^a	19.69 ± 0.85^a
Reducing sugar (mg/mL)	12.75 ± 0.46^b	118.43 ± 0.73^a
Total dietary fibre (%)	28.55 ± 0.98^a	16.55 ± 0.83^b
Soluble dietary fibre (%)	0.60 ± 1.65^b	4.32 ± 1.38^a
Insoluble dietary fibre (%)	27.94 ± 1.72^a	12.23 ± 1.77^b

*at optimum conditions with 1% (v/w) Viscozyme® L at pH 5 and 45 °C for 3 hrs.

According to Weinberg *et al*. (1990), reducing sugars were mainly generated from the hydrolysis of cellulose, hemicellulose, pectin,

and other polysaccharides. The enzymatic hydrolysis of these polysaccharides improved the permeability of the cell wall, facilitating better recovery of cell content. The SDF content of Cu-amaranth purees also increased from an initial value of 0.60% to 4.32% after 3 hours of enzymatic liquefaction. Soluble dietary fibres possess prebiotic, hypoglycemic, and hypolipidemic effects (Chawla and Patil, 2010) and thereby provide additional beneficial values to these enzyme-treated purees.

CONCLUSION

The results of this study demonstrate that enzymatic treatment has significantly improved juice yield, total phenolic content, and DPPH scavenging activity. This study has revealed that the enzymatic treatment of Cu-amaranth purees with Viscozyme® L (1% v/w) at pH 5 and 45 °C for 3 hours significantly improved their physicochemical quality characteristics, including total chlorophyll content, antioxidant activity, green colour, reducing sugar, and reduced viscosity. These findings thus suggest the efficacy of cell wall-degrading enzymes in improving the potential application of vegetable juice in the food industry.

ACKNOWLEDGEMENTS

REFERENCES

Akbar, S., Rahman, R., Mushtaq, A., Azeem, M.W., & Al Mahruqi, Z.M. (2017). Slender Amaranth: A review on botany, chemistry, pharmacological importance and potential benefits. *International Journal of Chemical and Biochemical Sciences*, 12: 152-156.

Amobonye, A. E., Bhagwat, P., Ruzengwe, F. M., Singh, S. & Pillai, S. (2022). Pear juice clarification using polygalacturonase from *Beauveria bassiana*: Effects on rheological, antioxidant and quality properties. *Polish Journal of Food and Nutrition Sciences*, 72(1): 57-67. https://doi.org/10.31883/pjfns/145704

Amin, I., Norazaidah, Y., & Hainida, K.I.E. (2006). Antioxidant activity and phenolic content of raw and blanched Amaranthus species. *Food Chemistry,* 94(1*)*: 47-52. https://doi.org/10.1016/j.foodchem.2004.10.048

Arsad, P., Wan Ibadullah, W.Z Mustapha, W.Z., Meor Hussin, A.S. & Sukor, R. (2015). Effects of enzymatic treatment on physicochemical properties of sugar palm fruit juice. *International Journal of Advanced Science Engineering Information Technology*, 5 (5): 308–312. https://doi.org/10.18517/ijaseit.5.5.577

Bashir, O., Hussain, S.Z. & Gani, G. (2021). Evaluating the physicochemical and antioxidant characteristics of apricot juice prepared through pectinase enzyme-assisted extraction from Halman variety. *Food Measure*. 15, 2645-2658. https://doi.org/10.1007/s11694-021-00833-w

Benzie, I.F. & Strain, J. (1996). The ferric-reducing ability of plasma (FRAP) is a measure of "antioxidant power". The FRAP assay. *Analytical biochemistry,* 239 (1): 70-76. https://doi.org/10.1006/abio.1996.0292

Brand-Williams, W., Cuvelier, M. & Berset, C. (1995). Use of a free radical method to evaluate antioxidant activity. *LWT-Food Science and Technology,* 28(1): 25-30. https://doi.org/10.1016/S0023-6438(95)80008-5

Buckenhüskes, H., Omran, H., Zhang, C. & Gierschner, K. (1990). Investigations on enzymatic liquefaction of red and white cabbage. *Food Biotechnology*, 4(1): 289-299. https://doi.org/10.1080/08905439009549741

Chauhan, M., Thakur, N.S., Thakur, A. & Hamid. (2017). Standardisation of enzymatic treatments for the extraction of juice from wild prickly pear (*Opuntia dillenii* Haw.). *Indian Journal of Ecology*, 44(6): 715-720.

Chawla, R. & Patil, G.R. (2010). Soluble dietary fibre. Comprehensive *Reviews in Food Science and Food Safety*, 9(2): 178-196. https://doi.org/10.1111/j.1541-4337.2009.00099.x

Chong, S.Y., & Wong, C.W. (2015). Production of spray-dried sapodilla (*Manilkara zapota*) powder from enzyme-aided liquefied puree. *Journal of Food Processing and Preservation,* 39: 2604-2611. https://doi.org/10.1111/jfpp.12510

Costache, Manuela, A., Gheorghe, C. & Gabriela, N. (2012). Studies concerning the extraction of chlorophyll and total carotenoids from vegetables. *Romanian Biotechnological Letters*, 17(5): 7703-7708.

Dere, S., Günes, T. & Sivaci, R. (1998). Spectrophotometric determination of chlorophyll-

A, B and total carotenoid contents of some algae species using different solvents. *Turkish Journal of Botany,* 22: 13-17.

Dias, J.S. & Ryder, E. (2011). World vegetable industry. *Production, Breeding, Trends. Hort Review,* 38: 299-356. https://doi.org/10.1002/9780470872376.ch8

Dueñas, M., Hernández, T. & Estrella, I. (2007). Changes in the content of bioactive polyphenolic compounds of lentils by the action of exogenous enzymes. Effect on their antioxidant activity. *Food Chemistry,* 101(1): 90-97. https://doi.org/10.1016/j.foodchem.2005.11.053

Galante, Y.M., De Conti, A. & Monteverdi, R. (1998). Application of Trichoderma enzymes in food and feed industries. In Harman, G.F. & Kubicek, C.P. (Eds), *Trichoderma and Gliocladium-Enzyme, Biological Control and Commercial Applications.* London, Taylor and Francis. pp. 327-342.

Godfrey, T. & West, S. (1996). Introduction to industrial enzymology. London. Macmillan Press. pp. 1-8.

Grabowski, J.A., Truong, V.D. & Daubert, C.R. (2008). Nutritional and rheological characterisation of spray-dried sweet potato powder. *LWT - Food Science and Technology,* 41(2): 206-216. https://doi.org/10.1016/j.lwt.2007.02.019

Grabowski, J., Truong, V.D. & Daubert, C. (2006). Spray-Drying of amylase hydrolysed sweet potato puree and physicochemical properties of the powder. *Journal of Food Science,* 71(5): E209-E217. https://doi.org/10.1111/j.1750-3841.2006.00036.x

Gurrieri, S., Miceli, L., Lanza, M., Tomaselli, F., Bonomo, R. P. & Rizzarelli, E. (2000). Chemical characterisation of Sicilian prickly pear (*Opuntia ficus indica*) and perspective for the storage of its juice. *Journal of Agriculture and Food Chemistry,* 48: 5424-5431. https://doi.org/10.1021/jf9907844

Guzmán, G. R., Dorantes, A. L., Hernández, U. H., Hernández, S. H., Ortiz, A. & Mora, E. R. (2002). Effect of zinc and copper chloride on the color of avocado puree heated with microwaves. *Innovative Food Science and Emerging Technologies,* 3(1): 47-53. https://doi.org/10.1016/S1466-8564(01)00053-4

Hesham, A. E. & Manal, F. S. (2015). Effect of incubation, enzymes and thermal pre-treatments

on the quality of pumpkin juice. *Journal of Nutrition and Food Science,* 5: 371. https://doi.org/10.4172/2155-9600.1000371

Hong, Y. H., Jung, E. Y., Park, Y., Shin, K. S., Kim, T. Y., Yu, K. W., Chang, U. J. & Suh, H. J. (2013). Enzymatic improvement in the polyphenol extractability and antioxidant activity of green tea extracts. *Bioscience, Biotechnology, and Biochemistry,* 77(1): 22-29. https://doi.org/10.1271/bbb.120373

Humphrey A.M. (2004). Chlorophyll as a color and functional ingredient. *J. Food Sci.,* 69: C422–C425. https://doi.org/10.1111/j.1365-2621.2004.tb10710.x

Isabelle, M., Lee, B. L., Lim, M. T., Koh, W. P., Huang, D. & Ong, C. N. (2010). Antioxidant activity and profiles of common fruits in Singapore. *Food Chemistry,* 123: 77–84. https://doi.org/10.1016/j.foodchem.2010.04.002

Jiménez-Aguilar, D.M. & Grusak, M.A. (2015). Evaluation of minerals, phytochemical compounds and antioxidant activity of Mexican, Central American and African green leafy vegetables. *Plant Foods for Human Nutrition,* 70: 357–364. https://doi.org/10.1007/s11130-015-0512-7

Kashyap, D.R., Vohra, P.K., Chopra, S. & Tewari, R. (2001). Applications of pectinases in the commercial sector. A review. *Bioresource Technology,* 77: 215-227. https://doi.org/10.1016/s0960-8524(00)00118-8

Koley, T. K., Walia, S., Nath, P., Awasthi, O. & Kaur, C. (2011). Nutraceutical composition of *Zizyphus mauritiana* Lamk (Indian ber): Effect of enzyme-assisted processing. *International Journal of Food Sciences and Nutrition,* 62(3): 276-279. https://doi.org/10.3109/09637486.2010.526930

Kotcharian, A., Kunzek, H. & Dongowski, G. (2004). The influence of variety on the enzymatic degradation of carrots and on functional and physiological properties of the cell wall materials. *Food Chemistry,* 87(2): 231-245. https://doi.org/10.1016/j.foodchem.2003.11.015

Lee, S. C., Prosky, L. & De Vries, J. (1992). Determination of total, soluble, and insoluble dietary fibre in foods. enzymatic-gravimetric method, MES-TRIS buffer. collaborative study. *Journal of AOAC International (USA),* 75: 395-416.

Lee, W.C., Yusof, S., Hamid, N.S.A. & Baharin, B.S. (2006). Optimising conditions for enzymatic

clarification of banana juice using response surface methodology (RSM). *Journal of Food Engineering,* 73(1): 55-63. https://doi.org/10.1016/j.jfoodeng.2005.01.005

Leunda, Maria, A., Norma, G. & Stella, M.A. (2000). Color and chlorophyll content changes of minimally processed kiwifruit. *Journal of Food Processing and Preservation,* 24(1): 17-38. https://doi.org/10.1111/j.1745-4549.2000.tb00403.x

Li, B.B., Smith, B. & Hossain, M.M. (2006). Extraction of phenolics from citrus peels. II. Enzyme-assisted extraction method. *Separation and Purification Technology*, 48(2): 189-196. https://doi.org/10.1016/j.seppur.2005.07.019

Li, H.B., Wong, C.C., Cheng, K.W. & Chen, F. (2008). Antioxidant properties in vitro and total phenolic contents in methanol extracts from medicinal plants. *LWT-Food Science and Technology,* 41(3): 385-390. https://doi.org/10.1016/j.lwt.2007.03.011

Liew Abdullah, A. G., Sulaiman, N. M., Aroua, M. K. & Megat Mohd Noor, M. J. (2007). Response surface optimisation of conditions for clarification of carambola fruit juice using a commercial enzyme. *Journal of Food Engineering,* 81(1): 65-71. https://doi.org/10.1016/j.jfoodeng.2006.10.013

Mavhungu, N. (2011). Antioxidant properties and cellular protective effects of selected african green leafy vegetables. PhD Thesis. Retrieved from http://repository.up.ac.za/handle/2263/25198. University of Pretoria, South Africa.

Norjana, I. & Noor Aziah, A.A. (2012). Quality attributes of Durian (*Durio zibethinus Murr*) juice after pectinase enzyme treatment. *International Food Research Journal,* 18: 1117-1122.

Östbring, Karolina, Marilyn, R., Ingegerd, S., Jennie, O. & Charlotte, E.A. (2014). The effect of heat treatment of thylakoids on their ability to inhibit in vitro lipase/co-lipase activity. *Food and Function*, 5 (9): 2157-2165. https://doi.org/10.1039/c3fo60651a

Özkan, G. & Bilek, S. E. (2015). Enzyme-assisted extraction of stabilised chlorophyll from spinach. *Food Chemistry*, 176: 152-157. https://doi.org/10.1016/j.foodchem.2014.12.059

Pocock, T., Król, M. & Huner, N. P. (2004). The determination and quantification of photosynthetic pigments by reverse phase high-performance liquid chromatography, thin-layer chromatography, and spectrophotometry. Photosynthesis Research Protocols: Springer: 137-148. https://doi.org/10.1385/1-59259-799-8:137

Puri, M., Sharma, D. & Barrow, C. J. (2012). Enzyme-assisted extraction of bioactives from plants. *Trends in Biotechnology,* 30(1): 37-44. https://doi.org/10.1016/j.tibtech.2011.06.014

Roslan, J., Ling, H.C., Sintang, M.D. & Saallah, S. (2020). Effect of heat treatment on rheological properties of bambangan (*Mangifera pajang kosterm*) fruit juice. *Advances in Agricultural and Food Research Journal*, 1(2). https://doi.org/10.36877/aafrj.a0000115

Sakhale, B., Pawar, V. & Gaikwad, S. (2016). Studies on effect of enzymatic liquefaction on quality characteristics of Kesar mango pulp. *International Food Research Journal*, 23(2): 860-865.

Saqib, A.A.N. & Whitney, P.J. (2011). Differential behaviour of the dinitrosalicylic acid (DNS) reagent towards mono- and di-saccharide sugars. *Biomass and Bioenergy*, 35(11): 4748-4750. https://doi.org/10.1016/j.biombioe.2011.09.013

Schweiggert, U., Hofmann, S., Reichel, M., Schieber, A. & Carle, R. (2008). Enzyme-assisted liquefaction of ginger rhizomes (*Zingiber officinale Rosc.*) for the production of spray-dried and paste-like ginger condiments. *Journal of Food Engineering,* 84(1): 28-38. https://doi.org/10.1016/j.jfoodeng.2007.04.013

Sharma, A., Sarkar, B. & Sharma, H. (2005). Optimisation of enzymatic process parameters for increased juice yield from carrot (*Daucus carota* L.) using response surface methodology. *European Food Research and Technology*, 221(1-2): 106-112. http://dx.doi.org/10.1007/s00217-005-1203-7

Shin, K. S. & Lee, J. H. (2021). Optimisation of enzymatic hydrolysis of immature citrus (*Citrus unshiu* Marcov.) for flavonoid content and antioxidant activity using a response surface methodology. *Food science and biotechnology*, 30(5): 663–673. https://doi.org/10.1007/s10068-021-00897-w

Siti Faridah M.A., Yusof, Y.A., Karim, R. & Muhammad, K. (2021). Effects of Enzymatic Liquefaction, Drying Techniques, and Wall Materials on the Physicochemical Properties, Bioactivities, and Morphologies of Zinc-Amaranth (*Amaranthus viridis* L.) Powders.

International Journal of Food Science, 2021: 1819104. https://doi.org/10.1155/2021/1819104

Stoll, T., Schweiggert, U., Schieber, A. & Carle, R. (2003). Process for the recovery of a carotene-rich functional food ingredient from carrot pomace by enzymatic liquefaction. *Innovative Food Science and Emerging Technologies*, 4(4): 415-423. http://dx.doi.org/10.1016/S1466-8564(03)00060-2

Sun, T., Powers, J. R. & Tang, J. (2007). Effect of enzymatic macerate treatment on rutin content, antioxidant activity, yield, and physical properties of asparagus juice. *Journal of Food Science,* 72(4): S267-S271. https://doi.org/10.1111/j.1750-3841.2007.00345.x

Tochi, B.N., Wang, Z., Xu, S.Y. & Zhang, W.B. (2009). The influence of a pectinase and pectinase/hemicellulases enzyme preparations on percentage pineapple juice recovery, particulates and sensory attributes. *Pakistan Journal of Nutrition,* 8(8): 1184-1189. http://dx.doi.org/10.3923/pjn.2009.1184.1189

Uhlig, H. (1998). *Industrial* enzymes *and their applications*, New York. John Wiley and Sons, Inc. pp. 435.

Umsza-Guez, M. A., Rinaldi, R., Lago-Vanzela, E. S., Martin, N., Silva, R. & Thoméo, J. C. (2011). Effect of pectinolitic enzymes on the physical properties of caja-manga (*Spondias cytherea Sonn.*) pulp. *Food Science and Technology (Campinas),* 31(2): 517-526. https://doi.org/10.1590/S0101-20612011000200037

Urlaub, R. (2002). Modern use of enzymes in fruit processing. *Fruit Processing,* 8: 360-361.

Wargovich, M.J. (2000). Anticancer properties of fruits and vegetables. *Hort Science,* 35: 573-575. https://doi.org/10.21273/HORTSCI.35.4.573

Weinberg, Z., Szakacs, G., Linden, J. & Tengerdy, R. (1990). Recovery of protein and chlorophyll from alfalfa by simultaneous lactic acid fermentation and enzyme hydrolysis (ENLAC). *Enzyme and Microbial Technology*, 12(12): 921-925.

Wong, C., Pui, L. & Ng, J. (2015). Production of spray-dried Sarawak pineapple (*Ananas comosus*) powder from enzyme liquefied puree. *International Food Research Journal,* 22(4).

Wrolstad, R.E., Acree, T.E., Decker, E.A., Penner, M., Reid, D., Schwartz, S., Shoemaker, C., Smith, D. & Sporns, P. (2005). Pigments, Colorants, Flavors, Texture, and Bioactive Food Components. In *Handbook of Food Analytical Chemistry*, John Wiley and Sons, Inc.

Yusof, S. & Ibrahim, N. (1994). Quality of soursop juice after pectinase enzyme treatment. *Food Chemistry*, 51(1): 83-88. https://doi.org/10.1016/0308-8146(94)90052-3